INDUCED SEISMICITY AND ITS IMPLICATIONS FOR CO_2 STORAGE RISK

Report: 2013/09

June 2013

INTERNATIONAL ENERGY AGENCY

The International Energy Agency (IEA) was established in 1974 within the framework of the Organisation for Economic Co-operation and Development (OECD) to implement an international energy programme. The IEA fosters co-operation amongst its 28 member countries and the European Commission, and with the other countries, in order to increase energy security by improved efficiency of energy use, development of alternative energy sources and research, development and demonstration on matters of energy supply and use. This is achieved through a series of collaborative activities, organised under more than 40 Implementing Agreements. These agreements cover more than 200 individual items of research, development and demonstration. IEAGHG is one of these Implementing Agreements.

DISCLAIMER

COPYRIGHT

ACKNOWLEDGEMENTS AND CITATIONS

This report describes research sponsored by IEAGHG. This report was prepared by:

CO2CRC

The principal researchers were:

- M. Gerstenberger, GNS Science
- A. Nicol, GNS Science
- C. Bromley, GNS Science
- R. Carne, GNS Science
- L. Chardot, GNS Science
- S. Ellis, GNS Science
- C. Jenkins, CSIRO
- T. Siggins, CSIRO
- E. Tenthorey, Geoscience Australia
- P. Viskovic, GNS Science

To ensure the quality and technical integrity of the research undertaken by IEAGHG each study is managed by an appointed IEAGHG manager. The report is also reviewed by a panel of independent technical experts before its release.

The IEAGHG manager for this report was:

Millie Basava-Reddi

The expert reviewers for this report were:

- Sue Hovorka, University of Texas
- Mike Godec, ARI
- Stefan Baisch, QCon
- Tom Daley, LBNL
- Steve Whittaker, Global CCS Institute
- Gunter Siddiqi, Swiss Federal Office of Energy
- Malcolm Wilson, PTRC
- Hubert Fabriol, BRGM
- David Lumley, University of Western Australia
- Dave Ryan, NRCan

The report should be cited in literature as follows:

'IEAGHG, Induced Seismicity and its Implication for CO_2 Storage Risk, 2013/09, June 2013.'

Further information or copies of the report can be obtained by contacting IEAGHG at:

IEAGHG, Orchard Business Centre,
Stoke Orchard, Cheltenham,
GLOS., GL52 7RZ, UK
Tel: +44(0) 1242 680753 Fax: +44 (0)1242 680758
E-mail: mail@ieaghg.org Internet: www.ieaghg.org

INDUCED SEISMICITY AND ITS IMPLICATIONS FOR CO_2 STORAGE RISK

Key Messages

- The risks associated with induced seismicity at CCS sites can be reduced and mitigated using a systematic and structured risk management programme.
- Statistical models presently show the most promise for forecasting seismicity, but improved physical models are under development and may be key in the future. Both types will need to be tailored to the injection site.
- Site performance and management guidelines should be established prior to injection to facilitate: 1) definition of the acceptable levels and impacts of induced seismicity; 2) optimisation of the monitoring and mitigation programmes; and 3) the establishing of key control measures. Such guidelines have been developed for Enhanced Geothermal Systems and should provide the starting point for a management strategy of induced seismicity at CCS sites.

Background to the Study

Induced seismicity refers to seismicity caused by human/external activity above natural background levels in a given tectonic setting and is distinguished from triggered seismicity, where human activity affects earthquake recurrence intervals, magnitude or other attributes. The physics of triggered and induced seismicity is thought to be identical and both need to be considered during geological storage of CO_2. Induced seismicity may be observed during impounding of dams, mining and tunnelling operations, quarrying, underground solids/cuttings disposal, waste fluids disposal, oil and gas production, geothermal energy production and geological storage of gases and occasionally by rainfall. In some cases induced seismicity has led to projects being suspended, for example enhanced geothermal activities in Basel, Switzerland.

Injection and consequent geological storage of CO_2 may affect subsurface stress and alter in-situ fluid pressure and hence potentially induce seismicity. It is necessary to evaluate potential for and effects of induced seismicity during risk assessment of storage projects. A best practice approach has already been proposed by the US WESTCARB Partnership based on protocols related to geothermal activities.

Induced seismicity may be caused by mechanical loads which can cause changes to the stress regime. Fluid pressures also play a key role in seismicity as pore pressures act against gravitational and tectonic forces and, if increased sufficiently, may cause rock failure. Pre-existing fractures may be stable in the stress regime before fluid injection, but fluid injection increases the pore pressure, which acts in opposition to the normal stress. If pore pressure is great enough to overcome the normal stress, then shear failure will occur.

Other factors that may affect seismicity are thermal and chemical stresses, which can have a weakening effect on the rock. This is likely in geothermal reservoirs, though usually occurs in conjunction with seismicity caused by changes in fluid pressure.

Induced seismicity can also be associated with hydraulic fracturing; this is when a rock is purposefully fractured by injecting water at high pressure with an aim to increase permeability. This has been observed during enhanced geothermal activities and in shale gas production.

Learnings from induced seismicity in other areas, e.g. geothermal activities and hydrocarbon exploration may be applied, but differences with CCS need to be taken into account; such as depth differences, type of sediment into which injection will take place, tectonic activity in the area, injection pressure, volume injected and the length of injection. These values will, for example be very different from those for enhanced geothermal activity which will likely be deeper, into basement rock, possibly in a tectonic area with higher injection pressures for short bursts.

Induced seismicity will also depend on several other factors, which may include the stress regime, fault orientation and locations, and rock friction. It is necessary that site characterisation takes into account any potential for induced seismicity; however, as more information becomes available during the lifetime of the project, through the monitoring programme, the risk in regards to induced seismicity can be reassessed. This may be in the form of real-time monitoring of any ongoing induced seismicity.

CO2CRC, a consortium based in Australia and New Zealand, was commissioned by IEAGHG to undertake this study.

Scope of Work

This study would provide a review of the mechanisms that cause induced seismicity and their application to geological storage of CO_2. The study would involve a detailed literature review of recent and ongoing research in this topic and an analysis drawn from the findings. Importantly, the study would focus on induced seismicity that may be caused by CO_2 injection and storage. Owing to the paucity of large scale CO_2 storage projects, it may be necessary to use findings from analogues (for example, steam assisted gravity drainage of heavy oil, cyclic steam stimulation in heavy oil recovery or produced water re-injection (also at hydraulic fracturing conditions) in oil and gas field operations). Particular issues to be considered and reviewed by the study include:

Weaknesses and threats to storage projects:

- Mechanisms that could potentially cause induced seismicity during injection and storage of CO_2 and the scale of the effect.
- Possible negative impacts on parameters associated with injection and storage, such as maximum injection pressure.

Strengths and Opportunities for storage projects:

- Increase in storage capacity owing to microseismic activity
- Monitoring of reservoir behaviour (caprock integrity) and displacement phenomena

General Overview of Risk Management Concepts (HSE Management):

- Hazards, threats, top events and consequences associated with induced seismicity
- Any preventative and recovery measures that may be taken

The study aims to highlight the current state of knowledge, to recommend further research priorities on these topics, and establish links and best practice sharing where applicable in other subsurface operations.

The contractor was referred to the following recent IEAGHG reports relevant to this study, to avoid obvious duplication of effort and to ensure that the reports issued by the programme provide a reasonably coherent output:

- Pressurisation and Brine Displacement (Permedia, 2010/15)
- Caprock Systems for CO_2 Geological Storage (CO2CRC, 2011/01)
- Injection Strategies for CO_2 Storage Sites (CO2CRC, 2010/04)
- Extraction of Formation Brine from CO_2 Storage (EERC, 2012/12)
- Potential implications of gas production from shales and coal for CO_2 geological Storage (to be published, ARI)

Findings of the Study

This study considered the causes of induced seismicity and examples from CO_2 storage as well as relevant analogues. Empirical data are analysed and the observed relationships documented. Predictive modelling was then reviewed as well as risk management.

Induced earthquakes are indistinguishable from natural earthquakes in terms of their physical parameters such as frequency-magnitude distributions or waveforms produced. For example, earthquakes, including induced earthquakes, typically follow the Gutenberg- Richter relationship; for every magnitude 3 earthquake, there will be roughly 10 magnitude 2, and 100 magnitude 1 earthquakes, and so on.

The magnitude scale is a logarithmic scale so an M5 earthquake is 10 times greater than a M4 earthquake, which is 10 times greater than an M3 earthquake. In many case studies the magnitude is not consistently reported, e.g. whether local or moment magnitude is used, so the specific magnitude scale is ignored.

Events of less than M2 are considered microseismic events and can only be detected using seismological equipment, whereas events greater that M2 may be felt at the surface.

The dominant mechanisms that can result in induced earthquakes, within or close to subsurface reservoirs, include changes in stress field, reservoir pore pressure changes, volume changes of the rock (e.g., thermally induced) and applied forces or loads.

Case Studies

Induced seismicity at commercial and experimental CO_2 storage sites have many features in common. In general, induced seismicity reported for CCS sites have small numbers (<100/yr) and low magnitudes (M-2 to 1), so cannot be felt. The low numbers of induced earthquakes will partly reflect the fact that most CO_2 storage sites are monitored by a limited number of sub-surface geophones within existing wells. While cost effective, these geophone configurations are generally not optimal for accurately locating events or discriminating between ambient noise and small magnitude induced events. This sampling problem is exacerbated for permeable sand formations and saline aquifers where injection produces very low amplitude recorded events. In such cases peak amplitudes may be in the order of 10^{-7} m/s and are close to the noise floor of geophones used in wells. Not-withstanding these problems, no injection induced events >M1 have been produced by, and recorded at CO_2 storage sites.

Given the paucity of induced seismicity data for CO_2 storage sites, it is necessary to consider induced seismicity produced by water injection. Supercritical CO_2 is more compressible and less dense than water at pressures and temperatures typical of CCS reservoirs and these differences could cause variations in their patterns of seismicity. Higher compressibility of CO_2 compared to water makes it a 'softer' medium and could mean that its injection produces lower pressure increases and seismicity rates than water. Despite differences in the properties of water and supercritical CO_2, it is now accepted that they probably produce comparable induced seismicity magnitudes and productivity.

Other case studies considered are from the fields of petroleum production and stimulation, hydrothermal and petrothermal enhanced geothermal systems and waste fluid disposal. The mechanisms causing induced events differ across the different analogues making direct comparison difficult; these mechanisms are explained below.

Induced earthquakes associated with oil and gas extraction result from a reduction of pore pressure in the reservoir, which causes a contraction of the volume surrounding the extraction wells. The resulting stress changes are transferred to the surrounding rock volume and may trigger slip on existing fractures or cause the creation of new fractures. In some cases this can cause subsidence at ground level. In the vast majority of hydrocarbon fields induced seismicity has either not been recorded, not studied in detail or not presented in the publically available literature. Due to this lack of information, there are limitations to what can be concluded about the causes, and associated risks of induced seismicity in hydrocarbon fields. It is clear however that induced earthquakes are generally small to moderate in magnitude ($M \leq 4.5$). In many cases, if present, induced seismicity must comprise events too small to be felt at the ground surface and recorded by regional seismograph networks ($M \leq 3$). It is possible that earthquakes in excess of M 7.0 were triggered by hydrocarbon operations, but for many proposed large magnitude induced events agreement has not been reached about their mechanical origins.

In a number of hydrocarbon fields the onset of seismicity has been linked to significant reductions or increases in reservoir pressures arising from production or water flooding.

Temporal relations between changes in reservoir conditions and induced seismicity are highly variable, with cases ranging from days to years.

The majority of induced seismicity in hydrocarbon fields appears to be from reactivation of pre-existing faults, while new faults are formed due to stresses caused by substantial subsidence. Differences in activity may be due to varying numbers of pre-existing faults or pre-extraction reservoir pressures. In an example in Texas (Cogdell field), induced seismicity was common at intersections or bends in basement faults; such fault complexities are often characterised by high densities of small-scale faults. Some of these apparent differences in the relative timing of changes in reservoir conditions and seismic productivity may be better resolved by improved datasets of the reservoir seismicity and dynamics. Additional data may also improve understanding of the relative importance of reactivation of pre-existing faults and generation of new faults for seismicity induced by hydrocarbon operations.

A range of geothermal sites were considered, both conventional, using low pressure fluid extraction and production and EGS (enhanced geothermal system) projects, where high pressure injection stimulation is required. Hundreds of geothermal fields are under production or development globally and the majority have not reported any felt induced seismicity. High temperature geothermal reservoirs are generally in tectonically active zones, where a high level of natural seismicity is expected. Where seismicity occurs in other areas, it is thought to be due to increases in pore pressure as well as changes in ‘roughness’ of a fault. Other factors are displacement stresses associated with volumetric contraction caused by fluid extraction, thermal stresses and chemical stresses associated with injection of brine. In the case of EGS projects, seismicity can be associated with hydraulic fracturing.

In the relatively small number of operating EGS projects, there have been no known cases where any large induced seismic events have caused major damage or injury. Whether larger, low probability events can yet occur is still to be determined. Geothermal activities were terminated at Basel, Switzerland after a M3 induced event, which indicates the importance of understanding induced seismicity and suggests that its risks go beyond infrastructural damage and have implications for an entire industry.

Some investigations indicate that the smaller the strain energy placed in the formation, the smaller the probability of generating larger seismic events. Injection at lower pressures over longer periods, or more slowly building up injection pressures, then slowly reducing pressures as the stimulation period ends, may be advantageous. However, more research is needed on this.

Injection of waste into deep non-communicative aquifers is used to dispose of hazardous fluids, oilfield brine and as part of solution mining. Well documented occurrences of seismicity related to waste fluid are rare relative to the total number of active injection wells. There is evidence that if reservoir and injection conditions are not closely monitored and understood, induced seismicity is a potential outcome. Reported studies to date of waste water injection projects have shown that small to moderate earthquakes can be induced and, in the case of the Rocky Mountain Arsenal, three $M \geq 5.0$ earthquakes that caused minor

damage in the city of Denver were the result. However, with careful planning and understanding of the reservoir, any risks can be minimised and should be low.

Observed Seismicity and Empirical Data Analysis

Empirical induced seismicity data from injection and extraction projects have potential value for informing risk management decisions at CCS sites. 35 sites from the literature were used for this analysis. Relationships were analysed between induced seismicity parameters; i.e. maximum magnitudes, seismicity rates, b-values, timing and locations; and other reservoir or injection/extraction specific parameters; reservoir permeabilities together with injection/extraction volumes, rates and timing; from the literature.

Of great importance to note is the bias of the data available. Most injection and extraction sites do not have any significant induced seismicity and there is a bias of published data towards productive and large magnitude sequences as seismicity data is not often published for sites without significant seismicity. It is also important to note that CCS will be more closely regulated and monitored than has been the case in the past for other analogous activities. This regulation has the potential to further reduce induced seismicity at CCS sites compared to other injection/ extraction projects.

The maximum earthquake magnitudes of induced earthquakes are generally ≤M4.5 but on very rare occasions may exceed M6. Observations from the literature and this compilation indicate that the maximum magnitude of induced events may increase with total volume of fluid injected/extracted and the injection/ extraction rate. The volume-maximum magnitude relationship may arise because larger volumes of injection fluid have the potential to modify the stresses in larger volumes of crust and to encounter larger faults. It should be noted that the largest observed earthquakes are for fluid extraction projects, and so it is not possible to be certain if this is due to the fluid volumes or the different mechanisms associated with extraction projects.

Rates of induced seismicity are also positively correlated with injection rate and may be attributed to the rise in reservoir pressures expected for higher injection rates.

The rate of seismicity and the proportion of smaller to larger induced earthquakes in a sequence, i.e. the *b*-value for the Gutenberg-Richter relationship, also appear to increase with decreasing reservoir permeability. Reservoirs with low permeabilities (e.g., <0.01 mD) may have high rates of seismicity and *b*-values because they promote locally high stresses which generate many small new fractures. Induced earthquakes are typically spatially and temporally clustered.

The depth of earthquakes inferred to be induced by fluid injection or extraction are mainly <5 km from (or beneath) the surface and located within, or immediately adjacent to, the depth of the reservoir. Clusters of induced seismicity grow in dimensions with injection time and increasing injected volume. Where induced events reactivate pre-existing large-scale faults they form elongate epicentre distributions which increase rapidly in dimension in the fault

strike and dip directions. Most (~70%) induced events occur during injection/ extraction with the number of events decreasing exponentially after injection/extraction ceases.

In all these analyses, it is important to note that other controlling factors, such as the state of stress and injection pressure and rates compared to formation pressure are not taken into account, due to the lack of information in the literature. These other controlling factors will need to be assessed for each site to get a fuller picture of the causes of induced seismicity.

Predictive Modelling of Induced Seismicity

Two main types of models, statistical and physical, have been used for modelling and predicting seismicity induced by fluid injection and both classes are in the relatively early stages of development.

A number of statistical models have been developed to predict temporal evolution, maximum magnitude and magnitude distribution of induced seismicity during and after injection. These statistical models, which were primarily developed for geothermal systems, typically rely on the Gutenberg-Richter relationship and/or the Omori-Utsu law and assume the occurrence of seismicity follows a Poisson distribution. Statistical models are now well established in the wider earthquake seismology community and could be developed to predict the seismic behaviour of a CCS injection system.

A particular challenge in developing robust statistical models to forecast induced earthquakes will be to test that they produce expected, unbiased and reproducible results. The development and refinement of induced seismicity forecast models will be facilitated by induced seismicity data for multiple projects being made widely available.

Many interacting factors contribute to the production of induced seismicity by fluid injection and numerical models need to fully couple fluid flow of different chemical species within a porous and fractured medium to elastic (and ideally, also inelastic) behaviour of the medium to account for the non-linearity effects.

Current numerical techniques are able to model multiphase flow and, in some cases, to couple fluid flow simulations with elastic models to account for the effect of pressure and temperature on strain/stress as well as the effect of strain/stress on permeability and porosity. Current models can highlight geometric and dynamic cases with significant risk of induced seismicity. Such models can be used to identify cases where the risk of induced seismicity can be minimized or avoided by adapting injection strategies.

The utility of these models is strongly dependent on the quality of the input data, including knowledge of the orientation and magnitude of the local stress field; the local fault network including any faults which may be effected by the pressure front; the hydraulic properties of the medium, such as permeability, diffusivity; and the elastic properties of the medium, such as elastic moduli and thermal expansion coefficient.

Obtaining these data and testing the model outputs using induced seismicity data will be critical for improving the utility of numerical models.

Only a few studies have considered the geochemical effects of CO_2 on fault friction and determining the long-term effects of CO_2 on fault rock behaviour is challenging, due to scaling issues.

Risk Assessment and Management

For the majority of existing fluid injection or extraction projects, induced seismicity has not significantly disrupted operations. The risks presented by induced seismicity are variable and include lack of public acceptance and support, damage to infrastructure and rupture of the seal or reservoir. Thresholds for triggering unacceptable risk may vary for different risk factors and CCS sites. Events near to (e.g., < 10 km) injection facilities and as small as M3 could cause damage to infrastructure and injury, while events as small as M2 may raise stakeholder concern.

A systematic and structured risk management programme in which risks associated with induced seismicity are identified and risk reduction, mitigation and control measures outlined will be critical for CCS projects. An eight step protocol for the assessment and management of induced seismicity has been proposed for EGS sites and should form the starting point for CCS sites. These steps are 1) Review laws and Regulations; 2) Assess Natural Seismic Hazard Potential; 3) Assess Induced Seismicity Potential; 4) Establish a Dialogue With Regional Authority; 5) Educate Stakeholders; 6) Establish Microseismic Monitoring Network; 7) Interact with Stakeholders; 8) Implement Procedure for Evaluating impact of induced seismicity

Risk reduction and mitigation measures (Table 1) should be carried out during pre-site selection, site selections and characterisation; and site operational phases:

Table 1: Summary of tasks recommended for risk reduction and mitigation of induced seismicity for CCS projects.

Phase	Risk Activity	Reduction and Mitigation Activity
Pre-site Selection (CCS Framework)	Stakeholder Uncertainty	Establish scientific and legal criteria for discriminating natural and induced earthquakes.
		Identify key stakeholders that will be impacted by induced seismicity and devise policies for engaging with stakeholders (e.g., government, regulators, public, NGOs).
		Introduce clear and usable CCS legislation for management of induced seismicity.
		Devise management protocols and acceptable earthquake magnitude thresholds for individual sites.
		Interact with stakeholders (e.g., regulators and operators) to ensure that risk assessment methods and process provides required outputs for induced seismicity.
		Governments regulate CCS and accept long-term liability for induced events.
	Seismicity	Preliminary regional assessment of potential for induced and natural seismicity.
	Public Acceptance	Survey public attitudes and perceptions toward and, knowledge of, seismicity induced by injection of fluid (and its risks) in local area of potential storage sites.

Site Selection and Characterisation	Seismicity	Site specific assessment of potential for induced and natural seismicity
		Measure reservoir stresses and predict change in reservoir stresses due to injection.
		Determine possible impact of rock properties and pre-existing faults on seismicity using fracture gradients and fault frictional properties.
		Integrate geomechanical, dynamic fluid flow and risk modelling for preferred storage site to forecast seismicity and estimate its impact on fluid flow.
	Monitoring	Develop mitigation and remediation plans (i.e. Induced Seismicity Management Plan) for potential seismic events using predefined magnitude and reservoir pressure thresholds.
	Public Acceptance	Educate and consult public about induced seismicity and risks.
	Economics	Develop economic modelling of CCS system for storage site incorporating induced seismicity. Highlight uncertainties in the economics arising from induced seismicity.
Site Operation	Monitoring	Record and analyse induced earthquakes in real time.
		Monitor reservoir pressures and plume migration to confirm pre-injection models.
		Modify monitoring and remediation plans as required.
	Mitigation	Adjust injection rates, injection intervals and number of wells to maintain induced earthquakes within pre-defined magnitude range and locations.
		Introduce financial compensation for damages and interference associated with induced seismicity.
	Public Acceptance	Reassess public response and perceptions to seismicity. Increase public communication and community support as required.
		Report induced seismicity to general public in near real time.
		Continue open dialogue with public regarding seismicity and general operations.
	Economics	Rerun economic models if critical seismicity thresholds are exceeded.

An understanding of the expected size, number, location and timing of induced earthquakes is required for risk assessment and management of seismicity generated by injection of CO_2. Tools for forecasting induced seismicity are of two main types: Tools that estimate generalities of induced seismicity prior to injection; and tools that provide more accurate estimates of the behaviour of the expected seismicity after injection has commenced. Category 1 tools are qualitative and include the use of empirical datasets together with preliminary physical and statistical models. Category 2 tools will be quantitative and include site-specific physical and statistical models. Statistical models presently show the most promise for forecasting induced seismicity; however, physical models could become key predictive tools in the future.

Monitoring and mitigation of induced seismicity should be an important component of commercial scale CO_2 storage projects. The design of monitoring networks for induced seismicity could vary between sites depending on a range of factors including; desired event magnitude range, site location and reservoir depth, levels of background seismicity and ambient noise and cultural site constraints (e.g., existing infrastructure and financial priorities). To optimise the utility of monitoring and mitigation programmes site performance and management, guidelines for induced seismicity should be established prior to injection.

Guidelines include setting the acceptable level (i.e. magnitude range and productivity) and impacts of seismicity and outlining the control measurements to be implemented if original expectations are exceeded.

There are also some potential benefits of induced seismicity to CCS. Firstly improved monitoring as mapping the locus of induced seismicity in real time provides a potential means of charting the movement of the pressure front associated with CO_2 injection, however further work is required to understand better relationships between locations of induced seismicity (for a given magnitude), pressure changes in the reservoir and the CO_2 plume. The pressure change would also need to be great enough to induce microseismicity, which will be dependent on a number of factors particular to the storage site. Secondly there will be increased permeability and therefore injectivity, due to hydraulic fracturing, though there is also the possibility that this could reduce sweep efficiency and therefore capacity; therefore effects must be determined on a site-by-site basis,

Expert Review Comments

Expert comments were received from 10 reviewers, representing industry (corporate sponsors of IEAGHG) and academia. The reviews were overall positive and key technical suggestions included more discussion on other controlling factors that could affect the current data and more discussion of the processes and mechanisms causing induced seismicity. These comments were addressed in the final report.

Conclusions

Induced seismicity has been widely reported over the last 40 years. To date few induced earthquakes have been recorded at CO_2 storage sites, however, the volumes of injected CO_2 are small and the onsite seismograph networks are often limited. Injecting commercial-scale volumes of CO_2 has the potential to produce induced seismicity at shallow depths of <5 km, but this will need to be considered on a site by site basis as there will be several controlling factors governing the likelihood of induced seismicity.

Observations from case studies and compilation of empirical data in this study indicates several potential relationships such as maximum magnitude of induced events may increase with total volume of fluid injected/extracted and the injection rate. The volume-maximum magnitude relationship may arise because larger volumes of injection fluid have the potential to modify the stresses in larger volumes of crust and to encounter larger faults. However, when considering empirical relationships, it is important to note the bias in the data and that the majority of sites do not produce induced seismicity to any significant degree. There are also a number of other controlling factors which will be specific to the site in question, but were not documented in enough detail to apply them to this study.

A particular challenge in developing robust statistical and physical models to forecast induced earthquakes will be to test that they produce expected, unbiased and reproducible, and, ultimately, informative results, which can be used as part of the risk assessment. The

risks associated with induced seismicity at CCS sites can be reduced and mitigated using a systematic and structured risk management programme.

Risks to CCS projects associated with induced seismicity may include:

1) loss of public support due to concern about potential seismicity or from actual observed events;
2) ground shaking causing damage to property or injury;
3) loss of integrity of the reservoir though fracturing of the reservoir or of the seal.

The risks associated with induced seismicity at CCS sites can be reduced and mitigated using a systematic and structured risk management programme. While precise forecasts of the expected induced seismicity may never be possible, a thorough risk management procedure will include some level of knowledge of the possible behaviour of induced seismicity. Risk management will require estimates of the expected magnitude, number, location and timing of potential induced earthquakes. Such forecasts should utilise site specific observations together with physical and statistical models that are optimised for the site. Statistical models presently show the most promise for forecasting induced seismicity after injection has commenced, however, with further development physical models could become key predictive tools that are informative prior to injection. Combining forecasts with real-time monitoring of induced seismicity will be necessary to maintain an accurate picture of the seismicity and to allow for mitigation of the associated risks as they evolve. Site performance and management guidelines should be established prior to injection to facilitate: 1) definition of the acceptable levels and impacts of induced seismicity; 2) optimisation of the monitoring and mitigation programmes; and 3) the establishing of key control measures. Such guidelines have been developed for Enhanced Geothermal Systems and should provide the starting point for a management strategy of induced seismicity at CCS sites.

A number of information and knowledge gaps have been identified for induced seismicity. Understanding of induced seismicity and the associated risks would be improved by;

1) Increasing the induced seismicity catalogues publically available for development and testing of physical and statistical models,
2) Undertaking more systematic studies of sites populated by well constrained subsurface information and seismicity catalogues that are completely recorded down to small magnitudes,
3) Improving the physical reality of physical models by modelling such factors as, poroelastic effects, multiple species of fluid and non-critically stressed systems,
4) Studying the scaling effects on seismicity associated with a move from pilot projects to full commercial implementation of CO_2 storage,
5) Developing standard risk management procedures and guidelines for induced seismicity for CCS projects and,
6) Filling induced seismicity knowledge gaps in the CCS community by collaborating with seismologists working in other industries.

Recommendations

Induced seismicity has not occurred to a significant degree on a CO_2 storage site and while analogues can be used for comparison and to help formulate a risk assessment plan, there are differences in the industries that cannot always be applied to CCS. Work is continuing in this area, with more CO_2 storage sites using microseismic monitoring and induced seismicity being accounted for in risk assessments.

It is recommended that IEAGHG continue to follow this topic, through the research networks (namely the risk assessment, modelling and monitoring networks).

Induced seismicity and its implications for CO_2 storage risk

[1,2]Gerstenberger, M, [1,2]Nicol, A, [2]Bromley, C, [2]Carne, R, [2]Chardot, L, [2]Ellis, S, [1,3]Jenkins, C, [1,4]Siggins, T, [1,5]Tenthorey, E, [2]Viskovic, P

November 2012
CO2CRC Report No: RPT12-4001

[1] Cooperative Research Centre for Greenhouse Gas Technologies (CO2CRC)

[2] GNS Science, PO Box 30368, Lower Hutt, New Zealand

[3] CSIRO, Pye Laboratory, Canberra, Australia

[4] CSIRO, Ian Wark Laboratory, Clayton, VIC, Australia

[5] Geoscience Australia, Canberra, ACT, Australia

CO2CRC
Technologies

CO2CRC Technologies Pty Limited

PO Box 1130, Bentley, Western Australia 6102
Phone: +61 8 6436 8655
Fax: +61 8 6436 8555
Email: dhilditch@co2crc.com.au
Web: www.co2tech.com.au

Table of contents

Figures

Tables

Executive Summary

Seismicity produced by human activities (i.e. induced seismicity) has been widely reported over the last 40 years. In this report we discuss induced seismicity that has been published in the scientific literature that resulted from: hydrocarbon stimulation and extraction; geothermal systems; waste fluid disposal; and carbon capture and storage (CCS). To date few induced earthquakes have been recorded at CO_2 storage sites, however, the volumes of injected CO_2 are generally small and the onsite seismograph networks are often limited. Injecting commercial-scale volumes of CO_2 (e.g., millions of tonnes) has the potential to produce induced seismicity at shallow depths (e.g., <5 km) that could have consequences for the successful completion of CCS projects. The largest risks to CCS projects associated with induced seismicity are likely to come from the loss of public support due to concern about, or the occurrence of, induced earthquakes. Additionally, fracturing of the seal reservoir must also be considered, and although no serious damage to property or serious injury has occurred due to induced seismicity associated with CCS projects, these risks may not be zero and should be understood. One of the principal reasons for studying induced seismicity arising from injection of CO_2, and a key driver for this report, is to improve the ability to assess and manage the associated risks.

A review of induced seismicity confirms that these events are typically small to moderate in magnitude (≤M4.5), but that induced events have not been observed or reported at an unknown, but likely large number of sub-surface injection or extraction sites. Rare large earthquakes of M≥5 have been observed, sometimes associated with hydrocarbon extraction, however, it is not clear if these events have anthropogenic origin and their cause is debated in the literature. While the mechanics of the earthquake process are generally understood, the key factors that control the magnitude range, seismicity rates and spatial and temporal distributions of events remain unknown at many sites. These uncertainties arise because the geomechanical parameters of the storage system are not well known and/or the records of induced events are poor. Despite these data issues, numerous published studies have investigated the relationships between fundamental reservoir properties and the behaviour of induced seismicity. In this report we have supplemented the published studies with a meta-analysis of all published data that we were able to obtain (i.e., 83 sites). In these analyses, a number of factors have been identified that could increase the risk of induced seismicity at CCS sites. Many of these factors are interrelated and include: injected volume, injection rates, reservoir pressure, injection depths, number of weak pre-existing faults, background seismicity rates, and reservoir permeability.

The risks associated with induced seismicity at CCS sites can be reduced and mitigated using a systematic and structured risk management programme. While precise forecasts of the expected induced seismicity may never be possible, a thorough risk management procedure will include some level of knowledge of the possible behaviour of induced seismicity. Risk management will require estimates of the expected magnitude, number, location and timing of potential induced earthquakes. Such forecasts should utilise site specific observations together with physical and statistical models that are optimised for the site. Statistical models presently show the most promise for forecasting induced seismicity after injection has commenced, however, with further development physical models could become key predictive tools. Combining forecasts with real-time monitoring of induced seismicity will be necessary to maintain an accurate picture of the seismicity and to allow for mitigation of the associated risks as they evolve. To optimise the utility of monitoring and mitigation programmes, site performance and management guidelines for the acceptable levels and impacts of induced seismicity together with key control measures should be established prior to injection. Such guidelines have been developed for Enhanced Geothermal Systems and should provide the starting point for a management strategy of induced seismicity at CCS sites.

A number of information and knowledge gaps have been identified for induced seismicity. Understanding of induced seismicity and the associated risks would be improved by; a) increasing the induced seismicity catalogues publically available for development and testing of physical and statistical models, b) undertaking more systematic studies of sites populated by well constrained sub-surface information and seismicity catalogues that are completely recorded down to small magnitudes, c) improving the physical reality of physical models by modelling such factors as, poroelastic effects, multiple species of fluid and non-critically stressed systems, d) studying the scaling effects on seismicity associated with a move from pilot projects to full commercial implementation of CO_2 storage, e) developing standard risk management procedures and guidelines for induced seismicity for CCS projects and, f) filling induced seismicity knowledge gaps in the CCS community by collaborating with seismologists and modellers working in other industries.

Introduction

The occurrence of earthquakes produced by human activities, or induced seismicity, is a phenomenon that has been observed to result from a number of industries over the last four decades (e.g., hydrocarbon and water extraction, wastewater sub-surface disposal, geothermal water injection and water impoundment by dams)(e.g., Figure 1 and Figure 3). Since the Basel earthquakes in December 2006, which resulted from water injection and reached a maximum magnitude of M 3.4, public awareness of earthquakes produced by human activities has increased significantly. More recently public debate has been heightened by the occurrence of a number of induced earthquakes including, events during February and March 2011 up to M 4.7 near Guy, Arkansas (USA), two earthquakes up to M 2.3 near Blackpool, UK, in April and May 2011, a M 5.1 earthquake in Lorca, southeast Spain on May 11 2011, and a M 4.0 event near Youngstown, Ohio (USA), on December 31 2011 (de Pater and Baisch, 2011; Healy, 2012; González et al., 2012; Zoback, 2012; Zoback and Gorelick, 2012). While none of these earthquakes were triggered by CO_2 injection, events of similar magnitudes could pose a risk to the successful completion of future CCS projects. Determining the magnitudes of these risks and how best to reduce their impact are important questions that require investigation.

A significant body of literature exists observing and modelling the occurrence of induced seismicity, however, the literature largely remains inconclusive about the detailed mechanics that control the behaviour of the earthquakes. This lack of clarity arises because numerous factors can influence earthquake behaviour. In many cases, the induced seismicity may be poorly recorded or the details of the related human activity are either poorly known, or not available. For carbon capture and storage (CCS) projects, as with other injection projects, understanding what controls the occurrence and behaviour of induced seismicity is important for developing a thorough and robust risk management plan. Such a plan will include assessment of the risk related to induced seismicity and will consider options for risk reduction and mitigation that will necessarily extend beyond the injection life of the project.

Research related specifically to the occurrence of induced seismicity in CCS is in relatively early stages of development; however, there is much to be learned by the CCS community from the broader industry and seismological communities which have a longer history of studying induced seismicity. Ultimately, induced earthquakes are similar in most aspects to natural earthquakes and the CCS community should learn from and interact with the traditional seismological research community. Here we present an overview of the induced seismicity literature from a broad spectrum of industries. The main purpose of this report is to summarise the relevant literature with regards to current state of knowledge and understanding of induced seismicity. With this knowledge we can then begin to estimate what the potential is for induced seismicity in CO_2 injection and storage projects. An ultimate goal of this report is to discover where important gaps in our understanding of induced seismicity exist and to highlight where future research may have the biggest impact in reducing the uncertainties associated with such events, and, hence, reduce the risk to CCS projects.

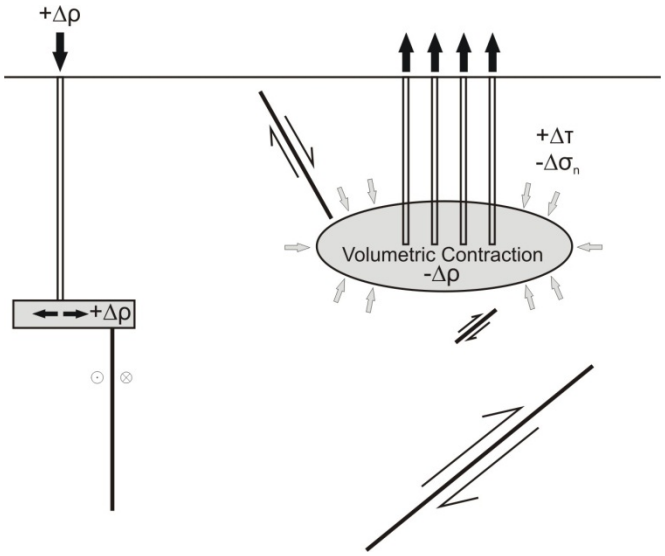

Figure 1: Seismicity induced by fluid injection at depth, and major oil and gas extraction operations (Modified from McGarr et al., 2002).

What is induced seismicity?

Induced seismicity occurs when human or anthropogenic activities encourage and cause a new or pre-existing fault to move in a single failure. The resulting fault slip typically takes place over seconds or less and the sizes of the earthquakes can cover many orders of magnitude. At the low end of the range micro-seismicity (M≤2) that may be of negative magnitude produced by maximum offset on the fault, or slip, and total rupture lengths is on the order of millimetres to centimetres. Events larger than M2 may be felt on the ground surface and have fault slip scales of meters and rupture scales of meters or more.

Often induced earthquakes are indistinguishable from natural earthquakes in terms of their physical parameters such as frequency-magnitude distributions or waveforms produced. For example, as explained in Section 6.5, earthquakes, including induced earthquakes, typically follow the Gutenberg-Richter relationship (Gutenberg and Richter, 1954). This means that for every magnitude 3 earthquake, there will be roughly 10 magnitude 2, and 100 magnitude 1 earthquakes, and so on. However, induced earthquakes are distinct from natural earthquakes in that they are caused by anthropogenic activities and arise from changes in physical or chemical properties of the reservoir (e.g., changes in stress, temperature and fluid chemistry) that these activities can cause. Such activities include:

- mining
- water impoundment reservoirs
- fluid extraction (e.g., groundwater and hydrocarbon) (Figure 1 and Figure 3)
- fluid and gas injection (e.g., waste water and CO2 (Figure 1 and Figure 3))
- Enhanced Geothermal Systems (EGS).

Induced seismicity has been attributed to fluid injection or extraction within subsurface reservoirs and are the focus of this report. Some particular examples are: 1) geothermal energy extraction such as the Rotokawa Geothermal Field, New Zealand (Bannister and Sherburn, 2007) and The Geysers Geothermal Field, USA (Mossop, 2001); 2) waste water disposal at Perry Nuclear Power Plant, USA (Ahmad and Schmidt, 1988) and Rocky Mountain Arsenal, USA (Healy et al., 1968; Hsieh and Bredehoeft, 1981); and 3) secondary oil recovery, Cogdell Oil Field, USA (Davis and Pennington, 1989).

A large part of the understanding of induced seismicity has been developed though empirical case studies and analytical modelling where particularly active or energetic sequences have been analysed using standard earthquake catalogue parameters such as earthquake magnitude, location and time. Systematic case studies of seismicity induced by fluid injection across multiple sites appear to be difficult to achieve and studies of catalogue data have been largely limited to individual sites with variable quality data (e.g., Healy et al., 1968; Kovach, 1974; Raleigh et al., 1976; Fletcher et al., 1977; Segall, 1989; Horner et al., 1994; Rutledge et al., 1998; Baisch et al., 2006, 2009a; Charléty et al., 2007). To begin to understand the overall behavioural patterns on induced seismicity, reviews and analyses of published data have been compiled by a number of authors (e.g., Nicholson and Wesson, 1990, 1992; Grasso, 1992a; Van Eijs et al., 2006; Baisch et al., 2009c; Suckale, 2009; Nicol et al., 2011; Evans et al., 2012). Additionally, research has been undertaken to develop computational models that specifically target the induced seismicity process and aim to understand the underlying physics that is driving it (e.g., Rutqvist et al., 2010; Cappa and Rutqvist, 2011b) including recent models being developed specifically for CO_2 injection and storage (e.g., Murphy, et. al., 2011; Zhao et. al., 2011).

As with populations of natural earthquakes, induced seismicity most often takes the form of small magnitude earthquakes, that are too small to be felt and that begin almost immediately after the onset of injection. The sequence of earthquakes typically continues for the duration of injection with a change in their character following the cessation of injection. Following the injection period, the rate of earthquakes typically follows an exponential decay as is seen in tectonic aftershock sequences (e.g., Charléty et al., 2007; Shapiro et al., 2007; Ladner and Haring, 2009). In some cases, induced seismicity continued for years or tens of years after injection has ceased (e.g., Healy et al., 1968; Seeber et al., 2004).

The relationships between operational parameters, such as injection rate, and the occurrence and behaviour of induced events is not completely understood; however, the earthquakes appear to be strongly influenced by the rate and volume of fluid injection and a corresponding increase in pressure as shown in Figure 2 (e.g. Healy et al., 1968; Charlety et al., 2007; Shapiro et al., 2007; Ladner and Haring, 2009). The spatial distribution of induced earthquakes often follows generally understood patterns, even if the scale and details of the pattern cannot be predicted ahead of time. Injection induced events typically commence adjacent to the injection well and migrate outwards from the well with time and increasing volume of injected fluid (e.g., Seeber et al., 2004; Baisch et al., 2006; Shapiro and Dinske, 2009).

The largest earthquakes attributed in the published literature to subsurface human activities have been associated with extraction of large volumes of hydrocarbons or water. Whether this is due to the nature of extraction, or simply a function of the larger volumes that have been extracted when compared to injected volumes is not clear. There is evidence that extraction induced events may be more variably distributed in terms of their location and their timing than events induced from injection (e.g., Grasso, 1992a; Nicholson and Wesson, 1992). For example, extraction induced earthquakes can occur kilometres from the reservoir in both horizontal and vertical directions (e.g., Simpson and

Leith, 1985; McGarr, 1991; Glowacka and Nava, 1996) and may occur many years after the beginning of the extraction operation (e.g., McGarr, 1991; Grasso, 1992a; Nicholson and Wesson, 1992).

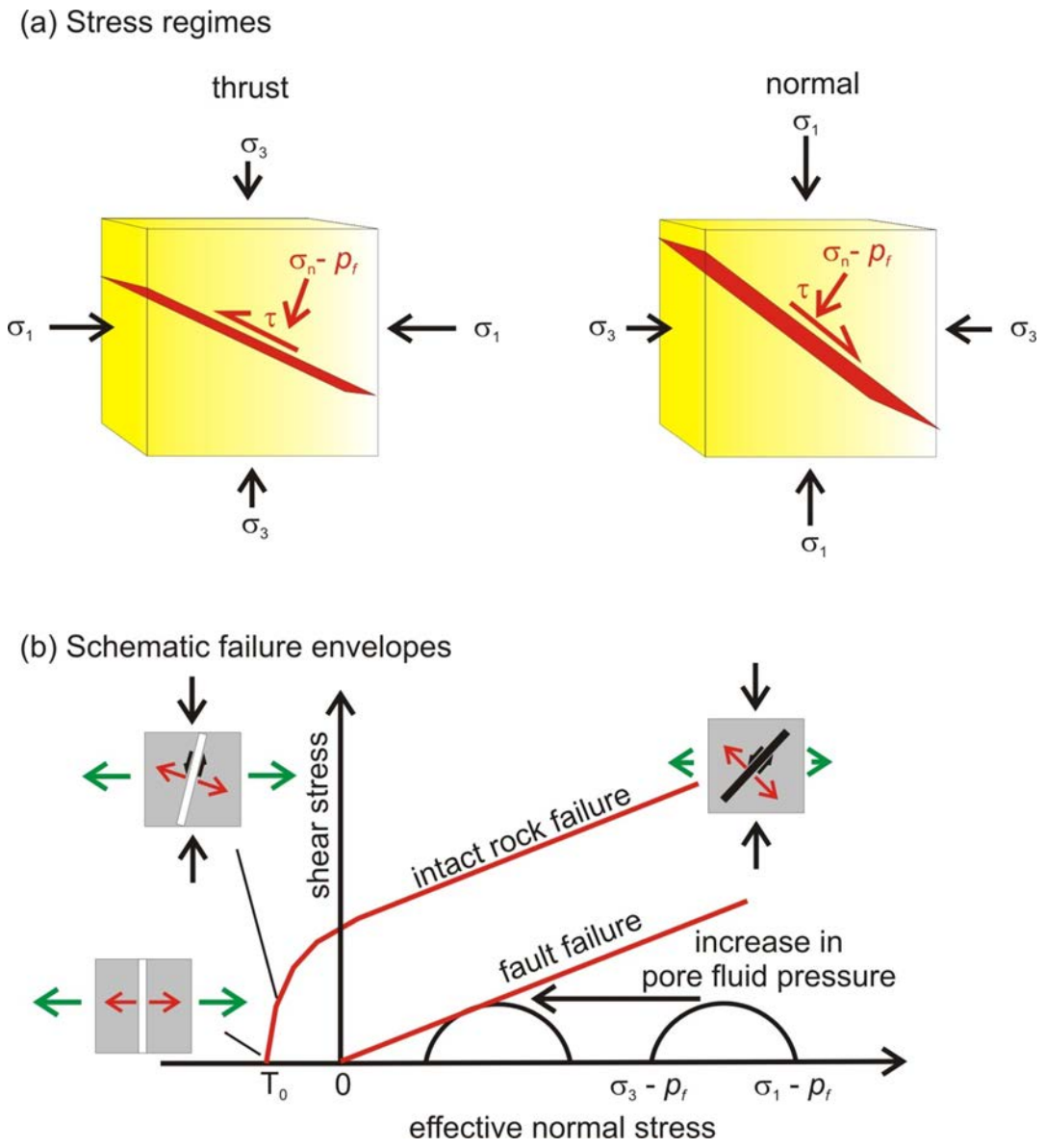

Figure 2: (a) Illustration of the stresses operating on the crust, and two of the common stress regimes under which failure can occur. σ_1, σ_3 are maximum and minimum principal stresses, respectively. Left-hand panel shows the stress conditions under which thrust faults activate, where maximum (compressive) principal stress is near-horizontal. Failure occurs once shear stress on the fault (τ) has been exceeded, according to frictional strength and the effective normal stress on the fault plane ($\sigma_1 - p_f$ where p_f is fluid pressure). Right-hand panel shows stress conditions for normal faulting, with steeper-dipping faults, and maximum principal stress near-vertical. (b) Schematic fault yield envelopes and related fractures for a compressive stress regime. The two red curves show yield for intact rock and for a pre-existing fault plane with zero cohesive strength. The Mohr circles span the difference between minimum and maximum effective normal stresses. As pore fluid pressure increases, the circles move to the left of the diagram and approach the failure envelopes (red lines). Shaded boxes show orientation of predicted failure planes and mechanism assuming initially intact rock. When effective normal stress is very low (e.g., because pore pressures exceed lithostatic pressure, and the tensile strength of the rock, T_0, is exceeded), tensile failure is predicted to occur (causing hydrofracturing, with open crack formation). With increasing normal stress, a hybrid crack opening/shearing failure mode develops, giving way to shear failure at higher effective normal stress. Figure modified after Twiss and Moores (1992).

In some cases, such as for EGS, induced seismicity will be an expected outcome from the fracturing created for increasing the permeability of the reservoir. In CCS any potential benefits are less certain but with appropriate monitoring instrumentation, micro-seismicity could be used to estimate the maximum radius of the pressure front and CO_2 plume. Additionally, one outcome of induced seismicity may be locally increased permeability; however, until the processes of induced seismicity and the likely impact of associated fractures on caprock integrity are better understood, it will not be prudent to use induced earthquakes for this purpose.

What produces it?

In our review of the literature, the dominant mechanisms that can result in induced earthquakes, within or close to subsurface reservoirs, include:

- changes in stress field (e.g., as caused by loading/unloading at the surface, most commonly due to induced changes in groundwater level)
- reservoir pore pressure changes (e.g., fluid injection or depletion; Figure 2)
- volume changes of the rock (e.g., thermally induced)
- applied forces or loads

All of these are mechanisms that can be caused by any of the previously mentioned anthropogenic activities (McGarr et al., 2002). Changes in pore pressure resulting from injection or extraction of fluids can cause sufficient stress changes that, with time, can lead to failure via an earthquake (Nicholson and Wesson, 1992). Often this is referred to as “advancing the clock” (e.g., Figure 4) which suggests that such triggered earthquakes would have happened at some point in the future, but have been brought forward in time by the stress changes and implies that very small stress changes can induce earthquakes. Figure 1 and Figure 3 provide schematic views of the seismicity induced by fluid injection and extraction at depth.

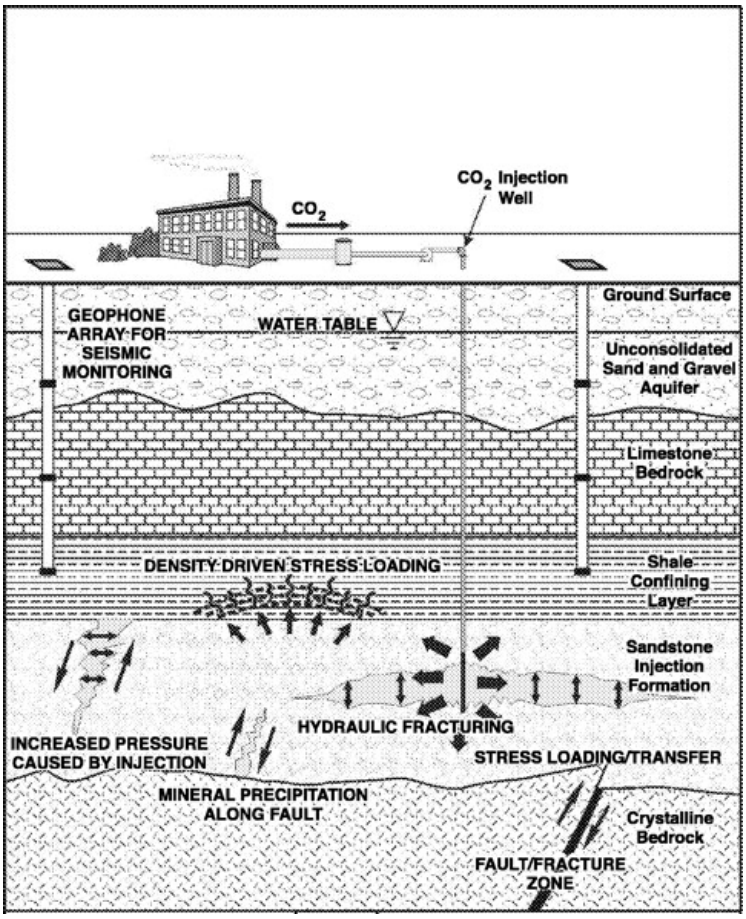

Figure 3: Processes inducing seismic activity at CO_2 injection sites (From Sminchak and Gupta, 2003).

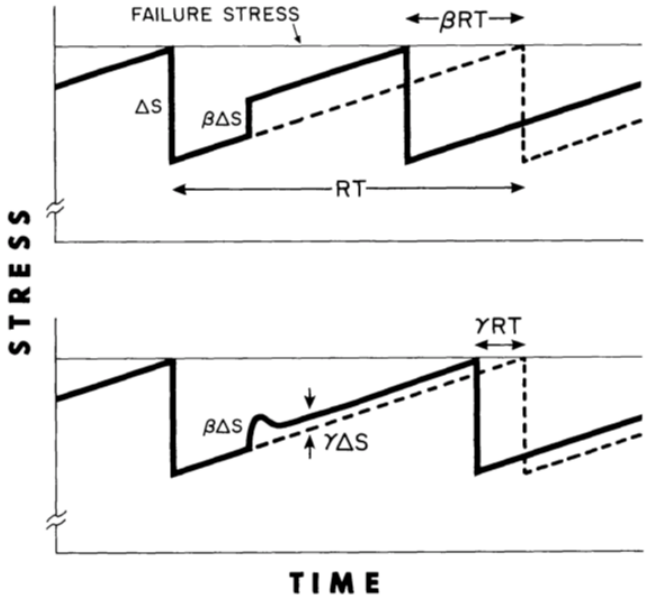

Figure 4: Schematic representation of stress on a fault zone, from Simpson (1986). Dashed line is normal earthquake cycle, showing cyclical buildup of shear stress on a fault plane with time, followed by release steps. The stress drop (ΔS) in an earthquake is recovered during an interseismic period with repeat time *RT*. Rupture occurs when the failure shear stress is reached. In an induced stress change $\beta\Delta S$ occurs, the repeat time is shortened to $\beta\Delta S$. In the lower diagram, the induced stress change includes a transient component.

Early understanding of the interaction between fluids and the stress field of a medium came from work by Terzaghi (1923) who showed the effect of pore pressure on stress, and how an increase in pore pressure can lead to an increase in the local stress. Hubbert and Rubey (1959) described the effect of fluid pressure on failure and proposed that an increase in pore pressure would reduce the "effective strength of rock" and therefore weaken a fault; thus facilitating failure of the fault (Figure 2b). In 1968, the first observation of the link between injection and seismicity was made when Healy et al. (1968) identified fluid pressure as a triggering mechanism for seismicity after the injection of waste water into a deep well in Denver, Colorado, USA.

Induced earthquakes can occur either on pre-existing faults and fractures or on newly formed faults and fractures created as a result of the human activities. The basic mechanisms for the seismicity may come from the following sequence of processes: 1) an increase in the pore pressure on faults in the rock volume surrounding the injection well from the fluid injection (McGarr et al., 2002), resulting in; 2) a reduction in the effective normal stress along pre-existing faults producing induced earthquakes when the fault slips due to the reduction in the frictional properties of the fault caused by the normal stress (Figure 2b; Hubbert and Rubey, 1959; Gupta, 1992; Nicholson and Wesson, 1992; Suckale, 2009; Zoback, 2007, 2012). Additionally, injection of fluids may increase the pressure in excess of the intergranular strength of the rock, and may cause local hydraulic fracturing of competent rock (Sminchak and Gupta, 2003), creating induced seismicity on newly formed faults and fractures; however, the mechanisms inducing seismicity cannot be this simple. For example, depletion of fluids can also induce seismicity (see below) yet this is not predicted purely on the basis of the change in effective normal stress as outlined in Figure 2b. Other mechanisms discussed in the relevant literature include: transfer of stress between faults (e.g., static Coulomb stress changes), pore-scale expansion or contraction of rocks, mineral precipitation along faults, chemically-induced fault weakening, and density-driven stress loading (Sminchak and Gupta, 2003; See section 7 of this report).

Induced earthquakes associated with oil and gas extraction result from a reduction in the pore pressure within the reservoir, which causes a contraction of the volume surrounding the extraction well(s) and can cause subsidence which can be observed at the ground surface (Nicholson and Wesson, 1992). Poroelastic mechanisms transfer the resulting stress changes from the reservoir to the surrounding rock volume by increasing the differential stress and bringing the rock closer to failure (e.g., Hillis, 2000). These stress perturbations may trigger slip or dilation on pre-existing structures and/or lead to the creation of new fractures both within and outside the reservoir. The resulting induced earthquakes typically have magnitudes that are not felt at the surface (Grasso, 1992a; McGarr et al., 2002), as is the case with almost all natural earthquakes. On a larger scale, hydrocarbon production can remove load from the upper crust reducing its average density and causing an isostatic imbalance. The ductile lower crust may deform in response to this imbalance, increasing the load on the seismogenic layer, which may then fail seismically (McGarr, 1991). Earthquakes associated with hydrocarbon operations may also arise due to water or CO_2 injection designed to enhance resource extraction, which is often referred to as Enhanced Oil Recovery (EOR) or Enhanced Gas Recovery (EGR), The impact of EOR/EGR can be inferred from the relative timing of these operations and the induced seismicity, however, in many cases the contributions of extraction and injection to the induced seismicity are uncertain.

Identifying whether or not any particular earthquake was triggered by anthropogenic means can be a difficult task. Often, overall clusters of earthquakes can be identified as being most likely to have been initiated by anthropogenic sources due to spatial and temporal clustering near to and during injection; however any individual earthquake within the cluster will have some probability of occurring without any anthropogenic influence. Determining the origin of seismicity becomes particularly challenging in active seismic areas where tectonically driven earthquakes occur at higher rates. Therefore,

determining whether or not earthquakes have been induced inevitably leads to debate within the community; this may particularly be the case for large events when issues of liability may be present.

Why is it important for CCS?

To reduce greenhouse gas emissions fully commercial CCS will require the injection of large volumes of CO_2 (e.g., > 20 Mt) into underground storage reservoirs (e.g. depleted hydrocarbon fields, saline aquifers) (Figure 3). Where the rate of injection exceeds the rate of CO_2 flow (and in-place brine) in the reservoir away from the injector well(s), pressures in the reservoir can be expected to rise as a result of the injection. Increases in the reservoir pressure have the potential to result in induced seismicity which could pose risks to the successful completion of some CCS projects, even if mitigation measures have been put in place (e.g., increase in the number of pressure-relief and injection wells or cessation of injection in problematic wells). Injecting large volumes of fluid into the ground poses three or more important risks to a CCS operation; induced earthquakes that may cause concern or be felt by the local community; induced earthquakes that are large enough to cause damage to infrastructure or injury, and; induced earthquakes that could rupture the CO_2 reservoir caprock, allowing the potential for CO_2 to escape from the primary container (e.g., Zoback and Gorelick, 2012). Figure 5 shows estimated containment risks at the Otway Storage Site, a CCS demonstration project in Australia and highlights the potential importance of induced seismicity is a risk profile (Rigg et. al., 2006).

Induced earthquakes felt by the local community may cause concern to the general public about the safety of the CCS injection operations, risking the continued operation of the CCS project. Also, if the potential for induced seismicity is not well understood, concerns about its occurrence also have the potential to negatively impact a CCS project prior to injection. The risk of inducing earthquakes large enough to cause damage to the infrastructure at the CCS site and any nearby properties is important to consider, particularly if the induced earthquakes occur at shallow depths (e.g., <3 km). Such damage could risk successful project completion by resulting in operational delays while infrastructure is restored, or resulting in the operation being shut down completely if damage to the site and nearby properties is significant enough that continued activity is considered unsafe. At the Basel Enhanced Geothermal System in Switzerland, hydraulic stimulation into granite at 5 km depth caused induced seismicity that exceeded acceptable levels in an urban area, resulting in suspension of the injection operation (Häring et al., 2008). A potential risk to a CCS operation is that of inducing an earthquake that could rupture the storage reservoir caprock, jeopardising the safe containment of CO_2. To date fluid or gas injection operations have not produced significant damage, loss of life or known rupture of the reservoir seal. To maintain this record and to assure stakeholders that the risks associated with induced seismicity are acceptably low, a risk management programme will be required at CO_2 storage sites.

At CCS sites, the availability of geomechanical data is generally limited. It is important to study the magnitude and frequency of induced earthquakes at sites of fluid injection with various geomechanical properties, and to investigate the mechanisms by which these induced earthquake occur (Figure 2 and Figure 3). By determining the likely location and timing of the largest induced earthquakes at an injection site, we can quantitatively assess the earthquake risk for a CCS operation.

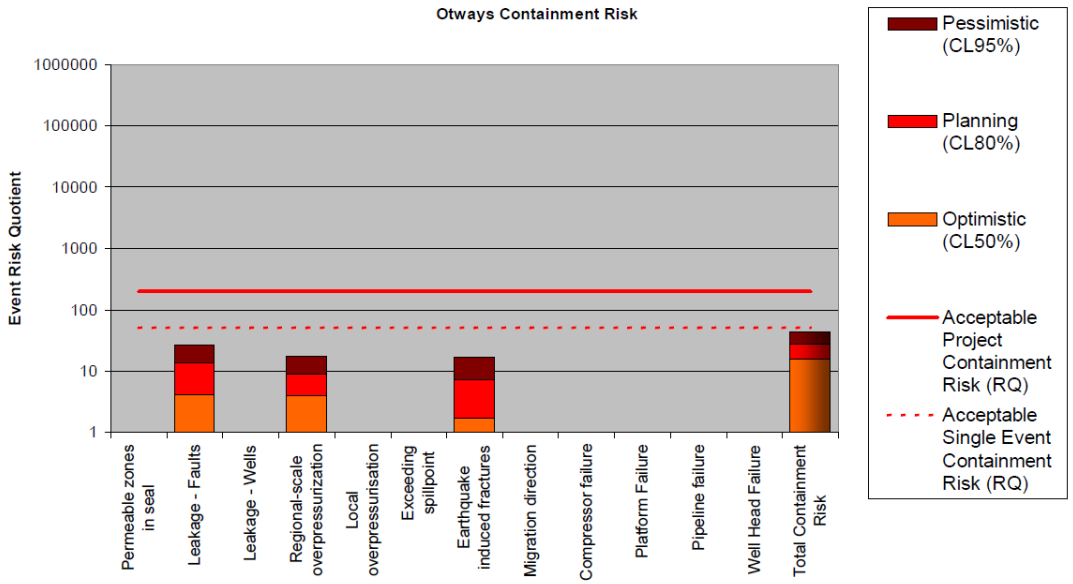

Figure 5: Containment Risks at the Otway CO_2 sequestration site, Australia (From Rigg et al., 2006).

Conventions in this report

The reporting of earthquake magnitudes and how they were determined is not consistently reported in the literature reviewed for this report. In some cases it was not clear what magnitude scale was used (e.g., local magnitude M_L or moment magnitude M_w;Hanks and Kanamori, 1979). For this reason we have chosen to ignore the specific magnitude scale used when reporting magnitudes in this report. In most cases a local magnitude estimate can be assumed for all but the largest events, which are often reported as M_w. Undoubtedly, some bias will be present on any analysis done using a combination of magnitudes scales and in some cases this bias may be significant. See Bethmann, et. al. (2011) for a discussion of the significant uncertainties introduced by differing magnitude estimates of induced earthquakes in the Basel, Switzerland EGS project.

Often the terms induced and triggered can take on different meanings. In this report we have taken the two terms to be synonymous. Because the two, no matter the definition, are ultimately driven by the same physical process, we have chosen to use them interchangeably to avoid any confusion. Similarly, the definitions of deterministic and probabilistic modelling can have different definitions based on the community that is using them, and we refrain from using them as much as possible in this report. However, when referring to probabilistic models, we are referring to a model that produces a probability of occurrence of an event, no matter how that probability is derived.

We have adopted the standard definition of micro-seismicity from the seismological community where it is used to indicate earthquakes less than or equal to Magnitude 2.0.

Report scope, methods and outline

Induced seismicity from the injection of CO_2 poses a potential risk for future CCS projects. A comprehensive understanding of the processes that produce induced seismicity at CO_2 storage sites may ultimately aid in reducing the risks. The objectives of this study are to consolidate and improve

our knowledge of induced seismicity associated with fluid injection and extraction using information from the literature and to provide some guidance to the CCS community on how this information may best be used and improved in the future. This includes the motivation for the CCS community to be able to provide accurate information about induced seismicity to the public. In this report we present a comprehensive review of published papers and conference presentations together with publically available reports on induced seismicity. To develop a database sufficiently large to draw robust conclusions about induced seismicity at CCS sites, publications on both fluid injection and extraction have been included in the review. Induced seismicity information from a range of fluid injection projects (e.g., waste storage, hydrocarbon extraction/secondary recovery, enhanced geothermal systems), has been collated and discussed. Support for this approach is provided from the literature which indicates that similar behaviour of induced earthquakes can be observed for injection and extraction (e.g., Nicol et al., 2011). In addition, differences between the physical properties of injected fluids (e.g., water and CO_2) do not appear to significantly modify the occurrence behavior of induced earthquakes (Verdon et al., 2010a). Care has been taken to identify potential source of bias in the data and the circumstances in which interpretations and conclusions drawn from these different types of operations might have implications for CO_2 injection and storage.

The observations and conclusions presented in this report are drawn mainly from published reports and papers in the scientific literature. We have kept to a minimum references to media articles, blogs, anecdotal reports and presentations not accompanied by explanation. Information from these sources was excluded to reduce subjectivity in the analyses presented and to provide defensible and transparent conclusions. This exclusion of material also means that anecdotal information from industry experts is not included if it has not been published. Therefore, it is likely that the data presented are biased towards those sites where seismicity has been observed (i.e. we tend not to write about what we don't see). This bias is discussed further in Section 6.

In compiling, presenting and discussing these induced seismicity data, priority has been given to the following topics:

- The mechanisms resulting in induced seismicity (including review of field observations, empirical data and numerical dynamic seismicity modelling);
- Discussion and conclusions from case studies of induced seismicity from petroleum extraction (Section 2), enhanced geothermal systems (Section 3), waste fluid disposal (Section 4) and CO_2 storage sites (Section 5);
- Relations between CCS and reservoir parameters (e.g., injected volumes, injection rates, reservoir pressures, rock properties) and induced seismicity rates, timing, locations and earthquake magnitudes (Section 6);
- Development and utilisation of statistical and physical models for induced seismicity (Section 7);
- The risks associated with induced seismicity (Section 8);
- Monitoring of induced seismicity at CO_2 storage sites (Section 8);
- Mitigation measures utilised by geothermal industry to address these risks (Section 8);
- Gaps in our present understanding that should be filled with further work/research (Section 9).

The report is a summary of the current state of knowledge for induced seismicity. Should the reader wish to delve more into the topic of induced seismicity the report has an extensive reference list which includes many of the main reports and publications on this topic. The discussion of gaps (Section 9) highlights areas of research which, if undertaken, will likely improve our understanding of induced seismicity and its risk management.

Petroleum Production and Stimulation

Introduction

Over the last 100 years it has become increasingly clear that hydrocarbon production and associated water flooding can induce ground deformation and seismicity (e.g., Pratt and Johnson, 1926; Grant, 1954; Kovach 1974; Yerkes and Castle, 1976; Raleigh et al., 1976; Rothe et al., 1983; Segall, 1989; Davis et al., 1989; Grasso, 1990, 1992a and b; Doser et al., 1991; Nicholson and Wesson, 1992; Segall et al., 1994; Zoback and Zinke, 2002; Van Eijis et al., 2006; Suckale, 2009). In the early 1920s geologists observed faulting, subsidence and earthquakes close to the Goose Creek oilfield, Texas, and proposed that deformation resulted from oil extraction (Pratt and Johnson 1926). Such observations for oil and gas fields are common, although by no means ubiquitous. At the Wilmington oilfield in Long Beach, California (USA), for example, six small-magnitude earthquakes (M2.4-3.3) occurred between 1947 and 1955 and surface subsidence reached 9 m in 1966 after 30 years of oil production (Richter, 1958; Kovach 1974; Segall, 1989). In addition to these cases of extreme deformation there are many hundreds of examples (perhaps several thousand in Texas alone; Davis and Pennington, 1989; Doser et al., 1992), where induced seismicity associated with hydrocarbon production has not been reported. The paucity of data for induced seismicity at hydrocarbon fields may reflect a combination of incomplete sampling, a propensity for these earthquakes to be small (i.e. not sufficiently large to be felt) and/or the resulting deformation being aseismic. It is presently unclear which of these explanations is of greatest importance. There are however a number of reasons why seismicity records will be incomplete, including; 1) induced earthquakes are too small to be felt by people or detected instrumentally. Detection issues are exacerbated by a general lack of local seismograph arrays designed to record induced earthquakes associated with hydrocarbon production. In these circumstances onshore events with magnitudes up to M3 may not be routinely recorded by all regional seismic networks (if these seismic networks are present at all), or felt by people. 2) In areas where active deformation and seismicity is being driven by plate tectonic processes distinguishing natural from induced earthquakes may be problematic. This could lead to masking of small to moderate magnitude induced earthquakes and/or to incorrect identification of larger natural events as being induced. 3) For many hydrocarbon fields there has been little operational or regulatory requirement to undertake research into induced seismicity. As a consequence, systematic data collection has not been undertaken for many sites, although it has become more common over the last decade. This lack of data is compounded by the fact that research conducted by petroleum companies is often not publically available. This lack of publically available data is highlighted by the fact that a recent literature review (Suckale, 2009) of hydrocarbon fields identified only 70 sites (probably a small fraction of the total number of fields worldwide) where induced seismicity had been unintentionally produced.

Like Suckale (2009) we do not review seismicity intentionally generated by hydraulic fracturing (often referred to as “fracking” or “fraccing’) of hydrocarbon reservoirs to increase permeability and stimulate fluid flow (such a review could constitute a report in its own right, e.g., see de Pater and Baisch, 2011). The maximum magnitude of these events is typically small (<M0), while the rates of seismic productivity can be high resulting in b-values in excess of 1 (see Section 6.5). On rare occasions events in excess of M2 appear to have been initiated by fluid injection during hydraulic fracturing; Events larger than M3 that occur in association with hydraulic fracturing (e.g., M4 2011 December 31 Youngstown, Ohio earthquake), often appear to have been induced by disposal of the wastewater used to generate the fractures and not by the stimulation itself (e.g., Zoback, 2012; Zoback and

Gorelick, 2012). For further information on hydraulic fracturing refer to the following publications (e.g., Fjaer, 2008; de Pater and Baisch, 2011; Healy, 2012).

In this section we provide a general overview of seismicity induced by hydrocarbon extraction and associated water flooding operations. We do not attempt to replicate the comprehensive review presented by Suckale (2009), but rather present six case studies together with general observations and conclusions. These case studies focus on fields where induced seismicity has been recorded and are biased towards sites where ground deformation or seismicity (e.g., productivity or maximum magnitudes) are relatively high. In a number of these cases water or CO_2 injection was initiated to maintain reservoir pressures, enhance hydrocarbon recovery and/or reduce near-surface deformation (including seismicity). Due in part to the availability of data the case studies are from North America and the former Soviet Union (see Figure 6 for locations).

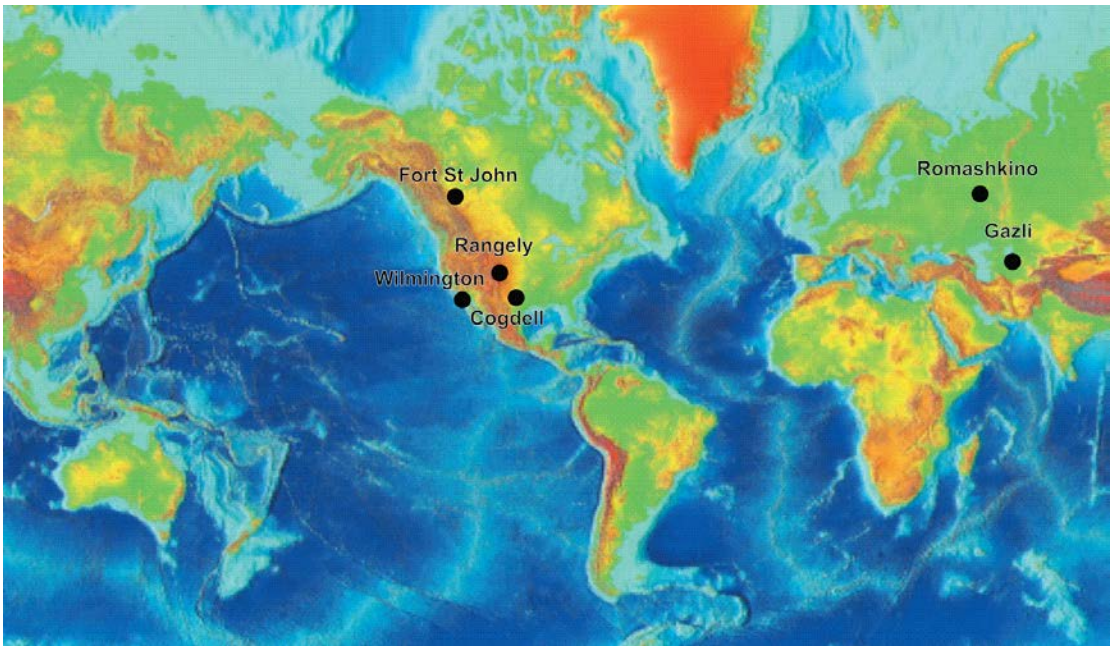

Figure 6: Location map of petroleum production sites reported in this study. Black circles are approximate locations of situations where petroleum production has resulted in induced seismicity.

Rangely, Colorado, USA

The Rangely oil and gas field is situated within the Rangely Anticline of Colorado, USA (Raleigh et al., 1976). Oil and gas production started in 1945 and continues today. The majority (~98%) of oil and gas production at Rangely is from the Pennsylvanian and Permian (245-315 million years ago) Weber sandstone which is about 350 m thick and produced from depths of 1700m (Raleigh et al., 1976; EMFI, 2005). The sandstone is fine-grained with average porosity of 12% and average permeability of 1 mD in the hydrocarbon producing zone. Due to the low permeabilities reservoir pressures and production rates declined rapidly following the start of hydrocarbon extraction. To arrest declining production rates and reservoir pressures and ensure access to large estimated reserves water flooding commenced in 1957 and continued until 1986 when the operators switched to CO_2 injection to maximise hydrocarbon recovery (EMFI, 2005). Water flooding resulted in induced seismicity. Small to moderate magnitude earthquakes (M1 to M3.4) were recorded in, or near to, the field between November 1962 and January 1970 by the Uinta Basin Observatory in the State of Utah (Gibbs et al., 1973). Following the discovery in 1966 that injection of waste fluid at high pressure triggered

earthquakes (Healy et al., 1968), the US Geological Survey designed an experiment to test the feasibility of controlled earthquake generation at Rangely. In 1967 a portable array of four seismographs was installed directly over the field. It began recording seismic events (40 small earthquakes < M 3 over an initial 10 day period) along a subsurface fault in two areas where water flooding had induced elevated pore-pressures. In 1969 an experiment was set up to test the relationships between injection rates, reservoir pressures and induced seismicity. To record seismicity a new seismic network consisting of 14 seismometers was installed over the field in 1969 (Raleigh et al., 1976). The project successfully initiated seismic activity by increasing the rates of water injection and subsequently halted recorded seismic activity by producing water from near the fault (Raleigh et al., 1976). In addition to showing that induced seismicity could be successfully managed the Rangely experiment demonstrated a positive correlation between variations in fluid pressure and amounts of seismicity, while also showing that induced seismicity productivity may increase in cases where water flooding for EOR and EGR (Enhanced Gas Recovery) elevates reservoir pressures. Insufficient data are available from most other sites to test these relations.

Gazli, Uzbekistan

The Gazli gas field is located on a large (38 km long and 12 km wide) asymmetric anticline in Uzbekistan. The gas field was discovered in 1956 and began production in 1962 at an average rate of 20 billion m^3/yr since 1966 (Dienes and Shabad, 1982). Three large magnitude earthquakes (M6.8, M7.3 and M7.2) occurred 10-20 km from Gazli with two events in 1976 and a third in 1984. The 1984 event caused more than 100 casualties, one death and extensive damage in the town of Gazli (Simpson and Leith, 1985). These events are the largest earthquakes widely inferred to have been induced by hydrocarbon production or fluid injection which warrants the inclusion of Gazli in these case studies.

Gazli field gas has been extracted from shallow (mostly < 1200m) stacked reservoirs within Cretaceous strata. Producing sandstone intervals, separated by clay beds, have average porosities of 20 to 32% and permeabilities from of all but one producing horizon of 675 to 1457 mD. Despite large amounts of water injection ($600x10^6$ m^3 between 1962 and 1976) reservoir pressures gradually decreased from 6.9 to 1.5 MPa between the 1960s and 1980s. The decline in pressures was associated with subsidence at the surface, with each ~0.1 MPa pressure decrease corresponding with 2 mm of subsidence in the central field area (Adushkin et al., 2000). Average subsidence rates increased from 10 mm/year between 1964 and 1968 to 19.2 mm/year from 1968 to 1974. The timing of the highest rates of subsidence approximately coincided with the greatest production rates from 1968-1971.

The Gazli gas field is located in an intra-plate region that exhibited relatively low levels of seismic activity prior to 1976 (Medvedev, 1968). On April 8th 1976, a magnitude M 6.8 earthquake ruptured the crust with an epicentre 20 km from the gas field boundary. This event was followed by a second earthquake of magnitude M 7.3 on May 17th 1976 and a third magnitude M 7.2 on March 20th 1984. Hypocenters for all three earthquakes were at 25 to 30 km depth and associated with many aftershocks. The three large magnitude earthquakes at Gazli are the largest recorded in Central Asia. The low levels of pre-1976 historical seismicity in the Gazli region, proximity of the large magnitude earthquakes to the Gazli gas field, the spatial coincidence of gradual subsidence associated with gas extraction and subsidence during the large magnitude earthquakes, and the modelled downward propagation of the 1984 rupture (Eyidogan et al., 1985) have been cited as evidence in support of the view that the Gazli earthquakes were triggered by exploitation of the gas field (Akramhodzhaev et al., 1984; Simpson and Leith, 1985; Adushkin et al., 2000). However, others suggest that the unloading

stresses induced by gas extraction were probably minimal (due in part to the extensive water injection) and that the earthquakes were tectonic in origin (Bossu and Grasso, 1996). If the Gazli earthquakes were triggered by gas extraction operations, they could have been induced by a decline of reservoir pressures, subsidence or variable production rates.

Romashkino, Russia

Romashkino, Russia, is the largest oilfield in the Volga-Ural basin. The Romashkino oil field has a maximum width of 70 km and comprises a succession of 10-30 m thick Devonian sandstones and carbonate rocks at depths of 1600-1800 m. The main reservoir interval contains interbedded sandstones and clays with the sandstones having permeabilities of 200 to 420 mD and porosities of 18.8 to 20.4%. Oil production commenced in 1948 and continues today with total production in excess of 15 billion barrels of oil (Adushkin et al., 2000). Water flooding was initiated in 1954 and by 1975 the total volume of fluid injected for EOR had reached 2.13×10^9 m^3 and exceeded the volume of extracted fluids. The water injection programme resulted in reservoir pressures rising from initial values of ~16-18 MPa to a maximum of ~20-25 MPa (Adushkin et al., 2000). With the rise in pressures associated with EOR small to moderate magnitude earthquakes ranging up to M4.0 were recorded by a local seismograph network throughout the 1980s and early 1990s.

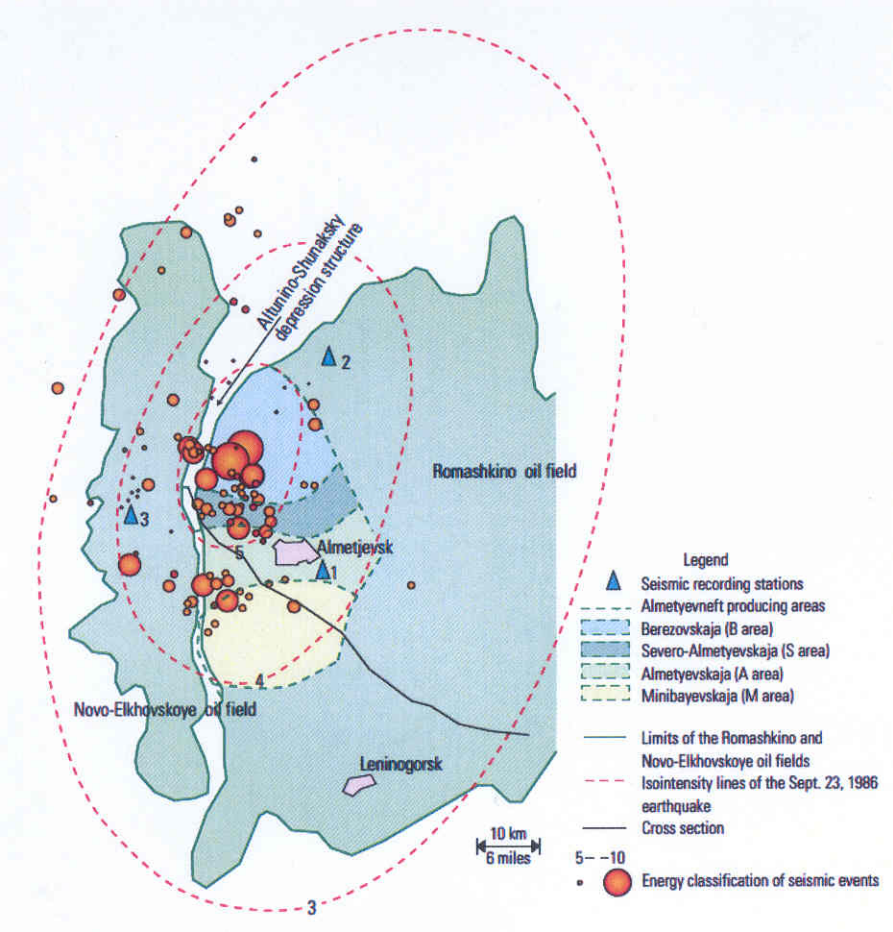

Figure 7: Seismicity in the region of the Romashkino oil field between 1986 and 1992. Event and seismograph locations are indicated by orange circles and green triangles, respectively. Map from Adushkin et al. (2000).

In 1982, after decades of production and water injection the residents of the township of Almetjevsk, near to the oilfield, began feeling earthquakes. In response to ongoing seismic activity a local seismic network was installed within the footprint of the Romashkino oilfield in 1985 (Figure 7). Between 1986 and 1992 the network recorded 391 local earthquakes with magnitudes of mainly M1.5 to M4.0. The largest earthquakes were a magnitude M3.8 on September 23rd 1986 and a magnitude M4.0 on October 28th 1991 (Adushkin et al., 2000). Despite the fact that we have no information on baseline seismicity in the region of the Romashkino oil field prior to the start of production, the clear temporal and spatial relationships between extraction/injection and seismicity strongly suggest that the two are related (Adushkin et al., 2000)(e.g., Figure 7). In particular, the seismic productivity was highest when the volume of water injected exceeded the volume of hydrocarbon extracted by the greatest amount (Figure 8). Conversely, the lowest rates of seismicity occurred when the volumes of fluid extraction exceeded water injection (Figure 8). These relationships support the view that seismic productivity was positively related to reservoir pressures. In addition, it has been noted that effectiveness of water injection for EOR decreased during periods of higher seismic activity (Adushkin et al., 2000). One possible explanation for this loss of effectiveness is that increased fault permeability arising from transient dilation during earthquakes may have channelized the flow of injected water in the reservoir, reducing the sweep of water flooding at these times (see Adushkin et al., 2000).

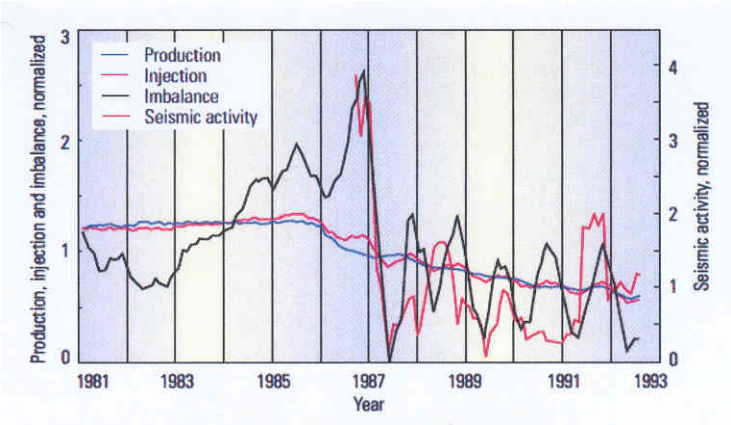

Figure 8: Comparison of the seismic productivity (red line) and the net extracted volume of oil (black line labelled imbalance in key) (i.e. the difference between the total volume of the extracted oil and the injected water), for the Romashkino oil field, Russia. Where the black (imbalance) line is above the blue production line injection exceeds extraction, where it is below extraction exceeds injection. Figure from Adushkin et al. (2000). Note that while there is a general correspondence of the imbalance and seismic activity lines their detailed geometries may differ.

Cogdell, Texas, USA

The Cogdell oil field is in the Midland basin of West Texas, USA (Figure 6). It is part of a chain of Palaeozoic limestone mounds which host seven major oilfields. The Canyon reefs limestone produces oil at a depth of 2.1 km. Although the producing interval comprises thin highly permeable fractured karst zones, average permeability (~6 mD) and porosity (~13%) in the field are low (Pennell and Ward, 2004). The field was first discovered in 1949 with production starting about 1950. EOR in the form of water injection was initiated in 1956 and augmented by CO_2 injection in 2001. The earliest verified earthquake in the field occurred in 1974 (Sanford et al., 1980), although the occurrence of earlier sub-resolution or unreported events cannot be ruled out. The largest earthquake occurred on June 16th 1978, with estimated M5.3 and caused minor damage, such as cracked windows, in the Snyder area (Davis et al., 1989).

A sequence of induced shallow earthquakes at the Cogdell oil field was recorded from about 1974 to 1982 (Harding et al., 1978; Harding, 1981; Davis and Pennington, 1989). Seismicity commenced at about the time of peak water injection and appears to have declined as the difference between the rates of water injection and production decreased. Subsequent to the onset of seismicity it is possible that water injection rates were reduced and water production increased as part of an induced seismicity management strategy, although documentation on the operation of the field is, to our knowledge, not publically available. Following the June 16th 1978 event the US Geological Survey located a further 20 events of ≤M3.9 from February 1979 to August 1981 using a local seismograph network at the Cogdell field (Harding, 1981). The earthquakes occurred in close spatial association with the field. The mean hypocentral depth of these events is 1.9 km, while the largest event had a depth of 3 km. These shallow depths together with the clustering of the epicentres near the field are consistent with suggestions that the seismicity was induced by high-pressure water flooding operations at the field (Harding et al., 1978). The rates and magnitudes of induced seismicity recorded in the Cogdell oil field are unusually high for Texas, where there are many producing oil fields using high-pressure water flooding techniques which have not produced recorded seismicity. Davis and Pennington (1989) suggest that geometries of injector wells around the periphery of the field, which contributed to formation of local high-pressure zones within the reservoir, may have been a factor contributing to the generation of relatively high levels of induced seismicity. In addition, it is also possible that for Texas oil and gas fields there is a positive relationship between the densities of pre-existing faults in basement and induced seismicity (e.g., Doser et al., 1992).

Wilmington, California, USA

Based on production figures, the Wilmington oil field is the largest in the Los Angeles basin, USA, having delivered over 2.5 billion barrels of oil from 1932 to 2001 (Clark and Phillips, 2003). Oil has been exploited from seven main sand intervals within Miocene and Pliocene turbidites at depths ranging from 600 to 3400 m, with the majority of extraction from the upper 1000 m of the depth range. Oil withdrawal from the reservoir intervals resulted in collapse of pore space and compaction, which produced significant bowl-shaped subsidence of the ground surface above the reservoir (Kovach, 1974). Between 1936 and 1966 onshore subsidence reached 9 m and was accompanied by horizontal displacements of up to 3.7 m (Figure 9). Subsidence caused damage to property, dropping some coastal areas below sea level, and triggered seismicity. Wilmington is presented because it provides an example where induced seismicity is thought to have been triggered by subsidence arising from extraction rather than by later injection of water.

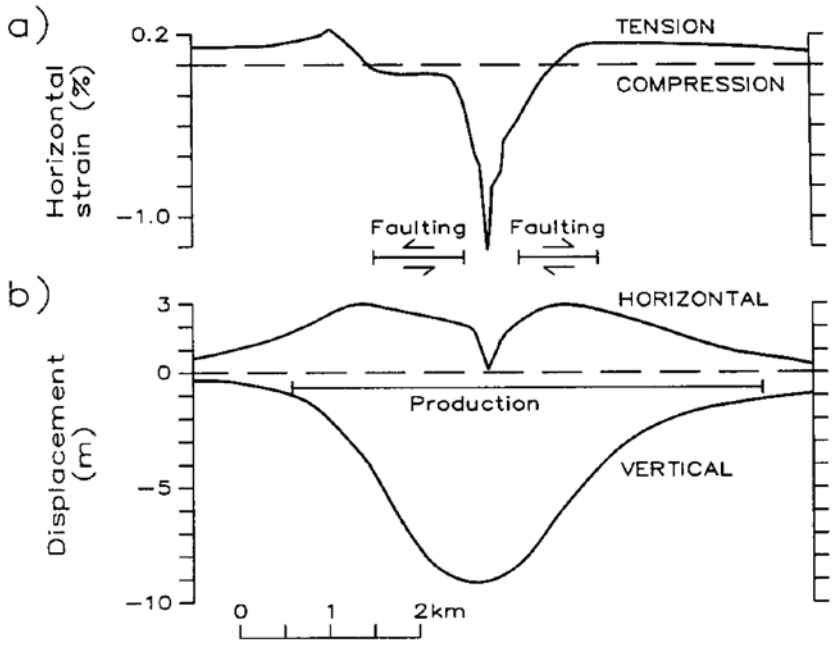

Figure 9: Surface horizontal strain change (a) and displacement (horizontal 1937-1962 and vertical 1928-1962) due to extraction at the Wilmington oil field, California. Locations of producing field and bedding-parallel faulting during earthquakes are also shown. Figure from Segall (1989) after Yerkes and Castle (1970).

Six shallow earthquakes were recorded within the Wilmington field in 1947, 1949, 1951, 1954, 1955, and 1961 (M2.4 to M3.3) by the Pasadena and Riverside seismographs in the Californian network (Richter, 1958; Kovach, 1974; Segall, 1989). All of these events occurred at shallow depths (~0.5 km) and produced both horizontal movement and subsidence at the ground surface (Figure 9). The earthquakes were generated by slip on bedding planes at depths of 470 to 520 m which offset tens to hundreds of wells over several square kilometres (for fault locations see Figure 9). In addition to disrupting drilling operations the earthquakes accelerated subsidence. The observed earthquakes are inferred to have relieved horizontal shear stresses produced by elliptical subsidence (Kovach, 1974). Fluid extraction causes the reservoir rock to contract which results in subsidence and high horizontal contractional strain gradients (Figure 9). These strain gradients are achieved via reverse and normal faults which primarily slip during induced earthquakes (Segall, 1989). Both the subsidence issues and the elevated rates of seismicity were successfully mitigated at Wilmington by water injection which commenced in 1956.

Fort St John, Canada

Seismicity was temporally and spatially related to oil production in the Eagle West and Eagle fields, in the Fort St John region of Canada (Horner et al., 1994). Oil production in these fields is from reservoir intervals at approximately 2 km depth within shallow marine inter-fingering sandstone and carbonate units of Permian age in the Belloy Basin. The Eagle (1972) and Eagle West (1976) oil fields were discovered in the 1970s and commenced production in the late 1970s. Reservoir pressures quickly went into decline and water flooding was initiated in 1980 (Eagle West) and 1985 (Eagle) to enhance oil recovery. Earthquakes large enough to be felt started in each field four and six years after the onset of water injection and have been inferred to be related to oil field operations (Horner et al., 1994). The earthquakes were reported to have produced minor damage (e.g., cracked plaster and fallen pictures), loud noises and to awaken people from their sleep.

Fort St John is an area of low seismicity with few earthquakes recorded instrumentally prior to 1984 (Horner et al., 1994). This is despite the fact that the regional network of seismograph stations in western Canada was capable of recording earthquakes of about M2.5 and greater. In November 1984 a sequence of seismic activity commenced comprising 25 events with magnitudes of 2.2 to 4.1 which were focused in three main time periods (November to December 1984, January to February 1992, December 1992 to January 1993). These events were followed by the largest recorded earthquake in the region, an M4.3 on May 22nd 1994 (Horner et al., 1994). Many of these events, including the M4.3 event, had epicentres within the footprint of the Eagle and Eagle West oil fields. Data from the regional seismograph network were supplemented by information from a temporary array of five stations deployed from January to March 1993. This array recorded a dozen events ranging in magnitude from <M1 to M3.5. Epicentres of the events recorded by the temporary array lie within the Eagle oilfield with focal depths of <5 km within a few kilometres of both production and injection wells (Horner et al., 1994).

There are temporal and spatial correlations between oil field operations and seismicity which, together with a number of additional observations, suggest that these earthquakes were induced. These observations include the fact that the seismic sequence at Fort St John occurred in a region of previously low level seismicity. On its own the low-seismicity argument cannot be used to categorically state that the earthquakes were induced. The location of earthquake epicentres over, or very near to, the Eagle oilfields provides additional supporting evidence. This inference is further supported by the propensity of events recorded by the temporary seismograph network to be located within a few kilometres of production and injection wells in the Eagle field. The timing of the events also supports the view that they were induced. Earthquakes within the Eagle and Eagle West field both commenced after water injection started and may have been triggered by rising injection pressures which reached 23-25 MPa. In the Eagle West field seismicity declined with decreasing production and injection pressure in the late 1980s. The available evidence supports suggestions that high-pressure fluid injection reactivated pre-existing faults, however, other mechanisms cannot be ruled out until better locations and focal mechanisms are available (Horner et al., 1994).

Summary

The case studies presented are a small sample of the 70 or so oil and gas fields globally where seismicity is believed to have been induced by extraction of hydrocarbons or by injection of fluids to maintain production rates as part of EOR or EGR operations. These case studies together with the available literature and recent reviews of the literature by Suckale (2009, 2010) provide the basis for the summary remarks below.

In the vast majority of hydrocarbon fields induced seismicity has not been recorded, not studied in detail or not presented in the publically available literature. The resulting lack of information creates limitations to what can be concluded about the causes, and associated risks of induced seismicity in hydrocarbon fields. It is clear however that induced earthquakes are generally small to moderate in magnitude (M≤4.5). In many cases, if present, induced seismicity must comprise events too small to be felt at the ground surface and recorded by regional seismograph networks (e.g. M≤3). It remains possible that earthquakes in excess of M 7.0 (e.g., M7.3 May 17th 1976 Gazli earthquake, Adushkin et al., 2000) were triggered by hydrocarbon operations but for many proposed large magnitude induced events (i.e. >M6) agreement has not been reached about their mechanical origins.

The available literature suggests that there is strong spatial and temporal links between induced seismicity and hydrocarbon operations (e.g., Kovach, 1974; Raleigh et al., 1976; Davis and

Pennington, 1989; Segall, 1989; Doser et al., 1991; Hornet et al., 1994; Van Eck et al., 2006). It is often the case that induced earthquakes occur within, or close to, the reservoir intervals. This is perhaps not surprising given that close spatial association between earthquake locations and reservoirs is one of the criteria used to infer that the earthquakes were induced. In a number of hydrocarbon fields the onset of seismicity has been linked to significant reductions or increases in reservoir pressures arising from production or water flooding during EOR/EGR operations (e.g., Raleigh et al., 1976; Harding, 1978; Davis and Pennington, 1989; Horner et al., 1994). The temporal relations between changes in reservoir conditions and in the induced seismicity are highly variable. In some cases these changes occur within days or months of each other (e.g., Raleigh et al., 1976), in others time lags of years are inferred (e.g., Kovach, 1974; Davis and Pennington, 1989; Hornet et al., 1994) and on occasions significant changes in reservoir conditions do not appear to affect the seismicity recorded (e.g., Davis and Pennington, 1989; Adushkin et al., 2000; Suckale, 2009).

Variable seismic response to changes in reservoir pressure suggests that other factors also influence the occurrence of induced seismicity. These factors could include changes in reservoir conditions (e.g., temperature and fluid chemistry), variations in the pre-extraction (and in some cases injection) stress state and differences in rock properties (e.g., rock strength and fault friction). Differences in the seismic productivity between hydrocarbon fields could, for example, be partly due to variations in the numbers and frictional properties of pre-existing faults or to pre-extraction reservoir overpressures (e.g., Doser et al., 1992; Zoback and Zinke, 2002; Van Eijs et al., 2006; Suckale 2009). Doser et al. (1992) noted that in Texas induced seismicity was common at intersections or bends in basement faults; such fault complexities are often characterised by high densities of small-scale faults (e.g., Gartrell et al., 2004). Some of these apparent differences in the relative timing of changes in reservoir conditions and seismic productivity may be better resolved by improved datasets of the reservoir seismicity and dynamics. Additional data may also improve understanding of the relative importance of reactivation of pre-existing faults and generation of new faults for seismicity induced by hydrocarbon operations.

Hydrothermal and Petrothermal Enhanced Geothermal Systems

Introduction

Injection or extraction of fluids from geothermal reservoirs has the potential to change reservoir pressures and temperatures sufficiently to perturb *in-situ* stress conditions and cause or trigger seismicity (Bromley and Mongillo, 2008; Cladouhos et al., 2010). Understanding of the mechanisms involved in geothermal induced seismicity has advanced to the stage that numerous models have been developed to simulate the process (e.g., Cacas, et. al., 1990, Baisch and Voros, 2010; McClure and Horne, 2010).

It is convenient to subdivide geothermal induced seismicity experiences into those associated with conventional projects involving low pressure fluid production and injection, and those associated with enhanced (EGS) projects where high pressure injection stimulation is usually a requirement.

Hundreds of geothermal fields are under production or development around the world, producing a total of about 11 GW_e (Gigawatt electrical) of installed power and 50 GW_{th} (Gigawatt thermal) of direct heating. Many fields have been producing for more than 25 years, and the majority have not reported any felt induced seismicity. In the few cases where significant induced seismicity has been reported, it has generally consisted of small magnitude earthquakes. The maximum magnitude induced event reported at a geothermal field was a M 4.6 at The Geysers, California, USA (Figure 10). While no significantly damaging events have been observed to date, the potential for such events in the future is a subject of research and highlights the need for thorough risk assessment.

Earthquakes have been induced by high pressure fluid injection experiments, as well as by injection or extraction of fluids during some routine geothermal operations. The high pressures are required to stimulate (artificially fracture) reservoirs for heat extraction (EGS, or Hot Dry Rock projects). The results of these experiments have been widely reported. There are no known cases in EGS settings of induced earthquakes causing severe damage (Majer et al., 2005; Baria et al., 2006). While felt events have been induced in several cases (e.g., Soultz-sous-Forêts, France and Cooper Basin, Australian), felt events in Basel, Switzerland are of particular importance. In the Basel case, several felt events were induced during and after a short-duration high-pressure injection experiment. The initial felt events exceeded a pre-determined threshold which led to the injection being stopped. Cracking of mortar in many buildings in Basel was reported and repaired under insurance. The cost of repairs, which exceeded $US8 million, and a subsequent review of risks (Baisch et. al., 2009c), led to the intended geothermal heat extraction project being suspended. By contrast, at The Geysers (California, USA), another well-known geothermal location for induced seismicity, many recorded local earthquakes are of sufficient magnitude to be felt, but this has been a regular and generally accepted part of routine geothermal operations for several decades. Induced seismicity at The Geysers has had negligible impact on infrastructure, although in 2009, a planned EGS demonstration project at The Geysers by AltRock Energy Inc. was suspended.

Induced seismicity is triggered by anthropogenic changes to the stress regime. Tectonic setting is an important variable to consider. High temperature geothermal reservoirs are typically located in active tectonic settings where high levels of natural seismicity are common; however, as observed in Basel and Cooper Basin, Australia, felt events can occur in areas of relatively low tectonic strain rate. Fluid

pressures also play a key role. If pore pressure is great enough to overcome the effective normal stress, then shear failure will occur. The process of seismicity triggering in these settings can be linked to a change in pore pressure and degree of 'roughness' of a fault. One suggested mechanism is that increasing pore pressure causes asperities (or locked points) on the 'rough' fracture surface to fail, thereby allowing movement on the naturally stressed fracture.

Other factors that may affect geothermal seismicity are: a) displacement stresses associated with volumetric contraction caused by fluid extraction; b) thermal stresses created by injection of cool fluids into hot rock; and c) chemical stresses associated with injection of brines or acid fluids, which can have a weakening effect on the rock.

Induced seismicity can be associated with hydraulic fracturing for geothermal reservoir expansion with the objective of increasing permeability. This has been observed during EGS experiments, and also sometimes observed during completion of conventional geothermal production wells when cooler water is injected for extended periods of time in order to enhance the near-wellbore permeability. Often there has been an observed increase of injectivity and/or productivity (through fracture controlled permeability increases), and an increase in reservoir volume. Induced seismicity in EGS is a necessary tool for creating and monitoring permeability.

The levels of induced seismicity (number of events and magnitudes) depend on a number of background factors, which include the local stress regime, fault orientation and locations, and friction, as well as controllable factors, such as injection pressure and temperature, volume injected, duration of injection, and injection ramping rates. However, the uncertainties involved, and variability between geological settings, make it difficult to establish reliable correlations between the level of seismicity and any of these factors that could be consistently applied to new settings (Evans, et. al., 2012).

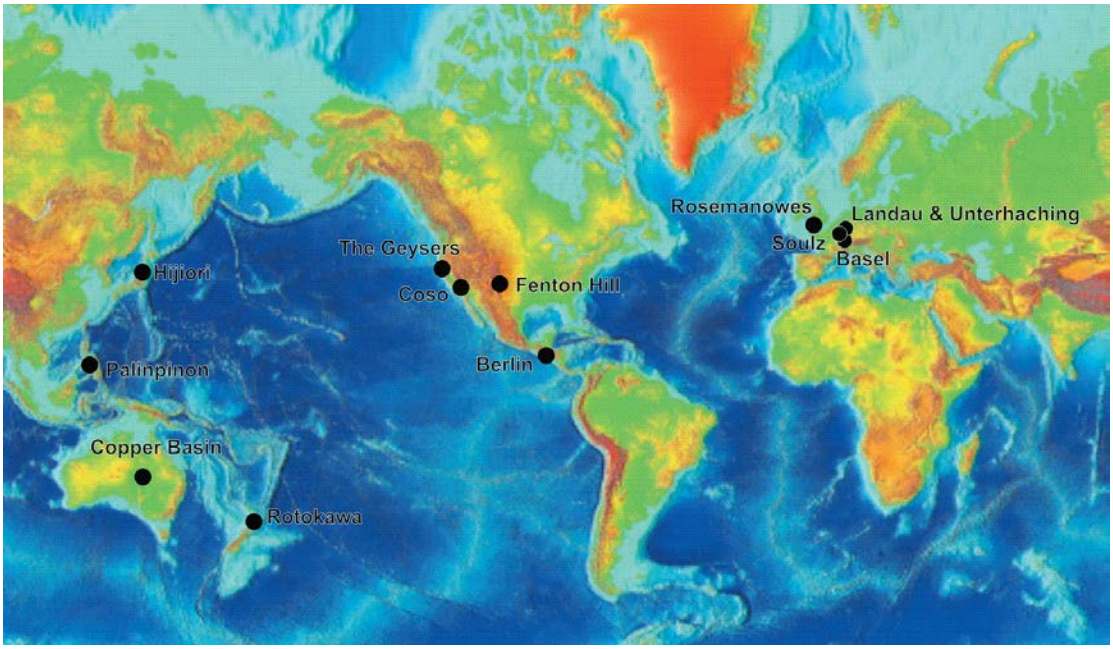

Figure 10: Location map of geothermal case studies reported in this study (see black filled circles and site names).

Conventional geothermal case studies

The Geysers Geothermal Field, California, USA

Induced seismicity at The Geysers, which is located in a tectonically active area and is classed as a steam-dominated geothermal system, has been well documented since 1975 (Figure 11). Approximately 1000 seismic events have been detected and located per year (M>1.5). Approximately 1 or 2 events per year have been of magnitude M>4.0 (maximum M4.6). One small community is close enough for ground motions from at least 10 events per week, on average, to be felt by residents (Majer et al., 2007). Although the area is close to the San Andreas fault, there are no mapped faults within The Geysers that are considered active in the last 10,000 years, and pre-development datasets suggest little seismicity occurred in the field for the 10 years prior to the start of commercial production.

Steam pressure in the reservoir has been in decline since production commenced. Seismicity was located throughout and above production zones, so a simple mechanism of hydraulic shear failure due to pore pressure increase is not favoured. Rates of seismicity are positively correlated with increasing injection rates of cool water, initially consisting of surplus steam condensates, but in 1997 and 2003 supplemented by treated waste water collected from nearby towns. This supplementary injection did not fully replace the mass extracted with lost to the atmosphere via cooling towers. Various triggering mechanisms are thought to be responsible for the induced seismicity. These include pore pressure changes, cooling contraction, and volumetric decline from net fluid loss and associated stress changes.

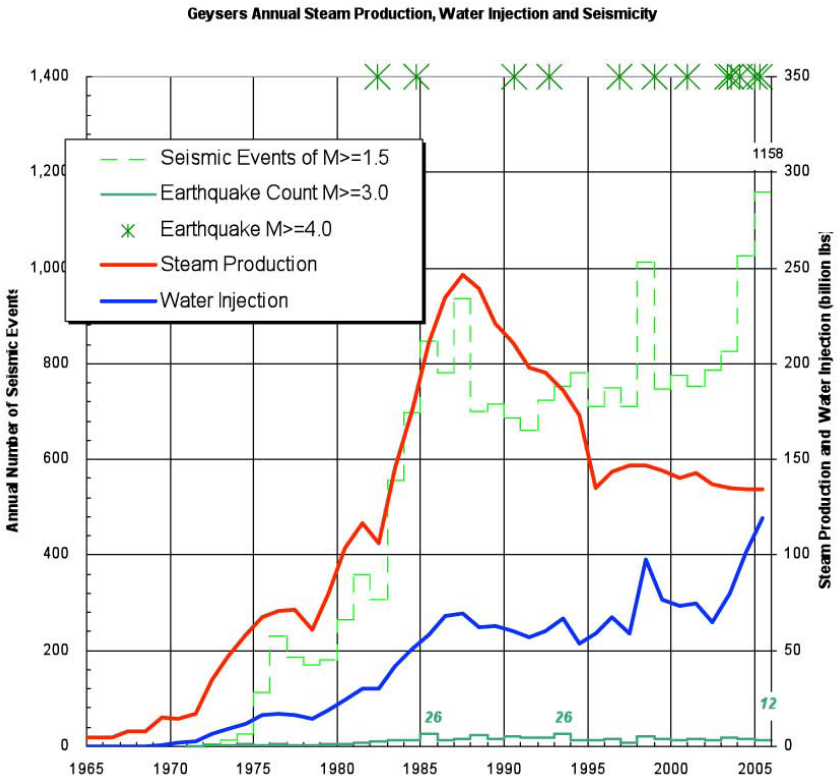

Figure 11: The Geysers annual steam production (red line) and water injection (blue line) 1965-2006 plotted with seismic productivity data (dashed green line events >M1.5, solid green line >M3.0 and stars >M4), and water injection (blue line). Figure from LBNL (2012).

Many studies at The Geysers have linked rates of induced seismicity to steam extraction and water injection (Majer and McEvilly, 1979; Allis, 1982; Eberhart-Phillips and Oppenheimer, 1984; Oppenheimer, 1986; Enedy et al., 1992; Stark, 2003; Foulger et al., 1997; Henderson et al., 1999; Kirkpatrick et al., 1999; Ross et al., 1999; Segall and Mossop, 1998, Smith et al., 2000; Majer and Peterson, 2005; Stark et al., 2005; Greensfelder et al., 2008). An approximate positive correlation between the annual injection volume in the field and induced seismicity rates (1000 events of M>1.5 for every 1.3 Mega-tonne of injection per year) was observed. However, this simple correlation has not always been in evidence throughout The Geysers; other factors clearly have an important role to play. A diverse set of mechanisms (Majer et al, 2007) are thought to operate independently, or in combination, to influence seismicity. Henderson et al. (1999) found that under constant injection conditions, small fluctuations in pore fluid pressure led to seismic activity, which locally inhibited further activity (dilatant hardening). Rapid injection overcame dilatant hardening, and triggered earthquakes through pore pressure diffusion. A statistical study by Segall and Mossop (1998) found that shallow seismicity was correlated to production rather than injection, with a lag time of ~500 days consistent with pressure diffusion rates between main fractures. They found that poro-elastic reservoir contraction increases shear stresses across fractures above the reservoir, leading to shear failure (and surface subsidence of up to 1 m over 20 years). The mechanism for deep seismicity was explained as a mixture of thermo-elastic stress due to evaporative cooling of boiling residual pore fluid, and thermal stresses associated with advective cooling from injected fluid.

In the past few years, a doughnut-shaped region of low seismic density surrounded by a region of higher seismic density has become visible in a high temperature zone that underlies the main reservoir and the area of highest volume injection (Beall et al., 2010; Boyle et al., 2011). It is thought that the observed local de-coupling between injection and induced seismicity may reflect accumulation of injectate as plumes within the reservoir.

In summary, because of a diverse set of mechanisms, and changing pressure, temperature and liquid/vapour phase states, it is difficult to draw consistent conclusions regarding the causes of induced seismicity at The Geysers.

Coso geothermal area, California, USA

The Coso geothermal field is located in an area characterised by a high occurrence of natural seismicity, and an underlying magmatic heat system. Geothermal energy recovery commenced in 1987. A direct correlation between the locations of micro-seismicity and the injection and circulation of geothermal fluid was observed by Feng and Lees (1998). They also observed a spatial, though not temporal, correlation with natural seismicity extending southeast of the field. Areas of high seismicity are interpreted to indicate pre-existing fracture zones and main flow paths. They also infer different stress patterns within the Coso geothermal field. Modelling by Fialko and Simons (2000) suggested that there is a transpressional (strike-slip movement and oblique compression) regime on the periphery of the field, whereas the geothermal area is characterised by a transtensional (strike-slip movement and oblique extension) regime. The stress regime observations are consistent with the conclusion from Feng and Lees (1998) based on focal mechanisms, and the explanation that different stress patterns are associated with fault-bounded geological blocks.

Ghassemi et al (2007) showed that thermal stresses play an important part in explaining induced seismicity at Coso. In particular, an observed delay between injection and seismicity might be explained by this mechanism.

Berlin (El Salvador)

Berlín geothermal field, located in a tectonically active area, was explored from 1968, commenced energy extraction in 1992 and was expanded in 1999. Long-term seismic monitoring began soon after the start of fluid extraction and injection. As Berlín is located adjacent to Tecapa volcano, in a region that was seismically active prior to geothermal operations commencing, it is difficult to differentiate between natural and induced or triggered seismic events. However, data from the local Berlin network suggests that some micro-seismicity is spatially correlated to areas of pressure and temperature change, in both production and injection areas (Rivas et al., 2005).

No clear correlation in timing was found between the monthly seismicity data and the mass injected or extracted, although there is a spatial correlation with the geothermal anomaly. Seismicity in the reservoir increased after the occurrence of two large nearby tectonic earthquakes (M_w=7.6 and M_w=6.6) in early 2001.

In 2003, a trial rock fracture stimulation operation was carried out using pressurized injection in a 'tight' injection well at 1-2 km depth to improve permeability in a hot part of the resource (Bommer et al., 2006). A calibrated real-time 'traffic-light' control system was put in place to reduce or stop injection operations if the levels of vibration (peak ground velocity) from injection-induced seismicity exceeded acceptable levels (normal background = 'green', significant felt events = 'orange', and damaging events = 'red'); additional detail is explained in Section 8: Risk Assessment and Management. The stability of local rural housing and shallow ground conditions were taken into account when setting acceptable thresholds. What eventuated were low levels of induced seismicity around the injection well induced by three episodes of pumping, over a total of 54 days. The 'traffic light' thresholds were not exceeded, and the project was not adversely affected. Two weeks after injection shut-in, a relatively large event was recorded (M4.4), and felt, although no damage was reported. This event was located about 3 km south of the injection well (in the production sector), and was associated with a swarm of nearby smaller events, so it was concluded that it was unlikely to have been directly related to the pressurized injection activities (Bommer et al., 2006).

In summary, the geothermal field is characterized by high levels of micro-seismic activity, and some events have been found to result from high-pressure rock fracture stimulation, but fractures within the reservoir apparently have a poor capacity to accumulate large amounts of stress, therefore strain energy is released frequently through swarms of low-magnitude events. These can be triggered by stress changes associated with external sources such as large regional earthquakes as well as by reservoir changes (Rivas et al., 2005).

Palinpinon (Philippines)

During the first few years (1983-86) of production and injection at Palinpinon, a Philippine geothermal project in a tectonically active area, a significant increase in the level of micro-seismicity (0<M<2.5) was observed (Bromley et al., 1987). Some high-frequency events were felt within the project area due to their shallow depth (1-4 km) and proximity. There was a correlation in space and time between swarms of micro-seismic events (up to 100 events/day) and changes in injection and production rates. Event hypocentres were distributed on fractures throughout the pressure-affected parts of the reservoir, and were not concentrated on major permeable fault planes. After 1986, the level of locally induced seismicity declined to pre-operation background levels, despite steadily increasing mass flows and lateral pressure gradients as development doubled in capacity.

0n 13 July 2007, a M5 earthquake occurred at shallow depth within the borefield. This was apparently triggered by a 70 km deep earthquake beneath the same area a minute earlier. These events were

judged by the Philippine authorities to be of natural tectonic origin, rather than induced by geothermal activities. The M5 event briefly tripped some of the generating turbines because of vibration sensor control, but caused no damage to the geothermal field infrastructure or nearby domestic dwellings.

Rotokawa (New Zealand)

Rotokawa geothermal system is located in the tectonically active Taupo Volcanic Zone of New Zealand. Swarms of micro-earthquakes typically occur throughout this zone above the temperature-controlled brittle-ductile boundary at about 8-12 km depth. Production and full injection at Rotokawa commenced in 1997 (for a 35 MWe binary plant). No abnormal seismicity was detected by the regional seismic network (http://www.geonet.org.nz) during the first 10 years of operation (at an average fluid flow rate of 5.5 MT/yr). At this time the bulk of the injection was into a central, shallow, two-phase aquifer (~400m depth). In preparation for a change to deeper, peripheral injection, and larger mass flows, two micro-earthquake surveys were conducted in 2005 and 2006 using portable instruments to investigate injection induced seismicity (Bannister et al., 2008). Although no direct temporal relationship between injection flow history and seismicity was found (for that time period), there was a spatial correlation between the earthquakes and an inferred northeast trending fault zone between the injection and production wells. Fluid pressure transients, or stress changes associated with injection-induced cooling, are thought to have indirectly triggered seismicity on this deeper fault structure. Since July 2008, micro-seismic monitoring using a local network has been operating continuously. To avoid short-circuiting of reinjected fluids along northeast trending faults (and fractures), deep reinjection locations were changed in October 2008 to the south-eastern side of the production zone, and there was an accompanying change in the locations of the micro-seismic events (with magnitudes of up to M2.8). This marked a change in pressure gradients and fluid flow paths within the reservoir. The subsequent events have been primarily concentrated on a different northeast fault zone located approximately midway between the injection and production zones and perpendicular to the injection-production fluid flow-path. In February 2010, production and injection mass flows increased four-fold to 22 MT/yr, pressure drawdown rate increased and the rate of induced seismicity (M>2) in the central part of the field was observed to double. Events are clustered in time and space, similar to natural swarms of micro-earthquakes (Bannister et al., 2008).

Other Geothermal Fields (Iceland, Italy, Kenya)

Low magnitude induced seismicity has also been noted in other geothermal fields. For example, seismicity has occurred during injection at some Icelandic geothermal fields, at Krafla (Tang et al., 2008), and at Hellisheidi in the Hengill Volcanic area (Jousset et al., 2011). Hellisheidi is located close to a CCS drilling project (CarbFix). Geothermal seismicity was also associated with low-pressure, cold-water injection to stimulate permeability through changes to thermal stresses (Axelsson et al., 2006). Newspapers (Iceland Review Online, 2011) reported that many felt induced earthquakes, up to a maximum M3.8, have been triggered by drilling/injection activities at Hellisheidi during September-October, 2011. However, no injection induced events were detected at Svartsengi (Brandsdóttir et al., 2002) or at Laugaland geothermal projects (Axelsson et al., 2000).

In Italy, induced seismicity (maximum M3.2), has been recorded at Larderello-Travale steam-dominated geothermal field (Batini et al., 1985) in association with cooled condensate reinjection, Monte Amiata in association with long-term injection, and in three other geothermal areas (Latera, Torre Alfina and Cesano) in response to pressurized injection testing (Evans et al., 2012). High levels of natural seismicity (swarms of small events), however, make identification of induced events difficult. In Olkaria Geothermal Field, Rift Valley, Kenya, induced seismicity (maximum M 1.5) was correlated to discharges from a production well in 1997 (Simiyu, 1999).

EGS case studies

EGS, Hot Dry Rock (HDR), or Hot Fractured Rock (HFR) reservoirs utilise high pressure hydraulic stimulation to fracture the rock. Fluid transmissivity is increased by creating new inter-connected fractures or by shearing of existing fractures through fluid injection. Some EGS fracturing experiments have involved small volumes of high pressure injection to induce rock failure, while others have involved larger volumes of fluid at lower pressure, and longer-term circulation tests. The purpose of the latter is to trigger seismicity through changes in pore pressure on existing fractures where fluid is flowing away from the injection point, or through transient thermal stresses associated with injection of fluids that are cooler than the in-situ rock. Recent experiments are generally very well instrumented, including borehole monitoring, and because induced seismicity is a necessary outcome of EGS, they typically record thousands of events.

During reservoir stimulation, the hydraulically-induced rock failure stops when the pressure induced by fluid injection drops below the rock fracture gradient. However, shear failure is generally observed at much lower fluid pressures due to triggering slip or dilation on pre-stressed fractures. A suggested mechanism is that of increased pore pressure or thermal contraction releasing asperities on fracture surfaces, thereby facilitating shear failure and stress release. Such triggered events are indistinguishable from natural earthquakes. Their moment magnitudes are dependent on the magnitude of local stress release and fracture surface area, rather than fluid pressure increase (Shapiro, 2008).

Once a connected fracture network has been created, EGS utilisation involves long-term fluid circulation between injection and production wells in order to extract useful heat from the system. The maintenance of reservoir transmissivity (long-term) may be enhanced by triggered seismicity that continues throughout the lifetime of the project in response to gradual stress changes associated with slow cooling, and diffusion of pressure transients into low permeability reservoir rock.

Fenton Hill, New Mexico, USA

Fenton Hill was one of the world's first experimental EGS reservoirs. Experiments were commenced by Los Alamos National Laboratory in the 1970s. The area is located on the western flank of the Valles Caldera where temperature gradients are elevated, but permeability is insufficient for a natural geothermal convecting system (Duchane and Brown, 2002). Four hydraulic stimulation experiments were conducted at 2.8 and 4.2 km depth using high pressure injection. The majority of the observed seismicity at Fenton Hill was due to shear failure (House et al., 1985; Cash et al., 1983; Fehler et al., 1987; Kaieda, 1984). Occasional long period micro-earthquakes also occurred (Bame and Fehler, 1986; Majer and Doe, 1986) and these were thought to represent tensile fracturing. The longer period events were observed during the early stages of injection, when fluid pressures were high enough to cause tensile failure. Many shear events also occurred in close proximity to tensile failure events, and at locations where fluid pressure is assumed to be sufficient to trigger shear failure, but insufficient for tensile failure. Seismicity was found to occur along pre-existing fracture surfaces that are favourably oriented with respect to the *in situ* stress-field, to allow shear slip (Cundall and Marti, 1978; Murphy and Fehler, 1986). The fracture plane with the highest ratio of shear to normal stress acting along it is the one most likely to slip, and micro-earthquakes occur when the normal stress on such a fracture plane is reduced by an increase in pore fluid pressure (Fehler et al., 1987; Fehler, 1989).

Rosemanowes, Cornwall, U.K.

Between 1978 and 1991, the Rosemanowes project (Cornwall) tested the viability of geothermal energy production by using high pressure fracture stimulation followed by fluid circulation at 2.2 km depth (Parker, 1999). The host rock is a thick batholith of granite, with anomalous heat generation and a temperature gradient of ~35°C km^{-1}. During the first phase of injection, microseismicity was observed at low flow rates and wellhead pressures of 3.1 MPa (Parker, 1999). During the second phase, Batchelor (1983) noted that injection of 30 kT at flow rates up to 100 L s-1 (pressure up to 14 MPa) caused a downward migration of microseismic event locations. This was ascribed to the pore pressure increase required for shear failure decreasing with depth. The intensity of the seismic activity was less than in the first phase. It was confirmed that the locations of the microseismic activity defined volumes of rock with increased fracture apertures and permeability (Parker, 1999).

The maximum observed event (M2) in July 1987 was felt but was less than the expected maximum magnitude of 3.5, which had been determined using a seismic hazard assessment based on a predicted maximum affected fault length of 100 m. The felt event did not generate any recorded complaints from residents of the Rosemanowes area, possibly as a result of early “rock and roll” public education initiatives (Baria, 2007).

Hijiori, Japan

The Hijiori site has been used for EGS experiments at 1.8 and 2.2 km depth, since 1985. A granodiorite basement is overlain by ~1.5 km of alluvium and volcanic deposits. Sasaki (1998) found that the induced seismicity is strongly dependent on the injection rate and wellhead pressure. However, he observed a lag between changes in the injection flow rate and the corresponding increases and decreases in seismicity, inferring that the seismicity is correlated to diffusion of pressure transients along fractures. The induced seismicity is caused by shear failure as the result of slip on joints, which, as noted previously, occurs when the effective stress is reduced by increasing the pore fluid pressure. The spatial orientation of the induced seismicity was coplanar with the caldera ring fault structure, suggesting a pre-existing fracture zone was being re-opened and developed. Sasaki and Kaieda (2002) confirmed that injection caused shear failure and opening of existing fractures in the direction of the maximum principal horizontal stress.

Soultz-sous-Forêts, France

EGS research at Soultz-sous-Forêts, near Strasbourg on the northern side of the Rhine Graben, commenced in 1987. The site is located in a zone of low to moderate natural earthquake activity. The development consists of four deep drill-holes, intersecting granite below 1.4 km depth. Hydraulic stimulation and circulation took place at 3-3.5 km depth during the first stage (1992-97), and at 4.5-5 km depth during the second stage (1998-2009). Maximum bottom hole temperatures reached about 200°C. Since 2010, circulation testing and operation of a pilot 1.5 MW_e ORC binary power plant has been supported by flows of ~35 l/s (~1.1 Mt/yr) from two production wells, and injection into the other deep well (Genter et al., 2010).

Induced seismicity was observed during reservoir stimulation at high pressure and flow rate (Dorbath et al, 2009) (Figure 12). The largest events were M1.9 during the initial stimulation and M2.9 during deeper stimulation. Although no structural damage was caused, public complaints led to restrictions on subsequent stimulation options. A possible consequence is that some wells do not have good hydraulic connection with other wells. Better public education about the project at an earlier stage might have been beneficial (Baria, 2007).

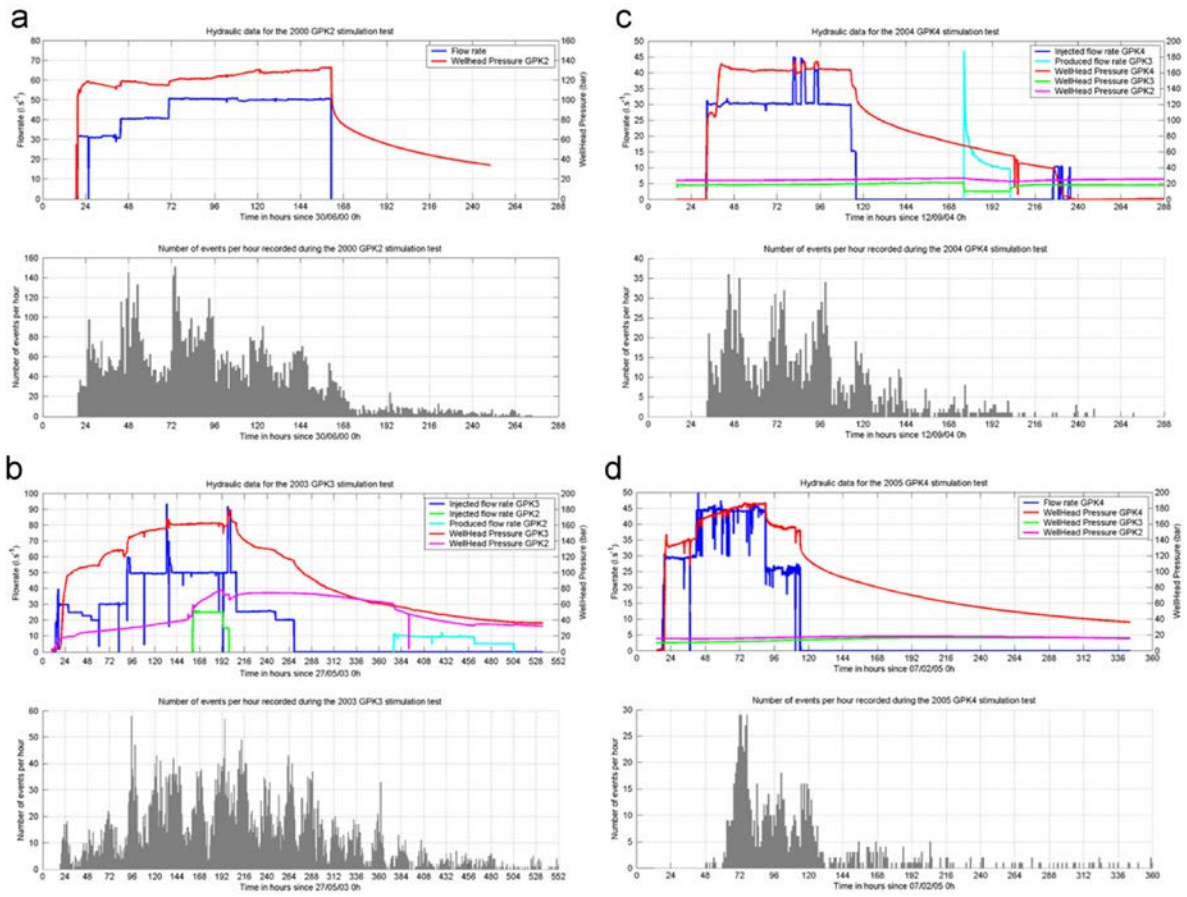

Figure 12: Number of seismic events (grey histograms) generated by injection stimulation of well GPK2 in 2000 (a), GPK3 in 2003 (b), and GPK4 in 2004 (c) and 2005 (d). Top graphs for each experiment show flow rate (dark blue and green lines), wellhead pressure (red and pink lines) and produced flow rate (light blue line).

Induced seismicity at Soultz commenced in September 1993 when injection tests of well GPK1 stimulated fracturing at differential pressures of up to 7.5 MPa. 12,000 micro-seismic events with moment magnitudes ranging from -2 to 1 were recorded starting 17 hours after the commencement of injection (Jones and Evans, 2001). This produced a sub-vertical zone of micro-seismicity, ~1 km^3 in volume. Some micro-seismic events were generated by seismic slip on sub-vertical, hydrothermally-altered, cataclastic shear zones, containing numerous limited-scale fractures with evidence of past movement from slickensides. These fractures are optimally oriented for strike-slip shear failure in the prevailing stress field. A downward progression of the induced seismicity was observed. Permeability was initially relatively low, but during the early stages of injection, induced seismicity created permeable fractures, and a self-propped high-permeability flow path developed, opening up vertical pathways, and facilitating downward propagation of fluids and further micro-seismicity. Evans et al. (2005) concluded that the micro-seismicity represents fluid penetration along existing structures, and enhanced permeability. No seismicity was detected during a 4 month circulation test of the 3.5 km deep system in 1997.

Stimulation of the second well GPK2 in 2000 generated 14,000 events. These were located using a downhole seismometer array. Stimulation continued for 6 days at a maximum flow rate of 50 L/s, wellhead pressures of 14 MPa, and a total injection of 25 kT. The largest event recorded was M2.5. The seismicity predominantly occurred during the first 4 days of injection (Charléty et al., 2007). After injection shut-in, the proportion of events with >M2 increased. An increase in event magnitude with

stimulation duration was noted. It was attributed by Baisch et al. (2010) to a geometrical effect, where stress criticality is approached over a larger reservoir volume, and therefore larger fracture area.

Stimulation of GPK3 in 2003 generated 8,345 locatable events, using the downhole array. Stimulation lasted 10.6 days at 50 L/s (with pulses up to 90 L/s) and wellhead pressures of 16 MPa (up to 19 MPa pulses) and total injection of 37 kT. The largest three events (up to M=2.9) occurred several days after the stimulation ended. As with Berlin, and Basel (see Section 7.1.2; Bachmann, et. al., 2011) the largest event occurred after injected was stopped and illustrates the limitations of a 'traffic light' protocol when applied to injection activities for risk management.

Stimulation of well GPK4 in 2004 and 2005 (32,288 events) involved 30 L/s at 17 MPa for 3.5 days in 2004 (9 kT), and 30 to 45 L/s at 14-18 MPa for 4 days in 2005 (12.5 kT). The largest recorded event was M2.7 after the first day of stimulation. After each shut-in, the numbers of induced events decayed exponentially with time (Charléty et al., 2007). As with natural seismicity, the induced seismicity during the injection tended to occur in temporal clusters (swarms).

Fluid circulation tests undertaken between wells in 2005, 2008, 2009 and 2010 resulted in several hundred locatable small magnitude events (Cuenot et al., 2011). Some of these reached magnitudes of 2 to 2.3. All tests were found to stimulate the same zones of the reservoir. Each test used different parameters (e.g. number of wells involved, artesian or pump-assisted circulation, and duration), illustrating that induced seismicity can occur under a broad range of operational conditions.

Cooper Basin, Australia

The Cooper Basin EGS project is located in a remote, sparsely populated area of central Australia. High heat generating granite basement (7-10 W m^{-3}, ~10 km thick, Chopra and Wyborn, 2003), below ca. 3.6km depth, and at ca. 250°C, is overlain by low-conductivity sediments. The stress regime is over-thrust. The minimum stress direction is vertical. Most induced fracture planes are therefore horizontal, although some are vertical. The developer (Geodynamics) has drilled 5 wells to depths of up to 4.6 km (temperatures of up to 264°C) and successfully fracture-stimulated and flow-tested some of them (up to 25 L/s at 210°C). Three sectors approximately 10km apart have been drilled to date (Habanero, Jolokia, and Savina). Casing failures and mud damage have delayed progress, but demonstration of economic heat extraction using a 1 MWe pilot plant is anticipated by the end of 2012. If successful this is planned to be followed by production of 40 MW_e and eventually 250 MW_e in modules, hence justifying the cost of grid connection to this remote location.

In December 2003, the initial pumped stimulation of well Habanero1 caused large numbers of micro-seismic events, 27,000 of which were located using a downhole array. The maximum magnitude was 3.7, but no damage was reported, and the remote location meant that there was little community concern. The induced-seismicity hazard at the project was assessed to be at an acceptable level (Morelli and Malavozos, 2008). Testing of the fracture zone revealed a high artesian pressure of ~34 MPa above hydrostatic (Baisch et al., 2006, 2009a). Earthquake hypocentres occur in a sub-horizontal layer with a lateral extent of 2 × 1.5 km, and a thickness of ~200 m. The induced seismicity displayed a high degree of spatio-temporal ordering: seismic activity migrated away from the injection well with time. Previously activated regions became seismically quiet, suggesting stress relaxation processes.

Further stimulation by injection of 25 kT in 2005 generated another 16,000 events, with magnitudes up to 2.9 (Baisch et al., 2009a). The immediate vicinity of the well remained seismically quiet as the result of the Kaiser effect (stress relaxation), (Kaiser, 1950). Seismicity was not detected until a day after the start of injection, and started at the outer boundary of the previously activated zone, following the

same sub-horizontal structure. The induced seismicity is primarily controlled by the fluid overpressure relative to the local stress state.

No direct relationship between the magnitude of the events and the hydraulic injection records was observed (Asanuma et al., 2005). Some larger events occurred after shut-in, suggesting that the initial stress state of the individual fractures, rather than the pore pressure amplitude, is the critical parameter. The larger events possibly break a hydraulic barrier, allowing extension of the seismic event 'cloud' into previously seismically quiet zones. Asanuma et al. (2005) hypothesize that the micro-seismic events are generated by slip or failure of asperities along existing fractures.

Basel, Switzerland

Deep drilling (to 5 km) and reservoir stimulation (pumping) was conducted in 2006 for a trial, deep heat extraction, EGS project within the city of Basel, Switzerland, located near the southern end of the tectonically active Rhine Graben. Several felt events occurred as a result of the high pressure pumping; the sequence of events is described below. As a consequence, and following a pre-determined "traffic-light" protocol, pumping was initially reduced and then stopped shortly after. Well head pressures were subsequently reduced by bleeding off. After a detailed seismic risk study, the project was eventually suspended (Baisch et. al., 2009c; Giardini, 2009).

The Basel area is subject to natural seismicity as evident from the historical and instrumental records. Additionally, two major fracture zones were identified in the borehole (Häring et al., 2008), but it is not clear if these are active, and a normal fault south of Basel is thought to be responsible for a large earthquake (M6.5-M6.7) in 1356, in which most of the town was destroyed (Meghraoui et al., 2009).

During stimulation of the well, a steady increase in seismicity rate and magnitude was observed with increasing flow rate and wellhead pressure (Deichmann and Giardini, 2009). A total of 10,500 events were recorded. On 8th of December 2006, a M2.6 event occurred after injection of 11.5 kT at maximum rates of 50 L/s and wellhead pressures up to 30 MPa (Häring et al., 2008). As these events exceeded the safety threshold for continued stimulation, it led to a reduction in flowrate to 30 L/s for 5 hours then shut-in. Two additional events of M2.7 and 3.4 were recorded in the subsequent 24 hours within the same source rock volume. After 5 hours of shut-in venting was initiated to reduce pressure. When the well head valve was opened, a third of the injected water flowed back (Häring et al., 2008). This resulted in decreased rates of seismicity. However, sporadic microseismic activity near the edge of the seismic cloud, with <M3.2, was still being detected in the stimulated rock volume (~500m from the casing shoe) 1-2 months after shut in, and minor seismic activity continued for some years afterwards (Deichmann and Giardini, 2009); the ongoing activity is behaving as a natural aftershock sequence and is expected to decay to background levels for the next 10 to 25 years (Bachmann, et. al., 2011). The on-going seismicity after shut down and pressure leak-off suggests longer-term static stress changes, perhaps in response to slow pressure diffusion or temperature changes.

The distribution of seismicity formed a lens-shaped, NNW trending, near-vertical cloud, about 1.2 km in diameter, and at 4-5 km depth. The focal mechanisms imply strike-slip or normal failure in mostly WNW oriented vertical fault planes (Deichmann and Ernst, 2009). This implies that the stimulated rock volume is composed of a complex network of individual fault segments oriented obliquely to the general trend of the microseismic cloud (Evans et al., 2010). During injection, seismicity migrated away from the borehole, implying a pressure diffusion process. Mukuhira et al (2008) noted that hypocenters of some of the deep large events during the stimulation were located within the zone that had previously been seismically active. They inferred that increases in pore pressure were not, therefore, the direct trigger and did not directly control the magnitude of seismic events. Instead, water

injection changes the physical conditions, including friction coefficient and stress state on the fracture plane, triggering failure. Additionally, the larger events showed a distance dependence of stress-drop (Goertz-Allman et. al., 2011; see Section 6.8). In conclusion, there are still uncertainties regarding the factors that controlled the magnitude of the seismic events at Basel.

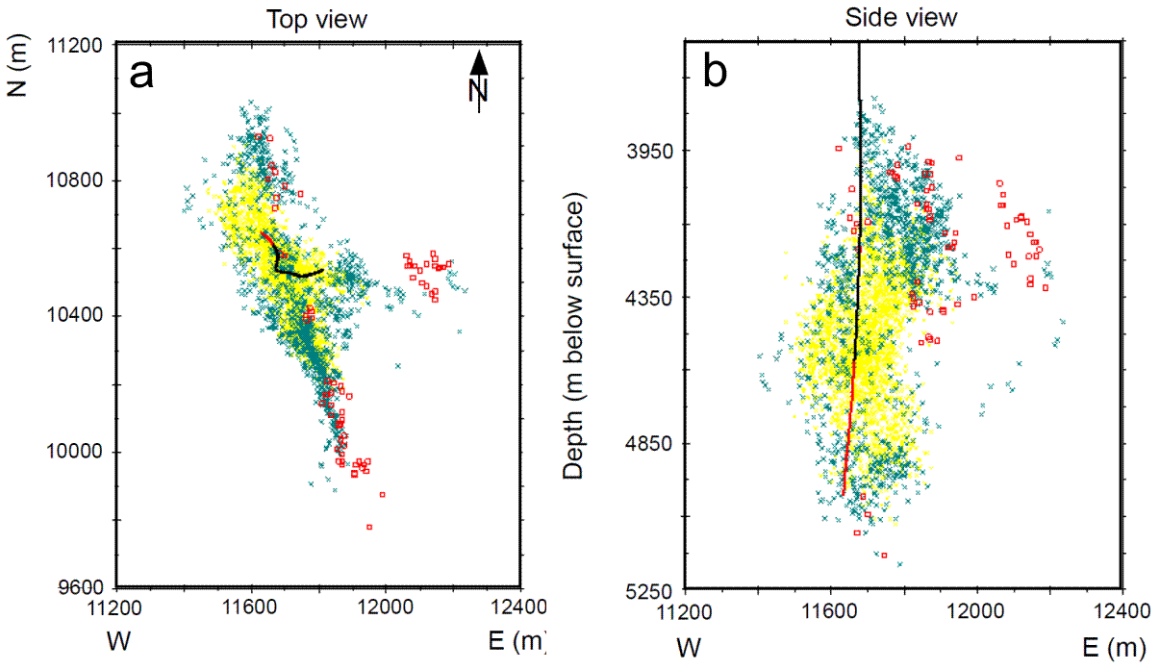

Figure 13: Absolute locations of seismic events from the Basel experiment shown in map (top) and cross sectional (middle and bottom) views. The timing of events is indicated by symbol colours: yellow crosses show events during the active injection phase from 2-8 December 2006, green crosses events from the early post-stimulation phase from 8 December 2006 - 2 May 2007, and red cubes events during the later post-stimulation phase from 3 May 2007 - 30 April 2009. The black and red line in cross sections shows the well location with black being cased and red open. Diagram modified from Figure 3 of Ladner and Häring (2009).

The consequences of relatively low magnitude induced seismicity at Basel have been unfortunate. A 2009 risk assessment (Baisch et. al., 2009c) for future EGS at Basel developed a rigorous and structured risk assessment including numerical modeling with a detailed geological model to estimate the potential for future induced seismic activity due to continued operation at the site. They concluded that, in terms of risk from induced seismicity, the Basel site was unfavourable. Additionally, they recommended that similar detailed risk assessments should be undertaken for future EGS sites in Switzerland.

Landau and Unterhaching, Germany

A combined heat and power plant at Landau, in the Rhine Graben near Soultz, started production of hot water for district heating and power generation in late 2007, using a well doublet and an organic Rankine cycle (ORC) binary plant (Baumgärtner et al., 2010, Schellschmidt et al., 2010). Injection occurs into lower units of a sedimentary sequence and granitic basement. The two wells were drilled to about 3.3 km depth; one was naturally permeable (intersected a fault) and the other was stimulated using high pressure injection (190 L/s at 13.5 MPa). There were no felt seismic events from the stimulation. The 3.8 MWe plant produces ~1.5 MWe net power and 5.1 MWt heat using re-circulated ~150°C fluid, at flow rates of ~65 l/s (~2 MT/yr). Injection pressures declined from 6 MPa to 3 MPa between February and September 2008, and rose back up from 4 MPa to 5.5 MPa between February and September 2009. Six micro-earthquakes ranging in magnitude from 1.6 to 1.9 were located by a

regional seismic network in the Landau area between February 2008 and May 2009, although their depths were poorly constrained.

After 2 years of operation, the project came under review in September 2009 as the result of local seismicity (Baisch et al., 2010). Two earthquakes (M2.4 and 2.7) were felt by the local population in August 2009, although no significant damage occurred. The latter, along with several other smaller events, occurred on 15th August, shortly after plant operation was halted for maintenance. It was located 1.5 - 2 km north of the plant at 2.3 - 3.3 km depth, so there was initially some uncertainty as to whether it was induced or natural. Plant operation was resumed in November 2009 with the maximum injection pressure lowered to 4.5 MPa in order to limit the potential for induced seismicity.

At Unterhaching, near Munich, a doublet of production-injection wells at 3.3 to 3.6 km depth, 4 km apart, intersect different faults within a sedimentary carbonate formation. The wells have high injectivity and are well connected. Since October 2007, operation for district heating has involved fluid circulation at 120 l/s, and an excess injection pressure of 2.5 MPa. From February to July 2008, several earthquakes (M2.1-2.4) were detected (2 felt) in this formerly aseismic region within several kilometres of the project (Kraft et al, 2009). In July 2008 a local network was established to improve the location accuracy.

In February 2009, electricity production commenced, with no change in circulation parameters. A series of 7 earthquakes (M0.7 to 2.1) were detected by the local network shortly afterwards, but none were felt. Analysis indicates that all hypocentres are located at a depth of 3.6 ± 1.5 km and 0.5 ± 0.3 km west of the injection interval at the fault intersection (Kraft et al., 2009).

Summary

Some of the specific conclusions from the study of induced seismicity at EGS sites are as follows.

- In the relatively small number of operating EGS projects (ca. 15), there have been no known cases where any large induced seismic events have caused major damage or injury; whether the avoidance of large events is due to the small number of operating EGS projects and larger, low probability events can yet occur is still to be determined. However, minor damage claims associated with some felt events have been lodged and settled.

- The termination of geothermal activities at Basel indicates the importance of understanding induced seismicity and suggests that its risks go beyond infrastructural damage and have implications for an entire industry (Giardini, 2009).

- Public perception of seismic risk is important and should be addressed at the start of a project. Expectations and fears should be taken seriously. All stakeholders, including the public should be actively engaged in a transparent and open-ended dialogue. This should include education about the effects of fracturing a reservoir and be ongoing during the project.

- When considering sites for development, especially urban locations, it is prudent to consult geological and seismological information to gauge suitability in relation to background natural seismicity, the state of stress, the existence of surface geology with potential for amplifying ground shaking, and the capability of existing buildings and services to withstand seismic shaking.

- As is done with seismic hazard for tectonic earthquakes, it is important to also define the criteria used for assessing the magnitude of induced seismicity in terms of ground acceleration and

frequency content, rather than just earthquake magnitude. Typically, the smaller magnitude events, that are most likely to be induced, generate ground shaking frequencies that are too high to cause significant structural damage, but may cause non-structural damage. Although larger events (M3-4) can generate lower frequency shaking that can potentially damage certain structures; therefore a case-by-case assessment of shaking hazard is prudent.

- Some investigations indicate that the smaller the strain energy placed in the formation, the smaller the probability of generating larger seismic events. Pumping at lower pressures over longer periods, or more slowly building up pumping pressures, then slowly reducing pressures as the stimulation period ends, may be advantageous. However, more research is needed to test this idea.

- A “Traffic-Light” approach has been suggested (Bommer et al., 2006; see Section 8), whereby communities are assured that high-pressure pumping activities will be amended or suspended if certain levels of large-magnitude induced seismicity are exceeded. The level of acceptability depends on local ground conditions, proximity of buildings, and susceptibility of infrastructure to vibration damage. This approach is reactive, however, and does not prevent larger triggered events that are significantly delayed by slow diffusion of pressures or stresses, a process that has been seen in practice and demonstrated by modelling (Baisch and Voros, 2010). An advanced traffic light system has been proposed by Bachmann et. al., (2011) and is discussed in Section 7.1.2.

- Further development of alternative hazard assessment techniques (e.g. extreme event based assessments) and a Probabalistic Seismic Hazard Assessment (PSHA) framework will be given high priority within the geothermal community; such a PSHA assessment has already been performed for the CO2CRC Otway Project (Stirling et. al, 2011).

Waste Fluid Disposal

Introduction

Injection of waste into deep non-communicative aquifers is used to dispose of hazardous fluids, oilfield brine and as part of solution mining. The first well documented instance of induced seismicity, related to a waste injection well is at Rocky Mountain Arsenal near Denver, Colorado, USA, in the mid-1960s. Since this time numerous examples of earthquakes associated with deep well injection have been documented (e.g., Nicholson and Wesson, 1990; Cox, 1991; Seeber et al., 2004).

Well documented occurrences of seismicity related to waste fluid injection are rare relative to the total number of active injection wells. This is because waste disposal wells typically inject at low pressures into large porous aquifers with high permeability. Due to these factors, and to the typically poor seismic instrumentation, there are few directly attributable events to waste fluid injection. The case studies that are covered in this section are plotted on Figure 14. As with the Petroleum section (Section 2) we have not discussed examples of wastewater disposal associated with hydraulic fracturing nor do we present detailed accounts of highly publicized 2011 earthquakes in the central USA which may have been induced by wastewater disposal (Zoback, 2012; Zoback and Gorelick, 2012). Little detail is published about these independent events and the associated injection projects, which can be summarized as follows: 1) near Guy, Arkansas in February, a sequence of earthquakes occurred with the largest being a M4.7; 2) during August in southern Colorado near Trinidad/Raton, a swarm of earthquakes up to M5.3 appear to have been triggered by wastewater injection from coalbed methane production; and 3) in late December, near Youngstown, Ohio, a sequence of more than 1,200 events up to M4.0 appear to have been induced by wastewater injection.

As with any potentially induced seismicity, there can be a significant challenge providing enough evidence to be confident that any one earthquake was induced. The southern Colorado sequence, for example, occurred in the same region as a swarm of earthquakes ($M \leq 4.6$) in 2001 with a history of earthquakes prior to injection (Meremonte et al, 2002). In an investigation of the 2001 swarm, which was located in an area with 10 gravity fed fluid disposal wells, Meremonte et al. (2002), concluded that while they could not rule out the possibility that the earthquakes were induced, there was not strong evidence that the earthquakes had been triggered.

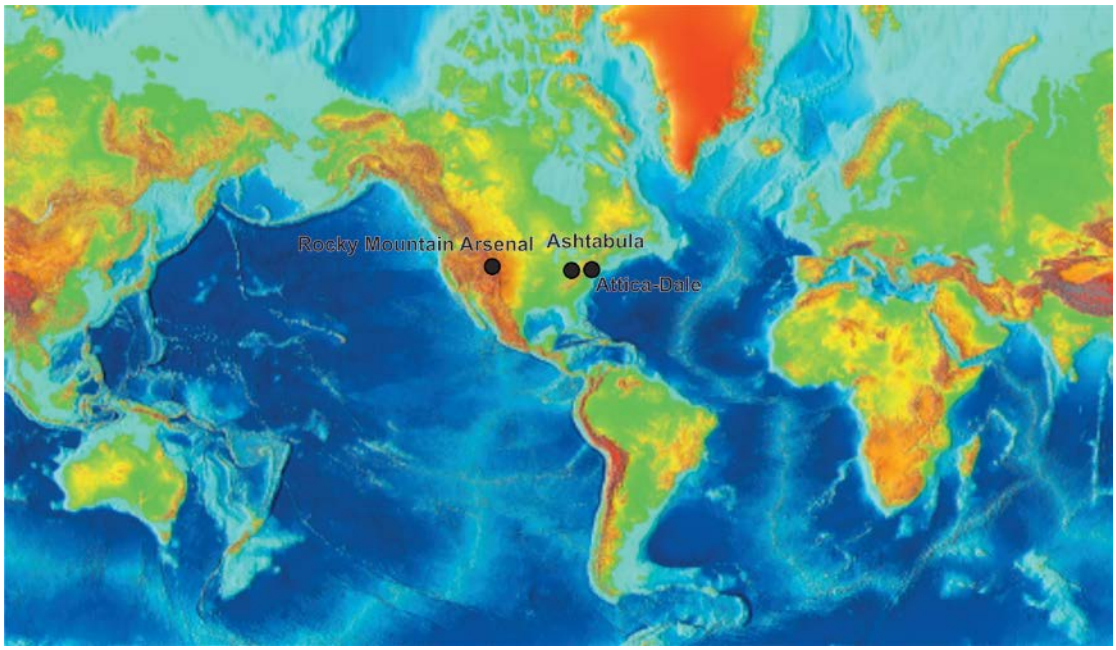

Figure 14: Location map of waste fluid injection sites reported in this section. Black circles are approximate locations of situations where fluid injection or solution mining has resulted in induced seismicity.

Rocky Mountain Arsenal

Waste fluid injection at the Rocky Mountain Arsenal in Denver, Colorado, USA, commenced in 1962 (Healy et al., 1968). Routine injection continued until September 1963 with ca. 21 million L/month injected into the well. Disposal of fluids started again in 1965 and was initially under gravity flow (ca. 7.5 million L/month) until pressurised injection recommenced at a rate of ca. 17 million L/month for 9 months, with a maximum of 478 L/min (Nicholson and Wesson, 1990). In February of 1966 injection was halted due to concerns that it was inducing recent local earthquakes (Healy et al., 1968).

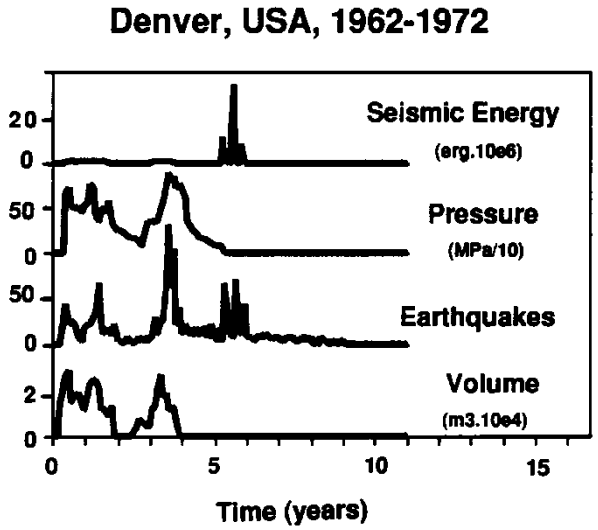

Figure 15: Temporal relationships between seismic energy, pressure, earthquake number and injection volume of waste water. Diagram from Grasso (1992a) and adapted from Healy et al. (1968).

Between 1962 and 1966, 1,281 earthquakes M≥1.5 were recorded with 22 M≥3.0 and two 4.0≤M≤4.4. After injection was halted in February of 1966, recorded earthquakes continued at a variable rate with as many as 71 recorded events per month. The most accurately located earthquakes were focused within kilometres of the injection well. In 1967, more than one year after injection was halted, three events of ≥M~5.0 occurred within the injection region (Nicholson and Wesson, 1990). These earthquakes caused damage in the Denver region. Based on proximity to the injection site and basic stress modelling, it was concluded that the occurrence of these earthquakes was consistent with the hypothesis that they were induced by sub-surface water disposal.

Rocky Mountain Arsenal was one of the first locations where clear relationships between injection volumes, pressure and productivity of induced earthquakes were demonstrated (Healy et al., 1968). Visual inspection of Figure 15 suggests a reasonable correlation between injected volume, numbers of earthquakes and pressure during water injection. However, these relationships are less clear during the post-injection period when pressures and injected volumes were zero (or close to it) yet seismicity continued and produced the largest events (M~5) in the sequence (indicated by the high seismic energy output between years 5 and 6). It has been suggested that the delayed timing of these larger magnitude events (relative the timing of injection) may reflect deferred stress transfer by propagation of the fluid pressure front along pre-existing faults which were close to failure prior to injection (Hsieh and Bredehoeft, 1981). Whatever the processes that produced these delayed M~5 events it is clear that injection parameters (e.g., injection rates, pressures and volumes) alone cannot be used to predict the timing and magnitude-frequency relationships of induced earthquakes.

Ashtabula, Ohio

Seeber et, al. (2004) describe a series of eight earthquake sequences near Ashtabula, Ohio, USA, that display characteristics of foreshock-mainshock-aftershock sequences. These earthquakes appear to have been triggered by injection of $60x10^3$ m^3 of waste fluid injection between 1987 and 1994. A M3.8 earthquake, the first felt event, occurred approximately one year after waste water injection began in a reservoir close to the city of Ashtabula. Felt events continued at the rate of about 1 per year through to 2004. The largest earthquake recorded has been a M4.3 in 2001, which caused slight damage.

The Ashtabula earthquake sequence occurred in association with hazardous waste water disposal in the Mt Simon sandstone (Nicholson and Wesson, 1990). The seismicity was recorded by a combination of regional broadband seismograms and local seismograph deployments in 1987, 2001 and 2003 (Figure 16). These different types of seismograph arrays have variable detection thresholds, levels of completeness and accuracy of hypocenter locations. The hypocentral locations of 42 events were determined local networks at Ashtabula. Despite these sampling issues the seismicity data provide a number of key insights. First, the recorded seismicity in the region was low prior to injection. The increase in seismic productivity, the locations of earthquakes close to injection site and the synchroneity of injection and seismicity have been interpreted to provide strong evidence for the events being induced (Nicholson and Wesson, 1990; Seeber et al., 2004). Second, the seismicity was focused within two sub-parallel east-west striking faults proximal to the injection site (Seeber et al., 2004). The faults are about 4 km apart and were active at different times. From the seismicity pattern the faults have lengths of 1.5 and 5 km and, like many faults reactivated by fluid injection, were not known to exist prior to the start of operations. Lastly, between 1988 and 2004 seismicity shifted southwards from close to the injector well (≤1 km) to up to 8 km away. This migration is interpreted to reflect movement of the pore-pressure front and associated reactivation of pre-existing faults further from the injector well (Seeber et al., 2004).

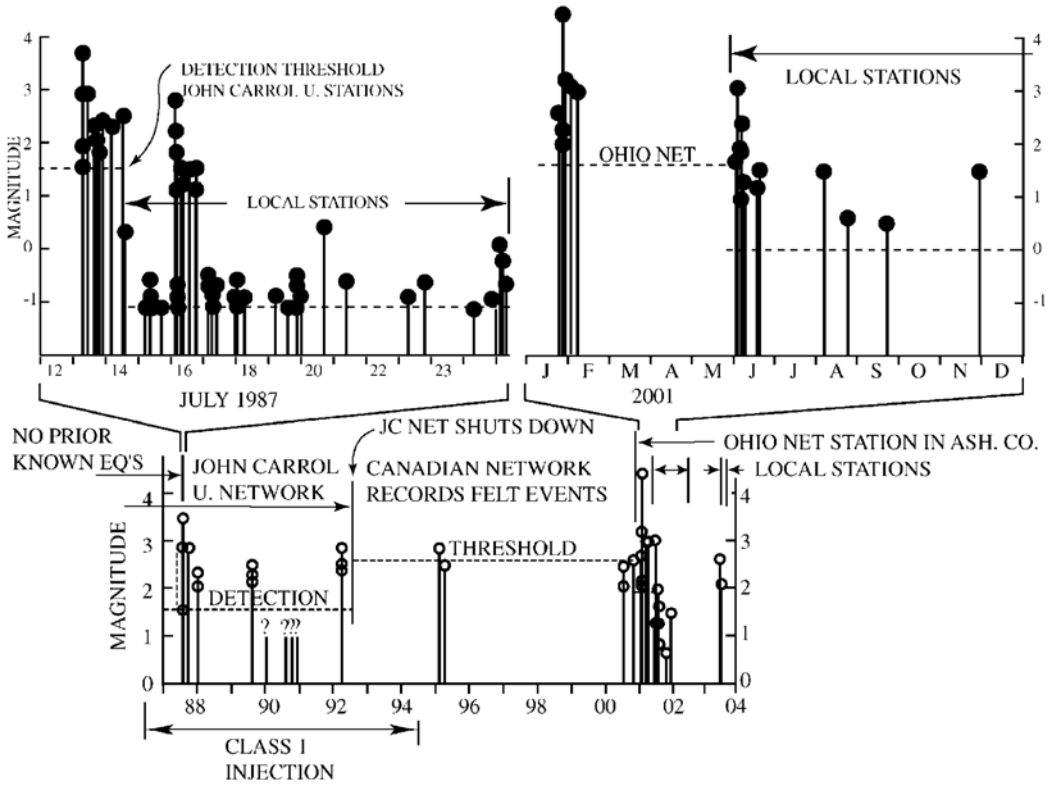

Figure 16: Temporal distribution of recorded seismicity and the history of seismography networks at Ashtabula, Ohio, USA. Prior to the onset of injection in 1987 the closest epicentre was about 30 km from Ashtabula. During and after injection seismicity was recorded by a combination of regional and local networks with estimated detection thresholds of M~1.5-2.6 and M~-1-0, respectively. The graphs illustrate the importance of detection threshold for the number of observed events.

Attica-Dale, New York

Nicholson and Wesson (1990) describe a sequence of seismicity that was likely induced due to injection related to solution mining of salt near Attica-Dale, New York, USA in 1971. Injection was at a depth of 426m and all observed seismicity reported was within 1km of the well. Minimal details of the recorded earthquake catalogue are reported, but estimated magnitudes are -1.0 ≤ M ≤ 1.0. How seismicity was recorded prior to injection and for what magnitudes, is not clear; however Nicholson and Wesson (1990) indicate that the background seismicity rate was “less than 1 event per month.” Based on stress measurements from hydrofracturing at a distance of 100km from the earthquakes, and Mohr-Coulomb failure analysis assuming cohesionless fractures, the injection pressures of 5.2-5.5 MPa, were very close to that required to induce failure. It should be noted that assuming cohesionless fractures will likely give a large underestimate of the pressure required and, particularly at shallow depths, hence, a lower bound. Once injection pressures were dropped below 5 MPa, the seismicity quickly declined. At the maximum, roughly 80 events per day were recorded, and the strong correlation of the seismicity with injection is in good agreement with the hypothesis that the seismicity was induced.

Paradox Valley

A brine injection project in Paradox Valley, Colorado, USA, represents one of the best monitored and documented cases of induced seismicity from the injection of wastewater. The project is a commercial project to remove excess salinity from the ground water and hence, the Dolores River. High pressure injection of the aquifer brine began in 1991. By 2005, more than $4x10^6$ m^3 of brine had been injected and that more than 4,000 earthquakes had been recorded by a surface network of 15 instruments (Ake et al., 2005). Seismicity has largely been in two clusters: one around the injection well, and another separated by a distance of approximately 8km from injection. Ake et Al. (2005) reported that the largest event recorded at that date was M4.3 and that approximately 15 felt events had occurred.

The injection operations have been adjusted several times in response to the seismicity and can best be described in four phases (Ake et al., 2005). Phase I lasted approximately 3 years and encompassed a number of short shutdowns in injection. Injection was at maximum capability (1290 L/min and approximately 33 MPa surface pressure). Earthquake occurrence was variable throughout this Phase, and 2,446 events were recorded. Injection was suspended following the occurrence of two larger events (M3.6 and M3.5) within a period of one month. Soon after, Phase II began with an altered injection strategy targeted at reducing the largest seismicity; injection continued at the same rate, but every six months a shutdown period of 20 days was scheduled. Seismicity rates were, in fact, reduced during this time period; however, the largest event recorded to date, an M4.3, occurred less than one year after the start of Phase II and injection was halted soon after.

Phase III began one month after the end of Phase II, and injection proceeded at a rate that was reduced by 33%. The rate of induced events reduced significantly to about 9 recorded events per month and the largest event recorded was M2.8. However, due to the nature of the project, this strategy was uneconomic and not sustainable. Therefore, after about two years, the strategy again changed, this time using the same injection protocol, but with altered injectate chemistry. This protocol was being followed until the publication of Ake et. al. (2005).

The Paradox Valley injection project represents a very well monitored and studied example of induced earthquakes. Some key findings from the recorded earthquakes follow: there is no observed correlation between anomalous wellhead pressure and recorded earthquakes; earthquake clusters rapidly cease when injection is halted; the events occurred in a narrow depth range; and, the observed seismicity is correlated to the injection rate, particularly those events within 2km of the injection well. Finally, by monitoring the occurrence of events and altering the injection strategy, the operators were able to reduce the rate of events produced, which likely indicates that there was also a reduced probability for the occurrence of larger events.

Summary

While it is still unclear if the recent 2011 earthquakes were induced, there remains strong evidence that if reservoir and injection conditions are not closely monitored and understood, induced seismicity is a potential outcome. Reported studies to-date of waste water injection projects have shown that small to moderate earthquakes can be induced and, in the case of the Rocky Mountain Arsenal, three M≥5.0 earthquakes that caused minor damage in the city of Denver, were the result. However, with careful planning and understanding of the reservoir, any risks can be minimized and should be low (Zoback, 2012).

Carbon Capture and Storage

Introduction

Globally CO_2 has been injected into the sub-surface at many sites. In the majority of cases this injection is for enhanced oil recovery (EOR) which has been a widely accepted practice in the petroleum industry for at least 30 years. The SACROC (Scurry Area Canyon Reef Operations Committee) project, for example, injected at least 55 Mt of trapped CO_2 near Snyder Texas (USA) for EOR between 1972 and 2005 (Crameik and Plassey, 1972; Han et al., 2010). Despite the large number of CO_2 EOR sites (e.g., >100) they provide few quantitative data on induced seismicity. This report focuses on sites where the primary purpose of CO_2 injection was long-term storage for the purposes of greenhouse gas reduction. These operations commenced at commercial scales (i.e. injection ≥1 Mt/yr) in 1996 and have had a short history compared to petroleum production, EGS and waste water injection. There are presently four commercial-scale CCS projects in operation internationally. These are: i) Weyburn in Saskatchewan, Canada; ii) In Salah in Algeria; and iii) Sleipner in the Norwegian sector of the North Sea and iv) Snøvit also in the Norwegian sector of the North Sea. In addition, a number of smaller mainly experimental sites (or pilot projects) have been in operation for short durations (mostly days to months) in the last 10 years. These include: Otway, Victoria, Australia; Cranfield field study, Natchez, Mississippi, USA; Nagoaka, Japan; Frio, Texas, USA and Ketzin, Germany. Because of the limited number of sites and the lack of extensive local microseismic monitoring networks at many commercial and experimental sites (including those where CO_2 injection is being used for EOR), there is little information on induced seismicity for CO_2 storage in the public domain; Weyburn and Cranfield are the notable exceptions (Verdon et al., 2010b). Given the limited amount of data it is not possible to draw robust conclusions about future induced seismicity at CO_2 storage sites directly from CCS specific data. The paucity of data may be addressed by examining seismicity induced at different types of fluid injection and extraction sites which are described in the previous sections. In this section we summarise induced seismicity for five CO_2 storage sites (Weyburn, Sleipner, In Salah, Ketzin and Otway; see Figure 17 for locations) and conclude that more information is necessary for risk management of induced seismicity at CCS projects.

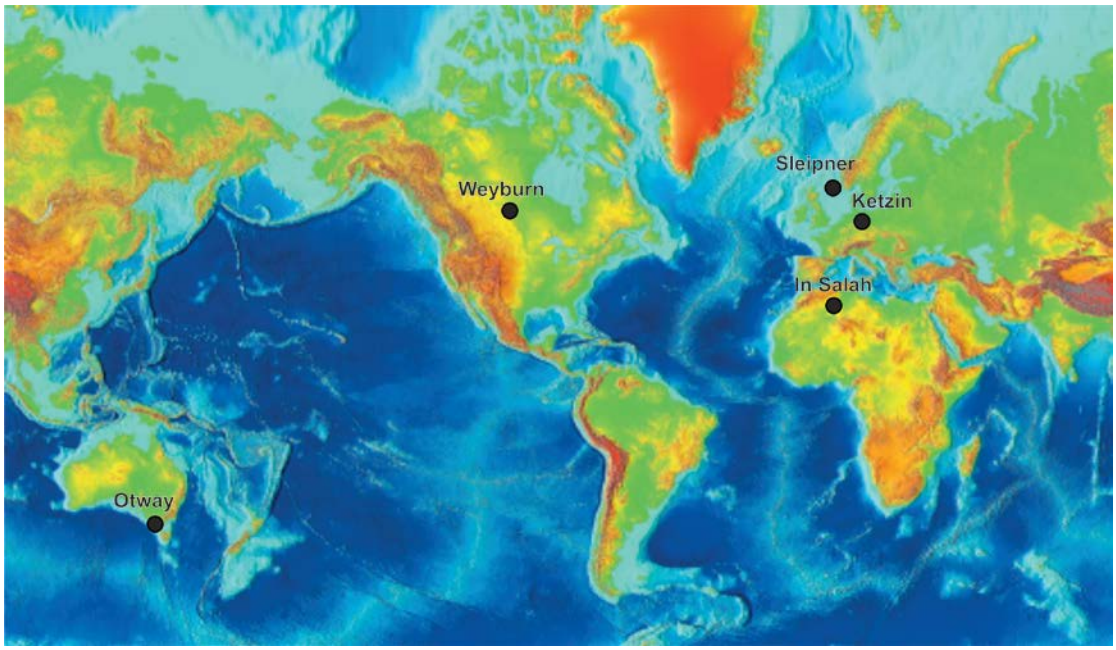

Figure 17: Location map of CO_2 storage sites (black filled circles) reported in this section.

Weyburn, Canada

The Weyburn oil field in south-eastern Saskatchewan, Canada, was discovered in 1954 and secondary oil recovery driven by water flooding commenced in the 1960s. In October 2000, EnCana and the International Energy Agency Greenhouse Gas Research and Development Programme (IEAGHG) started CO_2 injection to enhance oil recovery and to store CO_2 as part of a CCS programme. Initial injection rates were 2.69 million m³ per year rising to greater than 3 million m^3 per year (Verdon et al., 2010b). CO_2 is being injected via individual wells at rates of 50 to 500 tonnes per day into the reservoir (Midale interval in the Mississippian Charles Formation at a depth of ~1430 m) which is typically 20-30 thick with porosities of ~10-30% and relatively low permeabilities of ~10-50 mD (Ma and Morozov, 2010). As of January 2010 about 28 million m^3 of CO_2 had been injected and resulted in increases of about 5 MPa in reservoir pressures (Verdon et al., 2010b).

In 2003 a passive seismograph network consisting of eight triaxial 20 Hz geophones was installed in a vertical monitoring well, 50 m from a CO_2 injection well. Geophones were spaced at intervals of 25 m between depths of 1181 and 1356 m, roughly 200 m above the main reservoir. From August 2003 to December 2004 approximately 100 well located (~±100 m) earthquakes were recorded by the geophone array (Verdon et al., 2010b)(e.g., Figure 18). These events ranged in magnitude between M-3 and M-1. Due to the configuration and number of seismographs and the small size of the events, accurate source locations were difficult to obtain and distinguishing between seismic events and ambient noise was not easily done. Reduction of source location uncertainty requires additional down-hole instruments in multiple monitoring wells.

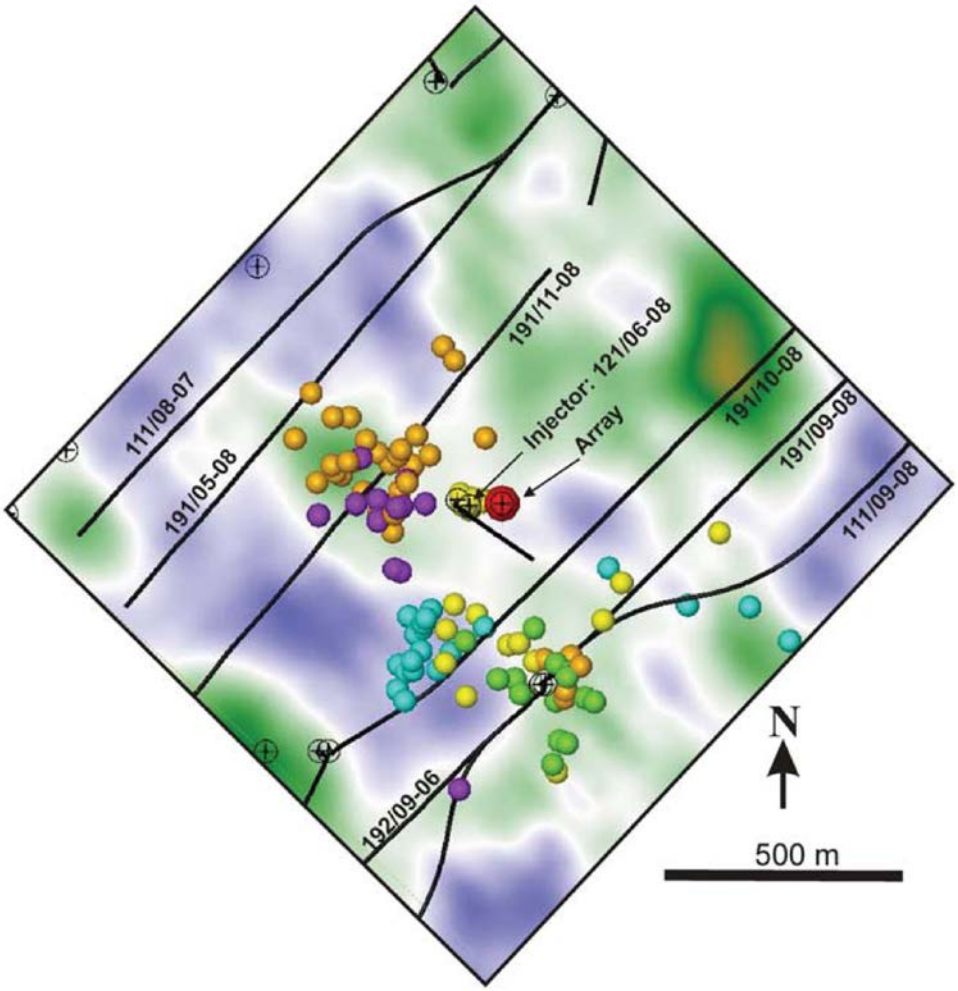

Figure 18: Seismic epicentre locations at Weyburn, Canada, from August 2003 to January 2006, superimposed on a 4D seismic amplitude difference map (figure from Vernon et al., 2010b). Green-to-orange and blue background colours represent negative and positive amplitude differences, respectively, within the Midale marly unit. Blue colours are interpreted to be zones where impedance has been reduced by the presence of injected CO_2. Events are colour-coded according to their timing: pre-injection period (yellow); initial injection (purple); production well shut-in 18–19 March 2004 (green); high-injectivity period (orange); low-frequency events during January 2006 (light blue). Locations of the injection, production, and monitoring wells are shown.

Induced earthquakes at Weyburn recorded between 2003 and 2008 were low in number and small in magnitude (M-3 to M-1) (Figure 19). The earthquakes induced by CO_2 injection were too small to be recorded on the Canadian regional network. In cases such as Weyburn, local networks comprising sub-surface instruments will be required to record the seismicity. Because seismographs were not recording continuously over the sample period (Figure 19) and water injections also occurred during this time the relations between seismicity and CO_2 injection rates are not well resolved. It is possible that elevated CO_2 injection rates and changes of water production in nearby wells correlate with higher rates of seismicity (Vernon et al., 2010b). The locations of some seismic events also correlate with the regions of CO_2 saturation identified using 4D seismic (e.g., Figure 18), which supports the view that CO_2 injection has affected the location of events. The spatial association of CO_2 saturation and seismicity may also suggest that the distribution of seismicity was influenced by chemical changes in the reservoir, although such a relationship has not been demonstrated. The low rates and magnitudes of seismicity indicate however, that seismic deformation of the reservoir is minor. Neither the deformation nor the seismicity have had an impact on the CO_2 injection operations at Weyburn.

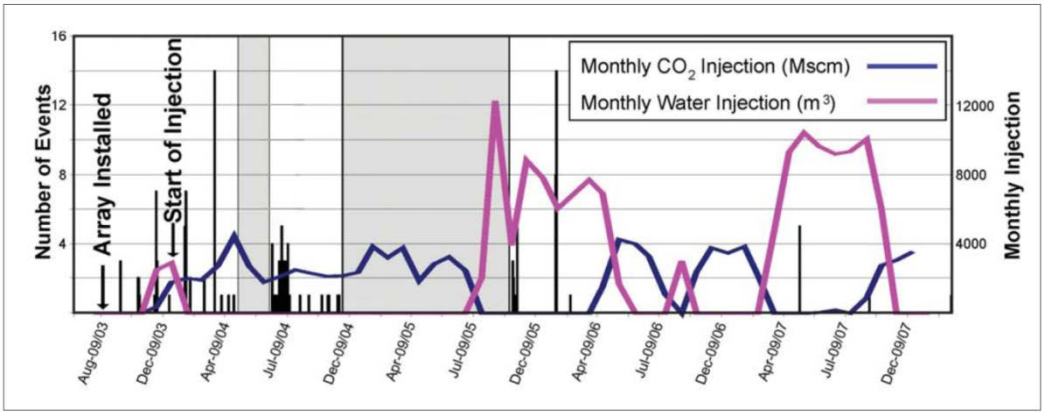

Figure 19: Timing of induced seismicity, water injection and CO_2 injection at Weyburn from August 2003 to January 2008. Numbers of events and monthly injection volumes (vertical well 121/06-08) are shown on the left-hand and right-hand sides of the graph, respectively. Grey shaded areas indicate periods when the passive seismic network was not recording. Figure from Verdon et al. (2010b).

Sleipner, Norwegian North Sea

CO_2 injection of about 1 Mt per year commenced in 1996 and continues today with about 11 Mt injected by 2008 (Korbol and Kaddour, 1995; Chadwick et al., 2010). Sleipner is in the Viking Graben in the Norwegian sector of the North Sea and stores CO_2 from the Sleipner-Vest natural gas reservoir beneath the Sleipner-A platform. Supercritical CO_2 has been injected into the Late Cenozoic Utsira Formation, a homogeneous fine sand with 35-40% porosity and 1-8 D permeability. CO_2 injection is taking place via a sub-horizontal well at a depth of about 1012 m which is approximately 200 m below the top of the Utsira Formation reservoir. The injected CO_2 is pumped at well head temperatures of 25^o with pressures of 6.2 – 6.4 MPa. Down-hole reservoir pressures may have increased <0.5 MPa due to injection (Chadwick, pers. comm, 2010).

The southern part of the Viking Graben is located in an area of moderate seismicity with several earthquakes of M2-3 recorded within 50 km of Sleipner-A platform by a regional seismograph network since CO_2 injection commenced. The regional network has not recorded seismicity induced by the injection programme (Evans et al., 2012). In addition, seismicity is not monitored on site and felt induced seismicity has not been reported from the Sleipner-A platform. In the absence of local microseismic monitoring induced seismicity due to CO_2 injection cannot be discounted. If, however, shallow seismicity (e.g., 5 km) were present it is unlikely that these events exceeded M3 as, at these magnitudes, they would probably have been felt on the Sleipner-A platform.

In Salah, Algeria

The In Salah commercial-scale storage project commenced in 2004 with CO_2 being injected into the aquifer leg of the Krechba gas field (Mathieson et al., 2004). As of February 2010, almost 3 Mt of CO_2 has been injected via three horizontal wells (KB-501, KB-502, KB-503) at a depth of 1850-1950 m into a 20 m thick Carboniferous sandstone reservoir. The reservoir has porosities of 13-20% and permeabilities of the order of 5-10 mD. The location of the plume and integrity of the caprock has been intensely monitored using a range of techniques including, 4D seismic reflection surveys, gravity, VSP, shallow aquifer wells, deep observation wells, InSAR and a microseismic passive geophone array. This array includes 48 3-component geophones at depths from 10 to 480 m, with 6-8 geophones recording seismicity at any one time (Daley et al., 2011, 2012). The test well containing the geophone array was drilled in 2009 and these instruments continue to record. To date in excess of 1000 events have been recorded at In Salah, with a cluster of activity in mid-2010. The largest magnitude for these events has been estimated at M0.5 (Daley et al., 2011, 2012).

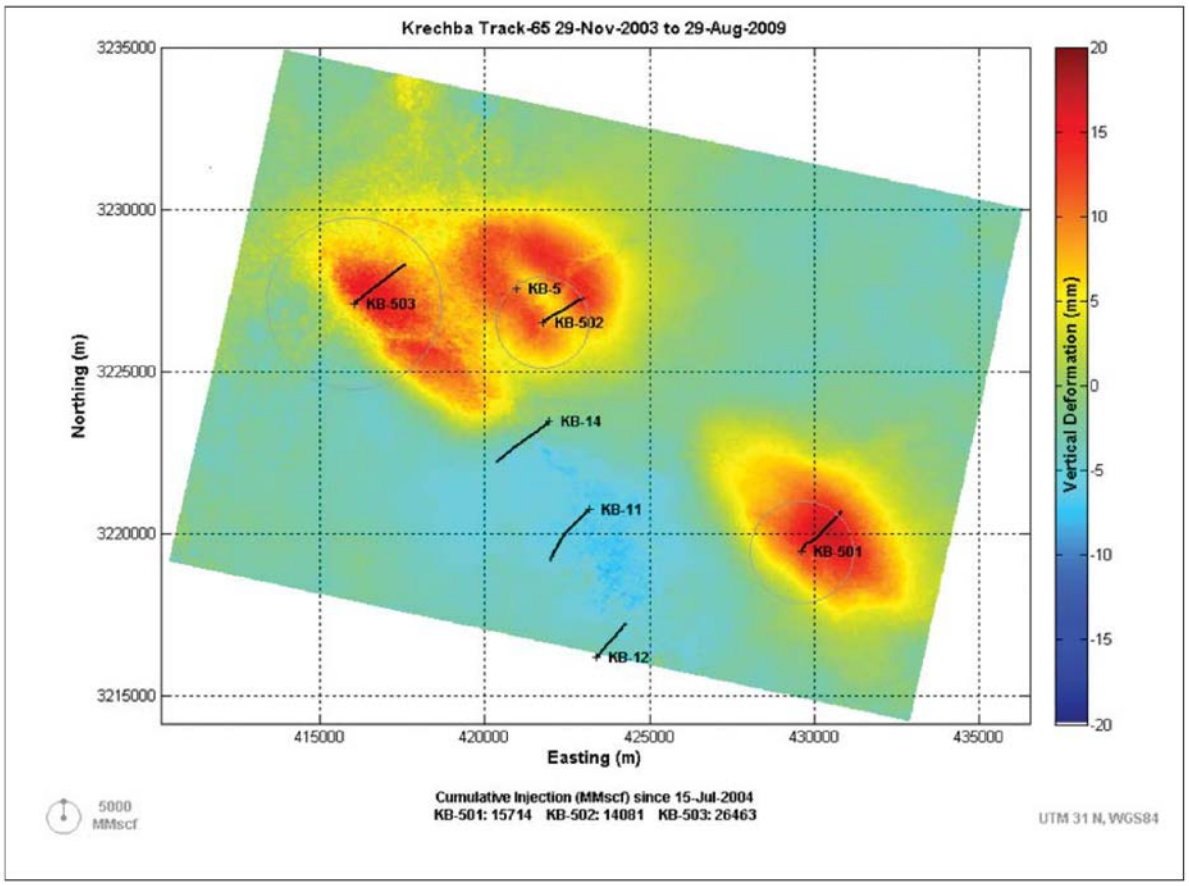

Figure 20: Vertical deformation at In Salah (Krechba) due to CO_2 injection between November 29 2003 and August 29 2009. Deformation measured by recording differences in the altitude of ground surface using InSAR satellite images collected 28 days apart. Figure from Mathieson et al. (2010) and originally provided by MDA/Pinnacle Technologies.

Given the paucity of the publically available seismicity data from In Salah, conclusions cannot be made about the primary factors contributing to induced events being triggered at this site. It is worth noting, however, that InSAR data clearly shows doming of the ground surface by up to 25 mm over each of the three injector wells (Mathieson at al., 2010)(e.g., Figure 20). This ground deformation, which results from the first 5 years of injection, is consistent with a ~10 MPa increase in reservoir pressures and dilational deformation of the reservoir (Rutqvist et al., 2010). Geomechanical modelling

indicates that deformation of the reservoir is likely to occur on pre-existing fractures rather than via generation of new hydraulic fractures (Rutqvist et al., 2011). Further analysis of the record from the geophone seismic array offers the prospect of testing the results of Rutqvist et al., (2011), characterising the brittle component (i.e. fracturing) of the deformation field and possible also of determining the important factors controlling the seismicity.

Ketzin, Germany

In June 2008 CO_2 injection commenced at the Ketzin (near Berlin), Germany, pilot project site, with approximately 58 000 tonnes injected as of January 29th 2012 (CO2Sink, 2012). CO_2 storage is in a saline aquifer within the Stuttgart Formation at depths of 632 m to 700 m. The reservoir is characterised by heterogeneous permeabilities of 50 and 100 mD (Wurdemann et al., 2010) and is overlain by the clay dominated Weser Formation seal.

CO_2 injection was achieved via one well (Ktzi-201) and was monitored in two nearby (<100 m from Ktzi-201) observation wells (Ktzi-200, Ktzi-202) (Prevedel et al., 2008). All three wells contained sensors installed in the casing to monitor 'Distributed Temperature Sensing' (DTS), 'Electrical resistivity Tomography' (ERT) and 'Gas Membrane Sensors' (GMS) (Wurdemann et al., 2010). CO_2 injection rates of 50 to 500 t per day increased pressure in the Stuttgart Formation to 8.1 MPa by the end of one year, 1.7 MPa above initial formation pressure (Wurdemann et al., 2010).

Background seismicity in the Ketzin region has been low with the nearest modern events recorded on regional seismograph networks located more than 100 km from the storage site. A local seismic network has been operational at the site since September 2009 and has detected events which may have been associated with CO_2 injection. However, the geometry of the seismograph array and local noise make it difficult to use these data to quantify the seismicity, which has not been presented in the literature (e.g., Evans et al., 2012). The Ketzin experience highlights a common issue with CCS microseismic monitoring, which is that their designs are often not optimal for detecting events above background noise levels or for determining accurate locations of events.

CO2CRC Otway Project, Australia

The CO2CRC Otway project is an experimental scale operation in south-western Victoria, Australia. CO_2 injection and storage occurred over two stages. In stage 1, from March 18th 2008 to August 29th 2009, over 65 000 tonnes of supercritical CO_2 was injected at an average rate of 145 tonnes per day via the CRC-1 into the Waare C Formation at a depth of about 2 km (Underschultz et al., 2011). Stage 2 consisted of injecting about 10 tonnes of CO_2 into the Paaratte Formation saline aquifer between May and September 2011 at a depth of about 1400 m in the CRC-2 well. The stage 2 experiment was designed to provide an estimate of residual trapping in a saline aquifer at Otway (Zhang et al., 2011).

Monitoring of seismicity at the Otway site commenced in September 2007, prior to the injection of CO_2, and consisted of a two-channel seismometer connected to a pair of triaxial geophones installed downhole above the reservoir at 10 m and 40 m depths. A second down-hole array of geophones and hydrophones was also installed at reservoir depth in the Naylor-1 well, but ceased to operate after several months and provided limited data. In March 2011 the two initial geophones were augmented by a further four geophones (two triaxial geophones at 10 m and 40 m depth in two more wells). The array presently operating now comprises 6 geophone stations arranged in a triangular geometry around the CRC-2 injection well.

During stage 1 CO_2 injection between 0 and 36 'seismic events' were recorded each day with possible magnitudes up to M1. For these data distinction between seismic events and ambient noise was often unclear and the lack of an extended geophone array contributed to many poor (>±100 m) event locations, while recording of the geophones was intermittent. These sampling issues make it difficult to draw conclusions about the relations between the induced seismicity and injection operations (e.g., changes in injection rates or to fluctuations in the reservoir pressure history). Following upgrade of the seismic monitoring array in March 2011 a significant number (>100) of mainly small events, M-1 to -2, were recorded during the stage 2 experiments. Only one event of ~M-1 triggered all 6 geophones in the array and appears to have been associated with CO_2/water injection. Further analysis of these data is required to constrain better their locations, magnitudes and origin (e.g., reservoir deformation or ambient noise).

Summary

Induced seismicity at commercial and experimental CO_2 storage sites has many features in common. In general, induced seismicity reported for CCS sites have small numbers (<100/yr) and low magnitudes (M-2 to 1). In addition to the case studies discussed in this section (i.e. Weyburn, Sleipner, In Salah, Ketzin and Otway), few seismic events have been recorded at the Cranfield field study, Frio field or Nagoaka site. In the latter case, a downhole array of hydrophones and a surface seismometer, failed to record seismic activity that could be associated with the CO_2 injection of 2 tonnes per day (Kikuta et al., 2004). The low numbers of induced earthquakes will partly reflect the fact that most CO_2 storage sites were monitored by a limited number (e.g., <10) of sub-surface geophones within existing wells. While cost effective, these geophone configurations were generally not optimal for accurately locating events (i.e. <±50 m) or discriminating between ambient noise (e.g., noises in pipe work and electrical pulses) and small magnitude (M-2 to M0) induced events. This sampling problem is exacerbated for permeable sand formations and saline aquifers where injection produces very low amplitude recorded events. In such cases peak amplitudes may be in the order of 10^{-7} m/s and are close to the noise floor of geophones used in wells. Not-withstanding these problems no injection induced events >M1 have been produced by, and recorded at, CO_2 storage sites.

Given the paucity of induced seismicity data for CO_2 storage sites, it will be necessary to consider induced seismicity produced by water injection. Supercritical CO_2 is more compressible and less dense than water at pressures and temperatures typical of CCS reservoirs (e.g., 20 MPa and 80°C), and these differences could cause variations in their patterns of seismicity (e.g., Sminchak et al., 2002). Higher compressibility of CO_2 compared to water make it a 'softer' medium and could mean that its injection produces lower pressure increases and seismicity rates than water (e.g., Maxwell et al., 2008). Despite differences in the properties of water and supercritical CO_2,they appear to produce comparable induced seismicity magnitudes and productivity. Verdon et al. (2010a), for example, concludes that "despite differences in compressibility, viscosity, density and relative permeability between the fluids, CO_2 and water have similar induced patterns of microseismicity". Given these observations it appears valid to use induced seismicity from water injection and petroleum production sites as analogues for induced seismicity at future CO_2 storage sites.

Observed Seismicity and Empirical Data Analysis

Introduction

Existing pilot (or experimental) and commercial-scale storage projects show that CO_2 geological storage is technically feasible (e.g., Hosa et al., 2011; Jenkins et al., 2012). Pilot projects do not, however, operate at a scale that will be necessary for mitigation of climate change arising from greenhouse gas emissions into the atmosphere. Commercial CCS projects will store several orders of magnitude greater volumes of CO_2 compared to pilot projects, possibly requiring CO_2 injection at higher rates, many more injector wells and/or injection for longer periods of time. While the four commercial-scale CO_2 storage projects (Weyburn, Sleipner, In Salah and Snovit) presently operating have not generated moderate or large magnitude earthquakes, they do not provide sufficient data to draw generic conclusions about future commercial-scale CO_2 storage sites. One means of circumventing the paucity of induced seismicity data for commercial-scale CO_2 storage projects and the potential gap in our knowledge is to review the seismicity induced by injection and extraction of different types of fluid (e.g., waste water, brine, and hydrocarbons) for volumes ranging from the size of CO_2 pilot projects (thousands of tonnes) to commercial CO_2 projects (millions of tonnes).

Empirical induced seismicity data from injection and extraction projects have potential value for informing risk management decisions at CCS sites. Although earthquakes induced by injection are of most relevance to CO_2 storage projects, seismicity associated with hydrocarbon extraction may in many cases be driven by water injection designed to maintain reservoir pressures (e.g., Raleigh et al., 1976; Horner et al., 1994). Induced seismicity resulting from fluid extraction appears to be consistent with examples of injection induced seismicity (e.g., Nicol et al., 2011; Shapiro et al., 2011) and inclusion of extraction sites provides earthquake information for larger fluid volumes than if we only focused on injection examples. The examples of extraction induced seismicity are therefore useful for understanding the potential magnitudes and rates of induced seismicity associated with commercial-scale volumes of CO_2 injection. The potential limitations and value in what can be learned from using data from other industries are discussed in Section 6.2.

Analysis of Published Data Sets

In the following sections we present an overview of existing observations and analyses of relationships between induced seismicity parameters and other reservoir or injection/extraction specific parameters. The induced seismicity parameters include the following:

- Earthquake magnitude, including maximum and distributions,
- Seismicity rates,
- Temporal distribution of seismicity,
- Spatial distribution of seismicity.

In addition to presenting the observations described in other published studies, we have compiled data from the literature to test and augment published results. Our compilation builds on previously published collations (e.g., Nicholson and Wesson, 1990; Grasso, 1992a; Van Eijs et al., 2006; Suckale, 2009; Nicol et al., 2011; Evans et al., 2012), however, the amount of data remain limited. Our data set is neither comprehensive nor are the interpretations drawn from it conclusive. Until more data, including more homogeneous datasets, are made available, the results presented here are considered preliminary and indicate that the behaviour of induced seismicity in injection systems needs to be understood better.

We use data from a global compilation of 34 (Figure 21) published fluid injection and extraction sites, primarily from North America and Europe, to examine the relations between operations and induced seismicity. The 34 sites provide data such as the volume and rate of fluid injection/extraction, the duration and dates of injection/extraction, reservoir permeability, earthquake magnitude-frequency scaling relationships (*b*-value), and the rates, location and timing of all induced earthquakes. The database includes sites of water or brine injection (e.g. waste disposal, secondary recovery of hydrocarbons and hot dry rock geothermal systems) and where hydrocarbons have been extracted. Injection operations range in duration from less than 24 hours to more than 35 years, with total injected fluid volumes of 200 m^3 to approximately 42 million m^3. Maximum induced magnitudes range between -1.1 and 5.5 (Table 1). Not all 34 sites are used in each plot. The data presented in Table 1 are plotted in Figure 23, in Table 2 for Figure 25 and in Table 3 for Figure 27, and Figure 28.

Extraction operations are generally longer than injection, with durations of 12 to 90 years. The extracted fluid volumes are also much greater, with total volumes extracted ranging from 4700 m^3 to ~548 million m^3. At the majority of sites where induced seismicity has been reported, magnitudes are small to moderate (≤ M4.5). There is considerable debate around the maximum magnitudes induced by extraction but reported maximum magnitudes range from M0.9 to M7.

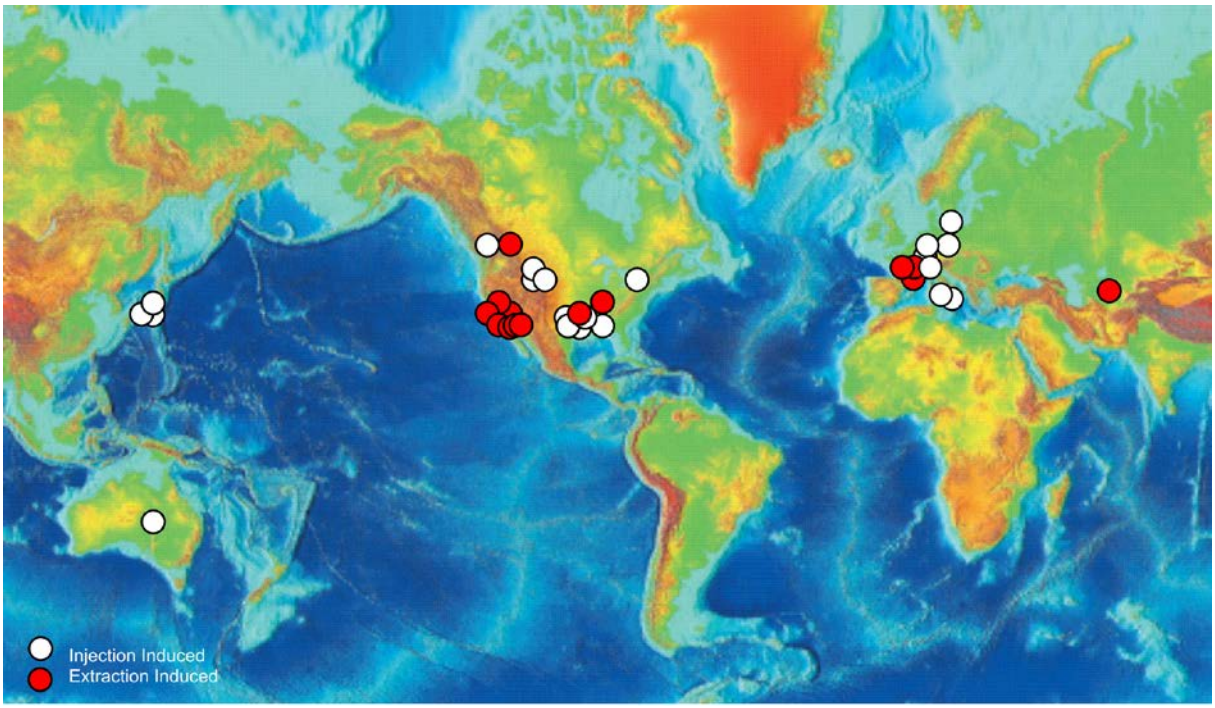

Figure 21: Location map of injection and extraction sites of induced earthquakes reported in this study (N=34) (see Table 1 to Table 3 and Figures 23, 25, 27 and 28). White circles are locations of injection induced earthquakes, and red circles are sites of extraction induced earthquakes.

Observational Data Bias and Limitations

As with any analysis of seismicity data, one must be aware of, and account for, the uncertainties, limitations and bias in the observed data set when attempting to interpret the data. There are four main data limitations that can cause difficulties when interpreting induced seismicity data: i) uncertainties in earthquake locations and magnitudes, ii) completeness of the recorded seismicity, and estimating this accurately iii) separation of induced earthquakes from tectonic earthquakes and, iv) bias of the published induced seismicity data toward productive and large magnitude sequences. The first two issues are common to all instrumental seismicity datasets (Mignan, et. al., 2011).

Uncertainties in Earthquake Locations and Magnitudes

For the purposes of this report we have used the published locations of induced earthquakes. The accuracy of these locations varies between sites and is dependent on a number of factors including the numbers and locations of recording stations near the reservoir, and the techniques used to derive the locations. At sites where seismograph arrays were established to record induced seismicity and the reservoir is within 1-2 km of the ground surface, errors on absolute locations are typically <±100 m (e.g., Seeber et al., 2004). For earthquakes recorded using standard networks, the errors can be as large as kilometres. These location errors do not impact on the validity of the first-order interpretations presented in this report.

In Section 1.4 we discussed the potential bias introduced by the use of different magnitude types within a catalogue of earthquakes. This bias is particularly important when estimating parameters that describe the behavior of a large population of earthquakes. An additional bias relates to uncertainties in the magnitude estimates. This bias is due to the nature of the negative exponentional Gutenberg-Richter distribution (Gutenberg and Richter, 1954), which describes the frequency-magnitude

distribution of earthquakes, When accounting for the uncertainty in the estimate of the magnitude, a population of earthquakes will be biased toward slightly higher magnitudes (Rhoades, 1995). This is because more events with a true magnitude less than some particular value will have an observed magnitude greater than this value than the opposite (Rhoades, 1995). However, in the context of this report, this bias is unlikely to significantly change any of the conclusions.

Minimum Magnitude of Completeness of the Recorded Seismicity

The magnitude of completeness (Mc) (also referred to as the minimum magnitude of completeness) is the magnitude below which the sampled earthquake population is incomplete. Mc applies to all earthquake datasets, including those for CO_2 storage sites, and varies depending on multiple factors including: the density and location of the seismograph array, number of down-hole seismographs, level of ambient 'noise', and the network analysts (Mignan, et. al., 2011). Mc strongly influences the number of earthquakes recorded and below Mc the frequency-magnitude distribution will not be accurately recorded. Numerous tools and methods are available for estimating Mc from a population of earthquakes; however the method used is not typically reported in the studies we have reviewed here. It is likely that a method based on estimating the point of maximum curvature in the frequency-magnitude distribution is used. This method is useful for a first order approximation, but is prone to errors. Future understanding of the behavior of induced earthquakes will be improved by better estimation and reporting of Mc.

In Figure 22 both the lower magnitude limit of earthquakes (approximately M-1.3) and the decline in earthquake frequency below M-0.6 are interpreted to derive from limitations imposed by the instrument technology together with the number and configuration of the seismograph array and not from an actual decrease in the numbers of earthquakes; in other words, the data set is incomplete below M-0.6. Mc is notoriously difficult to estimate accurately and care must be taken in doing so or erroneous seismicity parameters are likely to be estimated. Bachmann et. al. (2011) showed how Mc can vary by 0.3M within hours and hundreds of metres. The seismicity presented in Figure 22 from Cooper Basin, Australia, are typical of data gathered over the last 10 years using multiple down-hole instruments situated above the injection zone.

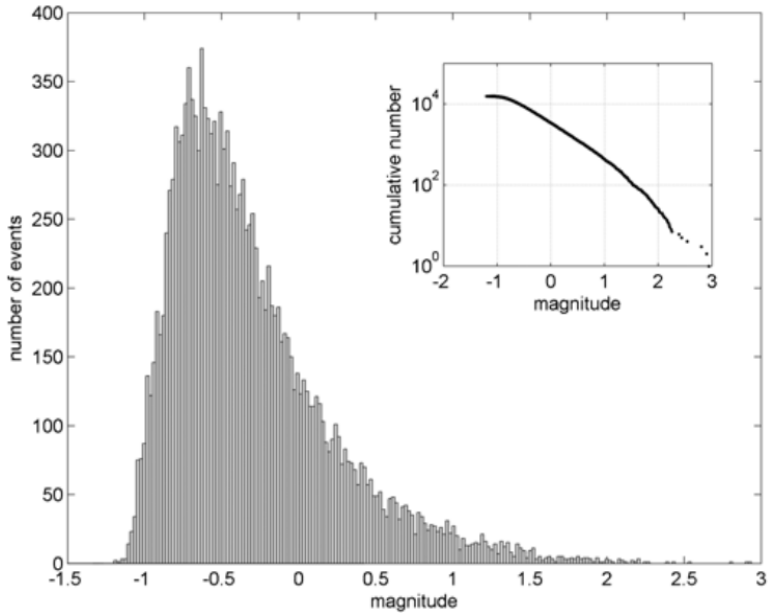

Figure 22: Gutenberg-Richter magnitude-frequency plot for induced earthquakes produced during the 2005 restimulation of the Cooper Basin HFR reservoir in Australia. During this restimulation, about 25,000 m^3 of water was injected at a depth of 4.25 km into the granitic crust, with maximum injection rates exceeding 31 L/s and the well head pressure peaking at ~62 MPa. Approximately 16,000 induced seismic events up to a maximum magnitude of M 2.9 were recorded during this restimulation. Seismicity was monitored by a local 8-station network activated prior to injection, consisting of geophones deployed in boreholes at depths of 70-1700 m (Baisch et al., 2009a).

Separating Induced Earthquakes from Tectonic Earthquakes

Distinguishing between induced and natural seismicity can be subjective. In cases where seismicity is clustered close to the reservoir during injection or extraction it is generally assumed to be induced (Nicholson and Wesson, 1992). In areas where the rates of seismicity were low prior to operations, the temporal and spatial clustering of seismicity and injection can provide strong evidence for these events being induced. Even in such cases however it remains possible that the seismicity was not induced; there are numerous examples (e.g., Christchurch September 4th 2010 Mw 7.1 earthquake, Kaiser et al., 2012) where natural earthquakes where preceded by low rates of seismicity. In addition, at some sites agreement has not been reached about whether the largest magnitude earthquakes (e.g., M>5) were induced by fluid injection or extraction, or constitute natural seismicity produced by tectonic activity (see Suckale, 2009). The largest magnitude earthquakes are more often associated with fluid extraction rather than injection. Such earthquakes have been considered to be induced if one or more of the following criteria have been met: 1) they are located close to, or within, the fluid injection/extraction reservoir; 2) the measured or calculated state of stress in the crust exceeds (or is likely to exceed) the rock strength; 3) the earthquakes occur during or immediately following injection/extraction and; 4) there is a clear temporal and/or spatial disparity between previous natural seismicity and the inferred induced events (Simpson and Leith, 1985; McGarr, 1991; Nicholson and Wesson, 1992; Suckale, 2009).

For the purposes of this report we have included in our database four large earthquakes (M5-7) that are inferred to have been induced by oil and gas extraction, but occurred up to 10 km outside the main reservoirs. Although debate still exists about the origin of these events (see discussion in Suckale, 2009), they represent a possible worst-case scenario and their inclusion in the following analysis is considered conservative from a risk perspective. These sites are: Gasli, Uzbekistan, where three M7 earthquakes occurred in 1976 and 1984 (despite this area being previously aseismic) and the

Coalinga Eastside (1983), Kettleman North Dome (1985) and Montebello Fields (1987)(California, USA), where earthquake magnitudes of M6.5, M6.1 and M5.9 occurred, respectively. The Gasli earthquakes represent the largest possible induced events identified to date and are discussed further in section 3.3.

Bias of the Published Induced Seismicity Data towards Productive and Large Magnitude Sequences

The database utilised in this study is dependent on published data and is therefore likely to not be fully representative of the true distribution of possibilities for induced earthquakes in injection and extraction projects. A key factor in this is that sites with low or no recorded seismicity, or without large magnitude earthquakes, are unlikely to be reported in the scientific literature; therefore the data set is biased toward sites with large magnitude earthquakes,higher seismicity rates or to sites where high seismicity rates were expected. It is not possible to determine the magnitude of the effect of the missing data. Until induced seismicity data is consistently recorded, reported, and available, this will remain the case.

In some cases this bias may occur because seismograph arrays were capable of recording larger earthquakes only (e.g., >M 2) and sites with no recorded events above this threshold were excluded (i.e. smaller events may have occurred but are not recorded by the network). Such a scenario generally applies to sites where seismicity was recorded by regional seismograph networks not specifically designed to measure local induced seismicity. In addition, the minimum detection threshold of earthquakes varies between sites and is generally lower where elevated rates, expected magnitudes, or predicted hydraulic fracturing demand deployment of dense networks or instruments in the sub-surface. Also, at sites where instrument deployment was triggered by elevated rates and magnitudes of seismicity, earthquakes in the sequence that pre-date network installation will not be recorded in the catalogue. The improved data quality resulting from installation of a local network is a feature of many Enhanced Geothermal Systems (EGS, previously referred to as Hot Dry Rock, HDR, sites) and for this reason these sites have been included here. The well head pressures and rates of seismicity at these sites are typically higher than at sites where no hydraulic fracturing occurs, however, the maximum magnitudes of earthquakes tend to be lower. The inclusion of these sites in our sample does not appear to have increased the maximum magnitudes or to impact on interpretations of Figure 23a. Finally, the quality of the data and the maximum magnitudes of the observed earthquakes will influence which studies are published and what data are available in the literature. Sites with low quality data where induced seismicity is of low magnitude and/or with low seismicity rates are more likely not to be published. These sites may be underrepresented in the in the present sample.

It should be noted that relevant reservoir engineering experience exists about the nature of the behavior of induced seismicity (e.g., induced seismicity is not an issue). Due to the subjective nature of this information, and the general lack of support from a seismic network capable of completely reporting small magnitudes, we do not discuss it in this report. While such experience can be kept in mind when interpreting the results of this report, care must be taken due to the subjective nature of the experience and to the very low expected rates of larger magnitude earthquakes which require a very large sample population to adequately quantify. However, such information, when supported by observational data, would be a valuable addition to this work in the future.

In analysing the data we have constructed a series of tables and plots which illustrate the most important relationships between the characteristics of the injection operations and the induced seismicity. The plots have been used to comment on the effects of various reservoir and operational

parameters (e.g., injection rate, injected volume, reservoir permeability and reservoir pressures) on the population of induced seismicity (rate, magnitude, *b*-value) together with timing and locations of earthquakes induced by fluid injection/extraction.

Table 1: Data used to construct plots in Figure 23. Data include reservoir name, maximum induced earthquake magnitude, total volume of fluid injected/extracted at each site, and average rate of fluid injection/extraction. Several sites have had multiple injection/extraction operations over their lifetime, and data for each operation have been plotted individually. For the purposes of this report these operations were delineated by time breaks in injection/extraction and/or changes in the rates of injection/extraction.

Reservoir name	Max EQ Magnitude	Total Volume (1000's m3)	Average Inj/ext rate (m3/day)	References
Injection				
Ashtabula	4.3	340	118.30	Seeber et al., 2004
Basel Bad Urach Cesano	3.4 1.8 2	12 5600 2	2000.00 2332.8 1296	Ladner and Haring 2009 Evans et al., 2012 Evans et al., 2012
Cogdell	4.6	41450	4368.00	Harding 1981; Davis and Pennington 1989
Cooper Basin	3.7	22.5	1125.00	Baisch et al., 2006; 2009a
Dallas-Fort Worth	3.3	30.524	113.05	Frohlich and Potter 2010
Eagle West Gross Schönebeck KTB	<4.3 -1.1 1.2	7872 13 0.2	1797.26 12960 80.00	Horner et al., 1994 Evans et al., 2012 Zoback and Harjes 1997
Matsushiro	2.8	2.883	169.59	Ohtake 1974; Sminchak and Gupta 2003
Nojima Fault Zone	1	0.258	17.20	Tadokoro et al., 2000
Ogachi 1	-1.1	5.443	1088.60	Shapiro et al., 2007
Ogachi 2	-0.9	4.147	829.40	Shapiro et al., 2007
Paradox Valley	4.2	2756.16	1900.80	Ake et al., 2005; Shapiro et al., 2007
Paradox Valley	3	1620	1296.00	Ake et al., 2005; Shapiro et al., 2007
Rocky Mountain Arsenal	4.8	646	442.47	Healy et al., 1968; Hsieh and Bredehoeft, 1981; Herrmann et al. 1981
Rocky Mountain Arsenal -1	4.2	210	575.34	Healy et al., 1968; Hsieh and Bredehoeft, 1981
Rocky Mountain Arsenal -2	4.2	189	517.81	Healy et al., 1968; Hsieh and Bredehoeft, 1981
Rocky Mountain Arsenal -3	2.7	30	82.19	Healy et al., 1968; Hsieh and Bredehoeft, 1981
Rocky Mountain Arsenal -4	3.7	180.5	494.52	Healy et al., 1968; Hsieh and Bredehoeft, 1981
Rocky Mountain Arsenal -5	3.7	34	93.15	Healy et al., 1968; Hsieh and Bredehoeft, 1981

Reservoir name	Max EQ Magnitude	Total Volume (1000's m3)	Average Inj/ext rate (m3/day)	References
Soultz-sous-Forets - GPK 2	2.6	25	4166.67	Charlety et al., 2007; Baisch et al., 2009b; Dorbath et al., 2009
SSF - GPK 2 (1)	2.2	2.7	2596.15	Charlety et al., 2007; Baisch et al., 2009b; Dorbath et al., 2009
SSF - GPK 2 (2)	2.6	16.56	4323.76	Charlety et al., 2007; Baisch et al., 2009b; Dorbath et al., 2009
Soultz-sous-Forets - GPK 3	2.9	37	3363.64	Charlety et al., 2007; Baisch et al., 2009b; Dorbath et al., 2009
Soultz-sous-Forets - GPK 4-1	2.3	9	1125.00	Charlety et al., 2007; Baisch et al., 2009b; Dorbath et al., 2009
SSF - GPK 4-1 (1)	2.1	3.6	3461.54	Charlety et al., 2007; Baisch et al., 2009b; Dorbath et al., 2009
Soultz-sous-Forets - GPK 4-2	2.7	12.5	3125.00	Charlety et al., 2007; Baisch et al., 2009b; Dorbath et al., 2009
SSF - GPK 4-2 (1)	2.7	7.2	3461.54	Charlety et al., 2007; Baisch et al., 2009b; Dorbath et al., 2009
SSF - GPK 4-2 (2)	2.0	2.16	2602.41	Charlety et al., 2007; Baisch et al., 2009b; Dorbath et al., 2009
Torre Alfina	3	4.2	3456	Evans et al., 2012
Extraction				
Coalinga Eastside	6.5	270000	9364	Segall 1985; McGarr 1991
Imperial Valley	6.6	157500	61644	Glowacka and Nava, 1996
Victoria	6.1	190000	65068	Glowacka and Nava, 1996
Cerro Prieto	5.4	547500	100000	Glowacka and Nava, 1996
Gasli	7	200000	36530	Simpson and Leith 1985
Gasli	7	400000	45662	Simpson and Leith 1985
Imogene	3.9	190720	10450	Pennington et al., 1986; Davis et al., 1995
Kettleman Hills North Dome	6.1	123000	5810	McGarr 1991
Montebello - Whittier Narrows	5.9	135000	5209	McGarr 1991
Seventy-Six	0.9	4.7	24	Rutledge et al., 1998
Wilmington	5.1	168288.057	24266	Ritchter 1958; Kovach 1974

Relevance of Case Studies to CCS

It cannot be emphasized strongly enough that this report does not contain quantitative information on seismicity that has not happened. Moreover, the number of CCS projects is limited (leaving aside EOR for the moment) and in none of these has there been any issue with induced seismicity. Even if the case studies and available data (which include some current CCS projects, but little on EOR) were clearly directly applicable to future CCS projects, the most that could be established is a worst-case scenario, that is, the likelihood of events large enough to be reported. What would trigger reporting is of course unclear and is likely to be vary between jurisdictions and at different times.

It is also worth noting that the closest analogy we currently have for large-scale CCS is EOR conducted using CO_2 injection (Table 2). EOR is a large industry which has been operating, particularly in the Permian Basins, for decades with little reported induced seismicity. While the level and importance of induced seismicity for CCS projects is impossible to quantify, the available information does suggest that CCS could manage the risks of induced seismicity to an acceptable level.

Some caution should be exercised however in extrapolating by analogy. Induced seismicity is determined by a potentially wide range of site-specific factors, including pressures, pressure history, stress state of the reservoir, pre-existing fault availability, lithology, geochemical effects, changes of state, layout of injection wells and general reservoir management and associated regulation. Most of these factors are not specific to the fluid that is injected.

Clearly site-specific details are not known for hypothetical future CCS projects. However, given the large number of injection and extraction projects that have taken place world-wide, it is a reasonable working assumption that the range of parameters and processes, possibly relevant to CCS-related induced seismicity, has been adequately represented in the available data. Accordingly, the trends and observations deduced from past projects are a useful guide, in a statistical sense, to the level of induced seismicity that will be experienced in CCS - on the assumption that over time CCS projects will occur in the same range of circumstances that are represented in the historical data.

There is of course uncertainty about whether this assumption will be borne out in practice. For instance, it may turn out that a typical CCS project will operate at higher pressures than today's typical EOR project, which would clearly affect the relevance of today's EOR experience. On the other hand, CCS may have to operate in tight, deep formations, making the evidence from geothermal projects may be more relevant than it currently seems.

The most obvious aspect of this historical data is that the vast majority of injection or withdrawal projects do not report induced seismicity. Furthermore it is likely that CCS will be more closely regulated and monitored than has been the case in the past for other analogous activities. This regulation has the potential to further reduce the induced seismicity at CCS sites compared to other injection/extraction projects.

Magnitudes of Induced Earthquakes

The maximum earthquake magnitudes of induced earthquakes are generally M ≤4.5 but on very rare occasions may exceed M6 (e.g., Nicholson and Wesson, 1990, 1992; Grasso, 1992a; McGarr, 1991; Van Eijs et al., 2006; Suckale, 2009; Nicol et al., 2011; Evans et al., 2012). Examination of the literature suggests that maximum magnitude may be influenced by volume of fluid injected/extracted and/or the injection. These relationships between maximum observed magnitude and volume of fluid and maximum observed magnitude and injection rate are discussed in the following sections.

A caveat is that in traditional probabilistic seismic hazard analysis (Cornell, 1968), the maximum possible (or modeled) magnitude is theoretically separate from the maximum observed magnitude. The theoretical upper limit for risk assessment may necessarily be larger than what has been observed.

Volume of Fluid Injected and Maximum Magnitude

Although some studies of empirical data from numerous fluid injection sites (e.g., Evans et al., 2012) have concluded that there are insufficient data to fully quantify a relationship between the volume of fluid injected or extracted and the maximum observed magnitude, some studies of individual sites support a positive correlation between these variables (e.g., McGarr, 1976; Smith et al., 2000; Baisch et al., 2006, 2009b; Shapiro et al., 2011). McGarr (1976) indicates that the total seismic moment of induced earthquakes increases with the volume of fluid injected. McGarr (quoted in Physics World March 2012, volume 25, number 3, page 15) also suggests that doubling the volume of injected water increases the maximum magnitude by about 0.4. In addition, a recent study of Enhanced Geothermal System sites indicates that the maximum magnitude of the induced seismicity is somewhat, but not completely, limited by the minimum dimension (L_{min}) of an volume defined by these events, which are assumed to define the stimulated reservoir (Shapiro et al., 2011). These observations are consistent with the view that increases in the injected mass and volume (and the associated plume dimensions) increase the probability of larger events being induced (e.g., Baisch et al., 2006, 2009b; Shapiro and Dinske, 2009). The physical basis for this relationship remains unclear. It may be that large volumes of injected/extracted fluid produce larger plumes which are more likely to intersect bigger faults and to drive these faults towards failure (e.g., Baisch et al., 2009b; Shapiro et al., 2011). Independent of the mechanism resulting in induced seismicity, monitoring the spatial growth of induced seismicity in real time could help constrain the risk of inducing damaging earthquakes (Shapiro et al., 2011).

Based on the dataset compiled in Table 1, a positive correlation is found between the maximum induced earthquake magnitude and the total volume of fluid injected/extracted, with larger volumes being associated with greater maximum induced earthquake magnitudes (Figure 23a). Because of the data biases, particularly the inferred under reporting of sites with no recorded induced seismicity, the lower bound of the distribution is considered to be a sampling artifact and is expected to move downwards with more data. This interpretation is supported by the data in Table 1 of Evans et al. (2012) in which 25 of 42 European injection sites had no reported seismicity and would plot below most of the data cloud in Figure 23a. The upper bound of the observed maximum magnitude data provides an approximation of the maximum earthquake magnitudes that could be expected given the injection/extraction volumes and geological conditions at the recorded sites. The upper bound of the observed maximum magnitude distribution also shows that observed maximum magnitudes increase with total fluid volumes; an order of magnitude increase in fluid volume produces about a 0.8 increase in maximum magnitude. This relationship, which does not change significantly if extraction events are excluded, is consistent for both injection (EGS and disposal projects) and extraction induced

earthquakes, with the total extracted volumes generally being far greater than the total injected volumes (Figure 23a). A general positive relationship between total volume and the maximum possible earthquake magnitude (Figure 23a) is consistent with previous studies (Smith et al., 2000; Baisch et al., 2009b; Shapiro et al., 2011), although the precise form of the relationship is poorly defined and may vary between studies and sites. For example, induced seismicity appears to be more common for fluid injection into crystalline rock than sedimentary rocks (Evans et al., 2012), while some sedimentary basins (e.g., Netherlands; Van Eck et al., 2006; Van Eijs et al., 2006) are more prone to induced seismicity than others. Lastly, because of the sampling biases inherent in the data used to populate Figure 23a and the expected variability in seismicity between sites the predictive value of these data for individual sites remains uncertain. At best the data in Figure 23a could be used to predict the maximum possible magnitude for all sites, although it should be recognized that this value will likely exceed the maximum magnitude at any given site. At worst the injected volume is not a suitable parameter for predicting maximum magnitude (Baisch et al., 2009c).

Table 2: A comparison of various industrial scale injection projects. A relative comparison is given in the colour coding: green = comparable, red = not comparable, yellow = partly comparable. Reproduced from Michael et al, (2011).

Characteristics	CO_2 Storage (large-scale)	Enhanced oil recovery	Acid-gas injection	Natural gas storage	Liquid waste disposal (Class 1)	Geothermal (Hot saline aquifers)
Purpose	Reduction of CO_2 emissions	Increase of oil production	Reduction of H_2S flaring and stripping of CO_2 from natural gas	Storage of gas for seasonal and backup energy use	Disposal of liquid waste	Energy production
Time scale	100s – 1000s of years	< 100 years	100s – 1000s of years	Seasonal, < 10 years	> 10,000 years	< 100 years
Injection depth	> 800 m	Variable	> 800 m	Variable	> 1500m	> 800 m
Total injection volume	> 100 Mt		< 20 Mt		< 20 Mt	
Injection rate	~ 4 – 20 Mt/year	< 2 Mt/year	< 1 Mt/year		< 1 Mt/year	< 1 Mt/year
Injection fluid	CO_2	CO_2 (+ water, NG)	H_2S + CO_2	Natural Gas	Water, organics, other	Water
Reservoir Geometry	Saline aquifers, depleted hydrocarbon reservoirs	Depleted hydrocarbon reservoirs	Saline aquifers (open), depleted hydrocarbon reservoirs	Depleted hydrocarbon reservoirs salt caverns & aquifers	Saline aquifers	Saline aquifers
Number of wells	10s to 100s	< 675	1 – 3		1 – 3	2 - 4
Well types	Injection + monitoring, pressure maintenance	Injection & production	Injection	Injection & production	Injection	Injection & production
Well completion	Corrosion resistant	Corrosion resistant	Corrosion resistant			
Monitoring	Comprehensive; pre-, syn-, and post-injection	Variable; syn-injection/ production	At the Wellhead, syn-injection	Comprehensive; syn-injection	Wellhead, annulus	Variable, syn-injection/ production

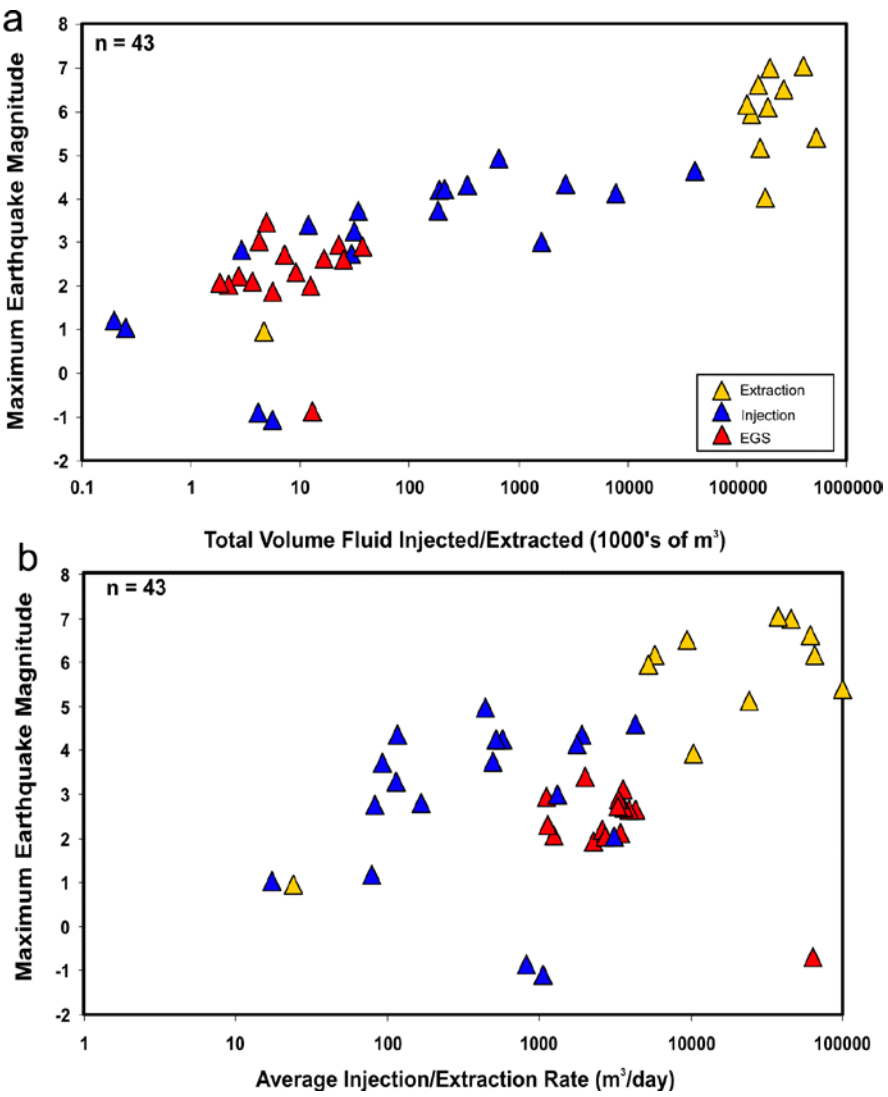

Figure 23: Maximum induced earthquake magnitude plotted against the total volume of fluid injected/extracted (top) and the average injection rates. Data and their sources for the graphs are presented in Table 1. These data are restricted to sites reported in the literature which are strongly biased towards the minority of examples where relatively high rates and magnitudes of seismicity were recorded (in the majority of cases induced seismicity was not detected and these could not be plotted on the graphs). Circled data for extraction sites indicate events >M6 for which the induced origin of these events remains contentious.

Injection Rate and Maximum Magnitude

A positive correlation between injection rate and maximum magnitudes has been observed at some sites. At Paradox Valley (Colorado, USA), for example, a total volume of 4 million m^3 of brine was injected at 4.3-4.8 km depth over 14 years. Most of the largest earthquakes occurred prior to ca. 1,400 days when the injection rates were about 50% higher than subsequent times (e.g., 22 L/s vs 13 L/s) (Figure 24). The largest induced earthquake at this site was M4.3, with 15 events of M greater than 2.5 felt locally and 14 of these occurring when injection rates were highest (Ake et al., 2005; Shapiro et al., 2007). A correlation between injection rate and the magnitudes of seismicity is widely inferred and is often attributed to a corresponding positive relationship between injection rate and increases in reservoir pressures (Healy et al., 1968; Raleigh et al., 1976; Smith et al., 2000; Ake et al., 2005; Baisch et al., 2006, 2009b). Increasing fluid pressures may trigger slip and earthquakes on pre-existing fault planes by decreasing the effective normal stress across these surfaces as proposed by Hubbert and Rubey (1959) and outlined in the modelling Section 7 of this report. The relationships between injection/extraction rate and maximum magnitude inferred for individual sites is not strongly supported by compilations of data from multiple injection and extraction sites (e.g., Suckale, 2009; Evans et al., 2012), perhaps partly because of insufficient data.

The compilation of data presented in Figure 23b shows a broad positive correlation between the average injection (or extraction) rate and the maximum induced magnitudes for sites compiled in Table 1. This relationship is to be expected for the data in Table 1 given that there are also positive relationships between fluid volume and maximum magnitude (Figure 23) and between volume and injection/extraction rates (Table 1). While arguments are frequently constructed in which higher injection rates lead to greater reservoir pressures which in turn lead to increases in seismicity rates and maximum magnitudes, it is presently not clear whether injection/extraction volumes or rates have the greatest influence on maximum magnitudes. The wide spread of data in Figure 23b is consistent with the view that relations between injection/extraction rates and seismicity vary between sites. One explanation for this variability is that factors in addition to injection/extraction rate and volume (e.g., pre-injection reservoir stress state and reservoir permeability, numbers, locations and strength of pre-existing faults, and duration of injection), could influence seismicity (Healy et al., 1968; Raleigh et al., 1976; Suckale, 2009; Evans et al., 2012). At many sites too few data are available to examine the interplay between these factors and seismicity.

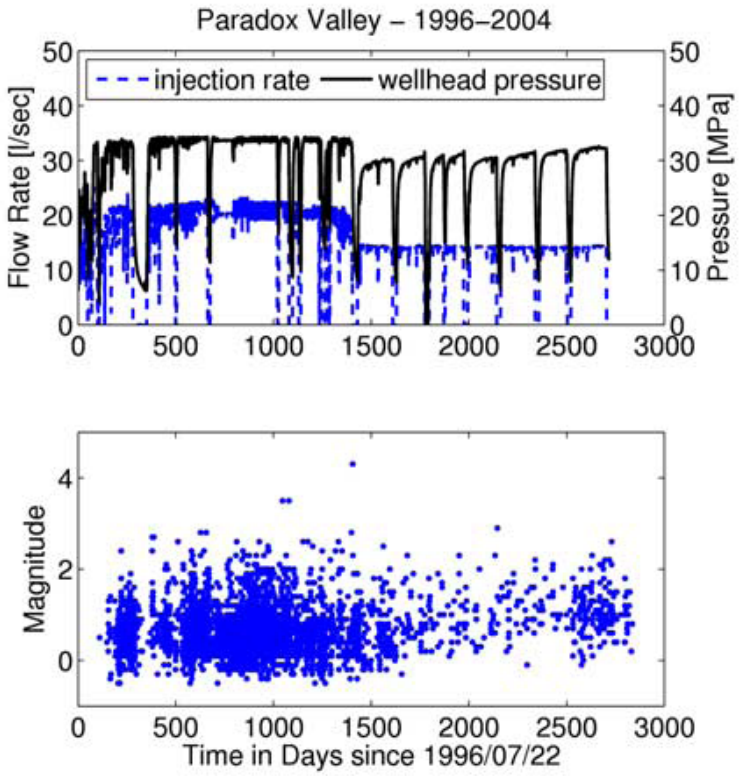

Figure 24: Variations in induced earthquake magnitude and frequency with changes to injection rate and wellhead pressure for injection operations at Paradox Valley, Colorado, USA during the period 1996-2004 (figure from Shapiro et al., 2007 and seismicity data original presented by Ake et al., 2005). Over 4,000 induced earthquakes were recorded by the 15-station Paradox Valley Seismic Network, which was installed in 1995 prior to the onset of injection.

Injection Rate and Seismicity Rate

The rate of induced seismicity is often positively correlated with the rate of injection (Healy et al., 1968; Raleigh et al., 1976; Zoback and Harjes, 1997; Charlety et al., 2007; Baisch et al., 2009a and b). Induced seismicity from Paradox Valley, for example, generally shows a positive correlation between numbers of earthquakes and injection rate for the duration of injection (Figure 24). Similar results have also been observed at Rock Mountain Arsenal (Healy et al., 1968), Rangely (Raleigh et al., 1976), KTB Borehole (Zoback and Harjes, 1997), Cooper Basin (Baisch et al., 2006, 2009a), Soultz-sous-Forêts (Charlety et al., 2007; Baisch et al., 2009b) and Basel (Ladner and Häring, 2009) sites. Our analysis of these data confirms the positive relationship between these parameters which, although showing significant temporal variability within individual sites, could be roughly linear in some cases. A correlation between the rates of injection and seismicity is most often attributed to higher reservoir pressures that accompany higher injection rates (Healy et al., 1968; Raleigh et al., 1976; Pearson, 1981; Smith et al., 2000; Ake et al., 2005; Baisch et al., 2006, 2009b). It should be pointed out that with a larger population of earthquakes, or with a larger volume of investigated crust, there will almost always be a higher probability of observing a larger magnitude earthquake due to the basic statistical distributions that earthquakes follow (Guternberg and Richter, 1954). Variations in geological and engineering conditions and data quality (e.g., recorded magnitude range and level of completeness) make detailed comparison of seismicity and injection rates between sites difficult.

Reservoir permeability and seismicity b-values

In addition to being dependent on operational parameters (e.g., volume and rate of injection/extraction) changes in reservoir pressures are also influenced by reservoir attributes, including rock permeability.

Table 3: Permeability and induced seismicity for the eight sites used to construct the plot in Figure 25. The data include the reservoir permeabilities, average permeability, range of b-values, and maximum induced magnitude at each site. Seismicity parameters are for the injection/extraction intervals. The data are from the publications indicated in the right-hand column and have not been re-evaluated as part of this study.

Site	Permeability range (mD)	Average Permeability (mD)	b-value range	Maximum EQ Magnitude	Reference
Cooper Basin	0.1-10	5.05	0.67-1.07	2.9	Baisch et al., 2006; 2009a
Basel	0.01-0.01	0.01	1.56	3.4	Ladner and Haring 2009; Bachmann et al. 2011
Cotton Valley	0.001-0.01	0.0055	2.5	-0.6	Shapiro and Dinske, 2009
Barnett Shale	0.000001-0.0001	0.0000505	2.5	-1.9	Shapiro and Dinske, 2009
Rocky Mountain Arsenal	32-178	105	0.6-0.9	5.5	Healy et al., 1968; Hsieh and Bredehoeft, 1981
Paradox Valley	1-1100	550.5	0.82	3	Ake et al., 2005; Shapiro et al., 2007
Rangely	0.1-1	0.55	0.81-0.96	3.1	Raleigh et al., 1976; 1972
Soultz GPK2	0.001-0.1	0.0505	0.9-1.2	2.9	Charlety et al., 2007; Baisch et al., 2009b; Dorbath et al., 2009
Soultz GPK3	0.001-0.1	0.0505	0.9-1.2	2.9	Charlety et al., 2007; Baisch et al., 2009b; Dorbath et al., 2009
Soultz GPK4 2004	0.001-0.1	0.0505	0.9-1.2	2.9	Charlety et al., 2007; Baisch et al., 2009b; Dorbath et al., 2009
Soultz GPK4 2005	0.001-0.1	0.0505	0.9-1.2	2.9	Charlety et al., 2007; Baisch et al., 2009b; Dorbath et al., 2009

Frequency-magnitude distributions for populations of earthquakes are typically described by the Gutenberg-Richter relationship (Gutenberg and Richter, 1954). For a population of N earthquakes greater than M, the relationship is as follows:

$$N = 10^{(a-bM)} \qquad \text{(Equation 1)}$$

where the *a*-value is related to the seismicity rate of the population. The *b*-value describes the relative proportion of small events to large events where a smaller *b*-value indicates relatively more large events in the region. Estimates of b-value are susceptible to errors due to incomplete recordings of earthquake magnitude bands and due to systematic bias introduced via the network for such things as magnitude estimates. For that reason, care must be taken in interpreting b-value results, particularly when full details of the network and data set are not available, as is the case here.

Over large populations of tectonic earthquakes *b*-values tend to be approximately 1.0 with higher *b*-values (e.g., 1-2.5) sometimes estimated for populations of induced events (Maxwell et al., 2009; Shapiro and Dinske, 2009; Bachmann et al., 2011; Shapiro et al., 2011). This increase in *b*-value has been attributed to decreases in permeability which promote the generation of many small new tensile fractures (Shapiro and Dinske, 2009). A recent study by Bachmann, et al., (2012) finds a decrease in b-value with distance from injection which they propose is correlated with a corresponding decrease in pore pressure.

A relationship with increasing *b*-value with decreasing permeability is hinted at by our analysis of permeability data ranging over 9 orders of magnitude (~0.000001 to 1100 mD) and presented in Table 3. Although limited in number, these data may indicate some preliminary observations regarding the relations between permeability and induced seismicity. Figure 25 plots the *b*-value against the reservoir permeability for eight selected sites where both *b*-value and reservoir permeability data are available (Table 3). It shows an apparent positive relationship between reservoir permeability and *b*-value for these sites. Sites with very low permeabilities (tight gas sand examples, e.g. Barnett Shale and Cotton Valley) display much higher *b*-values (ca. 2.5) than sites with higher permeabilities (0.6-1.3). The range of *b*-values at these higher permeability sites could produce profound differences in relative numbers of small and large earthquakes, however, due to the errors and potential errors in these estimates,we are careful not to draw any conclusions from this data. Table 3 indicates that in some cases increasing *b*-value at lower permeabilities are accompanied by decreased maximum earthquake magnitudes. This result is consistent with the findings of Shapiro and Dinske (2009) who suggest that increasing permeability could result in both an increase in maximum magnitude and a decrease in the seismic productivity.

Similarly, the data set suggests a change in b-value between tight gas and higher permeability sites in our limited data. High *b*-values have been attributed to fluid-rock interactions which result in localised pressure build-ups and the generation of many new small hydraulic tensile fractures (Shapiro and Dinske, 2009). These newly created small fractures produce high rates of seismic productivity and anomalously high *b*-values. By contrast, low *b*-values are attributed mainly to reactivation of slip on pre-existing fractures and may, in part, inherit the magnitude scaling relations (i.e., lower *b*-values and a greater number of larger earthquakes) of these earlier formed structures. At some sites both low and high *b*-values have been observed and appear to form by fracture reactivation and by initiation of new hydraulic fractures after and during injection, respectively (Maxwell et al., 2009).

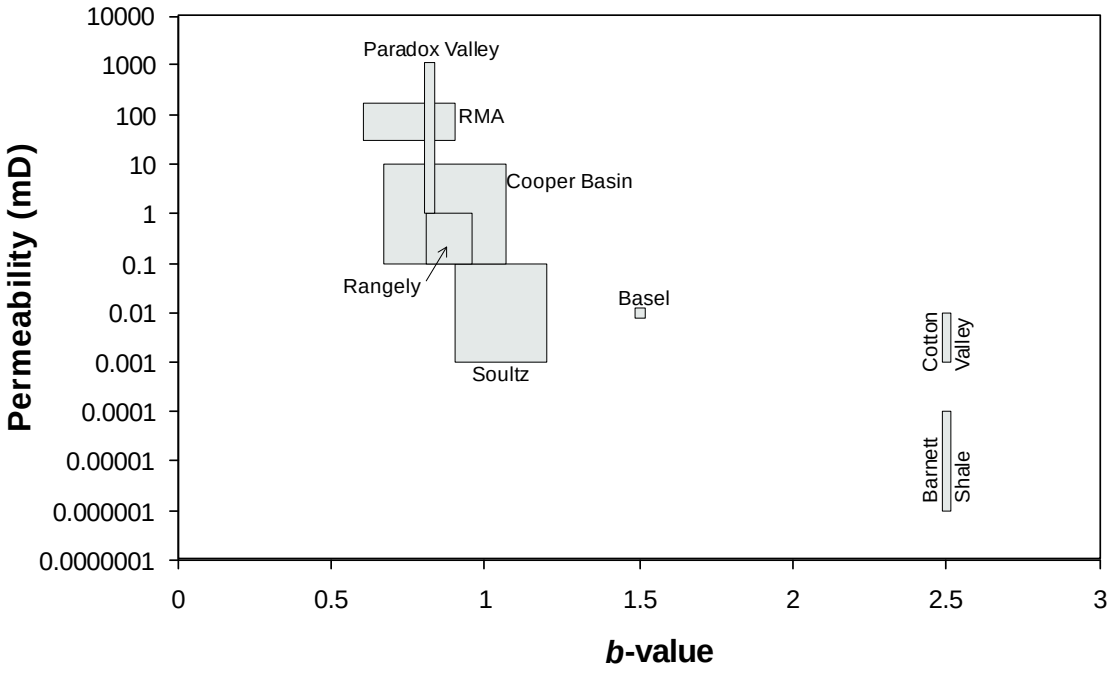

Figure 25: Range of reservoir rock permeabilities plotted against range of *b*-values for injection induced earthquakes at eight sites. Negative *b*-values are plotted as positive values (see Table 2 for data and references).

Spatial distribution of induced earthquakes

Predicting where induced earthquakes will occur is important for risk analysis and has been examined using the data compiled in Table 4. For the purposes of this report the location of an induced earthquake is measured by the depth and the radial horizontal distance of the earthquake epicentre from the injection/extraction well. The location of induced earthquakes have been analysed for all recorded events at some sites and the largest earthquakes at all sites in Table 4.

Depths of Induced Seismicity

The depth of earthquakes inferred to be induced by fluid injection or extraction operations are generally less than 10 km depth and in many cases are within 5 km of the surface (e.g., Nicholson and Wesson, 1992; Sminchak and Gupta, 2003; Suckale, 2009; Nicol et al., 2011). Induced earthquakes are most commonly located within, or immediately adjacent to, the depth of the reservoir. For fluid injection operations where the events are well-located (e.g., ≤±100 m) they often cluster around the reservoir defining an ellipsoidal volume which contains the reservoir and has a minor axis in the vertical direction (e.g., Figure 26). The shallow depths of induced seismicity and their general clustering about the reservoir interval are consistent with the compilation of injection data in Table 4. For the limited dataset presented in Table 4 the extraction induced earthquakes occur over a much greater depth range, and to far greater depths (>10 km) than the injection induced earthquakes. The greater focal depths for some extraction-related earthquakes have been interpreted to be a direct reflection of the fact that extraction of large volumes of fluids has the potential to induce crustal scale deformation and seismicity (see also McGarr, 1991; Grasso, 1992a; McGarr et al., 2002; Nicholson and Wesson, 1992).

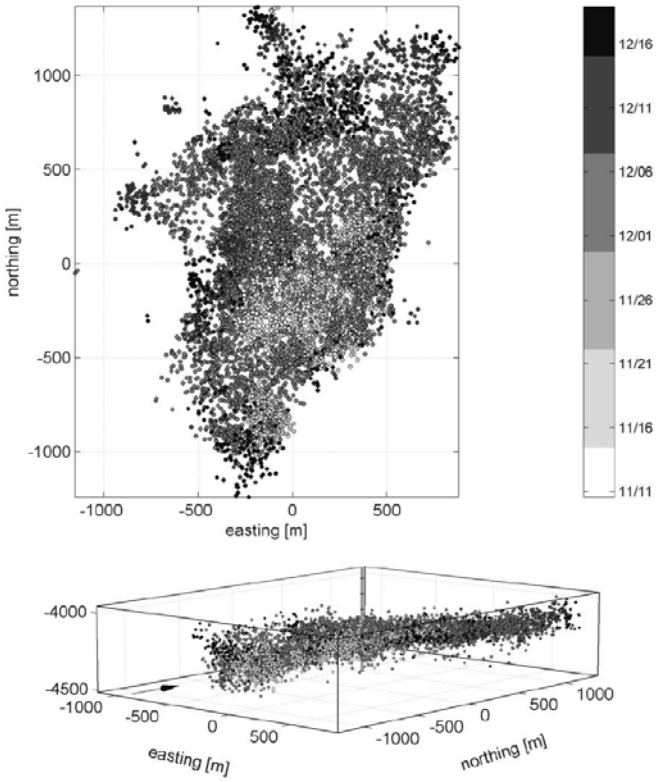

Figure 26: Induced seismicity epicentral (upper map) and hypercentral (lower diagram) locations with respect to the injection well (0, 0) during the first hydraulic fracture experiment at Cooper Basin, Australia. Timings of earthquakes with respect to the beginning of injection are colour coded where colours get darker with time following the onset of injection. Figure from Baisch et al. (2006).

Table 4: Data for injection and extraction sites used to construct the graphs in Figure 27, and Figure 28, including the reservoir name, average injection/extraction depth, depth range of main zone of seismicity, depth of largest magnitude earthquake, total volume of fluid injected/extracted, the maximum radius of seismicity from the injection/extraction site, and the earthquake timing relative to the beginning of injection normalised to the length of injection. Several of the sites have multiple injection/extraction operations over their lifetime, and data for these operations have been plotted individually.

Reservoir name	Average Inj/Ext Depth (km)	Seismicity Depth Range (km)	Depth Max M EQ (km)	Total Volume (1000's m3)	Seismicity Max Radius (km)	Max M EQ Normalised Timing	References
Injection							
Ashtabula	1.8	1.5-3.5	3.75	340	1	0.13	Seeber et al., 2004
Ashtabula	1.8	2-3.5	2.26	340	8	1.84	Seeber et al., 2004
Barnett Shale				2.7	0.6		Shapiro and Dinske 2009
Basel	5	3.8-5.2		12	1		Ladner and Haring 2009
Big Escambia Creek, Little Rock and Sizemore Creek	2.1	2-6			6	1.00	Gomberg and Wolf 1999
Cogdell	2.071	0-3	4.5	41450	5	0.64	Davis and Pennington 1989; Harding 1981
Cooper Basin	4.25	4-4.5	3	22.5	2		Baisch et al., 2006; 2009a
Cotton Valley				0.954	0.3		Shapiro and Dinske 2009
Dallas-Fort Worth	3.6	4.4-4.8		30.5	0.77	0.73	Frohlich and Potter 2010
Eagle West	2	3-4		7872		1.00	Horner et al., 1994
KTB	9.1	7.6-9.1		0.2	0.5	0.78	Zoback and Harjes 1997
Matsushiro	1.8	1-8		2.883	4		Ohtake 1974; Sminchak and Gupta 2003
Nojima Fault Zone	1.5	2-4		0.258	5.7		Tadokoro et al., 2000
Ogachi 1	1		6.5	5.443		0.82	Shapiro et al., 2007
Ogachi 2	1		3.8	4.147			Shapiro et al., 2007
Paradox Valley	4.3	3.5-6		2756.16	9	0.53	Shapiro et al., 2007; Ake et al., 2005
Paradox Valley	4.3	3.5-6		1620	9		Shapiro et al., 2007; Ake et al., 2005

Reservoir name	Average Inj/Ext Depth (km)	Seismicity Depth Range (km)	Depth Max M EQ (km)	Total Volume (1000's m3)	Seismicity Max Radius (km)	Max M EQ Normalised Timing	References
Rangely	1.9	1.25-4.25			3.5	0.03	Raleigh et al., 1976; 1972
Rocky Mountain Arsenal	3.671	4.5-5.5		646	6.2	1.25	Healy et al., 1968; Hsieh and Bredehoeft, 1981
Rocky Mountain Arsenal -1	3.671	4.5-5.5		210	6.2		Healy et al., 1968; Hsieh and Bredehoeft, 1981
Rocky Mountain Arsenal -2	3.671	4.5-5.5		189	6.2		Healy et al., 1968; Hsieh and Bredehoeft, 1981
Rocky Mountain Arsenal -3	3.671	4.5-5.5		30	6.2		Healy et al., 1968; Hsieh and Bredehoeft, 1981
Rocky Mountain Arsenal -4	3.671	4.5-5.5		180.5	6.2		Healy et al., 1968; Hsieh and Bredehoeft, 1981
Rocky Mountain Arsenal -5	3.671	4.5-5.5		34	6.2		Healy et al., 1968; Hsieh and Bredehoeft, 1981
Soultz-sous-Forets - GPK 2	5	4.25-5.5		25	0.9		Charlety et al., 2007; Baisch et al., 2009b; Dorbath et al., 2009
SSF - GPK 2 (1)	5	4.25-5.5		2.7	0.9	2.72	Charlety et al., 2007; Baisch et al., 2009b; Dorbath et al., 2009
SSF - GPK 2 (2)	5	4.25-5.5		16.56	0.9		Charlety et al., 2007; Baisch et al., 2009b; Dorbath et al., 2009
Soultz-sous-Forets - GPK 3	5	4-5.5		37	1.5	1.30	Charlety et al., 2007; Baisch et al., 2009b; Dorbath et al., 2009
Soultz-sous-Forets - GPK 4-1	5	4.25-5.25		9	0.6	1.13	Charlety et al., 2007; Baisch et al., 2009b; Dorbath et al., 2009
SSF - GPK 4-1 (1)	5	4.25-5.25		3.6	0.6		Charlety et al., 2007; Baisch et al., 2009b; Dorbath et al., 2009
Soultz-sous-Forets - GPK 4-2	5	4.25-5.5		12.5	0.6	0.58	Charlety et al., 2007; Baisch et al., 2009b; Dorbath et al., 2009

Reservoir name	Average Inj/Ext Depth (km)	Seismicity Depth Range (km)	Depth Max M EQ (km)	Total Volume (1000's m3)	Seismicity Max Radius (km)	Max M EQ Normalised Timing	References
SSF - GPK 4-2 (1)	5	4.25-5.5		7.2	0.6		Charlety et al., 2007; Baisch et al., 2009b; Dorbath et al., 2009
SSF - GPK 4-2 (2)	5	4.25-5.5		2.16	0.6		Charlety et al., 2007; Baisch et al., 2009b; Dorbath et al., 2009
Extraction							
Coalinga Eastside	2	10		270000	22		Segall 1985; McGarr 1991
Imperial Valley	1.5-3	10		157500	20	0.37	Glowacka and Nava, 1996
Victoria	1.5-3	12	10	190000	30	0.42	Glowacka and Nava, 1996
Cerro Prieto	1.5-3	5.6	10	547500	0	0.79	Glowacka and Nava, 1996
Fashing	3.2					1.03	Pennington et al., 1986; Davis et al., 1995; Segall 1989
Gasli	1.5	0-20	12	200000	25	1.17	Simpson and Leith 1985
Gasli	1.5	0-20	5.6	400000	25		Simpson and Leith 1985
Imogene	2.4		14	190720		0.83	Davis et al., 1995; Pennington et al., 1986
Kettleman Hills North Dome	1.5	11.4	8	123000	10	0.89	McGarr 1991
Lacq	3.5	0-9			12		Rothe 1977; Segal 1994
Montebello - Whittier Narrows	1.5	14.6	11.4	135000	7	0.93	McGarr 1991
Pau Basin	3.2-5.5	2.5-5			1		Segall 1989; Grasso and Wittlinger 1990
Seventy-Six			14.6	4.7			Rutledge et al., 1998
Strachan	3-5	4.7-5.2			5	0.16	Wetmiller 1986; Segall 1989
Wilmington		0.47-0.42		168288.057		0.03	Ritchter 1958; Kovach 1974

Areal Patterns of Induced Seismicity

Nearly all studies of induced seismicity for which the events are well located show strong clustering of earthquake epicentres (Raleigh et al., 1976; Zoback and Harjes, 1997; Baisch et al., 2006, 2009a, 2009b; Charlety et al., 2007; Suckale, 2009). Epicentres for earthquakes induced by fluid injection are generally clustered near to, and often enclose, injection/extraction wells (e.g., Figure 26). These clusters are typically well defined and contain 95% or more of the seismicity with roughly circular or elongate shapes (e.g., Figure 26). Elongation of the spatial distribution of induced seismicity epicentres is most commonly attributed to reactivation of pre-existing faults (e.g., Phillips et al., 2002; Sze, 2005; Ake et al., 2005; Arrowsmith and Eisner, 2006). The shape of the distribution may change through time due to reactivation and/or deactivation of pre-existing faults. For example, waste water disposal at Ashtabula, Ohio, induced a sequence of earthquakes during the year after injection began, on a fault ~0.7 km from the injection site. Fourteen years after that earthquake sequence, and seven years after injection operations ceased, a second earthquake sequence began on a fault ~5 km from the injection site, while the previously active fault remained inactive (Seeber et al., 2004). As discussed in Bachmann, et. al., (2011), post-injection induced seismicity behaves like a natural aftershock sequence where typical aftershock sequences can continue, with decreasing rates, for decades or more.

Changes in the shapes of the induced seismicity in map-view accompany growth in the areal extent of the seismicity, which is a widely observed phenomenon (Shapiro and Dinske, 2009). A clear example of seismicity migration throughout an injection operation is given by the Cooper Basin, Australia (Figure 26). During the first stimulation at this site, induced seismicity began in the area immediately surrounding the injection site and the radius of seismicity increased with both time and injected fluid volume. In the second stimulation, induced seismicity began in the area where seismicity had ceased in the previous experiment (Figure 26), and then migrated both toward and away from the injection site (Baisch et al., 2006; 2009a).

Growth in the size of induced seismicity clusters is consistent with the data in Figure 27. For the purposes of Figure 27 we have estimated the maximum radius of induced seismicity (i.e. the maximum horizontal distance from the injector well to the outer edge of the seismicity cluster) from published maps of induced seismicity. Figure 27 shows that with increasing cumulative volume of injection or extraction the maximum radius of seismicity also increases. Growth in the area of the induced seismicity may vary between sites due to changes in the Mc and the reservoir properties (e.g., porosities, permeabilities and reactivation of pre-existing faults). For example, the higher completeness for Paradox Valley (Mc=0.5) when compared to the other five sites ($-0.5 \leq Mc \leq -1.0$) (e.g., see Ake et al., 2005; Baisch et al., 2009a) may account for the shorter maximum radius for equivalent injection volumes at Paradox Valley (Figure 27). Higher Mc values may also decrease the radius measurements for the 16 additional sites (represented by yellow and grey diamonds in Figure 27), when compared to the detailed sites. Second, in some instances the increase in the maximum radius of seismicity is non-linear. In the case of Paradox Valley, which experienced a rapid increase in radius between ~100,000 and 600,000 m^3 of injected fluid, this increase has been attributed to reactivation of a pre-existing fault zone (Ake et al., 2005).

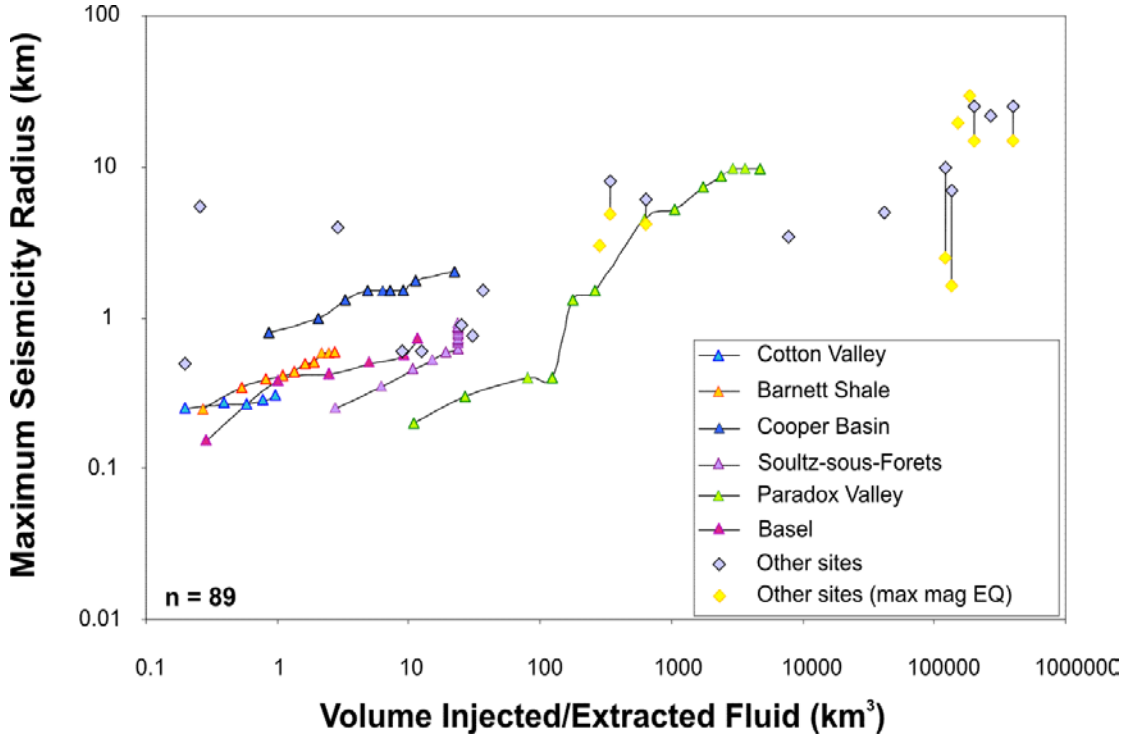

Figure 27: Maximum radius of induced seismicity from the injection well plotted against the cumulative volume of fluid injected at different stages of injection for six sites. Also plotted are an additional 16 sites where only the total injected volumes and the final maximum radius are reported (Table 4). Data for Cotton Valley and Barnett Shale are from Shapiro and Dinske (2009); Cooper Basin from Baisch et al., (2009a); Basel from Ladner and Haring (2009); Paradox Valley from Ake et al., (2005), and; Soultz-sous-Forêts from Baisch et al. (2009b).

Temporal Distribution of Induced Seismicity

Timing of Induced Seismicity

The timing of induced seismicity relative to the completion of injection/extraction operations has implications for risk. The risk to successful completion of injection would, for example, be much greater for an induced earthquake of moderate magnitude that occurs immediately after injection starts than for an event immediately prior to site closure. The seismic response to fluid injection/extraction is not instantaneous and may commence within hours to years of the onset of injection/extraction (e.g., Raleigh et al., 1976; Davis and Pennington, 1985; Rutledge et al., 1998; Shapiro et al., 2007; Shapiro and Dinske, 2009; Suckale, 2009). The timing of induced seismicity often follows the onset of extraction by years, consistent with the predictions of poroelastic modelling (Segall, 1985), while many injection operations generate a seismic response within days of the start of injection (e.g., Shapiro et al., 2007; Ladner and Häring, 2009; Shapiro and Dinske, 2009). For injection projects the majority of induced seismicity occurs during injection and the seismicity rate typically decreases after injection has ceased (e.g., Healy et al., 1968; Raleigh et al., 1976; Ladner and Häring, 2009). However, the timing of the largest events at each site may occur during or after the completion of injection/extraction. At Rocky Mountain Arsenal (M 5.1), near Denver (USA), for example, the largest magnitude earthquake occurred approximately 1 year after injection of 625,000 m^3 of contaminated waste water between 1962 and 1966. By contrast, at Basel a M_L 2.7 event was induced 6 days after injection commenced and caused the programme to be halted (Ladner and Häring, 2009). Several hours after the Basel 1 well was shut in the largest event (M_L 3.4) in the sequence occurred.

Clustering of Events

Describing the temporal relations between induced earthquakes in sequences and the manner in which they change through time has implications for seismic hazard. The Omori-Utsu law is a widely used law which can describe temporal clustering of earthquakes. The initial version of this law was first utilised to describe the decay in seismicity rate of the Nobi, Japan aftershock sequence in 1894 (Omori, 1894). The Omori-Utsu law (Utsu, et al., 1995) describes the relative productivity of an aftershock sequence and the decay in that rate through time:

$$N(t) = \frac{K}{(t+c)^P} \qquad \text{(Equation 2)}$$

K is the relative productivity of the sequence, *p* is the decay in productivity of the sequence, *t* is the time since the mainshock, and *c* is a constant related to the delay in onset of aftershock activity. A higher *p* indicates a relatively faster decay in aftershock productivity. As discussed in later sections, induced seismicity tends to follow similar clustering behaviour as tectonic earthquakes (Langenbruch and Shapiro, 2010; Bachmann et al., 2011; Barth, et al., 2011). Analysis of *p*-values of induced seismicity seems to indicate higher *p*-values and hence a quicker shut-off of activity than for normal tectonic aftershock sequences (e.g., Langenbruch and Shapiro, 2010; Bachmann et al., 2011).

In addition to the decay in seismic productivity, induced earthquakes have been investigated using inter event time distributions from six catalogues (Langenbruch et al., 2011). Using these catalogues from Basel and Soultz-sous-Forêts they concluded that the earthquakes are clustered in time and follow a non-homogeneous Poisson distribution. However, when transforming from the time domain to the injected volume domain, they find that the earthquakes are no longer clustered (i.e., they represent a homogeneous Poisson process). Their results suggest that coupling between events is weak and that injected volume is controlling the seismicity. They propose that using a Poisson model is appropriate for modeling of induced seismicity. Building on this type of model could provide a basis for predicting earthquakes at CCS sites and is further discussed in Section 7 of this report.

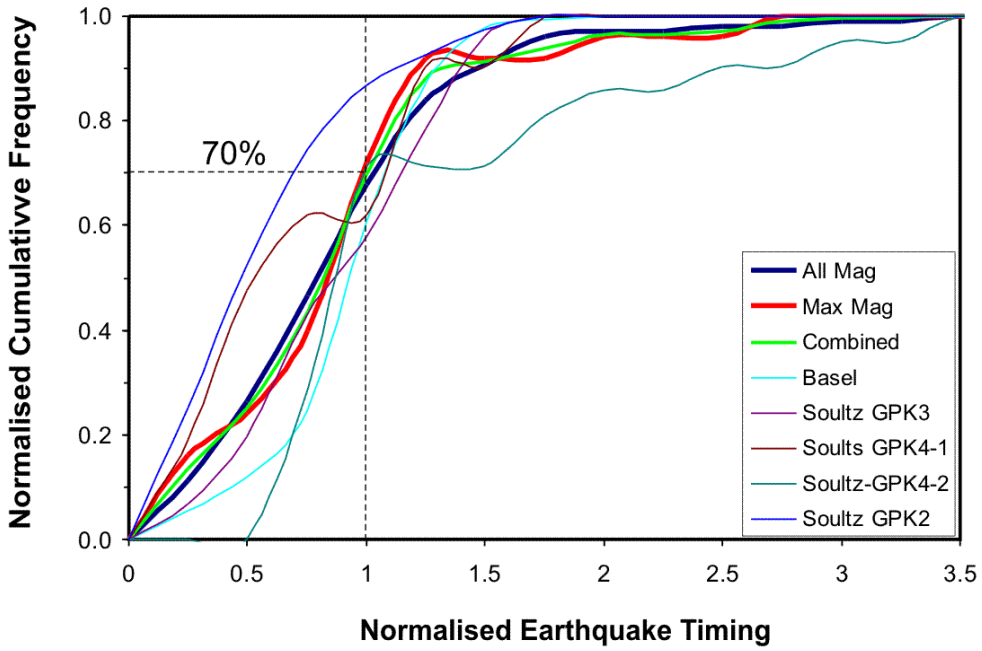

Figure 28: Normalised cumulative frequency plot of induced earthquakes for the sites in Table 4 and for all recorded events from the Basel and Soultz-sous-Forêts sites (Charlety et al., 2007; Ladner and Haring 2009). Thick blue, red and green lines show the timing for all data on the graph, maximum magnitude events and combined data, respectively (figure modified from Nicol et al., 2011). Timing has been normalised to the duration of injection/extraction.

To augment the general observations on the timing of induced earthquakes in the literature we have examined data from 21 sites in Table 4 and all recorded events at the Basel and Soultz-sous-Forêts sites (Charlety et al., 2007; Ladner and Haring 2009). To facilitate comparison of these data the timing of earthquakes has been plotted in Figure 28 relative to the duration of injection/extraction. The available data provide constraints for the timing of a range of earthquake magnitudes and are broadly similar for each of the curves in Figure 28a. The majority of induced seismicity (~70%) occurs during injection (i.e. normalised timing ≤1), with a further ~20% of the induced earthquakes occurring after operations cease between normalized times of 1 and 1.25. Importantly, the total duration of injection/extraction may include short shut-in periods of no injection, relative to the length of injection (e.g., Figure 24 top); the implications of this are not clear at this point and require further research. The remaining 10% of earthquakes occur over normalized times of up to 3.5 with an exponential decay of seismicity after injection stops (Figure 28). These data are consistent with previous observations (e.g., Nicholson and Wesson, 1992; Grasso, 1992a; Suckale, 2009; Evans et al., 2012), and support the view that the highest rates of seismic productivity can be expected during and immediately after injection/extraction.

Stress Drop of Induced Earthquakes

Goertz-Allmann, et al. (2011) estimated the stress drops for around 1,000 earthquakes induced in the Basel EGS project. Stress drop is a measure of the slip on a fault relative to the fault length and is often related to the local stress state in the crust and the fault strength; hence it can be related to pore pressure. For example, an increase in pore pressure may cause an increase in differential stress on the fault, which will result in relatively lower stress drop earthquakes. For the Basel earthquakes, Goertz-Allmann, et al. (2011) observed an increase in stress drop with increasing distance from the fault. They propose that stress drop may be used to map pore pressure changes in the reservoir and when using a linear pore pressure diffusion model, they find a good correlation of the pore pressure changes with the estimated stress drop changes.

Summary

Empirical induced seismicity data from injection and extraction projects have potential value for informing risk management decisions at CCS sites. This section reviews the observed relationships between induced seismicity parameters (i.e. maximum magnitudes, seismicity rates, b-values, timing and locations) and other reservoir or injection/extraction specific parameters (reservoir permeabilities together with injection/extraction volumes, rates and timing) from the literature. To test and augment these observations we have compiled data from the literature which permit preliminary conclusions to be drawn. The maximum earthquake magnitudes of induced earthquakes are generally ≤M4.5 but on very rare occasions may exceed M6. Both observations from the literature and our compilation indicate that the maximum magnitude of induced events may increase with total volume of fluid injected/extracted and the injection rate. The volume-maximum magnitude relationship may arise because larger volumes of injection fluid have the potential to modify the stresses in larger volumes of crust and to encounter larger faults. Rates of induced seismicity are also positively correlated with injection rate and may be attributed to the rise in reservoir pressures expected for higher injection rates. The rate of seismicity and the proportion of smaller to larger induced earthquakes in a sequence (i.e. the *b*-value for the Gutenberg-Richter relationship) also appear to increase with decreasing reservoir permeability. Reservoirs with low permeabilities (e.g., <0.01 mD) may have high rates of seismicity and *b*-values because they promote locally high stresses which generate many small new fractures. Induced earthquakes are typically spatially and temporally clustered. The depth of earthquakes inferred to be induced by fluid injection or extraction are mainly <5 km of the surface and located within, or immediately adjacent to, the depth of the reservoir. Clusters of induced seismicity grow in dimensions with injection time and increasing injected volume. Where induced events reactivate pre-existing large-scale faults they form elongate epicenter distributions which increase rapidly in dimension in the fault strike and dip directions. Most (~70%) induced events occur during injection with the number of events decreasing exponentially after injection/extraction ceases.

Predictive Modelling of Induced Seismicity

Predictive modelling of induced seismicity can be separated into two categories: 1) predictive statistical modelling; and 2) physical modelling; such models can be deterministic or probabilistic. Statistical modelling relies on fundamental laws of seismology (e.g., the Omori-Utsu law or the Gutenberg-Richter relationship) to predict the temporal, spatial and magnitude distributions of induced earthquakes. Currently these predictive models are not typically directly coupled with physics of the system and are based on the premise that what has happened in the past is most likely to happen in the future. Typically the models are based on relationships and parameters derived from "global data sets" comprising information from more than one region. If site or region specific data are available, the parameters may be optimised for the region of interest. For more complex models, the parameters may be optimised to a particular CCS project as CO_2 injection progresses.

Physical models endeavour to use the modellers understanding of the fundamental physical processes within the system to predict the seismic response to injection (e.g., Rutqvist et al., 2011). Physical models designed to simulate fluid flow within reservoirs have two main components, a "static model" and a "dynamic model". The static model represents the geological conditions of the reservoir and the injection site and is used as the starting conditions for the dynamic model. This static model is fed into the dynamic model which simulates the effect of the injected fluids on the reservoir and propagates the fluid through the system. Similar to the statistical class of models, the physical models attempt to predict the magnitude, spatial and temporal behaviour of induced earthquakes. Although not widely used outside the petroleum industry these terms have value because they help draw a distinction between the equations governing the physical processes ("dynamic model") and the input parameters used to populate these equations ("static model"). Differences in model output can derive from either changes in the dynamic or the static models. Drawing a distinction between the two components has value as it facilitates analysis of model uncertainties.

Statistical Predictive Modelling of Induced Seismicity

Using empirical seismicity relationships, such as the Omori-Utsu or Gutenberg-Richter relations, statistical models can be developed to predict the seismic behaviour of a CCS injection system. Because availability of induced seismicity data has been limited, and is probably heavily biased toward relatively seismically productive data sets, such predictive models are in the early stages of development. Much of the development of these models is being lead from the geothermal industry. Examples of such models range from predicting the maximum possible magnitude influenced by the geometry of the reservoir (Shapiro, et al, 2011) to predicting the frequency-magnitude and temporal distribution of earthquakes using methods that are based on well-established techniques in the study of aftershocks (Bachmann et al., 2011). In the following sections we explore several of the proposed models.

Predicting Maximum Magnitudes

Shapiro et al. (2011) have proposed a model for predicting the maximum possible magnitude that can be induced in a reservoir. They propose that the effective stress over a sufficiently large area of a rupture surface must be perturbed in order for a rupture of approximately that size to occur; in other words, the maximum possible magnitude is controlled by the geometric scale of the reservoir. By approximating a reservoir as an ellipsoid, they develop a model which indicates that the maximum possible magnitude is limited by the shortest axis of that ellipsoid. An assumption in the model

assumes that an earthquake's size (and rupture length) is predetermined before a rupture initiates; a fundamental question for which the seismological community has not reached a consensus. The authors show a good agreement of their model with a number of case studies and propose that by monitoring the spatial extent of induced seismicity, their model parameters can be developed and used to mitigate the earthquake hazard by limiting the spatial extent of the volume.

Predicting Probabilities of Future Earthquakes

Several models have been developed to predict the temporal evolution and magnitude distribution of induced seismicity (e.g., Parotidis and Shapiro, 2004; Langenbruch and Shapiro, 2010; Bachmann et al., 2011; Barth, et al, 2011). These models typically rely on the Gutenberg-Richter relationship and the Omori-Utsu law as described in section 7. Such models are now well established in the wider earthquake seismology community and have been utilised in multiple applications and studies (Ogata, 1998; Gerstenberger, et al., 2005; Lombardi, A.M. and Marzocchi, W., 2010).

Bachmann et al. (2011) have proposed a forecasting tool for induced seismicity based on Epidemic Type Aftershock Sequence (ETAS) models. An ETAS model differs from a simple Omori-Utsu sequence in that it allows for each earthquake (aftershock) to spawn its own aftershock sequence. Bachmann, et al, compared an ETAS based approach, with other modelling techniques, to the earthquake sequence induced by injection at the EGS in Basel, Switzerland in 2006. In retrospective testing, they found that an ETAS model that accounts for injection rate best predicted the observed seismicity when evaluated using likelihood based tests of the forecasts (Schorlemmer, et al., 2007). Bachmann et al. (2011) propose that such a model could be used in real-time to monitor the change in earthquake hazard throughout the life of an injection project. Such a tool highlights the possibilities for providing quantitative input into the risk management procedures for an injection project.

Two studies have specifically investigated modelling of the seismicity post-injection. Langenbruch and Shapiro (2010) built upon earlier work by Parotidis and Shapiro (2004) based on the assumption that pore pressure effects control the triggering of earthquakes in the reservoir. They develop a model for the seismicity rates through the life of an injection project with specific focus on the behaviour of seismicity post-injection. Similar to Bachmann et al (2011), they find that the rate and its decay can be modelled by the Omori-Utsu law. Langenbruch and Shapiro (2010) propose a model in which the decay rate of the Omori-Utsu law is proportional to the strength distribution of fractures within the reservoir; if the fractures are relatively weak a slow decay (i.e., a low p-value) is indicated. Qualitative comparisons of their model to two case studies and to synthetic data provide evidence in support of their model.

Similar to Bachmann et al. (2011), Barth et al. (2011) use both the Gutenberg-Richter relationship and the Omori-Utsu law to model the frequency-magnitude distribution and temporal decay of induced earthquakes; however they focus their model parameter development on the post shut-in phase. Using observed data from Basel, Switzerland and Soultz-sous-Forêts, they find results consistent with Bachmann, et al (2011) which show a decrease in the Gutenberg-Richter b-value (i.e., a decrease in b-value indicates a relatively larger proportion of large events) following the cessation of injection. Using a probability model they demonstrate how the decrease in the b-value following the end of injection can lead to a temporary increase in the probability of larger events.

A slightly different approach has been developed by Shapiro et al. (2010). They introduce the concept of the seismogenic index which characterises the seismotectonics of a local region and its expected seismic response to a stimulus such as injection of fluids. The seismogenic index can be empirically derived for a given injection site by its response to injection. Based on the seismogenic index, Shapiro

et al. (2010) develop a probabilistic model for the occurrence of future events during injection. Similar to the other models (Bachmann et al. 2011; Barth et al., 2011) they assume the occurrence of seismicity follows a Poisson distribution. Their model is combined with a Gutenberg-Richter relationship to derive the probability of occurrence for magnitude M or larger events during injection.

Testing of Statistical Predictive Models

A particular challenge in developing robust induced earthquake forecast models is in testing that the model performs as expected when tested in an unbiased fashion against data not used to develop the model. We distinguish this from history matching, which typically involves parameter optimization and does not normally involve prospective testing of models where a prediction is fully specified ahead of time and compared against observations at a later date (although in some cases this may be done). While history matching is valuable for parameter optimization, it is not necessarily informative about the true predictive power of the model or forecast tested. Earthquake forecast models, such as those described above, typically provide probability based forecasts which indicate the likelihood of observing an event of a particular magnitude or greater. Testing of probability based forecasts, although common for natural earthquakes, is not a straight forward procedure and is an active area of research in the larger seismology community (Schorlemmer et al., 2007; Zechar et al., 2010). Established techniques based on likelihood scores and the information gain per earthquake (Zechar et al., 2010) can be used to understand the consistency of the model with observed data and can be used to gain confidence in the appropriateness of using a particular model. However, because of the variability in behaviour of seismicity through time and space, developing robust forecast models will require testing over a large number of injection projects (e.g., the occurrence of maximum magnitude is by definition, a rare event, and is inherently difficult to test). The development and refinement of induced seismicity forecast models will be hindered until data for multiple projects are made widely available to the statistical seismology modelling community.

Physical Predictive Modelling of Induced Seismicity

Introduction

Early work related to understanding the link between stresses and fluids in the crust was carried out by Terzaghi (1923) who showed the effect of pore pressure on reducing effective normal stress. Later, Hubbert and Rubey (1959) described the effect of fluid pressure on failure of a pre-existing fault and proposed that an increase in pore pressure would reduce the effective strength of rock and thus weaken a fault. In 1968, Healy et al. first identified fluid pressure as a triggering mechanism for seismicity, after the injection of waste water into a deep well at the Rock Mountain Arsenal site.

Basic mechanisms for induced seismicity from introduction of excess pore pressure have been described in the literature (e.g., Zoback, 2007) where the injection of additional fluid changes the local stress field, and if the pressure of the injected fluid is too high, irreversible mechanical changes such as rock failure can occur. Ultimately, induced seismicity due to fluid pressure changes can result from two processes: either new faults are created by hydraulic fracturing or pre-existing faults are reactivated.

Hydraulic fracturing occurs when the fluid-injection pressure exceeds the rock fracture gradient (e.g., Majer et al., 2007). Although shear failure has been reported, tensile failure is most common and continues as long as the pressure remains higher than the fracture gradient. This can be intentional,

for example, one of the aims of hydrofracturing (e.g., EGS) is to increase the permeability of the reservoir through fracturing.

Basic stress failure analysis

Shear-slip on a pre-existing fault occurs if the shear stress acting on its plane is high enough to exceed its shear strength. The most fundamental relationship for fault slip is derived from the Coulomb failure criterion (e.g., Jaeger and Cook, 1979) (see Table 5 for a definition of symbols):

$$\tau = c + \mu_s \sigma'_n \quad \text{(Equation 3)}$$

Where from the effective stress law of Terzaghi (1923):

$$\sigma'_n = \sigma_n - P_f \quad \text{(Equation 4)}$$

and:

$$\mu_s = \tan(\varphi) \quad \text{(Equation 5)}$$

Table 5: Nomenclature of symbols.

Symbol	Definition
τ	Critical shear stress for slip occurrence
c	Cohesion of the fault
μ_s	Static friction coefficient of the fault
σ'_n	Effective normal stress
σ_n	Total normal stress
P_f	Fluid pressure
φ	Friction angle
σ_1	Maximum principal stress
σ_3	Minimum principal stress
δ	Angle between the fault plane and the σ1 direction
$\overline{P_f}$	Vertically averaged pressure
h	Hydraulic head
γ	Specific weight of the fluid
D	Hydraulic diffusivity
r	Distance from injection to seismic event
t	Time since the beginning of the injection

For 2D analyses, the shear and normal stress acting on a fault plane can be computed from the maximum and minimum principal stress (Figure 29a) using:

$$\tau = \frac{\sigma_1 - \sigma_3}{2\sin(2\delta)} \quad \text{(Equation 6)}$$

$$\sigma_n = \frac{\sigma_1 + \sigma_3}{2} - \frac{\sigma_1 - \sigma_3}{2\cos(2\delta)} \quad \text{(Equation 7)}$$

The Mohr-Coulomb criterion can be used to describe the response of a fault plans to shear and normal stresses; typically the criterion is visualised using Mohr circles as in Figure 2b and Figure 29b.

Figure 29b illustrates an increased likelihood of failure when pore pressure increases during injection of fluid, as both maximum and minimum principal effective stresses are reduced, shifting the Mohr circle closer to the failure envelope. One might think that a corresponding decrease in pore pressure e.g., during fluid extraction, would therefore suppress failure/seismicity; however, withdrawing large amounts of fluid also causes poroelastic contraction, and this induces stress changes in the surrounding rock that increase differential stress and therefore can also lead to faulting (e.g., Hillis, 2000).

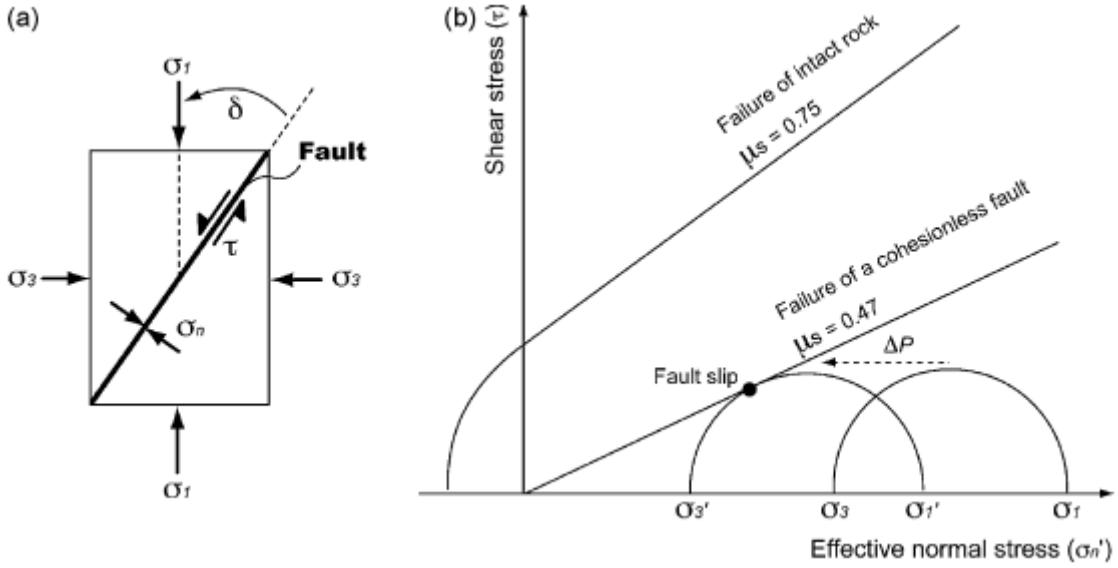

Figure 29: a) Normal and shear stresses resolved on a fault with a given orientation from the remote principal stresses. b) Mohr diagram of shear stress (τ) versus effective normal stress (σ'_n) showing how increasing fluid pressure (ΔP) may activate a well-oriented, cohesionless fault (causing fault slip) (from Cappa and Rutqvist, 2011a, Figure 30).

Initial principal stresses can be obtained from borehole stress measurements. The static friction coefficient, μ_s, of a pre-existing fault can be estimated from rock mechanical tests, and usually ranges from 0.6 to 0.85; however, it can also be as low as 0.2-0.4 when the faults contain weak clay gouge material (e.g., Morrow et al., 2000; Moore and Lockner, 2011).

Early attempts to analyse fault slip during reactivation of a pre-existing fault used analytical modelling (e.g., Streit and Hillis, 2004), relied on many assumptions (e.g., constant injection rate, homogeneous medium and properties) and were based on pre-injection stress characteristics corresponding to the remote or regional stress field. However, observations from depleted reservoirs show that the local stress field evolves in time and space during fluid injection (e.g., Hillis, 2001).

Effects of a fluid pressure increase on failure

Following Equation 3 and Equation 4, an increase in fluid pressure due to fluid injection may induce shear (i.e. slip) along a fault and it is of paramount importance to estimate the migration of the pressure front due to injection. In a study of induced seismicity produced by injection of nuclear waste water, Ahmad and Schmidt (1988) suggested that the pore-pressure increase depends upon three factors: 1) the rate of injection; 2) the reservoir permeability; and 3) the storage coefficient of the reservoir. Using these parameters reservoir pressure models can be constructed. Pressure changes due to fluid injection have been analysed, for example, using partial differential equation governing vertically averaged hydraulic head (h) buildup in the reservoir (Bear, 1979) as in Hsieh and Bredehoeft (1981). The vertically averaged fluid pressure increase $\Delta\overline{P}_{\mathrm{f}}$ is then obtained from h using:

$$\Delta\overline{P}_f = h\gamma \qquad \text{(Equation 8)}$$

Analytical estimates of fluid pressure effects on stresses are only feasible for simple geometries such as an infinite and anisotropic reservoir model, or a narrow fracture zone model when a single-phase fluid is injected. Such models are often too simplistic to explain complex phenomena and observations of real world injection experiments. For example, many model parameters such as permeability, fluid pressure and stress are inter-related. Induced seismicity can, for example, modify reservoir permeability which in turn will lead to a change in the reservoir response to fluid injection. This coupling produces non-linearity in the system which should be accounted for in the modelling procedure. The complexity and variability of the induced seismicity response to fluid injection is illustrated by observations summarized in Table 6.

Table 6: Summary and some examples of the main induced seismicity observations extracted from published literature.

Type of observation	Observation	Reference
Timing of the onset of seismicity	Immediately after the beginning of the injection (e.g., Rocky Mountain Arsenal waste water disposal, USA)	Hsieh and Bredehoeft (1981)
	Delayed from the onset of the injection (e.g., Cogdell Oil Field, USA)	Davis and Pennington (1989)
Occurrence of post-injection seismicity	Observed (e.g. Soultz-sous-Forêts EGS, France; Ashtabula waste water disposal, USA)	Baisch et al. (2010) Seeber et al. (2004)
Location of seismic events	Near field (around the injection well) (e.g., The Geysers geothermal field, USA)	Majer et al. (2007)
	Migration from near field to far-field (e.g., Cooper Basin geothermal field, Australia; The Geysers Geothermal Field, USA)	Baisch et al. (2006) Mossop (2001)
Number and size of seismic events	Low-magnitude events (e.g., Cooper Basin reservoir during the 2005 simulation)	Nicol et al. (2011)
	Large magnitude event (e.g., M = 3.4 event during the December 2006 injection at Basel, Switzerland; M > 2 after the injection stopped at Soultz-Sous-Forets, France)	Haring et al. (2008) Dorbath et al. (2009)
Correlation between injection rate and seismic activity	Observed (e.g., The Geysers geothermal field, USA)	Majer et al. (2007)
	Not observed (e.g., Rotokawa geothermal field, NZ)	Bannister and Sherburn (2007)
Correlation between injected volume and seismic events location	Maximum seismicity radius increases with volume injected	Nicol et al. (2011)

Additional factors influencing failure

Fluid temperature

Further complexity to the seismic response to injected fluids is provided by the effect of the injected fluid temperature on the stress field. If the injected fluid temperature is different from the surrounding rock, supplementary thermo-elastic strain may cause the medium to deform and potentially change the local stress state. If the fluid is hotter than the surrounding rock, the medium will expand; if the fluid is cooler, the medium will contract, potentially enhancing fracture openings and increasing permeability.

Poroelastic effects

Seismicity may be induced during fluid pressure depletion in oil fields. Pore pressure can change the magnitude of the minimum horizontal stress through the mechanics of poroelasticity (Hillis, 2000). This effect, not illustrated in the simple Mohr diagram of Figure 29, can cause failure during fluid extraction

in normal fault regimes. Depletion can also change the loading (overburden weight) and this may cause changes in the stress field bringing the system closer to failure.

Multi-phase effects and density changes

During CO_2 storage, the injected fluid is typically injected into the formation under supercritical conditions (where the CO_2 is held above the critical temperature and pressure in a supercritical fluid state). This allows more mass of CO_2 to be stored per bulk volume, as it has a higher density than when injected as a gas (see review by Shukla et al., 2010, and references therein). Once injected, the CO_2 can transition to multi-phase forms. For example, carbon dioxide which is injected at supercritical state into a saline aquifer forms a gas-like phase close to the injection zone, and partially dissolves in the aqueous phase (brine). This creates a multiphase (liquid, gas), multicomponent environment (NaCl, CO_2, water) thus complicating the prediction of pressure, density and flow considerably. Near an injection well, the supercritical CO_2 is less dense than the surrounding groundwater so will tend to migrate upwards and laterally due to density and pressure differences (e.g., Pruess et al., 2004). Over time, multiphase behaviour can initiate convective processes within the brine that can increase the rate of CO_2 uptake compared to diffusion alone, though this process may take hundreds or even thousands of years (Pau et al., 2010).

The initial development of the CO_2 plume involves the displacement of a wetting phase (brine) by a non-wetting phase (CO_2) similar to a drying process (Doughty and Pruess, 2007). A one-phase dry-out (gas) zone develops around the injection zone, surrounded by a two-phase zone (where CO_2 dissolves into the brine) then by a one-phase (liquid) brine zone. Accordingly, during injection, overpressure within the reservoir declines with distance away from the injection zone. This is shown in Figure 30 and Figure 31 (taken from Pruess and Garcia, 2002) where results are plotted as functions of the similarity variable (R^2/t) (Doughty and Pruess, 1992). As explained by the authors, these plots can be read as a snapshot in time, with radial distance R increasing along the x-axis, or they can be read as time-dependent data at fixed R, with time decreasing along the x-axis. For the latter interpretation, the figure indicates a pressure front migrating though the system in time; however, the study only considers behaviour for injection at a constant-rate, and does not describe post-injection pressure changes. Single phase fluid-mechanical models suggest that post-injection seismicity and pressure changes can occur as the high-pressure region diffuses away from the well (see following sub-section on post-injection seismicity).

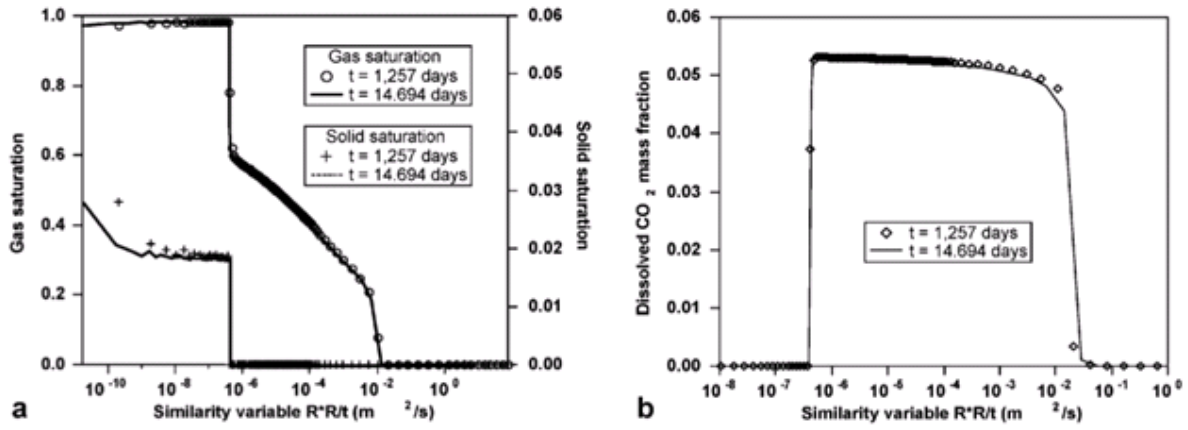

Figure 30: (from Pruess and Garcia, 2002, Fig. 6): a. Simulated gas and solid saturation, and b. Dissolved CO2 mass fractions as functions of the similarity variable. Simulation results are plotted at two different times.

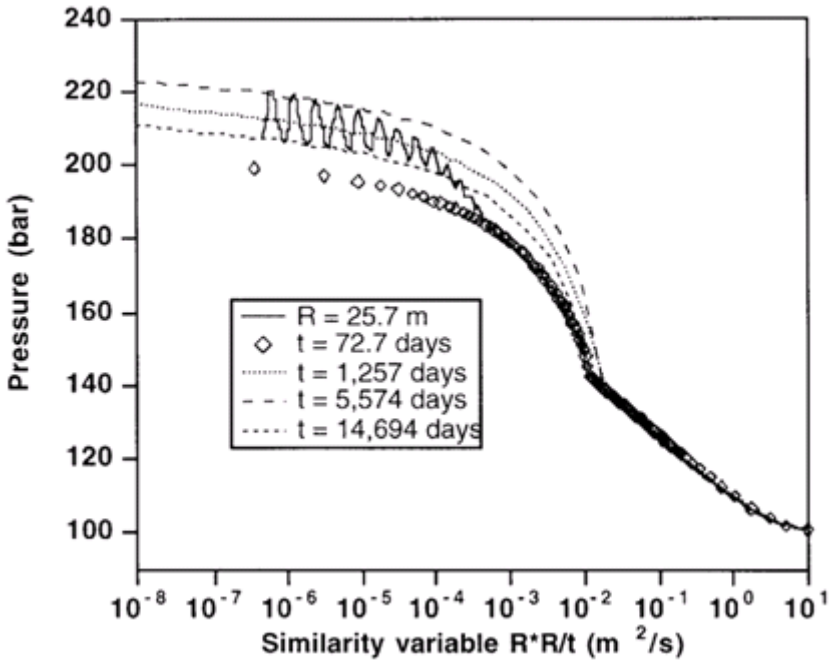

Figure 31: (from Pruess and Garcia, 2002, Fig. 7): Simulated pressures as function of the similarity variable. Arrows show interpretation either as increasing distance from the injection site, or time. The oscillations observed for *R* = 25.7m are attributed to discretization errors.

The experiments of Pruess and Garcia (2002) suggest consistent high pressures once the pressure front has passed. However, numerical experiments from Okwen et al. (2011), also assuming a constant injection rate, suggest that overpressure increases strongly at the beginning of the injection before decreasing slowly close to the well due to phase separation between the less dense and highly compressible carbon dioxide-rich (gas) phase and weakly compressible brine. These temporal variations in pressure near the well depend on the density contrast between the injected and native fluids, and vertical anisotropy of the injection formation. Mehnert and Okwen (2012) studied this effect for partially penetrating wells and confirmed that models predict lower pressures near the injection well perforation, but higher pressures occur near the top of the injection formation due to the buoyancy of CO_2. The pressure buildup close to the injection well will be higher if the formation is saline (compared to pure water) because of its higher viscosity. In the dry-out zone, salt may precipitate (Pruess and Muller, 2009) which can decrease the permeability of the medium, thus increasing the overpressure if the injection rate remains constant (according to Darcy's law).

Geochemical effects on formation integrity, permeability and faults

When CO_2 is injected into a deep aquifer, it can trigger geochemical reactions between the native fluid and the rock minerals comprising the aquifer formation. The dissolution and precipitation of various minerals in the formation can change its integrity and storage efficiency. Excess mineral dissolution can weaken the rock matrix and/or enhance porosity, increasing the risk of CO_2 escaping (e.g., Kharaka et al., 2006); conversely, precipitation of minerals such as carbonate helps bind CO_2 to the rock, potentially increasing storage stability. Precipitation may however also decrease porosity and permeability, enhancing pore pressure changes and decreasing the available volume for further bulk storage of CO_2. Since dissolution or precipitation cause changes in permeability, pore pressure and the strength of the rock matrix, they may impact on the likelihood of failure and induced seismicity.

The degree to which large-scale CO_2 injection induces changes in capillary trapping, dissolution, diffusion, convection, and chemical reactions depends partly on the nature of the formation and

aquifer into which it is injected. Xiao et al. (2009) used reactive transport modelling to investigate the trapping capacity and impact on reservoir rocks as a function of primary host mineral composition and the precise mixture of injected fluids. They found that significantly more CO_2 could be sequestered in siliclastic reservoirs compared to carbonate reservoirs; most injection scenarios caused a porosity increase close to the well and a porosity decrease away from it. Such predictions remain to be checked comprehensively in test CCS facilities; for example, at the Weyburn CO_2 monitoring and storage project in Canada, time-lapse geochemical monitoring is being undertaken in conjunction with reactive transport models in order to test the predictions from such models (Johnson, 2011). The timescale over which mineral reactions occur is problematic, as some reactions occur very slowly in nature. Shukla et al. (2006) note that reliable CO_2-brine-rock interaction models are still incomplete, that such models need validation against laboratory experiments and field data, and that without the ability to predict CO_2-fluid-rock interactions properly, there will always be some uncertainty regarding long-term effects of large-scale CCS projects on fluid pressures, and thus likelihood of frictional failure.

Only a few studies to-date have considered the geochemical effects of CO_2 on fault friction. Samuelson and Spiers (2012) concluded, based on direct shear experiments on simulated fault gouges relevant to a proposed CCS site, that the addition of brine or CO_2 did not significantly alter frictional properties of the gouge on short timescales. Determining the long term effects of CO_2 on fault rock behavior is challenging, because the necessary time scales cannot be accessed in laboratory experiments, and the topic of ongoing research.

Summary

To incorporate all of the effects discussed above, accurate predictions will only be obtained if we are able to account for:

- complex geometries involving the reservoir, caprock, and heterogeneities such as faults;
- multiphase flow of multiple fluids with heat transfer;
- coupled hydromechanical processes evolving through time (including poroelastic relationships between fluids, porosity and stresses);
- reactive transport and CO2-fluid-rock interactions, including dissolution and precipitation and their effect on aquifer and caprock permeability, porosity and strength
- tectonic loading

Currently, all of these effects can only be achieved via numerical modelling. However, analytical modelling can, for example, be used to get a first estimate of the maximum sustainable pressure before rock strength is exceeded during a fluid injection (Rutqvist et al., 2007) or to quickly assess potential storage capacity of sites (Schnaar and Digiulio, 2009).

Current State-of-the-art in Numerical Simulations: Numerical Procedures

Some numerical codes simulate fluid flow only, including TOUGH2 which is a simulator for nonisothermal flows of multicomponent, multiphase fluids in multidimensional porous and fractured media (Pruess et al., 1999). Other codes are primarily rock mechanics codes, such as ABAQUS (Borgesson, 1996) and FLAC (Itasca, 2009).

Coupling of fluid flow simulators to rock mechanics is still a significant challenge for numerical codes. Coupling TOUGH2 and FLAC (TOUGH-FLAC, Rutqvist et al., 2002) can, for example, account for the stress-dependency of permeability and porosity. However, TOUGH-FLAC does not employ “full coupling” as fluid and mechanical equations are solved sequentially rather than simultaneously. “Full” coupling via poroelastic equations is not yet a standard within models of CO_2 injection, and in addition, most codes do not explicitly model effects of fluid-mechanical interactions on seismicity.

Recently, other codes that sequentially couple thermo-hydro-mechanical processes have emerged, such as CODE_BRIGHT (Olivella et al., 1996), primarily designed for nonisothermal flow of brine and gas in saline media, and modified by Vilarrasa et al. (2010) to study CO_2 related problems. Such codes allow the simulation of complex fluid-mechanical feedbacks, for example the integrity of caprock (Rutqvist et al., 2007; Rutqvist et al., 2008; Vilarrasa et al., 2010) or possible reactivation of pre-existing faults (Rutqvist et al., 2007; Cappa et al., 2009; Cappa and Rutqvist, 2011a,b).

In numerical codes, the common procedure to derive a numerical solution for most problems can be summarized as:

- Step 1: choice of a mathematical model where the equations and the boundary conditions of the problem are defined.

- Step 2: discretisation of the problem in order to approximate the differential equations by a system of algebraic equations for the variables at a set of discrete locations in space and time. The most commonly used approaches in the geological sciences are: Finite Difference (FD) and Finite Element (FE). FD is the easiest method for simple geometries whereas FE can tackle more complex geometries and is more suitable when the domain changes during the simulation or when the desired precision varies over the domain. Usually, FE is used for analyses in structural mechanics whereas FD is preferred for fluid dynamics problems and when large deformation or non-linear material behaviors are involved. Both TOUGH2 and FLAC3D use a FD approach.

- Step 3: definition of the numerical grid which is a discrete representation of the geometric domain on which the problem is to be solved. This depends on the discretisation method chosen: structured (generally cartesian) grids are usually used with the FD approach while unstructured grids, where elements can have any shape, are best adapted to FE methods.

- Step 4: choice of a solution method for the system of algebraic equations (generally iterative, so that a convergence criterion is needed to stop the process) which depends on the problem: Jacobi or Gauss-Seidel methods are appropriate for linear equations whereas Newton's methods better suit non-linear problems.

For problems related to induced seismicity from fluid injection, the mathematical model (Step 1) needs to consider fluid flow equations coupled with elasticity models to assess when and where induced seismicity may occur. Governing equations for fluid flow, such as used by TOUGH2, describe the multiphase transport of several chemical species derived from Darcy's law and the elasticity model

relies on the equation of motion (as in FLAC3D). Then, a mechanical failure criterion needs to be defined; the most commonly used is the Mohr-Coulomb failure criterion.

Models can be 1D, 2D or 3D and typically involve an injection zone of CO_2, usually within an aquifer topped by a semi-permeable or impermeable caprock and possibly bounded by pre-existing fractures (Figure 32). Hydrologic and elastic parameters are defined for each component of the model as well as the duration of the injection and the injection rate. The coupling of TOUGH-FLAC, as presented by Rutqvist et al. (2002), accounts for the effect of stress changes on permeability, porosity and capillary pressure. Ideally, such models should also consider fluid and rock rheology such as the effect of frictional plasticity and/or creep on overpressure, but this remains challenging and is not currently addressed by numerical codes.

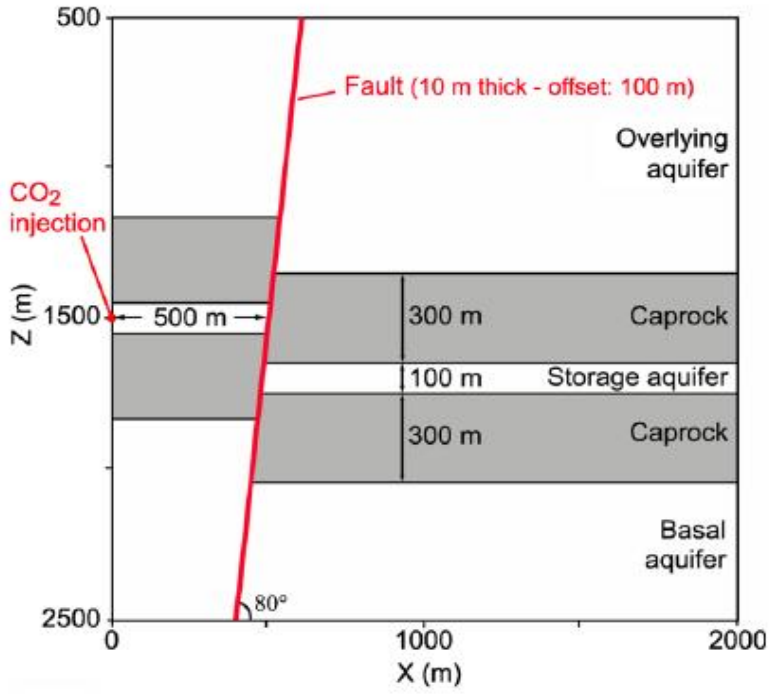

Figure 32: Schematic for TOUGH-FLAC modelling of discrete fault hydromechanical behavior during CO2 injection (from Rutqvist et al., 2007, Fig. 8).

To ensure that the size of the numerical problem remains manageable the grid should be appropriately designed for the problem of interest. For example, the mesh can be dense close to the injection zone if the purpose is to precisely assess small-scale effects around the injection well. If the objective is to see if the caprock remains intact through the simulation (due to density driven flow) or if a fault fails, then the mesh may be coarser close to the injection well but finer at the interface between the aquifer and the caprock/fault.

Both TOUGH2 and FLAC use the finite difference discretisation method and elements are usually rectangular. In FLAC, faults can be represented either by a zero-thickness interface (if the thickness is negligible compared to the size of the domain), or by an equivalent continuum using solid elements with a proper behavior (elastic, elasto-plastic or visco-plastic), or by a combination of solid elements and ubiquitous-joints oriented as weak planes (if the fault has strongly anisotropic mechanical behavior). Tests by Cappa and Rutqvist (2011a) suggest that results are similar for these differing representations of the fault.

Time-dependence: different processes dominant at different times

As summarized by Darcis et al. (2011), during CO_2 injection, the CO_2-rich phase spreads due to advective and buoyant forces, and is influenced by temperature effects, while dissolution and diffusion of CO_2 in the brine phase play a minor role. After the end of the injection, dissolution, diffusion and density-driven convection become the dominant processes while the advective and buoyant forces slowly decrease.

This time-dependence allows a potential simplification in the governing equations and modelling scheme according to the period of interest selected.

Post-injection seismicity

According to the Mohr-Coulomb criterion, failure is enhanced when the fluid pressure increases. Were this instantaneous failure criterion the only factor in play, then once injection stops, there should be no further induced seismicity, which is uncommon. Additionally, such delayed seismicity is also observed in reservoir impounding case studies (e.g., Howells, 1974; Bell and Nur, 1978).

To model better the time delay between cessation of injection and seismicity, Baisch et al. (2010) used a different approach to standard CO_2 sequestration models, by representing the fault by many smaller fault patches which may slip independently but are mechanically coupled to their neighbours (the so-called “block-spring” model). If a patch fails at a certain time step, its permeability increases for the next time step when fluid pressure is re-computed. With this approach, they managed to model occurrence of induced seismicity after the injection ceased, as well as the largest event of the sequence a couple of days after this shut-down. The time-scale over which seismicity persisted in their models depended on the failure-dependent permeabilities that were used. However, even without the fault patch approach, there will be a time-delay between the end of injection and the occurrence of seismicity as a result of fluid diffusion.

Characterisation of the Fracture Gradient

When fault reactivation is not a concern either because of the absence of faults or because of unfavourable fault orientation, induced seismicity may then be driven by the creation of new fractures in which the rock mass fails in tensile mode. Having a solid quantitative understanding of the pressure at which fracturing will occur is of first order importance for avoiding unwanted seismic activity. The fracture pressure generally increases with depth according to a fracture gradient, which is also the minimum horizontal stress gradient. The fracture gradient within a field or basin is usually based on borehole measurements from one or more wells. The most common tests used to determine the fracture gradient are leak off tests (LOT) or mini-frac tests. A leak off test (LOT) is a pressure test that is conducted immediately below a newly cemented casing shoe. During the test, mud is pumped into a newly drilled interval below the shoe, resulting in a pressure increase which is linear with time. At some point, mud loss into the formation accelerates and the pressure increase deviates from linear, indicating the onset of fracture formation. The pressure at which this occurs is referred to as the “leak off point”, and is generally taken to be broadly representative of the minimum horizontal stress. An extended LOT is very similar to a LOT, except that the test is continued past the leak off point until the formation breaks down via fracture propagation (Figure 33). Following fracture propagation, pumping ceases and the pressure is allowed to decay so that a fracture closure pressure (FCP) can be determined using a double tangent method. The FCP is an accurate measure of the minimum horizontal stress. ELOTs also involve successive pressurization and fracture propagation cycles which have the benefit of confirming the results of earlier cycles. Furthermore, during the second cycle and

beyond, the tensile strength of the formation does not need to be overcome as fracture formation has already been initiated.

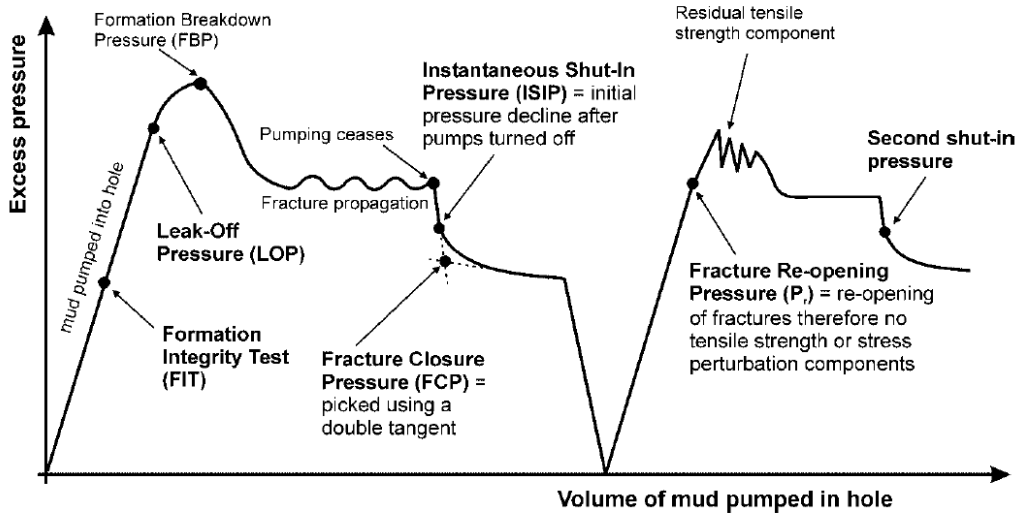

Figure 33: Illustration of an idealized extended leak off test (ELOT). The best estimate of the minimum horizontal stress is taken from the fracture closure pressure, which is determined by a double tangent method (White et al., 2002).

Mini-frac tests are similar in principle to an ELOT, albeit on a much smaller scale and with much better spatial control on fracture propagation. During a min-frac test, it is possible to isolate an interval as small as about 1 m, meaning that multiple measurements can then resolve changes in the fracture gradient which are usually caused by lithological variability. A mini-frac testing programme is performed once a well has been drilled and involves isolating an interval with inflatable packers, and then pressurising the interval until a fracture forms. Subsequently, pumping is stopped and the pressure allowed to decay, with the fracture closure pressure determined using the double tangent method (described previously). It is necessary to conduct multiple pressurization and propagation cycles during mini-frac testing, to ensure that the fracture propagates a distance of at least 4 borehole radii (and preferably 6-7 radii) so that wellbore stress distortion effects are eliminated (Carnegie et al., 2000). A detailed example of how LOT's, ELOTs and multiple mini-frac tests can be used to gain a better understanding of the fracture gradient can be found in Tenthorey et al. (2010).

In the previous paragraph, non-linearity of the fracture gradient was alluded to, and is certainly a topic that should be expanded upon for the purposes of this report. Leak of tests or mini-frac tests yield important information regarding fracture gradient immediately surrounding the well bore, under the prevailing fluid pressure conditions. However, injection or withdrawal of fluids from the reservoir can inherently alter the magnitude of the horizontal stresses via poroelastic effects, thereby changing the fracture gradient. This is generally referred to as the reservoir stress path and its effect on the reservoir and caprock may be understood conceptually as follows. As a liquid or gas is injected into a reservoir, pore fluid pressure builds up and the reservoir tries to expand in all directions (Figure 34). As the reservoir tries to expand laterally, there is a counteracting force that is imparted into the reservoir which causes the minimum horizontal stress to increase. In a normal faulting or strike slip faulting environment, an increase in the minimum horizontal stress does not favour reactivation of faults, but rather "stabilizes" existing faults by reducing the shear stress/normal stress ratio on the fault surface. However, the expected stress change in the overlying caprock is expected to be significantly different. This is due to the fact that the whole system must stay in equilibrium with the far-field stresses, and that elevated minimum horizontal stress (σ_h) at reservoir level will be counterbalanced

by reduced σ_h in the caprock above the reservoir and also in the formation below the reservoir. This is an example of stress transfer within a reservoir-caprock system. The implication of such a scenario is an increased propensity for tensile fracturing and reactivation of steeply dipping normal faults within the caprock (Figure 34), which may eventually cause induced seismicity.

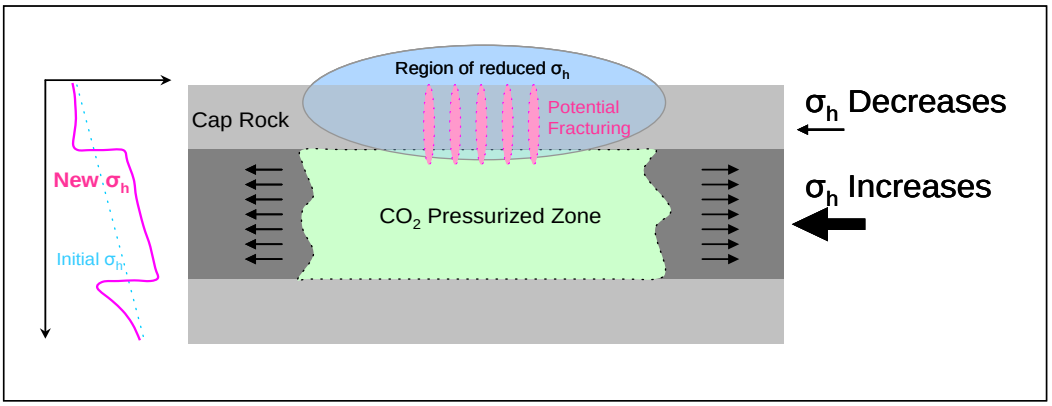

Figure 34: Schematic illustration to explain conceptually how the reservoir stress path operates. As a reservoir is pressurized with CO_2 or any other fluid, the reservoir tries to expand laterally due to poroelastic deformation. However, because the reservoir is confined laterally, the minimum horizontal stress increases together with the increase in pore pressure, albeit at a reduced rate. The increase in the minimum horizontal stress at reservoir level leads to a corresponding decrease in horizontal stress in the cap rock due to stress transfer processes. This reduced stress in the cap rock may lead to potential fracturing due to a lowering of the fracture gradient. The insert at the left of the diagram shows how the fracture gradient evolves from a linear state before injection, to one which varies significantly depending on the degree of pressurisation (modified from Marsden, 2007).

In summary, tests to measure the fracture gradient in advance of an injection or withdrawal project are not certain to accurately predict the pressure at which fracturing will actually occur. The measured fracture gradient should instead be used as a guide and operators must be aware of the properties of the rocks in, above and below the reservoir, as their mechanical properties will control the extent of stress transfer within the system. Having a solid understanding of the expected reservoir stress path is crucial to minimizing the risks associated with fluid injection or withdrawal, as it can enhance or impede fracturing in different parts of the system. In complex systems with heterogeneous lithologies it is therefore desirable to have detailed geomechanical models at ones disposal, as these simulations will allow the fracture gradient to be predicted both in terms of magnitude and spatial variations.

Summary of Statistical and Physical Modelling

Two main types of models have been used for modeling and predicting seismicity induced by fluid injection. Both classes of models, statistical and physical, are in the relatively early stages of development. A number of statistical models have been developed to predict the temporal evolution, maximum magnitude and magnitude distribution of induced seismicity during and after injection. These statistical models, which were primarily developed for geothermal systems, typically rely on the Gutenberg-Richter relationship and/or the Omori-Utsu law and assume the occurrence of seismicity follows a Poisson distribution. Statistical models are now well established in the wider earthquake seismology community and could be developed to predict the seismic behaviour of a CCS injection system. A particular challenge in developing robust statistical models to forecast induced earthquakes will be to test that they produce expected, unbiased and reproducible results. The development and refinement of induced seismicity forecast models will be facilitated by induced seismicity data for multiple projects being made widely available to the statistical seismology modelling community. For current use in risk assessment, the most robust results are most likely to be driven by statistical

modeling (as discuss in Section 8 Risk Assessment and Management), however, any such assessment will likely be best served by an ensemble model (i.e., the use of multiple models) and we expect that physical modeling will increasingly provide an important contribution to such ensemble models.

Many interacting factors contribute to the production of induced seismicity by fluid injection. Numerical physical models must fully couple fluid flow of different chemical species within a porous and fractured medium to elastic (and ideally, also inelastic) behavior of the medium to account for the non-linearity effects. Current numerical techniques are able to model multiphase flow and, in some cases, to couple fluid flow simulations with elastic models (e.g., TOUGH2-FLAC) to account for effect of pressure and temperature on strain/stress as well as the effect of strain/stress on permeability and porosity. Current models can highlight geometric and dynamic cases with significant risk of induced seismicity. Such models can be used to identify cases where the risk of induced seismicity can be minimized or avoided by adapting injection strategies. The utility of these models is strongly dependent on the quality of the input data, including knowledge of the: 1) orientation and magnitude of the local stress field; 2) the local fault network including any faults which may be effected by the pressure front; 3) the hydraulic properties of the medium, such as permeability, diffusivity; and 4) the elastic properties of the medium, such as elastic moduli and thermal expansion coefficient. Obtaining these data and testing the model outputs using induced seismicity data will be critical for improving the utility of numerical physical models.

Risk Assessment and Management

Introduction

The primary objective of commercial-scale CCS projects is to safely store millions of tonnes of CO_2 indefinitely to prevent large quantities of greenhouse gas entering the atmosphere. Risk assessment and management will be important components of CCS projects (Benson, 2005; IPCC, 2005; Stenhouse et al., 2005, 2006; IEAGHG, 2009; NETL, 2011; DNV, 2011; European Commission, 2011). They have been employed in many industries to understand better the likelihood and consequences of factors, such as those relating to economics or health, safety and environment (HS and E), which could have adverse effects on a particular operation or project. Risk assessment (i.e. identifying risk events together with their likelihoods and consequences) provides an important decision making tool that aids the management of potential risks (i.e. identification and implementation of risk reduction and mitigation measures). Risk management is an iterative process which develops as more information is gathered, uncertainties are reduced, new risks are identified and measures introduced to limit the impact of the risks. Risk assessment and management practices vary according to whether assessment encapsulates part or all of the sequestration process (i.e., capture, transport and/or storage), includes some or all risk factors (i.e. social, economic, engineering and/or geological), and the extent to which they are conducted before, during or after injection (Benson, 2005; IPCC, 2005; Stenhouse et al., 2005; IEAGHG, 2009; DNV, 2011).). Many tools and strategies are available for systematic and robust risk assessment of a CCS project (e.g., the references in this paragraph). In this section we focus on the specific needs of risk assessment related to induced seismicity.

Fluid injection and extraction projects over the last 70 years suggest that the injection and long-term storage of CO_2 could induce small to moderate magnitude earthquakes and large events at a low probability (e.g., Healy et al., 1968; Kovach, 1974; Raleigh et al., 1976; McGarr, 1991; Nicholson and Wesson, 1992; Van Eijis et al., 2006; Shapiro and Dinske, 2009; Baisch et al., 2009a and b; Suckale, 2009, 2010, Verdon et al., 2010b; Evans et al., 2012). Given the large volumes of CO_2 to be injected, it will become increasingly difficult to separate natural from induced seismicity; this may have potential complications for liability issues. For the majority of fluid injection or extraction projects induced seismicity has not significantly disrupted operations. Maintaining this record requires that we select sites judiciously and employ risk management to minimise the impact of these risks. One of the principal reasons for studying induced seismicity arising from injection of CO_2, and a key driver for this report, is to assess and manage risk. The risks presented by induced seismicity are variable and include those outlined in Table 7. Of these risks the lack of public acceptance and support, damage to infrastructure (and private property), and seal rupture may demand particular attention. The level of risk for each event will, however, vary between sites dependent on many factors, some of which may be unknown, but including proximity of CO_2 storage to populated areas, depth of injection, local site and rock conditions (e.g., pre-injection pressures and numbers of pre-existing faults), levels of background natural seismicity, injected volume and the dimensions of the reservoir, and uncertainties in the available data (Shapiro et al., 2011; Evans et al., 2012). Injection at sites with low natural seismicity in Europe, for example, typically does not produce felt events, suggesting that a low natural seismicity level may be a useful indicator of low induced seismicity risk, although the converse is not necessarily true (Evans et al., 2012). These factors highlight the importance for assessing risk of induced seismicity, of having good knowledge of the natural background seismicity, of the local geological setting, of the key stakeholders and of public opinion.

Thresholds for triggering unacceptable risk for each of the events in Table 7 will likely vary between sites and for different variables at the same site. For storage sites beneath, or close to, populated areas shallow (< 5 km hypocentral depth) induced earthquakes as small as M2 may be felt and raise public concerns that larger events are imminent. Public awareness and, in some cases, opposition to sub-surface operations such as hydraulic fracturing in the petroleum industry has increased in the last two years. Negative public opinions towards hydraulic fracturing and associated induced seismicity may increase project risks. These risks may be reduced by increasing our understanding of the behaviour of induced seismicity and controlling the reservoir conditions to minimise its occurrence and by engagement with public who are interested in the storage site (Bradbury et al., 2011; Kuijper, 2011). As with any risk assessment, effective communication of the state of knowledge in the project is key. Communication strategies are beyond the scope of this report, but by increasing our knowledge of induced seismicity, we can better inform all stakeholders involved in these discussions. With increasing distance from the storage site the magnitude of the smallest felt earthquake increases. Proximal (e.g., <10 km) earthquake magnitudes as low as M2 may be felt and could trigger public anxiety about project safety, while damage (either structural or cosmetic) is more likely to result from shallow earthquakes with magnitudes of ≥M3-4. While small events may not cause structural or reservoir damage, or increase the likelihood of leakage, the potential for such events could mean the risk of loss of public support for sites close to populated areas is significant, even when compared to other risk factors triggered by larger magnitude events. A key issue will be that of risk tolerance. It will be very unlikely to be able to absolutely exclude the possibility of a larger event (e.g., M≥5-6) and therefore, even though that probability may be very small, a policy of zero-risk tolerance will be challenging.

Table 7: Risk register for induced seismicity of CCS projects (Majer et al., 2007, 2008, 2011; Nicol et al., 2011).

Event	Cause	Mitigation
Incomplete operational framework	Uncertain whether earthquakes induced or natural. Acceptable earthquake magnitudes and risk poorly defined. CCS legislation and regulations for induced seismicity incomplete. Long-term liability for induced seismicity unresolved. Insurance/reinsurance for induced events not available.	Establish scientific and legal criteria for discriminating natural and induced earthquakes. Set acceptable earthquake magnitude thresholds for individual sites. Governments regulate CCS and accept long-term liability for induced events.
Lack of public acceptance and support	Small (M2-3) events felt raising safety issues and public concerns. Lack of trust of government and CCS operating companies releasing information on induced earthquakes. Low tolerance to risk.	Educate and consult about induced seismicity and risks. Transparent assessment and decision making process for induced events by government and CCS operating companies. Robust risk assessment and monitoring and verification programmes
Fragility of infrastructure, private property and human life	Damage to CCS and public infrastructure during induced earthquakes. Damage to private property. Loss of life.	Design CCS infrastructure to restrict damage associated with M3-5 events. Robust risk assessment and monitoring programmes. Maintain reservoir pressure below predetermined values (e.g., fracture gradients). Introduce pressure relief wells.
Human activity interference	Disruption of human activities by shaking/vibration or noise. Loss of sleep. Business disruption and loss of income.	Consult with community to ascertain level of concern. Mitigate to reduce magnitude and frequency of induced seismicity. Financial compensation.
Unexpected migration pathways	Earthquakes open unexpected fluid-flow pathways. Earthquakes rupture the seal allowing leakage of CO2.	Monitor location of the CO2 plume. Monitor leakage of CO2 at the surface and contamination of resources. Introduce migration management wells.
Not economically viable	Cost of data acquisition, numerical modelling and seismic monitoring too high. Revenue decrease due to decrease of CO2 injection rates or cessation of operations arising from unacceptably large induced earthquake. High cost of remediation following earthquake.	Increase price of carbon via taxation. Decrease the cost of CCS. Additional government funding (if considered of vital importance). Seek insurance for financial loss due to natural and induced earthquakes.

Event	Cause	Mitigation
Environmental Disruption	Fauna and flora interference. Habitat destruction.	Survey environment to determine level of disruption. Mitigate to reduce magnitude and frequency of induced seismicity. Restore environmental conditions. Relocate fauna and flora.

An understanding of the expected size, number, location and timing of induced earthquakes is required for risk assessment, management of seismicity generated by injection of CO_2, and for informing the public of the potential for induced earthquakes (see Sminchak and Gupta, 2003; Bommer et al., 2006; Majer et al., 2011; Myer and Daley, 2011; Nicol et al., 2011). This understanding could be achieved by data collection and modelling (initially undertaken prior to injection) and/or by microseismic monitoring for at least the duration of injection. While the general characteristics of potential induced earthquakes may be inferred from global empirical data (Section 6), detailed site specific analysis will generally be heavily reliant on modelling (Section 7) and seismic monitoring (Section 8.3). Forecasting future earthquakes arising from the storage of CO_2 using statistical and physical models requires information about the state of stress in the reservoir (and surrounding rock) prior to, during and after injection together with rock properties, including the presence of pre-existing faults or fractures, and earthquake temporal relationships (e.g., Rutqvist et al., 2002, 2007, 2008; Parotidis and Shapiro, 2004; Pruess et al., 2004; Zoback, 2007; Baisch et al., 2010; Langenbruch and Shapiro, 2010; Cappa and Rutqvist, 2011a and b; Bachmann et al., 2011; Barth, et al, 2011; Shapiro, et al, 2011). Alternatively, monitoring of induced seismicity alone may be considered appropriate if it can be argued, for example, that insufficient information will be available (at an acceptable cost) to constrain future events and/or that the risk of these events to stakeholders and infrastructure is low. However, reducing management of induced seismicity to monitoring coupled with mitigation fails to address the possibility that a larger than expected earthquake (e.g., magnitude 3-5) causes sufficient damage and public anxiety to terminate a project or operation. Such a scenario occurred in the Basel geothermal project during 2006 when, in a matter of hours after the commencement of injection, a magnitude M3.4 earthquake at 5km depth resulted in damage in Basel (Ladner and Häring, 2009; Bachmann et al., 2011). Therefore, it is recommended here that for commercial-scale projects both data acquisition/modelling and microseismic monitoring pre, syn and post injection be undertaken. For smaller pilot projects (e.g., injection of 10s of thousands of tonnes CO_2 over months) injection of CO_2 is less likely (than commercial-scale projects) to induce >M2 events (Figure 31a) and may pose a correspondingly lower risk to successful completion. However, such projects are proving useful for demonstrating the viability of CO_2 storage, for building the available databases and for improved understanding of seismicity induced by CO_2 injection. It may, therefore, also prove worthwhile to undertake both data acquisition/modelling and microseismic monitoring for pilot projects. The design and output from microseismic monitoring at CO_2 storage sites is discussed further in the Section 8.3.2.

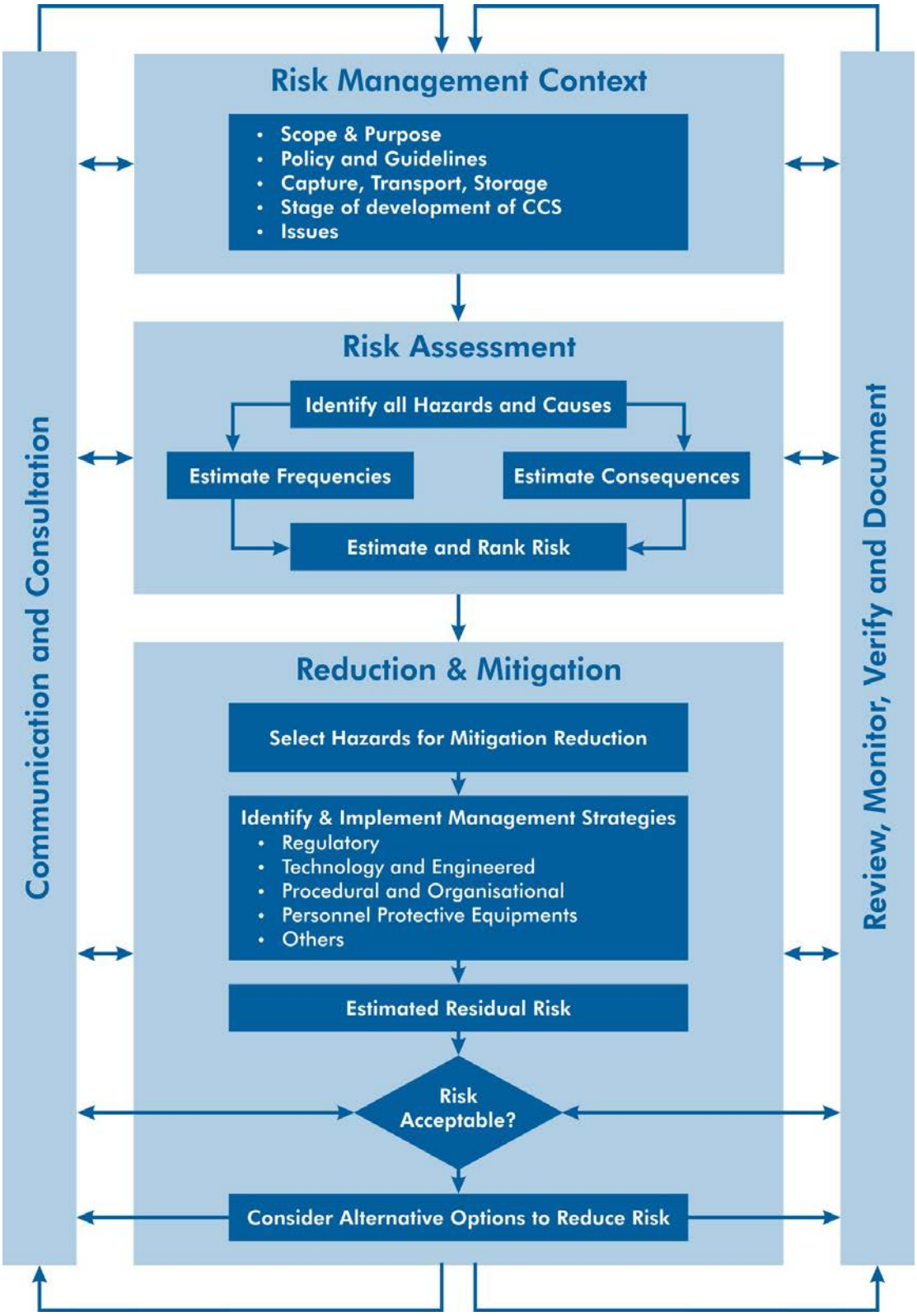

Figure 35: Risk management work flow for induced seismicity at CCS storage sites (based on IOS 31000 Risk Management, ISO, 2009).

Risk management strategy

A systematic and structured risk management programme in which the risks associated with induced seismicity are identified and risk reduction, mitigation and control measures outlined will be critical for CCS projects (Figure 35, Table 7 and Table 8). Protocols for the management of risks arising from enhanced geothermal systems have been proposed (Bommer et al., 2006; Majer et al., 2007, 2008, 2011) and should form the starting point for the development of risk management guidelines for CO_2 storage. The protocol for risk assessment and management of induced seismicity in enhanced geothermal systems has eight steps which range from preliminary site screening evaluation, through to quantification of risks from induced seismic events to development of a risk reduction and mitigation plan. These steps are outlined below (Majer et al., 2008):

- Step One: Review laws and Regulations
- Step Two: Assess Natural Seismic Hazard Potential
- Step Three: Assess Induced Seismicity Potential
- Step Four: Establish a Dialogue With Regional Authority
- Step Five: Educate Stakeholders
- Step Six: Establish Microseismic Monitoring Network
- Step Seven: Interact with Stakeholders
- Step Eight: Implement Procedure for Evaluating Damage

As is the case for enhanced geothermal systems, risk management of induced seismicity for CCS sites will contribute to site selection, and will continue to be applicable when potential CCS sites have been identified or finally selected.

Table 8 outlines a number of risk reduction and mitigation measures that should be undertaken for induced seismicity during the pre-site selection, site selection and characterisation, and site operational phases of CCS projects. Although some risk activities for induced seismicity will typically be conducted early, the precise range of activities and the order in which they are performed may vary between potential CO_2 storage sites. Establishing a regulatory and legislative framework will be necessary prior to detailed site characterisation to reduce the risks associated with stakeholder uncertainty. During the pre-site selection phase of risk assessment (see Table 8) it will also be necessary to establish the key stakeholders and levels of risk they find acceptable. In the site selection and characterisation phases, risk analysis should detail and document the risks and the information that is required to quantify them; additionally, any potential reduction and mitigation measure (Table 8) should also be highlighted. Qualitative and semi-quantitative risk registers and databases for induced seismicity should be developed for potential storage sites by expert elicitation techniques (e.g., Table 7), with formality and structure of the elicitation increasing as a project develops. A key feature of the risk management work flow (Figure 35, Table 8) is that the process is iterative with many aspects of the risk management continuing over multiple phases of the work programme. Updates of the initial risk assessment will be required throughout the project life cycle using new information on reservoir characterisation such as pressures and rock strengths, revised fluid flow models and simulations, monitoring of the magnitudes, numbers, locations and timing of earthquakes (Table 8). These data will be required to assure stakeholders (e.g., regulators,

government, NGOs and general public) that the risks remain acceptably low and CO_2 storage is safe. Risk management will require that seismicity, reservoir pressures and the plume location are closely monitored and reported (see Section 8.3.2). To gain full value from this monitoring it should commence prior to the onset of injection so that robust estimates of natural background seismicity can be determined. Establishing an understanding of the long-term background seismicity behaviour in the region will be important for distinguishing the contributions of natural and induced earthquakes to seismicity recorded during injection; it should be noted that developing such an understanding is not a trivial task and may take a very long time, or may not be possible within the uncertainties required for distinguishing between natural and induced events.

Initial informal risk registers will be an important intermediate step prior to the use of more quantitative tools and more structured elicitation procedures which are designed to derive probabilistic estimates for the occurrence of induced earthquakes. The probabilities of induced earthquakes of a given magnitude may be estimated using empirical global data (Section 6), statistical analysis of induced events at a site after injection has commenced (Section 7) and/or by the generation of synthetic seismicity from numerical models (Section 7). This quantification is required to use probabilistic risk assessment methods (e.g., Baysian Belief Networks - BBN, logic trees and Tesla triple value logic), which permit seismic risks to be propagated through a CCS system and in some cases (e.g., BBNs) allow risk interdependencies to be examined.

Table 8: Summary of tasks recommended for risk reduction and mitigation of induced seismicity for CCS projects.

Phase	Risk Activity	Reduction and Mitigation Activity
Pre-site Selection (CCS Framework)	Stakeholder Uncertainty	Establish scientific and legal criteria for discriminating natural and induced earthquakes.
		Identify key stakeholders that will be impacted by induced seismicity and devise policies for engaging with stakeholders (e.g., government, regulators, public, NGOs).
		Introduce clear and usable CCS legislation for management of induced seismicity.
		Devise management protocols and acceptable earthquake magnitude thresholds for individual sites.
		Interact with stakeholders (e.g., regulators and operators) to ensure that risk assessment methods and process provides required outputs for induced seismicity.
		Governments regulate CCS and accept long-term liability for induced events.
	Seismicity	Preliminary regional assessment of potential for induced and natural seismicity.
	Public Acceptance	Survey public attitudes and perceptions toward and, knowledge of, seismicity induced by injection of fluid (and its risks) in local area of potential storage sites.
Site Selection and Characterisation	Seismicity	Site specific assessment of potential for induced and natural seismicity
		Measure reservoir stresses and predict change in reservoir stresses due to injection.
		Determine possible impact of rock properties and pre-existing faults on seismicity using fracture gradients and fault frictional properties.
		Integrate geomechanical, dynamic fluid flow and risk modelling for preferred storage site to forecast seismicity and estimate its impact on fluid flow.
	Monitoring	Develop mitigation and remediation plans (i.e. Induced Seismicity Management Plan) for potential seismic events using predefined magnitude and reservoir pressure thresholds.
	Public Acceptance	Educate and consult public about induced seismicity and risks.
	Economics	Develop economic modelling of CCS system for storage site incorporating induced seismicity. Highlight uncertainties in the economics arising from induced seismicity.
Site Operation	Monitoring	Record and analyse induced earthquakes in real time.
		Monitor reservoir pressures and plume migration to confirm pre-injection models.
		Modify monitoring and remediation plans as required.
	Mitigation	Adjust injection rates, injection intervals and number of wells to maintain induced earthquakes within pre-defined magnitude range and locations.
		Introduce financial compensation for damages and interference associated with induced seismicity.

Phase	Risk Activity	Reduction and Mitigation Activity
	Public Acceptance	Reassess public response and perceptions to seismicity. Increase public communication and community support as required.
		Report induced seismicity to general public in near real time.
		Continue open dialogue with public regarding seismicity and general operations.
	Economics	Rerun economic models if critical seismicity thresholds are exceeded.

Reducing the Induced Seismicity Hazard and Risk

Monitoring, mitigation and prediction of induced seismicity should be important components of the risk management strategy for commercial-scale CO_2 storage projects, particularly if they are onshore and/or close to populated areas. This will require that seismicity and reservoir pressures in particular are closely monitored and reported at site selection, site characterization and site operation phases of CCS projects. Prediction of the potential seismicity prior to injection will permit identification of risk reduction measures that could be undertaken to maintain the levels of induced seismicity (i.e. numbers, magnitudes and locations) within acceptable limits. If however the level and impacts of seismicity exceed pre-injection expectations, then it may be necessary to put mitigation measures in place and establish a means of controlling the seismicity. Zoback (2012) has listed five steps that could be taken to reduce the probability of future induced earthquakes. These are; (i) Avoid injection into active faults, (ii) minimize pore pressure changes at depth, (iii) install local seismic monitoring networks, (iv) establish protocols for dealing with induced seismicity in advance, and (v) be prepared to alter plans or abandon wells. These measures are discussed further in Section 8.3.2.

Assessing Induced Seismicity Potential

Assessment of the potential for future induced seismicity will form a component of the risk assessment for all CCS projects. In previous sections we discuss various proposed methods for guiding the understanding of risk related to induced seismicity in a particular project. Here we consider the methods and procedures that could be used to assess the possibility of future induced earthquakes at the given site. Depending on the level of detail available at the time, this assessment can be purely qualitative, or it may contain some degree of quantification. A qualitative assessment may be based on purely descriptive terms which are likely to be the best available information early on in the life of a project. However, once the planning of a project begins to develop, and for certain stakeholders (e.g., regulators and project managers), a more quantitative assessment is likely to be required. With the current state of modelling of induced seismicity, as presented in this report, a quantitative assessment will most likely be probabilistic.

The risk assessment is likely to move through various phases, with multiple assessments done during the life of a project. In all stages, expert elicitation will likely be required. In an initial assessment, simplistic tools (e.g., risk registers and bow-tie diagrams) are likely to be the most useful and can be populated by informal expert elicitation. As the project develops, more structured tools may become more informative. Expert elicitation will still likely be required, particularly for defining appropriate risk thresholds, and in this case, the assessment may benefit from a more formal elicitation process (e.g., Cooke, 1996).

Current tools for estimating the behaviour of induced seismicity and informing expert elicitation can be broken down into two main categories: 1) tools that estimate generalities of induced seismicity prior to injection; and 2) tools that provide more accurate estimates of the behaviour of the expected seismicity after injection has commenced. Category 1 tools may include qualitative assessment using empirical induced seismicity data from many sites (see Section 6) and preliminary physical modelling from the site under consideration (see Section 8), or statistical modelling (see Section 7) that is not specific to the site in question (i.e. does not incorporate induced seismicity from the site). Category 2 includes physical and statistical modelling for the site under consideration with input data from locally measured reservoir parameters and induced seismicity. In some cases, category 2 tools may constitute mitigation (i.e. a measure undertaken after a risk event has occurred), which will reduce their effectiveness risk assessment. Therefore, category 2 tools can be separated into two further groups: mitigation tools, which provide some quantification of what has happened; and, risk assessment tools that analyse what has happened and provide some quantification of what may happen.

Currently neither empirical data (Section 6) nor physical and statistical models, whether deterministic, or probabilistic can adequately capture and describe the behaviour of induced seismicity. Using fundamental laws and relationships, as presented in Section 6, to estimate the behaviour of induced seismicity prior to injection will provide estimates with significant uncertainty until the characteristics of the reservoir are understood. Similarly, physical and statistical models are in the early stages of development for estimating induced seismicity associated with CCS projects and the uncertainties of any forecast of seismicity be significant. We expect that as physical models mature and constraints on the input data improve such models will become key tools in the future for predictive risk assessment of induced seismicity. Presently, statistical models appear to have greater utility than physical models for forecasting induced seismicity once injection and seismicity has commenced; however physically based modeling such as that done Baisch et al., (2009c) shows great promise. With the onset of injection and observations of the seismic response of the reservoir, statistical models proposed by Bachmann et al. (2011), Barth, et al. (2011) or Shapiro et al. (2010), show promise for generating revised and more accurate estimates of the expected induced seismicity. A critical step is then translating these expected rates of seismicity into hazard and risk (e.g., Bachmann, et al., 2011; Baisch et al., 2009c). With future development of these models, they could also provide useful risk assessment information prior to injection, particularly when coupled with data such as observations from stimulation of the reservoir of interest. Given the range of data and models available for forecasting induced seismicity, it is likely that the best possible predictive model will be an ensemble model that combines the results from any number of models. Doing so will allow the risk assessment to capture two types of uncertainty critical to a robust risk assessment: 1) epistemic uncertainty which is the uncertainty across models (i.e., different models represent the system in different ways and therefore capture a different portion of the uncertainity); and 2) aleatory uncertainty which is the randomness in the system and can be captured through such things as different parameter distributions.

Although a discussion of expert elicitation is beyond the scope of this report, it should be noted that a rigorous risk assessment including induced seismicity is likely to be heavily reliant on expert judgment. The manner in which an expert workshop is designed together with the processes used to collect and combine expert judgment, can have a significant impact on the final result (Cooke, 1996).

As with existing geothermal projects, it is expected that any risk assessment will be heavily supplemented with monitoring and mitigation tools that facilitate an improved understanding of the expected seismicity as injection progresses. Some examples of such tools are discussed in the following section.

Monitoring and Mitigation

Monitoring of the injected CO_2 plume location and of reservoir conditions (e.g., pressure and temperature) is widely considered to be an essential component of risk management for CCS sites (e.g., Benson, 2004, 2005; Stenhouse et al., 2006; IEAGHG, 2009; DNV, 2011). Monitoring is important for measuring the amount of CO_2 stored, for carbon accounting and crediting, to manage the injection process and reservoir performance (including induced seismicity), and to confirm that CO_2 is behaving as predicted and not migrating from the storage reservoir. Monitoring of CCS sites provides a means of assuring stakeholders (e.g., public, Government, Non-Government Organisations and site operators) that CO_2 storage sites are being operated safely and without detrimental impacts on the environment, existing resources or people. These assurances are important for building stakeholder confidence in CO_2 storage, especially in early projects before the technology has been widely tested, and to ensure that carbon credits awarded for CO_2 as part of Emissions Trading Schemes remain in the ground (IPCC, 2005).

Monitoring and mitigation of induced seismicity should be an important component of commercial-scale CO_2 storage projects. International experience suggests that monitoring programmes will generally be tailored for each site due to variations between sites in accessibility (e.g., whether the site is onshore or offshore), the perceived level of risk stakeholders and infrastructure, the total amount of CO_2 to be injected, the original purpose of the site (e.g., depleted oil and gas field or enhanced oil recovery operation), geology, topography, land use, technical requirements and the intended use of the microseismic data (Benson et al., 2005; Pearce et al., 2005; Jenkins et al., 2012). At some sites, for example, operators may wish to use the locations of induced events to track spatial and temporal changes in reservoir pressures which may help constrain the location of the injected CO_2. Use of induced seismic to locate the injected CO_2 may be of value where there are few sample wells and the quality of 4D seismic reflection data is too poor to aid plume location. Utilising induced seismicity to locate sub-surface CO_2 requires that the errors on absolute locations of seismic events are small (e.g., $<\pm$50m) and that the spatial relations between these events and the CO_2 plume are well understood. More research is required to develop robust models for the spatial relationships between the locations of the CO_2 plume and induced seismicity. Such models could, in the future, represent one of the few advantages of seismicity induced by CO_2 injection.

Conclusions of Evans, et al., (2012) tentatively suggest that CCS sites for which induced seismicity presents the greatest risk include those close to urban areas with potential for reservoir pressures to exceed rock strength where the background natural seismicity is high; however, more data is needed to better understand this. Risks may also be elevated by the injection of larger volumes of CO_2 (e.g,, tens of millions of tonnes) (McGarr, 1976; Nicol et al., 2011; Shapiro et al., 2011). In these circumstances monitoring induced seismicity may be particularly important. However, given the paucity of induced seismicity data for CCS and the need to avoid induced seismicity issues while CCS is gaining public acceptance, it may be prudent to initially set up seismic monitoring at all sites.

Design requirements for seismic recording arrays at CCS sites will depend on a number of factors including; the desired minimum recorded magnitude and location accuracy, the depth of the reservoir, the level of background earthquake activity, the proximity to sources of ambient noise (e.g., urban or industrial activity) and financial or site constraints on the number and locations of instruments (e.g., Mathieson et al., 2010; Verdon et al., 2010b; Zhou et al., 2010). In Table 9 below potential acquisition parameters and technical requirement are listed for recording induced seismicity at CO_2 storage sites. Instrument choice is also important and the instruments need to be able to record the dominant frequencies radiated by the earthquakes (i.e., the instrument should have a flat response over the

anticipated frequencies in the seismograms); failure to do so will hinder the ability of the network to provide accurate magnitude estimates and may effect such things as b-value estimates.

Table 9: Potential acquisition parameters and technical requirements for local seismograph networks installed to record induced seismicity at CCS sites. The acquisition parameters and technical requirements may change between sites depending on the predicted level (numbers and magnitudes) of induced seismicity and the associated risks.

Acquisition Parameters	Technical Requirements
Reservoir depths 0.8-3 km	Downhole seismometer array close to the reservoir (e.g. within ca.200 m, depending on location accuracy required), to reduce attenuation effects on the signal (affected by travel path length), and to provide optimal location accuracy
Earthquake completeness magnitude above ≥M-1	Downhole 3+ component seismometer array, (but not necessarily to the reservoir depth for ≥ M -1). Continuous recording rather than triggered recording, allows retrieval of smaller (M -1) magnitude events later in processing, which may otherwise be missed by 'triggered' recording.
Absolute location accuracy ≤±20m	Suitable 3+ component downhole array pre-designed for optimal location accuracy. Velocity control data necessary for the reservoir (e.g. from earlier VSP and tomography work), for accurate location analysis. Accuracy of locations is also affected by the recorded frequency of signal, and the sampling rate of recording – the sampling rate should be 0.5 ms or less.
Real-time monitoring and analysis	Real-time monitoring requires streaming of data from individual downhole sensors back to a centralized recording-monitoring unit, which is relatively standard. Real-time analysis requires calibration of detection and location parameters for the specific reservoir, requiring that the number of sensors is adequate (> 10) and the background anthropogenic noise level is relatively low for frequencies > 20 Hz
Measurement of PGA	Downhole 3-component accelerometers, at ~100 m depth, with a reasonable dynamic range, to handle +/- 2g accelerations.
Baseline seismicity record	A sub-surface array (minimum of 4-5 sensors, 3-components, at ca.50-200 m depth) would be necessary to detect background natural > M 1 events in the vicinity of the reservoir. This array may not necessarily attempt to record M-1 or M-2 events.

To optimise the utility of monitoring programmes, site performance and management guidelines should be established before injection commences. These guidelines or protocols and the process by which they are set should be agreed by key stakeholders at each site before injection start. Guidelines include setting the acceptable level (i.e. magnitude range and productivity) and impacts of seismicity and outlining the control measurements to be implemented if original expectations are exceeded. To our knowledge no such guidelines have been developed for CCS sites. An induced seismicity management system, referred to as the 'traffic light' system, has however been proposed for the Enhanced Geothermal Systems (Bommer et al., 2006; Majer et al., 2007, 2011). The 'traffic light' system is for real-time monitoring and management of the induced seismicity. The system continuously calculates and plots a cumulative window of the ground motion (usually PGV) as a

function of injection rates and time. It has been implemented in the Berlin geothermal field in El Salvador (Bommer et al., 2006) and at the Basel, Switzerland EGS project (Haering et al., 2008). The tool is aimed at managing risks related to: 1) the public response to the geothermal project due to felt events; and 2) infrastructural damage from shaking. The system may use two or more thresholds to define the current status of the project in terms of induced seismicity. The thresholds are relative shaking levels based on the anticipated response of the local population, and the specifics of the building stock in the region. To implement the system, Bommer et al. (2006) calculates an equivalent magnitude earthquake, which is an earthquake at 2km depth which would produce the same peak ground velocities, and compares the pre-defined thresholds to the cumulative rate of equivalent magnitude earthquakes.

The thresholds for induced seismicity, in terms of guiding decisions regarding the pumping operations, are as follows (Bommer et al., 2006, Majer *et al.*, 2007):

Red: The lower bound of the red zone is the level of ground shaking at which damage to buildings is expected to set in. To mitigate the risk pumping is suspended immediately.

Amber: The amber zone has been defined by ground motion levels at which vibrations occur and people are aware of seismic activity associated with stimulation, but damage is considered unlikely. Pumping is permitted to proceed with caution, possibly at reduced flow rates, and observations are intensified.

Green: The green zone was defined by levels of ground motion that are either below the threshold of general detectability or, at higher ground motion levels, at occurrence rates lower than the already-established background activity level in the area. In such cases pumping operations proceed as planned.

The 'traffic light' system highlights a number of challenges for risk management of induced seismicity. First, an intuitive and convenient measure of induced seismicity is its comparison against the long-term background seismicity rate within a region. Such a background can be challenging to estimate, particularly in low seismicity areas, or even in higher seismicity areas due to the non-stationarity of seismicity; in other words, natural seismicity rates can change significantly over a short time-period without any anthropogenic influence. Therefore the difficulty in estimating such rates must be taken into account and care taken in the risk management plan. Second, the system does not explicitly address the issue of induced seismicity that occurs after all Enhanced Geothermal System pumping activities cease (Majer et al., 2011). Such cases highlight the need to set guidelines for the termination of monitoring that are defined by the levels of seismicity compared to background and not simply by the time interval following cessation of sub-surface operations. Coupling of a 'traffic light' system with modelling as presented in Section 7 (e.g., Bachmann et al., 2011; Barth, et al., 2011) may provide a basis for quantifying the levels of seismicity beyond injection and estimating how long monitoring may be required. Lastly, for CCS sites induced seismicity well above acceptable levels may require actions beyond the termination of injection. These actions could include extraction of water or CO_2 via pressure relief wells. Numerical physical modelling may provide a basis for optimally locating pressure relief wells prior to the start of operations or before acceptable induced seismicity limits are exceeded.

Benefits of Induced Seismicity

Much of the available literature on induced seismicity focuses on the risks that may arise from these earthquakes, however, in some circumstances, if managed appropriately, these events may provide some benefit to CCS projects. Benefits presented by induced seismicity fall into one of two main groups, improved monitoring and elevated reservoir hydraulic conductivity.

The location of epicenters for induced earthquakes, which are typically clustered close to injection or extraction wells (see Section 6.6.2), records disequilibrium of the rock arising from addition of fluid to, or subtraction of fluid from, the reservoir. The spatial distribution of epicenters of induced earthquakes is generally thought to provide a first-order measure of the extent of pore pressure changes arising from injection/extraction (Shapiro and Dinske, 2009; Shapiro et al., 2011). Therefore, mapping the locus of induced seismicity in real time provides a potential means of charting the movement of the pressure front associated with CO_2 injection. Transmission of the pressure front does not require migration of fluid and in many cases will take place more rapidly than migration of the CO_2 plume. Because of these differences in rate, pressure changes in the reservoir are likely to take place beyond (i.e. further from the injector well) the CO_2 front. In such cases the spatial distribution of the outer limits of seismicity may provide an indication of the extent of pore pressure changes and of the CO_2 plume. More work is required, however, to understand better relationships between locations of induced seismicity (for a given Mc), pressure changes in the reservoir and the CO_2 plume. These observations may improve the utility of induced seismicity as a monitoring tool.

Rising pressures due to CO_2 injection also provide an opportunity to increase the reservoir permeability and injectivity through fracturing (e.g., Fjaer, 2008). Induced seismicity is a by-product of the fracturing process which may be a valuable reservoir management tool, particularly in lower permeability reservoirs (e.g., < 10 mD). Improvements to reservoir permeability arising from stimulation have the potential to increase the rates and total volumes of CO_2 that could be injected via individual wells. These increases in rates have the potential to improve the economics of the injection process. Well stimulation is a mature technology which is widely used in the petroleum industry and in the vast majority of cases is conducted with no adverse effects. However, it will be important to ensure that fractures are restricted to the reservoir and do not negatively impact on the sealing properties of the caprock. In addition, given the present negative public perceptions of hydraulic fracturing (e.g., see de Pater and Baisch, 2011; Healy, 2012) the benefits it offers should be weighed against the potential negative impacts that its use may have on public attitudes towards CCS projects.

Summary

One of the principal reasons for studying induced seismicity arising from injection of CO_2, and a key driver for this report, is to assess and manage the associated risks. For the majority of existing fluid injection or extraction projects induced seismicity has not significantly disrupted operations. Maintaining this record requires that operators select sites judiciously and employ risk management to minimise the impact of these risks. The risks presented by induced seismicity are variable and include lack of public acceptance and support, damage to infrastructure (and private property), and rupture of the seal or reservoir. Thresholds for triggering unacceptable risk may vary for different risk factors and CCS sites. Events near to (e.g., < 10 km) injection facilities and as small as M3 could cause damage to infrastructure and injury, while events as small as M2 may raise stakeholder concern.

A systematic and structured risk management programme in which the risks associated with induced seismicity are identified and risk reduction, mitigation and control measures outlined will be critical for

CCS projects. An eight step protocol for the assessment and management of induced seismicity has been proposed for EGS sites (e.g., Bommer et al., 2006; Majer et al., 2008) and should form the starting point for CCS sites. These steps are:

- Step One: Review laws and Regulations
- Step Two: Assess Natural Seismic Hazard Potential
- Step Three: Assess Induced Seismicity Potential
- Step Four: Establish a Dialogue With Regional Authority
- Step Five: Educate Stakeholders
- Step Six: Establish Microseismic Monitoring Network
- Step Seven: Interact with Stakeholders
- Step Eight: Implement Procedure for Evaluating impact of induced seismicity

An understanding of the expected size, number, location and timing of induced earthquakes is required for risk assessment and management of seismicity generated by injection of CO_2. Tools for forecasting induced seismicity are of two main types. 1) Tools that estimate generalities of induced seismicity prior to injection; and 2) tools that provide more accurate estimates of the behaviour of the expected seismicity after injection has commenced. Category 1 tools are qualitative and include the use of empirical datasets together with preliminary physical and statistical models. Category 2 tools will be quantitative and include site-specific physical and statistical models. Statistical models presently show the most promise for forecasting induced seismicity, however, physical models could become key predictive tools in the future. Such models may be either deterministic or probabilistic.

Monitoring and mitigation of induced seismicity should be an important component of commercial-scale CO_2 storage projects. The design of monitoring networks for induced seismicity could vary between sites depending on a range of factors including; desired event magnitude range, site location and reservoir depth, levels of background seismicity and ambient noise, and cultural site constraints (e.g., existing infrastructure and financial priorities). To optimise the utility of monitoring and mitigation programmes site performance and management guidelines for induced seismicity should be established prior to injection. Guidelines include setting the acceptable level (i.e. magnitude range and productivity) and impacts of seismicity and outlining the control measurements to be implemented if original expectations are exceeded. Such guidelines have been established for EGS which should provide the starting point for CCS induced seismicity guidelines.

Gaps in Understanding and Further Work

One of the primary aims of this report is to raise awareness that injection of CO_2 has the potential to induce earthquakes of magnitudes that pose a risk to CCS projects. Sub-surface storage of CO_2 for the purposes of greenhouse gas abatement is in its infancy and, although CO_2 has been widely used for EOR over the last 30 years, there are few data available in the literature on induced seismicity produced by the injection of CO_2. In addition, the data that are available from fluid injection projects are sparse. In this report we have attempted to summarise the relevant literature and, in an attempt to overcome some of inadequacies in these data we have combined data from waste water injection, Enhanced Geothermal Systems water injection and hydrocarbon extraction sites. The validity of the collective treatment employed in this report and the assumption that these provide information about seismicity produced by CO_2 injection requires further investigation, however, the indications are that differences in the density and compressibility of CO_2 and water, for example, do not significantly alter their ability to generate induced seismicity when injected into the sub-surface (e.g., Verdon et al., 2010a).

Six main areas of research require further investigation to improve our understanding of induced seismicity processes, the associated risks they pose to CO_2 storage projects and the risk reduction measures that may be employed. These main areas are summarized below.

1. **Across-Industry Induced Seismicity Catalogue Database:** development of the understanding of induced seismicity would be improved by better access to seismicity data from existing injection and extraction projects. Examination of the literature confirms that relevant data exist (e.g., seismicity catalogues, reservoir properties and injection histories), yet they do not appear to be freely and easily available. Such data are critical for the development and validation of statistical and physical models. Creation of a central database for global injection induced seismicity observations and encouragement of data sharing will greatly facilitate model development and improve induced seismicity forecasting. To ensure that such data are collected it is recommended that microseismic networks (including some down-hole instruments) are operated at all CCS sites prior to, during and following injection. Work is underway in the geothermal community for establishing a common data format and protocols.

2. **Fundamental Induced Seismicity Relationships:** Results presented in Sections 7 and 8 indicate that progress is being made in understanding fundamental relationships that describe the behaviour of induced seismicity. Statistical studies to date have largely been focused on either case studies or on global studies where the compiled data sets suffer from lack of completeness or other potential bias. The understanding of the fundamental relationships driving induced seismicity is not yet well developed. To improve predictive models, this work must move to systematic studies on complete data sets (i.e. seismicity catalogues, reservoir properties and injection histories). As more data becomes available, future studies will undoubtedly begin to reduce the uncertainties in the forecast induced seismicity parameters, such as the largest possible magnitude or the expected rate of events for a site. Uncertainty reduction is important for robust quantitative risk assessment. Additionally, by working across industry and compiling datasets we can also more quickly rigorously test predictive models of induced seismicity behaviour (e.g., Bachmann, et. al, 2011).

3. **Physical modelling:** The development of physical models is at an early stage but shows promise for informing induced seismicity predictions. In order to provide improved predictions these models must incorporate well quantified system parameters (e.g., porosities, permeabilities, pore pressures, rock strength, temperatures and fluid compositions) and more accurately replicate system processes. Future models could be improved by: modelling of poroelastic effects through full coupling between fluid flow and elasticity; incorporation of inelastic rock rheology; the effect of the presence of multi-phase fluids on fault rheology and fault friction, including chemical effects; modelling of non-critically stressed systems; and coupling of deterministic and stochastic models. For both validation and testing of the codes and models it is important that codes continue to be benchmarked against each other and tested, in a rigorous and prospective sense, against observations of induced seismicity.

4. **Scaling from pilot projects to production:** CCS projects to date have mainly consisted of pilot projects. The volumes of injected CO_2 for these pilot projects are probably orders of magnitude less than what will be required to achieve the ultimate goal of reducing the amount of CO_2 in the atmosphere to slow global warming and climate change. It is currently not well understood how the processes will scale to the much larger and potentially more complex reservoirs that will be required; additionally it will need to be understood if it is necessary and possible to include this complexity into physical modelling.

5. **Risk management protocol:** A CCS specific protocol or guideline for risk management specific to induced seismicity does not yet exist. Such protocols have been developed for other areas of CCS (e.g., DNV, 2011) and for induced seismicity in other industries (e.g., Majer, et. al., 2008). A CCS specific protocol would need to describe the major steps necessary to manage the induced seismicity risk through to guidelines for monitoring during injection and beyond. Such a protocol would educate stakeholders and project managers and ease the risk management process and would need to be coupled with a best practice guideline.

6. **Induced Seismicity Collaboration:** Induced seismicity is not a CCS specific problem and a number of industries (e.g., waste water disposal and EGS) are currently devoting time and resources towards improving our understanding of this topic. It will be very much to the CCS communities benefit to integrate with, and learn as much as possible from, other communities who are more advanced in their understanding of induced seismicity. For example, through international collaboration, including the IEA-Geothermal Implementing Agreement (Annex 11) and the International Partnership for Geothermal Technology induced seismicity working groups, research into geothermal induced seismicity attributed to EGS projects is ongoing. These groups will target a number of topics, including; discriminating between EGS induced and natural seismic events, defining how far relevant stress field pertubations can extend from EGS operations and designing downhole EGS operations to minimize ground shaking.

Conclusions

Induced seismicity has been widely reported over the last 40 years. To date few induced earthquakes have been recorded at CO_2 storage sites, however, the volumes of injected CO_2 are typically small (compared to those required for commercial-scale storage of CO_2) and the onsite seismograph networks are often limited. Injecting commercial-scale volumes of CO_2 (e.g., millions of tonnes) has the potential to produce induced seismicity at shallow depths (e.g., <5 km) that could have serious consequences for the successful completion of CCS projects. Risks to CCS projects associated with induced seismicity may include: 1) loss of public support due to concern about potential seismicity or from actual observed events; 2) ground shaking causing damage to property or injury; 3) loss of integrity of the reservoir though fracturing of the reservoir or of the seal. One of the principal reasons for studying induced seismicity arising from injection of CO_2, and a key driver for this report, is to improve the ability to assess and manage the associated risks. Through a better understanding the underlying processes that drive induced seismicity, the community will be better able to minimise the risk to CCS projects through a thorough risk management plan and may ultimately be able to control the behaviour of induced events.

Some case histories for petroleum extraction and stimulation, enhanced geothermal systems, waste water sub-surface disposal and CO_2 storage are presented in the report. These cases histories confirm that extraction and injection of fluids and gas can produce induced seismicity. In combination with our collective analysis of published induced seismicity data the case histories suggest that induced earthquakes are generally small in magnitude but can be of larger size (M≥4) in some cases. In many projects seismicity may not be observed, and, if present, it must comprise events too small to be felt at the ground surface or recorded by regional seismograph networks (e.g. M≤2-3). It remains possible that earthquakes in excess of M 7.0 (e.g., M7.3 May 17th 1976 Gazli earthquake, Adushkin et al., 2000) were triggered by hydrocarbon operations, but for many of these events, agreement has not been reached about whether the events were induced or tectonic. There are no known cases of large magnitude events being triggered by enhanced geothermal operations, while few induced earthquakes of any magnitude have been attributed to CO_2 storage. Little significance can be attributed to the low rates of induced seismicity at CCS sites because of the very few operational sites, due to the low injected CO_2 volumes and because the sites are generally not well-instrumented with seismographs. As a counter to the CCS experience, we have reported numerous cases where induced seismicity resulted in public disturbance and minor damage; however, with the notable exception of the 2006 M3.4 Basel earthquake, these events have not significantly impacted injection or extraction operations. The available case-study literature suggests that there can be strong spatial and temporal links between induced seismicity and hydrocarbon operations. It is often the case that induced earthquakes occur within, or close to, the reservoir intervals. In a number of hydrocarbon, geothermal and waste water fields the onset of seismicity has been linked to significant reductions or increases in reservoir pressures arising from production or water flooding. The temporal relations between changes in reservoir conditions and in the induced seismicity are highly variable. In some cases these changes occur within days or months of each other, in others, time lags of years are inferred and on occasions significant changes in reservoir conditions do not appear to affect the seismicity recorded.

Both observations from case studies and our compilation of empirical data indicate that the maximum magnitude of induced events may increase with total volume of fluid injected/extracted and the injection rate. The volume-maximum magnitude relationship may arise because larger volumes of injection fluid have the potential to modify the stresses in larger volumes of crust and to encounter larger faults. Rates of induced seismicity are also positively correlated with injection rate and may be

attributed to the rise in reservoir pressures expected for higher injection rates. The rate of seismicity and the proportion of smaller to larger induced earthquakes in a sequence (i.e. the *b*-value for the Gutenberg-Richter relationship) also appear to increase with decreasing reservoir permeability. Reservoirs with low permeabilities (e.g., <0.01 mD) may have high rates of seismicity and high *b*-values because they promote locally high stresses which generate many small new fractures. The depth of earthquakes inferred to be induced by fluid injection or extraction are mainly within 5 km of the surface and located within, or immediately adjacent to, the depth of the reservoir. Clusters of induced seismicity grow in dimensions with injection time and increasing injected volume. Most (~70%) induced events occur during injection with the number of events decreasing exponentially after injection/extraction ceases.

Two main types of models have been used for modelling and predicting seismicity induced by fluid injection. Both classes of models, statistical and physical, are in the relatively early stages of development. A number of statistical models have been developed to predict the temporal evolution, maximum magnitude and magnitude distribution of induced seismicity during and after injection. These statistical models, which were primarily developed for geothermal systems, typically rely on the Gutenberg-Richter relationship and the Omori-Utsu law and assume the occurrence of seismicity follows a Poisson distribution. Such statistical models are now well established in the wider earthquake seismology community and the developing injection specific models could be optimized for the seismic behaviour of a CCS injection system. Current physical models can highlight geometric and dynamic cases with significant risk of induced seismicity. Such models can be used to identify cases where the risk of induced seismicity can be minimized or avoided by adapting injection strategies. The utility of these models is strongly dependent on the quality of the input data, including knowledge of: 1) the orientation and magnitude of the local stress field; 2) the local fault network including any faults which may be effected by the pressure front; 3) the hydraulic properties of the medium, such as permeability, diffusivity; 4) the elastic properties of the medium, such as elastic moduli and thermal expansion coefficient; and 5) the reservoir mineralogy and geochemistry of in-situ fluids (in order to predict likely fluid-gas-rock interactions). A particular challenge in developing robust statistical and physical models to forecast induced earthquakes will be to test that they produce expected, unbiased and reproducible, and, ultimately, informative results.

The risks associated with induced seismicity at CCS sites can be reduced and mitigated using a systematic and structured risk management programme. While precise forecasts of the expected induced seismicity may never be possible, a thorough risk management procedure will include some level of knowledge of the possible behaviour of induced seismicity. Risk management will require estimates of the expected magnitude, number, location and timing of potential induced earthquakes. Such forecasts should utilise site specific observations together with physical and statistical models that are optimised for the site. Statistical models presently show the most promise for forecasting induced seismicity after injection has commenced, however, with further development physical models could become key predictive tools that are informative prior to injection. Combining forecasts with real-time monitoring of induced seismicity will be necessary to maintain an accurate picture of the seismicity and to allow for mitigation of the associated risks as they evolve (e.g., Bachmann, 2011). Site performance and management guidelines should be established prior to injection to facilitate: 1) definition of the acceptable levels and impacts of induced seismicity; 2) optimisation of the monitoring and mitigation programmes; and 3) the establishing of key control measures. Such guidelines have been developed for Enhanced Geothermal Systems and should provide the starting point for a management strategy of induced seismicity at CCS sites.

A number of information and knowledge gaps have been identified for induced seismicity. Understanding of induced seismicity and the associated risks would be improved by; a) increasing the

induced seismicity catalogues publically available for development and testing of physical and statistical models, b) undertaking more systematic studies of sites populated by well constrained sub-surface information and seismicity catalogues that are completely recorded down to small magnitudes, c) improving the reality of physical models by modelling such factors as poroelastic effects, multiple species of fluid and non-critically stressed systems, d) studying the scaling effects on seismicity associated with a move from pilot projects to full commercial implementation of CO_2 storage, e) developing standard risk management procedures and guidelines for induced seismicity for CCS projects and, f) filling induced seismicity knowledge gaps in the CCS community by collaborating with seismologists working in other industries.

References

Adushkin, V.V., Rodionov, V.N., Turuntaev, S. and Yudin, A.E., 2000. Seismicity in the oil field. Oilfield Rev., Vol. 12, No.2, 2-17.

Ahmad, M.U. and Smith, J.A., 1988. Earthquakes, injection wells, and the Perry Nuclear Power Plant, Cleveland, Ohio. Geology, Vol. 16, 739-742.

Ake, J., Mahrer, K., O'Connell, D. and Block, L., 2005. Deep-Injection and Closely Monitored Induced Seismicity at Paradox Valley, Colorado: Bulletin of the Seismological Society of America, Vol. 95, No. 2, 664-683.

Akramhodzhaev, A.M., Sitdikov, B.B. and Begmetov, E.Y., 1984. About Induced Nature of Gazli Earthquakes in Uzbekistan, Geological Journal of Uzbekistan, Vol. 4, 17-19 (in Russian).

Allis, R.G., 1982. Mechanism of induced seismicity at The Geysers geothermal reservoir, California Geophys. Res. Lett., Vol. 9, 629-632.

Arrowsmith, S.J. and Eisner, L., 2006. A technique for identifying microseismic multiplets and application to the Valhall field, North Sea. Geophys. Vol. 71, No. 2, V31-V40.

Asanuma, H., Nozaki, H., Niitsuma, H. and Wyborn, D., 2005. Interpretation of microseismic events with larger magnitude collected at Cooper Basin, Australia. Geothermal Resource Council Transactions, Vol. 29, 87-91.

Axelsson, G., Flovenz, O.G., Hjartarson, A., Hauksdottir, S., Sverrisdottir, G., Arnason, F., and Arnason, A. and Bodvarson, R., 2000. Thermal energy extraction by reinjection from Laugaland geothermal system in North Iceland. In: Proceedings: World Geothermal Congress, Kyushu Tohoku, Japan, May 28–June 10, 3027–3032.

Axelsson, G., Thórhallsson, S. and Björnsson, G., 2006. Stimulation of geothermal wells in basaltic rock in Iceland. In: Proceedings ENGINE Workshop 3: Stimulation of Reservoir and Microseismicity, Ittingen, Switzerland, 29 June–1 July, 17–25.

Bachmann, C.E., Wiemer, S., Goertz-Allman, B.P. and Woessner, J. 2012. Influence of pore-pressure on the event-size distribution of induced earthquakes. Geophysical Research Letters, Vol. 39, L09302, 7 pp. doi:10.1029/2012GL051480

Bachmann, C.E., Wiemer, S., Woessner, J. and Hainzl S., 2011. Statistical analysis of the induced Basel 2006 earthquake sequence: Introducing a probability-based monitoring approach for Enhanced Geothermal Systems, Geophys. Journ. Int., doi: 10.1111/j.1365-246X.2011.05068.x.

Baisch, S. and Vörös, R., 2010. Reservoir induced seismicity: Where, when, why and how strong? In: Proceedings of the World Geothermal Congress 2010, Bali, Indonesia, Paper 3160, 5 pp.

Baisch, S., Carbon, D., Dannwolf, U., Delacou, B., Devaux, M., Dunand, F., Jung, R., Koller, M., Martin, C.,Sartori, M., Secanell, R., and Voeroes, R. 2009c. Deep heat mining Basel - seismic risk analysis, Tech. rep.,Serianex.

Baisch, S., Schrage, C. and Kreuter, H., 2010. Induced seismicity – a challenge for geothermal project development in Germany. Geothermal Resource Council Transactions, Vol., 34, 291-293.

Baisch, S., Voros, R., Rothert, E., Stang, H., Jung, R. and Schellschmidt, R., 2009b. A numerical model for fluid injection induced seismicity at Soultz-sous-Forêts: International Journal of Rock Mechanics and Mining Sciences, Vol. 47, No. 3, 405-413.

Baisch, S., Voros, R., Rothert, E., Stang, H., Jung, R. and Schellschmidt, R., 2010. A numerical model for fluid injection induced seismicity at Soutz-sous-Forets. International Journal of Rock Mechanics and Mining Science Vol., 47 (2010), 405-413.

Baisch, S., Voros, R., Weidler, R. and Wyborn, D., 2009a. Investigation of Fault Mechanisms during Geothermal Reservoir Stimulation Experiments in the Cooper Basin, Australia: Bulletin of the Seismological Society of America, Vol. 99, No. 1, 148-158.

Baisch, S., Weidler, R., Vörös, R., Wyborn, D. and de Graaf, L., 2006. Induced seismicity during the stimulation of a geothermal HFR reservoir in the Cooper Basin, Australia. Bulletin of the Seismological Society of America, Vol. 96, 2242-2256.

Bame, D. and Fehler, M., 1986. Observations of long period earthquakes accompanying hydraulic fracturing. Geophysical Research Letters, Vol. 13, 149-152.

Bannister, S. and Sherburn S., 2007. Induced seismicity in Rotokawa geothermal field. GNS Science Consultancy Report.

Bannister, S., Sherburn, S., Powell, T. and Bowyer, D., 2008. Microearthquakes at the Rotokawa Geothermal Field, New Zealand, GRC Transactions, Vol. 32, 259-264.

Baria, R., 2007. Induced seismicity in geothermal systems and public concern, Proceedings of the First European Geothermal Review, Mainz, Germany.

Baria, R., Majer, E., Fehler, M., Toksoz, N., Bromley, C. and Teza, D., 2006. International cooperation to address induced seismicity in geothermal systems. In: Proceedings of the 31st Workshop on Geothermal Reservoir Engineering, Stanford University, Stanford, CA, USA, 3 pp.

Barth, A., Wenzel, F. and Langenbruch, C., 2011. Probability of earthquake occurrence and magnitude estimation in the post shut-in phase of geothermal projects, J. Seismol., doi:10.1007/s10950-011-9260-9.

Batchelor, A.S., 1983. Hot Dry Rock reservoir stimulation in the UK: an extended summary. Proceedings of European Geothermal Update: Third International Seminar on EEC Geothermal Research, Munich, November 1983, European Patent Office, Munich (EUR8853EN), 693-758.

Batini, F., Console, R. and Luongo, G., 1985. Seismological study of Larderello-Travale geothermal area. Geothermics Vol. 14, No. 2/2, 255-272.

Baumgärtner, J., Teza, D., Hettkamp, T., Gandy, T. and Schindler, M., 2010. Geothermal reservoir development in the Upper Rhine Graben – “Concepts, Techniques and Experiences”, the geothermal projects in Landau and Insheim. In: Presented at Second European Geothermal Review, Bestec GmbH, Landau, Germany, Mainz, Germany, June 21–23, p. 31.

Beall, J.J., Wright, M.C., Pingol, A.S. and Atkinson, P., 2010. Effect of high rate injection on seismicity in the Geysers. Geothermal Resources Council Transactions, Vol. 34, 47-52.

Bear, J., 1979. Hydraulics of Groundwater. McGraw-Hill, New York.

Bell, M.L. and Nur A. 1978. Strength changes due to reservoir-induced pore pressure and stresses and application to Lake Oroville. Geophys. J. Res. Vol. 83, 4469-4483.

Benson, S.M., 2005. Lessons Learned From Industrial and Natural Analogs for Health, Safety and Environmental Risk Assessment for Geologic Storage of Carbon Dioxide. in D.C. Thomas and S.M. Benson (Eds.) Carbon Dioxide for Storage in Deep Geologic Formations Chapter 25, Elsevier: 1133-1141.

Benson, S.M., Gasperikova, E. and Hoversten, M., 2004. Overview of Monitoring Techniques and Protocols for Geologic Storage Projects. IEA Report Number PH4/29, 99 pp.

Bethmann, F., Diechmann, N., and Mai, P.M. 2011. Scaling Relations of Local Magnitude versus Moment Magnitude for Sequences of Similar Earthquakes in Switzerland, Bulletin of the Seismological Society of America, Vol. 101 no. 2 p. 515-534.

Bommer, J., Oates, S., Cepeda, J. M., Lindholm, C., Bird, J., Torres, R., Marroquin, G. and Rivas, J., 2006. Control of hazard due to seismicity induced by a hot fractured rock geothermal project, Engineering Geology, Vol. 83, 287-306.

Borgesson, L., 1996. ABAQUS. In: Stephansson, O., Jing, L., Tsang, C.-F (Eds), Coupled Thermo-Hydro_Mechanical Processes of Fractured Media, Developments in Geotechnical Engineering, Elsevier Vol. 79, 565-570.

Bossu, R. and Grasso, J.R., 1996. Stress analysis in the intraplate area of Gazli, Uzbekistan, from different sets of earthquake focal mechanisms. Journal of Geophysical Research 101(B8), 17645-17659.

Boyle, K., Jarpe, S., Hutchings, L., Peterson, J. and Majer, E., 2011. Preliminary investigation of an aseismic 'doughnut hole' region in the northwest Geysers, California. Proceedings 36th workshop on Geothermal Reservoir Engineering, Stanford California, 614-620.

Bradbury, J., Greenberg, S. and Wade, S., 2011. Communicating the risks of CCS: The Global CCS Institute.

Brandsdóttir, B., Franzson, H., Einarson, P., Árnason, K. and Kristmannsdóttir, H., 2002. Seismic monitoring during an injection experiment in the Svartsengi geothermal field, Iceland. Jokull, Vol. 51, 43-52.

Bromley, C. and Mongillo, M., 2008. Geothermal energy from fractured reservoirs – Dealing with induced seismicity. Open Energy Technology Bulletin, 48, 7 pp. Available at: http://www.iea.org/impagr/cip/pdf/Issue48Geothermal.pdf

Bromley, C.J., Pearson, C.F. and Rigor, D.M., 1987. Microearthquakes of the Puhagan Geothermal Field, Philippines - a case of induced seismicity. Journal of volcanology and geothermal research, Vol. 31, No. 3/4, 293-311.

Cacas, M. C., Ledoux, E., De Marsily, G. and Tillie, B. 1990. Modeling Fracture Flow with A Stochastic Discrete Fracture Network: Calibration and Validation: 1. The Flow Model. Water Resources Research, 26(3), 479-489

Cappa, F. and Rutqvist, J. 2011a. Modeling of coupled deformation and permeability evolution during fault reactivation induced by deep underground injection of CO_2. International Journal of Greenhouse Gas Control, Vol. 5, No. 2, 336-346.

Cappa, F. and Rutqvist, J. 2011b. Impact of CO_2 geological sequestration on the nucleation of earthquakes. Geophysical Research Letters, Vol. 38 (L17313).

Cappa, F., Rutqvist, J. and Yamamoto, K., 2009. Modelling crustal deformation and rupture processes related to upwelling of deep CO_2 -rich fluids during the 1965-1967 Matsushiro earthquake swarm in Japan. Journal of Geophysical Research, Vol. 114 (B10304).

Carnegie, A., Thomas, M., Efnik, M.S., Hamawi, M., Akbar, M. and Burton, M., 2000, An advanced method of determining insitu reservoir stresses: Wireline conveyed micro-fracturing. SPE Paper 78486.

Cash, D., Homuth, E., Keppler, H., Pearson, C., and Sasaki, S., 1983. Fault plane solutions for microearthquakes induced at the Fenton Hill hot dry rock geothermal site: implications for the state of stress near a quaternary volcanic center. Geophysical Research Letters, Vol. 10, 1141-1144.

Chadwick, R. A., Williams, G., Delepine, N., Clochard, V., Labat, K., Sturton, S., Buddensiek, M.-L. Dillen, M., Nickel, M., Lima, A. L., Arts, R., Neele, F. and Rossi, G., 2010. Quantitative analysis of timelapse seismic monitoring data at the Sleipner CO_2 storage operation. The Leading Edge, Vol. 29, No. 2, 170–177.

Charléty, J., Cuenot, N., Dorbath, L., Dorbath, C., Haessler, H. and Frogneux, M., 2007. Large earthquakes during hydraulic stimulations at the geothermal site of Soultz-sous-Forêts. International Journal of Rock Mechanics and Mining Sciences, Vol. 44, 1091-1105.

Chopra, P. and Wyborn, D., 2003. Australia's first hot dry rock geothermal energy extraction project is up and running in granite beneath the Cooper Basin, NE South Australia. In Blevin, P., Jones, M., Chappell, B. (eds.), Magmas to Mineralisation: The Ishihara Symposium, Geoscience Australia, Record 2003/14, 43-46.

Cladouhos, T., Petty, S., Foulger, G., Julian, B. and Fehler, M., 2010. Injection induced seismicity and geothermal energy. Geothermal Research Council Transactions, Vol. 34, 1213-1220.

Clarke, D. D. and Phillips, C.C., 2003, Three-dimensional geologic modeling and horizontal drilling bring more oil out of the Wilmington oil field of southern California, *in* T. R. Carr, E. P. Mason, and C. T. Feazel, eds., Horizontal wells: Focus on the reservoir: AAPG Methods in Exploration No. 14, 27–47.

Class, H., Ebigbo, A., Helmig, R., Dahle, H., Nordbotten J.M., Celia, M.A., Audigane, P., Darcis, M., Ennis-King, J., Fan, Y., Flemisch, B., Gasda, S.E., Krug, S., Labregere, D., Min, J.,Sbai, A., Thomas, S.G. and Trenty, L., 2009. A benchmark study on problems related to CO_2 storage in geologic formations. Comput. Geosci., Vol. 13, 409-434.

CO2Sink, 2012. http://www.co2sink.org/. Accessed April 10th 2012.

Cooke, R., 1991. Experts in Uncertainty. Oxford University Press. 321pp.

Cornell C.A. 1968. Engineering Seismic Risk Analysis. Bulletin of the Seismological Society of America, 58(6):1583-1606

Cox, R.T., 1991. Possible Triggering of Earthquakes by Underground Waste Disposal in the El Dorado, Arkansas Area: Seismological Research Letters, Vol. 62, 113-122.

Crameik, T.D. and Plassey, J.A., 1972. Carbon Dioxide Injection Project SACROC Unit, Scurry County, Texas Annual Meeting Papers, Division of Production, March 6-8, 1972, Houston, TX.

Cuenot, N., Frogneux, M., Dorbath, C., and Calo, M., 2011. Induced microseismic activity during recent circulation tests at the EGS site of Soultz-sous-Fôrets (France). Proceedings 36th workshop on Geothermal Reservoir Engineering, Stanford California, 638-649.

Cundall, P. and Marti, J., 1978. Computer modeling of jointed rock masses. Report N-78-4. U.S. Army Corps of Engineers, Waterways Experiment Station, Vicksburg, Missouri.

Daley, T.M., Peterson, J.E., Korneev, V., 2011. GE-SEQ Subtask 2.3.4: Microseismic Monitoring and Analysis, Report LBNL-4597E, Lawrence Berkeley National Laboratory, May 2011.

Daley, T.M., Peterson, J.E., Korneev, V., Mathieson, A., Oye, V., Siggins, A., 2012. Microseismic monitoring at In Salah and Otway sequestration sites, 11th Annual Carbon Capture, Utilisation and Sequestration Conference, April 30 – May 2, 2012, Pittsburg, PA.

Darcis, M., Class, H., Flemisch, B. and Helmig, R., 2011. Sequential model coupling for feasibility studies of CO_2 storage in deep saline aquifers. Oil and Gas Science and Technology – Rev. IFP Energies nouvelles Vol. 1, 93-103.Davis, S. D., Nyffenegger, P. A. and Frohlich, C., 1995. The 9 April 1993 Earthquake in South-Central Texas: Was it Induced by Fluid Withdrawal? Bulletin of the Seismological Society of America, Vol. 85, No. 6, 1888-1895.

Davis, S. D. and Pennington, W. D., 1989. Induced Seismic Deformation in the Cogdell Oil Field of West Texas. Bulletin of the Seismological Society of America, Vol. 79, No. 5, 1477-1494.

de Pater, H. and Baisch, S. 2011. Geomechanical Study of Bowland Shale Seismicity. Synthesis Report prepared for Cuadrilla Resources, Ltd.

Deichmann, N. and Ernst, J. 2009. Earthquake focal mechanisms of the induced seismicity in 2006 and 2007 below Basel (Switzerland), Swiss J. Geosci, 102, 457–466.

Deichmann, N. and Giardini, D., 2009. Earthquakes induced by the stimulation of an enhanced geothermal system below Basel. Seismological Research Letters, Vol. 80, 784-798.

Dienes, L. and Shabad, T., 1982. *The Soviet Energy System,* John Wiley, New York, 298 pp.

DNV (Det Norske Veritas), 2011. CO2WELLS Guidelines for the risk management of existing wells at CO2 geological storage sites (No. 2011-0448). Hovik, Norway.

Dorbath, L., Cuenot, N., Genter, A. and Frogneux, M., 2009. Seismic response of the fractured and faulted granite to massive water injection at 5 km depth at Soultz-sous-Fôrets (France). Geophysical Journal International, 177 (2), 653-675.

Doser, D. I., Baker, M. R. and Mason, D. B., 1991. Seismicity in the War-Wink Gas Field, Delaware Basin, West Texas, and its Relationship to Petroleum Production. Bulletin of the Seismological Society of America, Vol. 81, 971-986.

Doser, D. I., Baker, M. R., Luo, M., Marroquin, P., Ballesteros, L., Kingwell, J., Diaz, H.L. and Kaip, G., 1992. The not so simple relationship between seismicity and oil production in the Permian Basin, West Texas. Pure and Applied Geophysics, Vol. 139, No. 3/4, 481-506.

Doughty C. and K. Pruess, A similarity solution for two-phase water, air, and heat flow near a linear heat source in a porous medium, Journal of Geophysical Research, 97, B2, 1821-1838, 1992.

Doughty C. and K. Pruess, Modeling supercritical carbon dioxide injection in heterogeneous porous media, Vadose Zone Journal, 3, 837-847, 2004.

Doughty C., Modeling geologic storage of carbon dioxide: comparison of non-hysteretic and hysteretic characteristic curves, Energy Conversion and management, 48, 1768-1781, 2007.

Duchane, D. and Brown, D., 2002. Hot Dry Rock (HDR) geothermal energy research and development at Fenton Hill, New Mexico. Geo-Heat Center Bulletin, Vol. 23, 13-19.

Eberhart-Phillips, D. and Oppenheimer, D.H., 1984. Induced seismicity in the Geysers Geothermal area, California, Journal of Geophysical Research, Vol. 89, 1191-1207.

EMFI, 2005. http://emfi.mines.edu/emfi2005/ChevronTexaco.pdf. Accessed May 2012.

Enedy, S.L., Enedy, K.L. and Maney, J., 1992. Reservoir response to injection in the Southeast Geysers. Geothermal Resource Council Special Report, Vol. 17, 211-219.

European Commission. 2011. Implementation of Directive 2009/31/EC on the Geological Storage of Carbon Dioxide, Guidance Document 1, CO2 Storage Life Cycle Risk Management Framework.

Evans, K.F., Moriya, H., Niitsuma, H., Jones, R.H., Phillips, W.S., Genter, A., Sausse, J., Jung, R. and Baria, R., 2005. Microseismicity and permeability enhancement of hydrogeologic structures during massive fluid injections into granite as 3 km depth at the Soultz HDR site. Geophysical Journal International, Vol. 160, 388-412.

Evans, K.F., Zappone, A., Kraft, T., Deichmann, N. and Moia, F., 2012. A survey of the induced seismic responses to fluid injection in geothermal and CO2 reservoirs in Europe. Geothermics, Vol. 41, January 2012 p30-54. http://dx.doi.org/10.1016/j.geothermics.2011.08.002.

Eyidogan, H., Nabelek, J. and Toksōz, M.N., 1985. The Gazli, U.S.S.R., March 19, 1984 earthquake: the mechanism and tectonic implications. *Bulletin of the Seismological Society of America,* Vol. 75, 661-675.

Fehler, M., House, L. and Kaieda, H., 1987. Determining planes along which earthquakes occur: method and application to earthquakes accompanying hydraulic fracturing. Journal of Geophysical Research, Vol. 92, 9407-9414.

Fehler, M.C. 1989. Stress control of seismicity patterns observed during hydraulic fracturing experiments at the Fenton Hill Hot Dry Rock geothermal energy site, New Mexico. International Journal of Rock Mechanics and Mineral Science- Geomechanics Abstracts, Vol. 26, 211-219.

Feng, Q. and Lees, J.M., 1998. Microseismicity, stress and fracture in the Coso geothermal field, California. Tectonophysics, Vol. 289, 221-238.

Fialko, Y. and Simons, M., 2000. Deformation and seismicity in the Coso geothermal area, Inyo County, California: Observations and modeling using satellite interferometry. Journal of Geophysical Research, Vol. 105, 21781-21793.

Fjaer, E., 2008. Mechanics of hydraulic fracturing. Petroleum related rock mechanics. Developments in petroleum science (2 ed.). Elsevier. p. 369. ISBN 978-0-444-50260-5.

Fletcher, J.B. and Sykes, L. R. 1977. Earthquakes Related to Hydraulic Mining and Natural Seismic Activity in Western New York State: Journal of Geophysical Research, Vol. 82, 3767-3780.

Foulger, G.R., Grant, C.C., Julian, B.R. and Ross, A., 1997. Industrially induced changes in Earth structure at The Geysers geothermal area, California. Geophysical Research Letters, Vol. 24, 135-137.

Frohlich, C. and Potter, E., 2010. Dallas-Fort Worth earthquakes coincident with activity associated with natural gas production: The Leading Edge, Vol. 29, No. 3, 270-275.

Gartrell, A., Zhang, Y., Lisk, M. and Dewhurst, D. 2004. Fault intersections as critical hydrocarbon leakage zones: Integrated field study and numerical modeling of an example from the Timor Sea, Australia. Marine and Petroleum Geology, Vol. 21, No. 9, 1165–1179, doi:10.10161059 /j.marpetgeo.2004.08.001.

Genter, A., Evans, K.F., Cuenot, N., Fritsch, D. and Sanjuan, B., 2010. The Soultz geothermal adventure: 20 years of research and exploration of deep crystalline fractured rocks for EGS development. Comptes Rendus Geoscience, Vol. 342, 502–516, doi:10.1016/j.crte.2010.01.006.

Gerstenberger, M.C., Wiemer, S., Jones, L.M. and Reasenberg, P.A., 2005 Real-time forecasts of tomorrow's earthquakes in California. Nature, Vol. 435(7040), 328-331.

Ghassemi, A., Tarasovs, S. and Cheng A.H.-D., 2007. A 3-D study of the effects of thermo-mechanical loads on fracture slip in enhanced geothermal reservoirs. International Journal of Rock Mechanics and Mining Sciences, Vol. 44 (2007), 1132–1148.

Giardini, D., 2009, Geothermal quake risk must be faced. Nature, 462, 848-849. doi:10.1038/462848a.

Gibbs, J.F., Healy, J.H., Raleigh, C.B. and Coakley, J., 1973. Seismicity in the Rangely, Colorado, Area; 1962-1970. Bulletin of the Seismological Society of America, Vol. 63, No. 5, 1557-1570.

Glowacka, E. and Nava, F. A., 1996. Major Earthquakes in Mexicali Valley, Mexico, and Fluid Extraction at Cerro Prieto Geothermal Field. Bulletin of the Seismological Society of America, Vol. 86, No. 1A, 93-105.

Goertz-Allmann, B. P., Goertz, A. and Wiemer, S. 2011. Stress drop variations of induced earthquakes at the Basel geothermal site. Geophysical Research Letters, Vol. 38, L09308, doi:10.1029/2011GL047498.

Gomberg, J. and Wolf, L., 1999. Possible cause for an improbable earthquake: The 1997 Mw 4.9 southern Alabama earthquake and hydrocarbon recovery. Geology, Vol. 27, No. 4, 367-370.

González, P.J., Tiampo, K.F., Palano, M., Cannavo, F. and Fernández, J., 2012. The 2011 Lorca earthquake slip distribution controlled by groundwater crustal unloading. Nature GeoScience. Published online: 21 October 2012. DOI: 10.1038/NGEO1610. Advance online Publication. www.nature.com/naturegeoscience. [Accessed 29 October 2012].

Grant, U. S., 1954. Subsidence of the Wilmington Oil Field, California. California Division of Mines Bulletin, Vol. 170, 19-24.

Grasso, J.-R. and Wittlinger, G. 1990. Ten Years of Seismic Monitoring over a Gas Field Area. Bulletin of the Seismological Society of America, Vol. 80, 450-473.

Grasso, J.-R., 1990. Hydrocarbon Extraction and Seismic Hazard Assessment. EOS Transactions, American Geophysical Union, Vol. 71, 1454.

Grasso, J.-R., 1992a. Mechanics of Seismic Instabilities Induced by the Recovery of Hydrocarbons. Pure and Applied Geophysics, Vol 139, No. 3/4, 507-534.

Grasso, J.-R., 1992b. Effects of the Gas Extraction on the Seismic and Aseismic Slips in the Neighborhood of Meillon-St-Faust Gas Field, Report to EIF-Aquitaine Company, Feb 1992, 60 pp.

Greensfelder, R., Cladouhos, T.T. and Jupe, A., 2008. Induced seismicity report, Engineered Geothermal System Demonstration Project Northern California Power Agency, The Geysers CA. Internal report to AltaRock (Appendix B).

Gupta, H.K., 1992. Reservoir – Induced Earthquakes. Developments in Geotechnical Engineering, 64, 364 pp.

Gutenberg, B. and Richter, C.F., 1954. Seismicity of the Earth and Associated Phenomena. Princeton Univ. Press, Princeton, N.J., 2nd Ed., 310 pp.

Han, W.S., McPherson, B.J., Lichtner, P.C., Wang, F.P., 2010. Evaluation of trapping mechanisms in geological CO_2 sequestration: case study of SACROC northern platform a 35-year CO_2 injection site. American Journal of Science 310, 282-324.

Hanks, T.C. and Kanamori, H., 1979. Moment magnitude scale. Journal of Geophysical Research 84 (B5): 2348–50. doi:10.1029/JB084iB05p02348

Harding, S. T., 1981. Induced Seismicity in the Cogdell Canyon Reef Oil Field, U.S. Geological Survey Open-file Report, No. 81-167, 452-455.

Harding, S. T., Carver D, Henrisey, R.F., Dart, R.L. and Langer, C.J., 1978. The Scurry County, Texas, earthquake series of 1977-1978, induced seismicity? (abstract), *Earthquake Note*, Vol. 49, No. 3, 14-15.

Häring, M.O., Schanz, U., Ladner, F. and Dyer, B.C., 2008. Characterization of the Basel 1 enhanced geothermal system. Geothermics, Vol. 37, 469-495.

Healy, D., 2012. Hydraulic Fracturing or 'Fracking': A Short Summary of Current Knowledge and the Potential Environmental Impacts. A small scale study for the Environmental Protection Agency (Ireland) under the Science, Technology, Research & Innovation for the Environment (STRIVE) Programme 2007-2013. http://www.epa.ie/downloads/pubs/research/sss/UniAberdeen_FrackingReport.pdf. [Accessed 29 October 2012].

Healy, J. H., Rubey, W. W., Griggs, D. T. and Raleigh, C. B., 1968. The Denver Earthquakes: Science, Vol. 161, No. 3848, 1301-1310.

Henderson, J.R., Barton, D.J. and Foulger, G.R., 1999. Fractal clustering of induced seismicity in the Geysers Geothermal area, California. Geophysical Journal International, Vol. 139, 317-324.

Herrmann, R.B., Park, S-K. and Wang, C-Y., 1981. The Denver earthquakes OF 1967-1968 Bulletin of the Seismological Society of America, Vol. 71, No. 3, 731-745.

Hillis, R., 2000. Pore pressure/stress coupling and its implications for seismicity. Exploration Geophysics, v31, 448-454.

Hillis. R.R., 2001. Coupled changes in pore pressure and stress in oil fields and sedimentary basins. Petroleum Geoscience, Vol. 7, 419-425

Horner, R. B., Barclay, J. E., and MacRae, J. M., 1994. Earthquakes and Hydrocarbon Production in the Fort St. John Area of Northeastern British Columbia: Canadian Journal of Exploration Geophysics, Vol. 30, No. 1, 39-50.

Hosa, A., Esentia, M., Stewart, J., and Hazeldine, S., 2011. Injection of CO_2 into saline formations: Benchmarking worldwide projects. Chemical Engineering Research and Design, Vol. 89, 1855-1864, doi:10.1016/j.cherd.2011.04.003.

House, L., Keppler, H., and Kaieda, H., 1985. Seismic studies of a massive hydraulic fracturing experiment. Geothermal Resource Council Transactions, Vol. 9,105-111.

Howells, D.A., 1974. The time for a significant change of pore pressure. Engineering Geology Vol. 8, 135-138

Hsieh, P. A., and Bredehoeft, J. D., 1981. A Reservoir Analysis of the Denver Earthquakes: A Case of Induced Seismicity: Journal of Geophysical Research. Vol. 86, No. B2, 903-920.

Hubbert, M.K. and Rubey, W.R., 1959. Role of fluid pressure in mechanics of overthrust faulting: 1. Mechanics of fluid-filled porous solids and its application to overthrust faulting. Bulletin of the Seismological Society of America, Vol. 70, 115-166.

Iceland Review Online, 2011. News report 17.10.2011 14:00 on Hellisheidi induced seismicity.http://www.icelandreview.com/icelandreview/daily_news/Hveragerdi_Residents_Angry_about_Manmade_Quakes_0_383317.news.aspx

IEAGHG. 2009. A review of the international state of the art in risk assessment guidelines and proposed terminology for use in CO2 geological storage, 2009/TR7.

IPCC, 2005. IPCC Special Report on Carbon Dioxide Capture and Storage. Prepared by Working Group III of the Intergovernmental Panel on Climate Change [Metz, B, Davidson, O, de Coninck, H C, Loos, M and Meyer, L A (Eds.)]. Cambridge University Press, New York.

ISO. 2009. ISO 31000:2009 Risk management - Principles and guidelines, International Organization for Standardization.

Itasca. FLAC^{3D}, 2009. Fast Lagrangian Analysis of Continua in 3 Dimensions, Version 4.0. Minneapolis, Minnesota, Itasca Consulting Group 438 pp.

Jaeger, J.C. and Cook, N.G.W., 1979. Fundamentals of Rock Mechanics. Third ed. Chapman and Hall, New York pp. 28-30.

Jenkins, C.R., Cook, P.J., Ennis-King, J., Undershultz, J., Boreham, C., Dance, T., de Caritat, P., Etheridge, D.M., Freifeld, B., Hortle, A., Kirste, D., Paterson, L., Pevzner, R., Schacht, U., Sharma, S., Stalker, L. and Urosevic, M. 2012. Safe storage of CO2 in a depleted gas field - the CO2CRC Otway Project, Proc. Natl. Acad. Sci., Vol. 109, No. 2 E35-E41.

Johnson, J.W., 2011. Geochemical assessment of isolation performance during 10 years of CO2 EOR at Weyburn, Energy Procedia, v4, 3658-3665.

Jones, R.H. and Evans, K.F., 2001. Improved source parameter estimates from microseismic events occurring during the 1993 injections of GPK1 at Soultz-sous-Forêts. In: Final report to New Energy Development Organisation (NEDO), Japan for the Project 'Universal Understanding and Design of Engineered Geothermal Systems.

Jousset, P., Haberland, C., Bauer, K., and Arnason K., 2011. Hengill geothermal volcanic complex (Iceland) characterized by integrated geophysical observations. Geothermics, Vol. 40, No. 1, 1-24.

Kaieda, H., 1984. Hypocenter distribution and fault plane solutions of microearthquakes induced by hydraulic fracturing as determined by observations from a surface seismic network. EOS Trans., 65, 101.

Kaiser, A.E., Holden, C., Beavan, R.J., Beetham, R.D., Benites, R.A., Celentano, A., Collet, D., Cousins, W.J., Cubrinovski, M., Dellow, G.D., Denys, P., Fielding, E., Fry, B., Gerstenberger, M.C., Langridge, R.M., Massey, C.I., Motagh, M., Pondard, N., McVerry, G.H., Ristau, J., Stirling, M.W., Thomas, J., Uma, S.R. and Zhao, J.X., 2012 The Mw 6.2 Christchurch Earthquake of February 2011 : preliminary report. New Zealand journal of geology and geophysics, Vol. 55, No. 1, 67-90; doi:10.1080/00288306.2011.641182.

Kaiser, J., 1950. Untersuchungen über das Auftreten von Geräuschen beim Zugversuch. PhD thesis, Fak. F. Maschinewesen, TH München, Germany.

Kharaka, Y.K., Cole, D.R., Hovorka, S.D., Gunter, W.D., Knauss, K.G., Freifeld, B.M., 2006. Gas-water-rock interactions in Frio Formation following CO_2 injection: implications for the storage of greenhouse gases in sedimentary basins. Geology v34, 577-80

Kikuta K., Hongo S., Tanase D. and Ohsumi T., 2004. Field test of CO2 injection in Nagaoka, Japan. In: *Proceedings of the 7th International Conference on Greenhouse Gas Control Technologies (GHGT-7) Vancouver, Canada, September 5–9, 2004* (ed. M. Wilson, T. Morris, J. Gale and K. Thambimuthu), pp. 1367–1372. ISNB 008044704.

Kirkpatrick, A., Peterson, J.E., Majer, E.L., and Nadeau, R., Proceedings of the 24th Workshop on Geothermal Reservoir Engineering, Stanford University, Stanford, CA, USA (1999), pp. 236–242

Korbol, R. and Kaddour, A., 1995. Sleipner Vest CO2 Disposal – Injection and Removed CO2 into the Utsira Formation, Energy Convers. Mgmt. 36, 509–512,

Kovach, R. L., 1974. Source Mechanisms for Wilmington Oil Field, California, Subsidence Earthquakes. Bulletin of the Seismological Society of America, Vol. 64, 699-711.

Kraft, T., Wassermann, J., Deichmann, N. and Stange, S., 2009. The 2008 earthquakes in the Bavarian Molasse Basin – possible relation to geothermics? In: Proceedings of European Geophysical Union General Assembly Research Abstracts, European Geophysical Union. Vol. 11, EGU2009105936, Vienna, Austria, April 19–24, p.1.

Kuijper, M., 2011. Public acceptance challenges for onshore CO2 storage in Barendrecht. Energy Procedia, Vol. 4, 6226-6233.

Ladner, F. and Haring, M. O. 2009. Hydraulic Characteristics of the Basel 1 Enhanced Geothermal System. Geothermal Resources Council Transactions, Vol. 33, 199-203.

Langenbruch, C. and Shapiro, S.A., 2010. Decay rate of fluid-induced seismicity after termination of reservoir stimulations: Geophysics, Vol. 75, MA53-MA62.

Langenbruch, C., Dinske, C. and Shapiro, S.A., 2011. *Inter event times of fluid induced earthquakes suggest their Poisson nature*. Geophysical Research Letters, Vol. 38, L21,302.

LBNL, 2012. EGS: The Geysers: What is the history of seismicity at The Geysers? http://esd.lbl.gov/research/projects/induced_seismicity/egs/geysers_history.html. Accessed on May 24th, 2012.

Lombardi, A.,M., and Marzocchi, W., 2010. The ETAS model for daily forecasting of Italian seismicity in the CSEP experiment. Annals of Geophysics, Vol. 53, No. 3, 155-164.

Ma, J. and Morozov, I., 2010. AVO modeling of pressure-saturation effects in Weyburn CO_2 sequestration. The Leading Edge, Vol. 29, No. 2, 178-183.

Majer, E. and Doe, T., 1986. Studying hydrofractures by high frequency seismic monitoring. Int. J. Rock Mech. Min Sci and Geomech. Ahstr., Vol. 23, 185-199.

Majer, E., Baria, R. and Stark, M., 2008. Protocol for induced seismicity associated with enhanced geothermal systems. Report produced in Task D Annex I (9 April 2008), International Energy Agency-Geothermal Implementing Agreement (incorporating comments by: C. Bromley, W. Cumming, A. Jelacic and L. Rybach). Available at: http://www.iea-gia.org/documents/ Protocol for Induced Seismicity EGS-GIADoc25Feb09.pdf [Accessed February 9, 2011].

Majer, E., Baria, R., Fehler, M., 2005. Cooperative research on induced seismicity associated with enhanced geothermal systems. Geothermal Resource Council Transactions, Vol. 29, 99-101.

Majer, E., Nelson, J., Robertson-Tait, A., Savy, J. and Wong, I., 2011. Protocol for addressing induced seismicity associated with enhanced geothermal systems (EGS) – Final Draft. Available at: http://www1.eere.energy.gov/geothermal/pdfs/egs-is-protocol-final-draft-20110531.pdf [Accessed June 27, 2011].

Majer, E.L. and McEvilly, T.V., 1979. Seismological investigations at The Geysers geothermal field. Geophysics, Vol. 44, 246-269.

Majer, E.L. and Peterson, J.E., 2005. Application of microearthquake monitoring for evaluating and managing the effects of fluid injection at naturally fractured EGS sites. Geothermal Resource Council Transactions, Vol. 29, 103-107.

Majer, E.L., Baria, R., Stark, M., Oates, S., Bommer, J., Smith, B. and Asanuma, H., 2007. Induced seismicity associated with Enhanced Geothermal Systems. Geothermics, Vol. 36, 185-222.

Marsden, R., 2007. Geomechanics for reservoir management. Algeria Well Evaluation Conference: 398.

Mathieson, A., Midley, J., Dodds, K., Wright, I., Ringrose, P. and Saoul, N., 2010. CO_2 sequestration monitoring and verification technologies applied at Krechba, Algeria, The Leading Edge, Vol. 29, No. 2, 216-222.

Mathieson, A., Wright, I., Roberts, D., and Ringrose, P., 2009. Satellite imaging to monitor CO_2 movement at Krechba, Algeria, Energy Procedia, Vol. 1, 2201-2209.

Maxwell, S. C., Jones, M., Parker, R., Miong, S., Leaney, S., Dorval, D., D'Amico, D., Logel, J., Anderson, E. and Hammermaster, K., 2009. Fault Activation During Hydraulic Fracturing: Society of Exploration Geophysicists Expanded Abstract, 28, 1552.

Maxwell, S. C., Shemeta, J., Campbell, E. and Quirk, D., 2008, Microseismic deformation rate monitoring: Annual Technical Conference and Exhibition, Society of Petroleum Engineers, SPE 116596.

McClure, M. and Horne, R., 2010. Numerical and analytical modeling of the mechanisms of induced seismicity during fluid injection. Geothermal Resource Council Transactions, Vol. 34, 381-394.

McGarr, A. 1991. On a possible connection between three major earthquakes in California and oil production. Bulletin of the Seismological Society of America, Vol. 81, No. 3, 948-970.

McGarr, A., 1976, Seismic moments and volume changes. Journal of Geophysical Research Vol. 81, No. 8, 1487-1494.

McGarr, A., Simpson, D., Seeber, L., 2002. Case Histories of Induced and Triggered Seismicity. In: International Handbook of Earthquake and Engineering Seismology. Volume 81A, 647-661.

Medvedev, S.V., 1968. S.V. Medvedev (Ed.), Seismic Zoning of the USSR, Nauka, Moscow (1968), p. 476 (in Russian)

Meghrauoi, M, Delouis, B., Ferry, M., Giardini, D., Huggenberger, P., Spottke, I. and Granet, M., 2009. Active normal faulting in the upper Rhine Graben and paleoseismic identification of the 1356 Basel Earthquake, Science, Vol. 293, 2070-2073.Meremonte, M.E., Lahr. J.C., Frankel, A.D., Dewey, J.W., Crone, A.J., Overturf, D.E., Carver, D.L., and Bice, W.T. 2002, Investigation of an Earthquake Swarm near Trinidad, Colorado, August-October 2001. United States Geological Survey Open-File Report 02-0073

Mehnert E. and R.T. Okwen, Near-well pressure distribution of CO2 injection in a partially penetrating well, Proceedings TOUGH Symposium 2012, 2012.

Michael, K., Neal, P.R., Allinson, G., Ennis-King, J., Hou, W., Paterson, L., Sharma., S., and Aiken, T., 2011, Injection Strategies for large-scale CO2 Storage Sites, Energy Procedia, Volume 4, 2011, Pages 4267–4274

Mignan, A., M. J. Werner, S. Wiemer, C.-C. Chen and Y.-M. Wu. 2011. Bayesian Estimation of the Spatially Varying Completeness Magnitude of Earthquake Catalogs. Bulletin of the Seismological Society of America, 101, doi: 10.1785/0120100223

Moore, D.E., and Lockner, D.A., 2011. Frictional strengths of talc-serpentine and talc-quartz mixtures, J. geophys. Res., 116, B01403, doi:10.1029/2010JB007881, 2011.

Morelli, C.P. and Malavozos, M., 2008. Analysis and management of seismic risks associated with engineered geothermal system operations in South Australia. Proceedings of the Australian Geothermal Energy Conference 2008, 113-116.

Morrow, C.A., Moore, D.E., and Lockner, D.A., 2000. The effect of mineral bond strength and adsorbed water on fault gouge frictional strength, Geophys Res. Lett., 27, 815-818.

Mossop, A.P., 2001. Seismicity, subsidence and strain at the Geysers geothermal field. PhD Thesis, Stanford University.

Mukuhira, H., Asanuma, H., Niitsuma, H., Schanz, U. and Häring, M., 2008. Characterization of microseismic events with larger magnitude collected at Basel, Switzerland in 2006. Transactions Geothermal Resources Council 32, 87–94.

Murphy, H. and Fehler, M., 1986. Hydraulic fracturing of jointed formations. Soc. Petrol. Engrs, Int. Mg Petrol. Engineering, March 17-20, Beijing, China. SPE, Paper 14088.

Murphy, S., O'Brien, G.C., Bean, C.J., McCloskey, J., and Nalbant, S.S. 2011. Modelling induced seismicity due to fluid injection. Abstract S42B-05 presented at 2011 Fall Meeting, AGU, San Francisco, California. 5-9 December 2011.

Myer, L.R. and Daley, T.M., 2011. Elements of a best practices approach to induced seismicity in geological storage. Energy Procedia Vol. 4, 2011, 3707-3713

NETL (National Energy Technology Laboratory U.S. Department of Energy), 2011. Best Practices for: Risk Analysis and Simulation for Geologic Storage of CO2.

Nicholson, C. and Wesson, R. L., 1990. Earthquake Hazard Associated with Deep well Injection. U.S. Geol. Survey Bull 1951, 74 pp.

Nicholson, C. and Wesson, R. L., 1992. Triggered Earthquakes and Deep Well Activities: Pure and Applied Geophysics, Vol. 139, No. 3/4, 561-578.

Nicol, A., Carne, R., Christopersen, A. and Gerstenberger, M., 2011. Induced seismicity and its implications for CO_2 sequestration risk. Oral preseantation, GHGT-10 Conference Amsterdam, 20-23 September 2011. Energy Procedia 4 (2011), 3699-3706.

Ogata, Y., 1998. Space-time point-process models for earthquake occurrences, Annals of the Institute of Statistical Mathematics, Vol. 50, 2, 379-402.

Ohtake, M., 1974. Seismic Activity Induced by Water Injection at Matsushiro, Japan. Journal of Physics of the Earth, Vol. 22, 163-176.

Okwen R.T., M.T. Stewart and J.A. Cunningham, Temporal variations in near-wellbore pressures during CO2 injection in saline aquifers, International Journal of Greenhouse Gas Control, 5, 1140-1148, 2011.

Olivella, S., Gens, A., Carrera, J. and Alonso E. E., 1996. Numerical formulation for a simulator (CODE_BRIGHT) for the coupled analysis of saline media. Engineering Computations, Vol. 13, 87-112.

Omori, F., 1894. On the aftershocks of earthquakes. Journal of the College of Science, Imperial University of Tokyo 7, 111–200.

Oppenheimer, D.C., 1986. Extensional tectonics at The Geysers geothermal area, California. Journal of Geophysical Research, Vol. 91, 11463-11476.

Parker, R., 1999. The Rosemanowes HDR project 1983-1991. Geothermics, Vol. 28, 603-615.

Parotidis, M. and Shapiro, S.A., 2004. A statistical model for the seismicity rate of fluid-injection-induced earthquakes. Geophysical Research Letters, Vol. 31, L17609, DOI: 10.1029/2004GL020421.

Parotidis, M., Shapiro, S.A. and Rothert, E., 2004. Back front of seismicity induced after termination of borehole fluid injection. Geophysical Research Letters, Vol. 31 (L02612)

Pau, G. S. H., Bell, J. B., Pruess, K., Almgren, A. S., Lijewski, M. J. , Zhang, K., 2010. High resolution simulation and characterization of density-driven flow in CO2 storage in saline aquifers', Advances in Water Resources, 33, 443-455.

Pearce, J., Chadwick, A., Bentham, M., Holloway, S., and Kirby, G., 2005. Technology Status Review—Monitoring Technologies for the Geological Storage of CO_2. UK Department of Trade and Industry.

Pearson, C., 1981. The Relationship between Microseismicity and High Pore Pressures during Hydraulic Stimulation Experiments in Low Permeability Granitic Rocks. Journal of Geophysical Research, Vol. 86, 7855-7864.

Pennell, S., and Ward, J.B., 2004. Cogdell Unit CO_2 flood yields positive results. Oil and Gas Journal, Vol. 102, No. 14, 12 April 2004, 48-49.

Pennington, W. D., Davis, S. D., Carlson, S. M., DuPree, J., and Ewing, T. E., 1986. The Evolution of Seismic Barriers and Asperities Caused by the Depressuring of Fault Planes in Oil and Gas Fields of South Texas. Bulletin of the Seismological Society of America, Vol. 76, No. 4, 939-948.

Pratt, W. E., and Johnson, D. W., 1926. Local Subsidence of the Goose Creek Oil Field. Journal of Geology, Vol. 34, 577-590.

Prevedel, B., Wohlgemuth, L., Henninges, J., Krüger, K., Norden, B., Förster, A., 2008. The CO2-SINK boreholes for geological storage testing. Scientific Drilling Vol. 6, 32–37, doi:10.2204/iodp.sd.6.04.2008.

Pruess K. and J. Garcia, Multiphase flow dynamics during CO2 injection into saline aquifers, Environmental Geology, 42, 282-295, doi:10.1007/s00254-001-0498-3, 2002.

Pruess K. and N. Muller, Formation dry-out from CO2 injection into saline aquifers: 1. Effects of solids precipitation and their mitigation, Water Resources Research, 45, W03402, doi:10.1029/2008WR007101, 2009.

Pruess, K., García, J., Kovscek, A.R., Oldenburg, C., Rutqvist, J., Steefel, C. and Xu, T., 2004. Code intercomparison builds confidence in numerical simulation models for geologic disposal of CO_2. Energy, Vol. 29, 1431-1444.

Pruess, K., Oldenburg, C. and Moridis, G., 1999. TOUGH2 Users' Guide, Version 2.0, Report LBNL-43134, Lawrence Berkeley National Laboratory, Berkeley, California 198pp.

Raleigh, C. B., Healy, J. H., and Bredehoeft, J. D., 1972. Faulting and Crustal Stress at Rangely, Colorado: A.G.U., Geophysical Monograph, no 16, p. 275-284. San Andreas Fault, EOS Transactions, American Geophysical Union, No. 71, 1652.

Raleigh, C. B., Healy, J. H., and Bredehoeft, J. D., 1976. An Experiment in Earthquake Control at Rangel y, Colorado. Science, Vol. 191, 1230-1237.

Rhoades, D.A. 1995 Estimation of the Gutenberg - Richter relation allowing for individual earthquake magnitude uncertainties. Tectonophysics, 258 (1/4), 71-83

Richter, C. F., 1958. Elementary Seismology. W. H. Freeman and Co., San Francisco, 768pp.

Rigg, A, et al, 2006. Callide Oxyfuel Project feasibility study part 6: desk-top study on CO2 Storage, southeast Queensland, Australia. Cooperative Research Centre for Greenhouse Gas Technologies, Canberra, Australia, CO2CRC Publication Number RPT06-0186. 8pp.

Rivas, J.A., Castellón, J.A., and Maravilla, J.N., 2005. Seven years of reservoir seismic monitoring at Berlín Geothermal Field, Usulut´an, El Salvador. In: Proceedings of the World Geothermal Congress 2005, Antalya, Turkey, April 24–29, 2005, Paper 0215, 8 pp.

Ross, A., Foulger, G.R. and Julian, B.R., 1999. Source processes of industrially-induced earthquakes at The Geysers geothermal area, California. Geophysics, Vol. 64, 1877-1889.

Rothe, G. H., and Lui, C. Y., 1983. Possibility of Induced Seismicity in the Vicinity of the Sleepy Hollow Oil Field, SW Nebraska. Bulletin of the Seismological Society of America, Vol. 73, 1357-1367.

Rothe, J.-P., 1977. Seismes artificiels et exploitation petrolieres: L'exemple de Lacq, France. Annali di Geofisicia, Vol. 30, 369-383.

Rutledge, J. T., Scott Phillips, W., and Schuessler, B. K., 1998. Reservoir characterization using oil-production-induced microseismicity, Clinton County, Kentucky. Tectonophysics, Vol. 289, 129-152.

Rutqvist, J., Birkholzer, J., Cappa, F. and Tsang, C.-F., 2007. Estimating maximum sustainable injection pressure during geological sequestration of CO_2 using coupled fluid flow and geomechanical fault-slip analysis. Energy Conversion and Management, Vol. 48, 1798-1807.

Rutqvist, J., Birkholzer, J.T. and Tsang, C.-F. 2008. Coupled reservoir-geomechanical analysis of the potential for tensile and shear failure associated with CO_2 injection in multilayered reservoir-caprock systems. International Journal of Rock Mechanics and Mining Sciences (2008) Vol. 45, 132-143.

Rutqvist, J., Liu, H-H., Vasco, D.W., Pan, L., Kappler, K., and Majer, E., 2011. Coupled non-isothermal, multiphase fluid flow, and geomechanical modeling of ground surface deformations and potential for induced micro-seismicity at the In Salah CO2 storage operation. Energy Procedia 4 (2011), 3542–3549.

Rutqvist, J., Vasco D., and Myer L., 2010. Coupled reservoir-geomechanical analysis of CO2 injection and ground deformations at In Salah, Algeria. International Journal of Greenhouse Gas Control, Vol. 4, 225–230.

Rutqvist, J., Wu, Y.-S., Tsang, C.-F. and Bodvarsson, G., 2002. A modeling approach for analysis of coupled multiphase fluid flow, heat transfer, and deformation in fractured porous rock. International Journal of Rock Mechanics and Mining Sciences Vol. 39 429-442.

Samuelson, J., and Spiers, C.J., 2012. Fault friction and slip stability not affected by CO_2 storage: Evidence from short-term laboratory experiments on North Sea reservoir sandstones and caprocks, int. J. Greenhouse Gas Control, in press October 2012.

Sanford, A. R., Sanford, S., Wallace, T.A., Barrows, L., Sheldon, J., Ward, R.M., Johansen, S., and Merritt, L., 1980. Seismicity in the area of the Waste Isolation Pilot Plant (WIPP), Sandia Laboratories Rept. SAND 80-7096.

Sasaki, S., 1998. Characteristics of microseismic events induced during hydraulic fracturing experiments at the Hijiori hot dry rock geothermal energy site, Yamagata, Japan. Tectonophysics, Vol. 289, 171-188.

Sasaki, S., and Kaieda, H., 2002. Determination of stress state from focal mechanisms of microseismic events induced during hydraulic injection at the Hijiori hot dry rock site. Pure and Applied Geophysics, Vol. 159, 489-516.

Schellschmidt, R., Sanner, B., Pester, S., and Schulz, R., 2010. Geothermal energy use in Germany. Proceedings of the World Geothermal Congress, Bali, Indonesia May 2010, IGA.

Schnaar, G. and Digiulio, D.C., 2009. Computational Modeling of the Geologic Sequestration of Carbon Dioxide. Vadose Zone Journal, Vol. 8, No. 2, 389.

Schorlemmer, D., Gerstenberger, M.C., Wiemer, S., Jackson, D.D. and Rhoades, D.A., 2007 Earthquake likelihood model testing. Seismological research letters, Vol. 78, No. 1, 17-29.

Seeber, L., Armbruster, J.G. and Kim, W.-Y. 2004. A Fluid-Injection-Triggered Earthquake Sequence in Ashtabula, Ohio: Implications for Seismogenesis in Stable Continental Regions. Bulletin of the Seismological Society of America, Vol. 94, No. 1, 76-87.

Segall P., and Mossop, A., 1998. Investigation of induced seismicity and surface deformation at The Geysers Geothermal Field, N. California. 1998 final report for US DOE, Geothermal Energy R&D Program, Reservoir Technology, Chapter 3, 138-141.

Segall, P., 1985. Stress and Subsidence resulting from subsurface Fluid Withdrawal in the Epicentral Region of the 1983 Coalinga Earthquake. Journal of Geophysical Research, Vol. 90, No. B8, 6801-6816.

Segall, P., 1989. Earthquakes triggered by fluid extraction. Geology, Vol. 17, 942-946.

Segall, P., Grasso, J.-R., and Mossop, A., 1994. Poroelastic stressing and induced seismicity near the Lacq gas field, southwestern France. Journal of Geophysical Research, Vol. 99, No. B8, 15423-15438.

Shapiro, S. A., and Dinske, C., 2009. Scaling of seismicity induced by nonlinear fluid-rock interaction. Journal of Geophysical Research, Vol. 114, B09307.

Shapiro, S. A., Dinske, C., and Kummerow, J., 2007. Probability of a given-magnitude earthquake induced by a fluid injection. Geophysical Research Letters, Vol. 34, L22314.

Shapiro, S. A., Dinske, C., Langenbruch, C. and Wenzel, F., 2010. Seismogenic index and magnitude probability of earthquakes induced during reservoir fluid stimulations. The Leading Edge 29, No. 3, 304-309.

Shapiro, S.A., Huenges, E. and Borm, G., 1997. Estimating the crust permeability from fluid-injection-induced seismic emission at the KTB site. Geophysical Journal International, Vol. 131, F15-F18

Shapiro, S.A., Kruger O.S., Dinske C., and Langenbruch C., 2011. Magnitudes of induced earthquakes and geometric scales of fluid-stimulated rock volumes. Geophysics 76, Issue 6 WC55 (2011); http://dx.doi.org/10.1190/geo2010-0349.1

Shukla, R., Ranjith, P., Haque, A., and Choi, X., 2010. A review of studies on CO2 sequestration and caprock integrity, Fuel, v89, 2651-2664.

Simiyu, S., 1999, Induced micro-seismicity during well discharge: OW-719, Olkaria, Kenya rift. Geothermics, Vol. 28, No. 6, 785-802.

Simpson, D. W., and Leith, W., 1985. The 1976 and 1984 Gazli, USSR, Earthquakes – Were they induced? Bulletin of the Seismological Society of America, Vol. 75, No. 5, 1465-1468.

Simpson, D.W., 1986. Triggered earthquakes. Ann. Rev. Earth Planet. Sci., v14, 21-42.

Sminchak, J., and Gupta, N., 2003. Aspects of induced seismic activity and deep-well sequestration of carbon dioxide. Environmental Geosciences, Vol. 10, No. 2, 81-89.

Sminchak, J., Gupta, N., Byrer, C. and Bergman, P., 2002, Issues related to seismic activity induced by the injection of CO_2 in deep saline aquifers. Journal of Energy and Environmental Research, Vol. 2, 32–46.

Smith, J.L.B., Beall, J.J., and Stark, M.A., 2000. Induced seismicity in the SE Geysers field. Geothermal Resource Council Transactions, Vol., 24, 24-27.

Stark, M., 2003. Seismic evidence for a long-lived enhanced geothermal system (EGS) in the Northern Geysers Reservoir. Geothermal Research Council Transactions, Vol. 24, 24-27.

Stark, M.A., Box, W.T., Beall, J.J., Goyal, K.P., and Pingol, A.S., 2005. The Santa Rosa Geysers recharge project, Geysers Geothermal Field, California. Geothermal Resource Council Transactions, Vol. 29, 145-150.

Stenhouse, M., Zhou, W., Kozak, M. and Wilson, M., 2006. Risk Assessment and Geological Storage of CO2 Briefing Document, Report MSCI-2512 to IEA GHG, v1.1, Monitor Scientific LLC.

Stenhouse, M., Zhou, W., Savage, D., and Benbow, S., 2005. Framework Methodology for Long-Term Assessment of the Fate of CO2 in the Weyburn Field. in D.C. Thomas and S. M. Benson (Eds.) Carbon Dioxide for Storage in Deep Geologic Formations Chapter 31, Elsevier: 1251-1262.

Streit, J.E. and Hillis, R.R., 2004. Estimating fault stability and sustainable fluid pressures for underground storage of CO_2 in porous rock. Energy Vol. 29, 1445-1456.

Suckale, J., 2009. Induced seismicity in hydrocarbon fields. Advances in Geophysics, Vol. 51, 55–106.

Suckale, J., 2010. Moderate-to-large seismicity induced by hydrocarbon production. The Leading Edge 29, No. 3, 310-319.

Sze, E., 2005. Induced seismicity analysis for reservoir characterization at a petroleum field in Oman. PhD Thesis. Massachussets Institute of Technology.

Tadokoro, K., and Ando, M., 2000. Induced earthquakes accompanying the water injection experiment at the Nojima fault zone, Japan: Seismicity and its migration. Journal of Geophysical Research, Vol. 105, No. B3, 6089-6104.

Tang, C., Rial, J.A., and Lees, J.M., 2008. Seismic imaging of the geothermal field at Krafla, Iceland using shearwave splitting. Journal Volcanology Geothermal Research 176, 315–324, doi:10.1016/j.volgeores.2008.04.017.

Taron, J. and Elsworth, D., 2009. Thermal–hydrologic–mechanical–chemical processes in the evolution of engineered geothermal reservoirs. International Journal of Rock Mechanics and Mining Sciences, Vol. 46, No. 5, 855-864.

Tenthorey, E, John, Z and Nguyen, D, 2010. CRC-2 Extended Leak-Off and Mini-Frac Tests: Results and Implications. Cooperative Research Centre for Greenhouse Gas Technologies, Canberra, Australia, CO2CRC Publication Number RPT10-2228. 23pp.

Terzaghi, K., 1923. Die Berechning der Durchlassigkeitziffer des Tonesaus dem Verlauf Spannungserscheinungen, Akad. Der Wissenchafen in Wien, Sitzungsberichte, Mathematisch-naturwissenschafttliche Klasse Part lia 142 (3/4), 125-138.

Twiss, R.J., and Moores, E.M., 1992. Structural Geology. W.H. Freeman and Company. 532 pp.

Underschultz, J., Boreham, C., Dance, T., Stalker, L.,Freifeld, B., Kirste, D., and Ennis King J., 2011. CO2 storage in a depleted gas field: An overview of the CO2CRC Otway Project and initial results. International Journal of Greenhouse Gas Control, Vol. 5 (2011), 922–932.

Utsu, T., Ogata, Y., Matsu'ura, R.S., 1995. The centenary of the Omori formula for a decay law of aftershock activity, Journal of the Physics of the Earth, Vol. 43, 1–33.

Van Eck, T., Goutbeek, F., Haak, H., and Dost, B., 2006, Seismic hazard due to small magnitude, shallow-source, induced earthquakes in The Netherlands. Environmental Geology, Vol. 87, 105–121.

Van Eijs, R.M.H.E., Mulders, F.M.M., Nepveu, M., Kenter, C.J., and Scheffers, B.C., 2006, Correlation between hydrocarbon reservoir properties and induced seismicity in the Netherlands. Environmental Geology, Vol. 84, 99–111.

Verdon J.P., Kendall, J-M., White, D.J., Angus, D.A., Fisher, Q.J. and Urbancic, T., 2010b. Passive seismic monitoring of carbon dioxide storage at Weyburn. The Leading Edge, Vol. 29, No. 2, 200-206.

Verdon, J.P., Kendall, J-M. and Maxwell, S.C., 2010a. A comparison of passive seismic monitoring of fracture stimulation from water and CO2 injection. Geophysics, Vol. 75, No. 3 P. MA1–MA7, doi:10.1190/1.3377789.

Vilarrasa, V. Bolster, D., Olivella, S. and Carrera, J., 2010. Coupled hydromechanical modeling of CO_2 sequestration in deep saline aquifers. International Journal of Greenhouse Gas Control, Vol. 4, 910-919.

Wetmiller, R. J. 1986. Earthquakes near Rocky Mountain House, Alberta, and Relationship to Gas Production. Canadian Journal of Earth Sciences, Vol. 32, No. 2, 172-181.

White, A.J., Traugott, M.O., Swarbrick, R.E., 2002. The use of leak-off tests as a means of predicting minimum in-situ stresses. Petroleum Geosciences 8, 189-193

Würdemann, H., Möller, F., Kühn, M., Heidug, W., Christensen, N.-P., Borm, G. and Schilling, F.R., 2010. CO2SINK – from site characterisation and risk assessment to monitoring and verification: one year of operational experience with the field laboratory for CO2 storage at Ketzin, Germany. International Journal Greenhouse Gas Control, Vol. 4, 938–951, doi:10.1016/j.ijggc.2010.08.010.

Xiao, Y., Xu, T., Pruess, K., 2009. The effects of gas-fluid-rock interactions on CO2 injection and storage: Insights from reactive transport modeling. Energy Procedia, v1, 1783-1790.

Yerkes, R.F. and Castle, R.O., 1970. Surface deformation associated with oil and gas field operations in the United States. In: Land subsidence; International Association of the Science of Hydrology, UNESCO Publication 89, Vol. 1, 55-66.

Yerkes, R.F. and Castle, R.O., 1976. Seismicity and faulting attributable to fluid extraction, Eng. Geol., Vol. 10, No. 2-4, 151-167.

Zechar, J.D., Gerstenberger, M.C. and Rhoades, D.A., 2010. Likelihood-based tests for evaluating space-rate-magnitude earthquake forecasts. Bulletin of the Seismological Society of America, Vol. 100, No. 3, 1184-1195. doi:10.1785/0120090192.

Zhang, Y., Frefield, B., Finsterle, S., Leahy, M., Ennis-King, J., Paterson, L. and Dance, T., 2011. Single-Well Experimental Design for Studying Residual Trapping of Supercritical Carbon Dioxide. International Journal of Greenhouse Gas Control, Vol. 5, No. 1, 88-98.

Zhao, X. P. et al. . 2011. Numerical Modelling of Microseismicity Induced by CO2 Injection. Proceedings of the 73rd European Association of Geoscientists and Engineers Conference, Vienna.

Zhou, R., Huang, L. and Rutledge, J., 2010. Microseismic event location for monitoring CO_2 injection using double difference tomography. The Leading Edge, Vol. 29, No. 2, 208-214.

Zoback M.D. and Gorelick S.M., 2012 Earthquake triggering and large-scale geologic storage of carbon dioxide. *PNAS* 2012, 1-5, www.pnas.org/cgi/doi/10.1073/pnas.1202473109.

Zoback, M. D. and Harjes, H.-P. 1997. Injection-induced earthquakes and crustal stress at 9 km depth at the KTB deep drilling site, Germany: Journal of Geophysical Research, Vol. 102, No. B8, p. 18477-18491.

Zoback, M.D. and Zink, J.C., 2002. Production-induced normal faulting in the Valhall and Ekofisk oil fields, Pure and Applied Geophysics, Vol. 159: 403-420.

Zoback, M.D., 2007. Reservoir Geomechanics. Cambridge University Press.

Zoback, M.D., 2012. Managing the seismic risk posed by wastewater disposal, Earth Magazine, April. http://www.earthmagazine.org/article/managing-seismic-risk-posed-wastewater-disposal. [Accessed 29 October 2012].